

DEVELOPMENT OF SPRAY DRIED CHITOSAN-BASED NANOAGGREGATES
CONTAINING LIPID NANOPARTICLES FOR ORAL DELIVERY TO BRAIN
TARGETING USING BROMOCRIPTINE AND ASIATIC ACID AS DRUG
MODELS

Miss Siti Zahliyatul Munawiroh



จุฬาลงกรณ์มหาวิทยาลัย

CHULALONGKORN UNIVERSITY

บทคัดย่อและแฟ้มข้อมูลฉบับเต็มของวิทยานิพนธ์ตั้งแต่ปีการศึกษา 2554 ที่ให้บริการในคลังปัญญาจุฬาฯ (CUIR)
เป็นแฟ้มข้อมูลของนิสิตเจ้าของวิทยานิพนธ์ ที่ส่งผ่านทางบัณฑิตวิทยาลัย

The abstract and full text of theses from the academic year 2011 in Chulalongkorn University Intellectual Repository (CUIR)
are the thesis authors' files submitted through the University Graduate School.

A Dissertation Submitted in Partial Fulfillment of the Requirements
for the Degree of Doctor of Philosophy Program in Pharmaceutical Technology

Department of Pharmaceutics and Industrial Pharmacy

Faculty of Pharmaceutical Sciences

Chulalongkorn University

Academic Year 2015

Copyright of Chulalongkorn University

การพัฒนานาโนแอกกริเกตจากโคโตซานพ่นแห้งที่ประกอบด้วยอนุภาคนาโนไขมันสำหรับการ
นำส่งทางปากสู่เป้าหมายที่สมอง โดยใช้โบรโมคริปตินและกรดเอเซียติกเป็นยาต้นแบบ



วิทยานิพนธ์นี้เป็นส่วนหนึ่งของการศึกษาตามหลักสูตรปริญญาวิทยาศาสตรดุษฎีบัณฑิต
สาขาวิชาเทคโนโลยีเภสัชกรรม ภาควิชาวิทยาการเภสัชกรรมและเภสัชอุตสาหกรรม

คณะเภสัชศาสตร์ จุฬาลงกรณ์มหาวิทยาลัย

ปีการศึกษา 2558

ลิขสิทธิ์ของจุฬาลงกรณ์มหาวิทยาลัย

สตีชวลียาตุล มุนะวีโร : การพัฒนานาโนเอกกริเกตจากไคโตซานพ่นแห้งที่ประกอบด้วยอนุภาคนาโนไขมันสำหรับการนำส่งทางปากสู่เป้าหมายที่สมองโดยใช้โบรโมคริปตินและกรดเอเซียติกเป็นยาต้นแบบ (DEVELOPMENT OF SPRAY DRIED CHITOSAN-BASED NANOAGGREGATES CONTAINING LIPID NANOPARTICLES FOR ORAL DELIVERY TO BRAIN TARGETING USING BROMOCRIPTINE AND ASIATIC ACID AS DRUG MODELS) อ.ที่ปรึกษาวิทยานิพนธ์หลัก: ศ. ญ. ดร. กาญจน์พิมล ฤทธิเดช, อ.ที่ปรึกษาวิทยานิพนธ์ร่วม: รศ. ญ. ดร. วิมลมาศ ลิปิพันธ์, 4 หน้า.

การ พัฒนาอนุภาคนาโนเอกกริเกตพ่นแห้งที่มีไคโตซานเป็นสารพื้นฐาน ซึ่งประกอบด้วย อนุภาคนาโนลิปิด 2 ชนิด อนุภาคนาโนไขมันแข็ง แข็ง (SLN) และตัวพาลีปิดที่มีโครงสร้างนาโน (NLC) โดยใช้โบรโมคริปติน มิสิเลท (BM) และกรดเอเซียติก (AA) เป็นยาต้นแบบ มีวัตถุประสงค์เพิ่มการดูดซึมเมื่อรับประทาน และนำส่งสู่สมอง การพัฒนาหาสภาวะที่เหมาะสมที่สุดของการพ่นแห้งประสบความสำเร็จด้วยวิธีการตอบสนองพื้นผิวโดยใช้การออกแบบชนิด rotatable composite กระบวนการพ่นแห้งทำให้เกิดการเกาะกลุ่มของอนุภาคนาโนลิปิดทั้ง 2 ชนิด (เช่น อนุภาคนาโนไขมันแข็ง และตัวพาลีปิดที่มีโครงสร้างนาโน) ซึ่งเพิ่มขนาดของอนุภาคนาโนลิปิดเหล่านี้ การเติมไคโตซานลงในการพ่นแห้ง SLN และ NLC ไม่ได้ให้พ่นแห้งที่มีการไหลไม่ดี จากการศึกษาดูด้วยเทคนิคเอกซเรย์ดิฟแฟรคชัน(WXRD) และ ดิฟเฟอเรนเชียลสแกนนิ่งแคลอริมิเตอร์ (DSC) พบว่า พ่นแห้งของอนุภาคนาโนลิปิด (AASLN/AANLC) เป็นอัญฐานที่มีขนาดไมโครเมตร ซึ่งสามารถกระจายตัวได้ง่าย เป็นนาโนเอกกริเกตของ SLN/NLC ที่มีตัวโบรโมคริปติน มิสิเลท และกรดเอเซียติก ทั้ง AA และ BM สามารถถูกกักเก็บใน SLN และ NLC ได้ดี ความคงอยู่ของ BM และ AA จากพ่นแห้งที่ได้จะเพิ่มขึ้นอย่างมีนัยสำคัญเมื่อเติมไคโตซานในระบบของ SLN และ NLC ซึ่งจะส่งผลให้ระยะเวลาการปลดปล่อยกรดเอเซียติกได้ดีกว่าที่ไม่ใส่ไคโตซาน เมื่อเปรียบเทียบกับกระจ่ายตัวในน้ำของอนุภาคนาโนลิปิด พ่นแห้งของ AASLN และ AANLC แสดงการเพิ่มความคงตัวระหว่างการเก็บรักษา จากการศึกษาร่างด้านไฟฟ้าผ่านผิวเซลล์ (TEER) และการศึกษากว้างจูลทัศน์ชนิด confocal พบว่าการเติมไคโตซานในการพ่นแห้ง AASLN และ AANLC แล้วกระจายตัวอีกครั้ง สามารถเปิด tight junction เพื่อเพิ่มการขนส่งยาเป็น 4.9 เท่า และ 4.23 เท่า ตามลำดับเมื่อเปรียบเทียบกับสารละลายกรดเอเซียติกเพียงอย่างเดียว ผ่านทาง Caco-2 cells ด้วยกระบวนการระหว่างเซลล์ การแพร่ของพ่นแห้งอนุภาคนาโน AASLN และ AANLC เมื่อกระจายตัวในน้ำอีกครั้ง ผ่าน Caco-2 cells จะเป็น 2.1 และ 1.6 เท่าตามลำดับของการกระจายในน้ำก่อนการพ่นแห้ง การศึกษา TEER และ confocal microscopy ใน bEnd3 cells พบว่า สารละลายในชั้นพื้นผิวหลังจากการซึมผ่าน Caco-2 cells ของสูตรพ่นแห้งอนุภาคนาโนที่มีการเติมไคโตซาน (cAASLN และ cAANLC) จะซึมผ่านเซลล์ด้วยกระบวนการเข้าภายในเซลล์ การศึกษานี้แสดงให้เห็นว่าอนุภาคพ่นแห้งของอนุภาคนาโนไขมันแข็ง และตัวพาลีปิดที่มีโครงสร้างนาโน ที่มีไคโตซานเป็นสารพื้นฐานสามารถใช้ด้วยการรับประทานเพื่อนำส่งเข้าสู่สมอง

ภาควิชา วิทยาการเกษตรกรรมและเกษตรอุตสาหกรรมสมัยใหม่นิเทศ
 สาขาวิชา เทคโนโลยีเกษตรกรรม
 ปีการศึกษา 2558
 ลายมือชื่อ อ.ที่ปรึกษาหลัก
 ลายมือชื่อ อ.ที่ปรึกษาร่วม

ACKNOWLEDGEMENTS

The present dissertation would not been accomplished without her adviser, Professor Garnpimol C Ritthidej, who not only originated this work, but also provided guidance, intensive suggestions and discussions, constructive criticisms, encouragement and opportunity to research in her research group. She also would like to extend her appreciation to her co-advisor, Associate Professor Vimolmas Lipipun (Department of Biochemistry and Microbiology, Faculty of Pharmaceutical Sciences, Chulalongkorn University) for her valuable advice and discussions during culturing caco-2 cells and bEnd3 cells.

She is deeply indebted to National Research University (NRU) Project of CHE and the Ratchadaphiseksomphot Endowment Fund (Project code HR1166I) and the Center of Innovative Nanotechnology, IIAC, Chulalongkorn University Centenary Academic Development Project for fully support this research. She is grateful for collaboration scholarship from Directorate General of Higher Education, Ministry of Education, Republic of Indonesia, University Islam of Indonesia, and Pharmaceutical Technology (International) Program. In addition, she acknowledges ASEAN scholarship, Chulalongkorn University for supporting her study for last one year.

She would like to express her deep gratitude to Associate Professor Parkpoom Tenganmuay, Ph.D as chairman of committee, Assistant Professor Nontima Vardhanabhuti, Ph.D, Assistant Professor Walaisiri Muangsiri, Ph.D as examiner and Professor Narong Sarisuta, Ph.D as external examiner for their valuable criticisms and suggestions to this research. She also would like to knowledge all board members and lecturers in Pharmaceutical Technology (International) Program who not only taught her but also provided recommendations and valuable discussions during study in this Program.

Deep gratitude is expressed to Buchi Thailand Ltd. and staffs for allowing her to use their B90 Nano Spray Dryer and providing guidance during research. She also would like to thank to Center of Nano Imaging, Mahidol University and their staffs who help during her research on using Confocal Laser Microscopy Study. She also wishes to thank the staffs in STREC (Science and Technological Research Equipment Centre), for SEM analysis, FTIR analysis, and WXRd analysis. In addition, she thanks to Petroleum and Petrochemical Collage and their staffs who help on TEM analysis.

Special thanks to all staffs in Pharmaceutics and Industrial Pharmacy Laboratory Department for their hospitality and helps during her stud and research in Faculty of Pharmaceutical Sciences, Chulalongkorn University.

She wishes to thank to all Ajarn Garnpimol's group members and also friends in Pharmaceutical Technology (International) Program for their friendship, helps and all good memorable moments.

Finally, she would like to dedicate all the best things in this dissertation to her country and family for their love, encouragement and continuously inspiration.

CONTENTS

	Page
THAI ABSTRACT	iv
ENGLISH ABSTRACT.....	v
ACKNOWLEDGEMENTS.....	vi
CONTENTS.....	vii
LIST OF ABBREVIATIONS.....	xiii
LIST OF FIGURES	xvii
LIST OF TABLES.....	1
CHAPTER I.....	1
INTRODUCTION	1
CHAPTER II.....	7
LITERATURE REVIEW	7
1. Blood Brain Barrier (BBB)	7
2. Human Colon Carcinoma Cell Line (Caco-2) Cells as Model for Intestinal Epithelial.....	11
3. Alzheimer’s Disease.....	13
4. Parkinson’s Disease.....	14
5. Bromocriptine.....	17
6. Asiatic Acid.....	21
7. Solid Lipid Nanoparticles.....	22
8. Nanostructure Lipid Carrier (NLC).....	24
9. Chitosan.....	25
10. Spray Drying	27
11. Response Surface Methodology and Central Composite Design.....	31
CHAPTER III	35
MATERIALS AND METHODS	35
1. Materials.....	35
1.1 Chemicals	35
1.2 Cell culture	36

	Page
1.3 Equipments	37
2. Methods	38
2.1 Preparation and Characterizations of Lipid Nanoparticles	38
2.1.1 Preparation of BMSLN	38
2.1.2 Particle size and zeta potential measurement.....	39
2.2 Preparation of Spray Dried SLN Chitosan-based.....	39
2.2.1 Preparation of SLN chitosan-based containing BM.....	39
2.2.2 Experimental design.....	40
2.3 Spray Dried Powder Characterization	45
2.3.1 % product yield.	45
2.3.2 Moisture content.....	45
2.3.3 Size and zeta potential measurement of spray dried powder redispersion BMSLN chitosan-based (RSPcBMSLN).	45
2.3.4 Particle size measurement	46
2.3.5 Particles flowability determination	46
2.3.6 TEM analysis	47
2.3.7 SEM analysis.....	47
2.4 Development of Spray Dried Powder of BMNLC Chitosan- based (SPcBMNLC)	47
2.4.1 Preparation of BMNLC.....	47
2.4.2 Spray drying of BMNLC chitosan-based (cBMNLC) ...	48
2.5 Chemical Characterization of BMSLN, BMNLC, Spray Dried Powder of BMSLN Chitosan-based (SPcBMSLN) and Spray Dried Powder of BMNLC Chitosan-based (SPcBMNLC).....	48
2.5.1 HPLC procedure.....	48
2.5.2 Drug Entrapment Efficiency (DEE).....	49
2.5.3 Drug retention (DR)	50

	Page	
2.6	Development and Comparison of Spray Drying BMSLN/BMNLC and Nanospray Drying BMSLN/BMNLC Chitosan-based.....	50
2.6.2	Wide angle X- ray diffraction analysis	52
2.7	Development and Comparison of Spray Dried Powder of AASLN/AANLC Chitosan-based	52
2.7.1	Preparation of AALN/NLC.....	52
2.7.2	Spray drying of AASLN/AANLC chitosan-based.....	53
2.7.4	HPLC procedure.....	55
2.7.5	Drug Entrapment Efficiency (DEE).....	55
2.7.6	Drug Retention (DR).....	56
2.7.7	<i>In vitro</i> release profile	56
2.7.8	Stability studies	57
2.8	<i>In vitro</i> Absorption Studies of Redispersed Spray Dried Powder of AASLN and AANLC Chitosan-based (RSPcAASLN and RSPcAANLC) on Caco-2 cells.....	58
2.8.1	Cell culture	58
2.8.2	Confocal laser scanning microscopy (CLSM)	59
2.8.3	Assessment of cell viability	59
2.8.4	Transport assay.....	60
2.8.5	Transepithelial electrical resistance (TEER) measurement	62
2.8.6	Nanoaggregate size and zeta potential measurement of cAASLN/cAANLC redispersion (RSPcAASLN/RPScAANLC) before and after passing Caco-2 cells.....	63
2.9	<i>In vitro</i> Absorption of cAASLN and cAANLC Redispersion (RSPcAASLN and RSPcAANLC) on bEnd3 Cells Cocultured with CTX-TNA2.....	63
2.9.1	Cell culture	64
2.9.2	Coculture of bEnd3 cells with CTX TNA2 cells	64

	Page
2.9.3 Confocal Laser Scanning Microscopy (CLSM).....	66
2.9.4 Cell viability.....	66
2.9.5 Permeability and uptake studies.....	67
CHAPTER IV	68
RESULTS AND DISCUSSIONS.....	68
1. BMSLN, Chitosan and Non-Chitosan-based	68
2. Experimental Design	70
2.1 Validation of Model Equations.....	79
2.2 Selection of Optimum Formulation	83
3. Effects of Inlet Temperature, Pump Rate and Feed Concentration on Responses	86
3.1 Effects on % Product Yield	86
3.2 Effects on Moisture Content.....	88
3.3 Effect on Nanoaggregate Size	89
4. Characterization of Spray Dried Powder of cBMSLN and cBMNLC.....	92
4.1 Physical Characterizations.....	92
4.1.1 Size, moisture and product yield characterizations.....	92
4.1.2 SEM analysis.....	98
4.1.3 TEM analysis	102
4.2 Chemical Properties Characterization	103
4.2.1 BM assay method.....	103
4.2.2 Drug Entrapment Efficiency (DEE).....	106
4.2.3 Drug retention	106
6. Development and Comparison of Spray Drying and Nanospray Drying BMSLN and BMNLC Chitosan-based	108
6.1 Characterization and Comparison of Spray Drying and Nanospray Drying of BMSLN and BMNLC Chitosan-based....	108
6.1.1 Size, zeta potential and polydispersity characterization	108
6.1.2 SEM characterization.....	110

	Page
6.1.3	TEM characterization..... 115
6.1.4	FTIR characterization..... 117
6.1.5	WXR D characterization..... 118
7.	Development and Comparison of Spray Dried Nanoaggregates Containing Asiatic Acid SLN and NLC Chitosan-based..... 120
7.1	Size, Zeta Potential and Yield Characterization..... 122
7.2	SEM Characterization..... 128
7.3	TEM Characterization 129
7.4	FTIR Characterization 130
7.5	DSC Characterization 132
7.6	WXR D Characterization..... 135
7.7	Chemical Properties Characterization 138
7.7.1	AA assay 138
7.7.2	Drug entrapment efficiency..... 143
7.7.3	Drug retention 144
7.7.4	<i>In vitro</i> release study profile 145
7.8	Stability Study 149
7.8.1	Chemical stability of drug content 149
7.8.2	Chemical stability of entrapped drug 152
7.8.3	Stability size and polydispersity index..... 154
7.9	Permeability Study of Redispersed Spray Dried Powder of AASLN and AANLC Chitosan-based on Caco-2 Cells..... 156
7.9.1	Confocal Laser Scanning Microscopy (CLSM) study . 156
7.9.2	Toxicity Study on Caco-2 cells 160
7.9.3	Permeability on Caco-2 cells 162
7.9.4	Uptake study on Caco-2 cells..... 167
7.9.5	TEER study on Caco-2 cells 169
7.9.6	Size and zeta potential behavior in permeability study on Caco-2 cells..... 171

	Page
7.10 Permeability Study on bEnd3 Cells Cocultured with CTX-TNA2 Cells.....	174
7.10.1 Confocal Laser Scanning Microscopy (CLSM) study .	174
7.10.2 Toxicity study on bEnd3 cells cocultured with CTX-TNA2	178
7.10.3 Permeability study on bEnd3 cells cocultured with CTX-TNA2	180
7.10.4 Uptake study on bEnd3 cells cocultured with CTX-TNA2.....	183
7.10.5 TEER study on bEnd3 cells cocultured with CTX-TNA2.....	185
CHAPTER V	188
CONCLUSIONS	188
REFERENCES	190
APPENDIX A.....	208
APPENDIX B	212
APPENDIX C	215
APPENDIX D.....	218
APPENDIX E.....	222
APPENDIX F	231
APPENDIX G.....	239
APPENDIX H.....	242
APPENDIX I	265
APPENDIX J	291
APPENDIX K.....	303
VITA.....	307

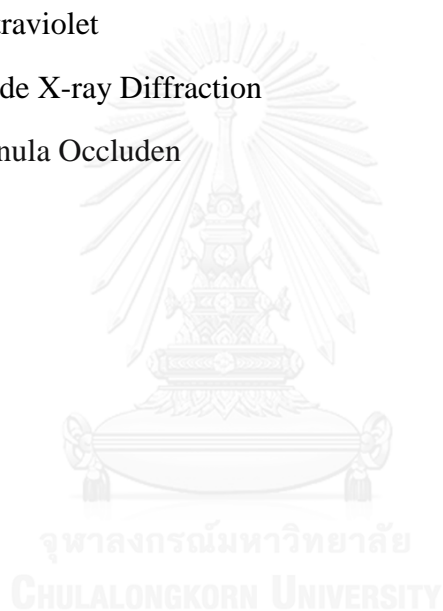
LIST OF ABBREVIATIONS

3D	: 3 Dimension
µg/mL	: microgram/mili Liter
AA	: Asiatic Acid
AANLC	: Asiatic acid nanostructures lipid carrier
AASLN	: Asiatic acid solid lipid nanoparticles
A-B	: Apical to Basolateral
AD	: Alzheimer's Disease
ANOVA	: Analysis of Variance
B-A	: Basolateral to Apical
BBB	: Blood Brain Barrier
BC	: Bromocriptine (2-bromo α -ergocriptine)
bEnd 3 cells	: Mouse Brain Endothelial Cells
BM	: Bromocriptine Mesylate
BMNLC	: Bromocriptine loaded Nanostructured Lipid Carrier
BMSLN	: Bromocriptine loaded Solid Lipid Nanoparticles
BMVECs	: Brain Microvascular Endothelial cells
Caco-2 cells	: Human Colon Carcinoma Cell Line
CCD	: Central Composite Design
CLSM	: Confocal Laser Scanning Microscope
CNS	: Central Nervous System
CYP3A4	: Cytochrome P450 3A4
DA	: Dopamine
DEE	: Drug Entrapment Efficiency
DHA	: Docosahexaenoic acid
DMEM	: Dulbecco's modified Eagle medium

EDTA	: Ethylenediaminetetraacetic acid
FBS	: Fetal Bovine Serum
FTIR	: Fourier
GIT	: Gastrointestinal
GRAS	: Generally Regarded As Safe
HPLC	: High Performance Liquid Chromathography
IgG	: Immunoglobulin
kDa	: kilo Dalton
kHz	: kilo Hertz
L/min	: Liter/minute
L-DOPA	: Levo-dihydroxyphenylalanine (DOPA)
L-MDR1	: L-Multi Drug Resistance 1
MDCK	: Madin-Darby canine kidney
MEE	: Microencapsulated Entrapment Efficiency
MESO	: Micoencapsulated Sunflower Oil
mL/h	: mili Liter/ hour
mM	: micro Molar
MPI	: Milk Protein Isolates
MTT	: 3-[4,5-dimethylthiazol-2-yl]-2,5-diphenyl-tetrazoliumbromide
MWCO	: Molecular Weight Cut-Off
NEAA	: Non essential amino acid
NFT	: Neuro Fibrillary Tangles
NLC	: Nanostructured Lipid Carrier
O/W	: Oil in Water
Papp	: Apparent permeability coefficient
PBS	: Phosphate-buffered saline
PD	: Parkinson's disease
P-gp	: P-glycoprotein

R6g	: Rhodamine 6G
RH	: Relative Humidity
RR	: Reverse Ratio
RSM	: Response Surface Methodology
RSPAANLC	: redispersed spray dried powder of Asiatic acid nanostructure lipid carrier
RSPAASLN	: redispersed spray dried powder of Asiatic acid solid lipid nanoparticles
RSPBMNLC	: redispersed spray dried powder of bromocriptine nanostructures lipid carrier
RSPBMSLN	: redispersed spray dried powder of bromocriptine solid lipid nanoparticles
RSPcAANLC	: redispersed spray dried powder of Asiatic acid nanostructure lipid carrier chitosan based
RSPcAASLN	: redispersed spray dried powder of Asiatic acid solid lipid nanoparticles chitosan based
RSPcBMNLC	: redispersed spray dried powder of bromocriptine nanostructures lipid carrier chitosan based
RSPcBMSLN	: redispersed spray dried powder of bromocriptine solid lipid nanoparticles chitosan based
SEM	: Scanning Electron Microscope
SLN	: Solid Lipid Nanoparticles
SO	: Sunflower Oil
SPAANLC	: spray dried powder of Asiatic acid nanostructure lipid carrier
SPAASLN	: spray dried powder of Asiatic acid solid lipid nanoparticles
Span 80	: Sorbitane monooleate
SPBMNLC	: spray dried powder of bromocriptine nanostructures lipid carrier
SPBMSLN	: spray dried powder of bromocriptine solid lipid nanoparticles
SPcAANLC	: spray dried powder of Asiatic acid nanostructure lipid carrier chitosan based
SPcAASLN	: spray dried powder of Asiatic acid solid lipid nanoparticles chitosan based

SPcBMNLC	: spray dried powder of bromocriptine nanostructures lipid carrier chitosan based
SPcBMSLN	: spray dried powder of bromocriptine solid lipid nanoparticles chitosan based
TEER	: Transendothelial electrical resistance
TEER	: Transepithelial electrical resistance
TEM	: Transmission Electromagnetic Microscope
TJ	: Tight Junctions
Tween 80	: Sorbitane polyoxyethylene monooleate
UV	: Ultraviolet
WXRD	: Wide X-ray Diffraction
ZO	: Zonula Occluden



LIST OF FIGURES

Figure 2.1	Illustration of blood brain barrier (modified from Benny and Pakneshan, 2009)	7
Figure 2.2	The illustration of the presences tight junctions and adherents junctions at BBB that causes limitation of paracellular penetration, and P-glycoprotein that effluxes the compound out from the brain and the presence of flattened end-feet astrocyte (Cardoso et al. 2010). ...	9
Figure 2.3	AD patient's brain (https://www.premedhq.com/alzheimers-disease) ...	13
Figure 2.4	The sites of neurodegeneration and neurochemical pathway in Parkinson' disease (modified from Lang and Lozano, 1998).....	16
Figure 2.5	Chemical structure of bromocriptine (Siegel et al. 1999).....	19
Figure 2.6	Chemical structure of Asiatic Acid (AA), molecular weight of 488.70 g/mol (Zhang et al. 2012).....	21
Figure 2.7	Chemical structure of chitosan (Agrawal et al. 2010)	26
Figure 2.8	Mini Buchi Spray Dryer B-290.....	29
Figure 2.9	Schematic of the Nanospray Dryer (Li et al. 2010)	31
Figure 2.10	Central composite design with k=3 (Montgomery, 2005).....	32
Figure 3.1	Schematic of dosing and sampling drug transport study (Wandel et al. 2002).	61
Figure 3.2	Coculturing of bEnd3 cells and CTX-TNA2 cells on different sides of the Transwell filter with 0.4µm diameter pores. The Transwell filters were coated with rat tail collagen type I (a). CTX-TNA2 cells were seeded onto the abluminal side of the inverted Transwell™ filter at a density of 5x10 ⁵ cells per filter, (b). allowed to adhere for 1.5 h, (c). filter was flipped back and the CTX-TNA2 were cultured for 3 days, (d). bEnd3 cells were seeded onto the luminal side of Transwell filter at a density of 5x10 ⁵ cells per filter and (e). cocultured with astrocytes (CTX-TNA2) for an additional 6 days.....	65
Figure 4.1	TEM characterization of a. SLN dispersion and b. SLN chitosan-based. Scale bars equal to 1.0µm.	69

Figure 4.2	Normal % probability plot of model equation for a) Yield of product, b) moisture content and c) redispersed nanoaggregate size of spray dried powder cBMSLN.....	80
Figure 4.3	Plots of predicted values versus studentized residual; a) yield, b) moisture content and c) redispersed nanoaggregate size of spray dried powder cBMSLN.....	81
Figure 4.4	Cook's distance plots of three models; a) yield, b) moisture content and c). redispersed nanoaggregates size of spray dried powder cBMSL.....	82
Figure 4.5	Response surface for 1. product yield of cBMSLN powder; a. effects of inlet temperature and feed concentration, b. effects of feed rate and inlet temperature, c. effects of inlet temperature and feed rate, 2. A. effect of feed concentration and feed rate on moisture content, 3. nanoaggregate size of RSPcBMSLN; a. effect of inlet temperature and feed concentration, b. effect of feed concentration and feed rate. ...	90
Figure 4.6	Normal size distributions by volume of BMSLN systems	96
Figure 4.7	Normal size distributions by volume of BMNLC systems.....	97
Figure 4.8	Log-normal size distribution by volume graph (a) and SEM characterization (b) of spray dried nanosystems of : 1) BMSLN, 2) cBMSLN, 3) BMNLC, 4) cBMNLC.	101
Figure 4.9	TEM characterization of 1.a, BMSLN dispersion 1.b redispersed spray dried of BMSLN (RSPBMSLN) 1.c redispersed spray dried of cBMSLN (RSPcBMSLN) and 2.a BMNLC dispersion, 2.b redispersed spray dried of BMNLC (RSPBMNLC) 2.c redispersed spray dried of cBMNLC. (RSPcBMNLC).....	103
Figure 4.10	Chromatogram of bromocriptine mesylate (HPLC condition of acetonitrile: 10 mM buffer ammonium = 70:30, v/v, flow rate 1.0 mL/min, detected 300nm).....	104
Figure 4.11	Standard Curve of BM (HPLC condition of acetonitrile: 10 mM buffer ammonium = 70:30, v/v, flow rate 1.0 mL/min, detected 300nm).	105
Figure 4.12	The calibration curve was shown the linearity of the method (HPLC condition of acetonitrile: 10 mM buffer ammonium = 70:30, v/v, flow rate 1.0 mL/min, detected 300nm).....	105
Figure 4.13	Significance difference of average nanoaggregate size of spray and nanospray dried powder. * = significant at $p < 0.05$	110

- Figure 4.14 SEM characterization: a. spray dried powder of SLN in chitosan – based, b. spray dried powder of NLC in chitosan –based, c. spray dried powder of SLN non chitosan-based, d. spray dried powder of NLC non chitosan-based, e. nanospray dried powder of SLN in chitosan based, f. nanospray dried powder of NLC in chitosan based, g. nanospray dried powder of SLN non-chitosan based and h. nanospray dried powder of NLC non-chitosan based..... 115
- Figure 4.15 TEM characterization of redispersed of dried powder containing lipid nanoparticles (BM-SLN/NLC): a. nanospray dried SLN in chitosan-based, b. nanospray dried NLC in chitosan-based, c. nanospray dried SLN non chitosan-based and d. nanospray dried NLC non chitosan-based. Bars scale equal to 1.0µm length. 117
- Figure 4.16 FTIR characterization of spray dried of SLN and NLC systems compared to bromocriptine (BM) a. nanospray dried BM-SLN chitosan-based, b. nanospray dried BM-NLC chitosan-based, c. spray dried BM-SLN chitosan-based and d. spray dried BM-NLC chitosan-based 118
- Figure 4.17 WXR D characterization of spray dried SLN systems; a. bromocriptine, mesylate, b. pluronic f127, c. tristearin, d. trimyristin, e. spray dried powder of BMSLN chitosan-based and f. nanospray dried powder of BMSLN chitosan-based 119
- Figure 4.18 WXR D characterization of spray dried NLC systems; a. bromocriptine, mesylate, b. pluronic f127, c. tristearin, d. trimyristin, e. spray dried powder of BMNLC chitosan-based and f. nanospray dried powder of BMNLC chitosan-based 120
- Figure 4.19 Log distribution size by volume of a. AASLN systems and b. AANLC systems 125
- Figure 4.20 Log-normal size distribution by volume graph of a. SPcAASLN and b. SPcAANLC..... 127
- Figure 4.21 SEM characterization: a. spray dried SLN loaded AA chitosan-based (SPcAASLN) and b. spray dried NLC loaded AA chitosan-based (SPcAANLC)..... 129
- Figure 4.22 TEM characterization: a. SLN loaded AA, b. Redispersed spray dried SLN chitosan-based loaded AA c. NLC loaded AA and d. Redispersed spray dried NLC chitosan-based loaded AA. Scale bars equal to 1.0µm. 130

- Figure 4.23 FTIR characterization of AASLN systems; a. Asiatic acid (AA), b. physical mixture of AASLN, c. spray dried powder of AASLN chitosan-based (SPcAASLN), d. physical mixture of AANLC and e. spray dried powder of AANLC chitosan-based (SPcAANLC). 131
- Figure 4.24 DSC characterization, (1) Heating (5°C/min) and cooling (1°C/min) of SLN; a. Bulk SLN lipid (tristearin:trimyrustin=7:3) after tempering, b. SLN Blank and c. AASLN, (2) Heating (5°C/min) and cooling (1°C/min) of NLC a. Bulk NLC lipid (tristearin:trimyrustin:castor oil=2:1:2) after tempering and c. AANLC, (3) Heating (5°C/min) of a. BM, b. tristearin, c. trimyrustin, d. pluronic F127, e. Maltodextrin, f. Physical mixture of AASLN (PMAASLN), g. spray dried powder of cAASLN (SPcAASLN), h. physical mixture powder BMNLC (PMAANLC) and i. spray dried powder of cAANLC (SPcAANLC). 135
- Figure 4.25 WXR D characterization of spray dried AASLN and AANLC chitosan-based; a. AA, b. tristearin, c. trimyrustin, d. pluronic F127, e maltodextrin, f. physical mixture AASLN chitosan-based, g. spray dried powder of AASLN chitosan-based (SPcAASLN), h. physical mixture AANLC chitosan-based and i. spray dried powder of AANLC chitosan-based (SPcAANLC) 138
- Figure 4.26 Chromatogram of Asiatic acid (AA) (HPLC condition of acetonitrile: 10 mM buffer phosphate = 28:72, v/v, pH 7.7, flow rate 1.0 mL/min, detected 210nm). 139
- Figure 4.27 The calibration curve was shown the linearity of systems on the range of concentration 0. 4-8 µg/mL of AA (HPLC condition of acetonitrile: 10 mM buffer phosphate = 28:72, v/v, pH 7.7, flow rate 1.0 mL/min, detected 210nm). 140
- Figure 4.28 Calibration curve was shown the linearity of the method (HPLC condition consisting of acetonitrile: 10 mM buffer phosphate = 28:72 v/v, pH 7.7, flow rate 1.0 mL/min, detected at 210nm). 141
- Figure 4.29 *In vitro* release of AA of SLN and NLC in situ pH change. AA were released from AASLN and AANLC at pH 1.2 for 2 h then replaced to medium to pH 6.8 for 6 h. Error bars represent standard deviations of the mean based on three replicates. 146
- Figure 4.30 *In vitro* released of Asiatic acid of SPAASLN and SPAANLC in situ pH change. AA from SPAASLN and SPAANLC were released at pH

- 1.2 for 2 h then replaced to medium to pH 6.8 for 6 h. Error bars represent standard deviations of the mean based on three replicates.... 148
- Figure 4.31 *In vitro* released of AA of SPAASLN and SPcAANLC in situ pH change. AA from SPcAASLN and SPcAANLC were released at pH 1.2 for 2 h then replaced to medium to pH 6.8 for 6 h. Error bars represent standard deviations of the mean based on three replicates.... 149
- Figure 4.32 Comparison of stability of drug content (AA) in nanoparticles dispersion and in their dry powder; a). Content of AA in AASLN and spray dried powder of SLN (SPcAASLN) and b). Content AA in AANLC and spray dried powder of NLC (SPcAALNC). Error bars represent standard deviations of the mean based on three replicates.... 151
- Figure 4.33 Drug entrapment efficiency stability; a. SLN and spray dried powder of SLN chitosan-based and b. NLC and spray dried powder of NLC chitosan-based. Error bars represent standard deviations of the mean based on three replicates. 153
- Figure 4.34 Comparison of size stability (average size and polydispersity index (PdI) value); a. AASLN system with their RSPcAASLN and b. AANLC system with their RSPc AANLC..... 155
- Figure 4.35 Confocal Laser Scanning Microscopy (CLSM) study of R6gSLN, RSPR6gSLN, RSPcR6gSLN, R6gNLC, RSPR6gNLC and RSPcR6gNLC on Caco-2 cells for 2 h incubation. Paracellular localization of R6g fluorescence was noted (arrow)..... 159
- Figure 4.36 Toxicity study on Caco-2 cells between different treatment groups; AA free, SLN blank, RSPSLN Blank, RSPcSLN Blank, AASLN, RSPAASLN and RSPcAASLN. Toxicity study were conducted in equal concentration of AA concentration at 100 μ M, 50 μ M, 25 μ M and 12.5 μ M. Error bars represent standard deviations of the mean based on three replicates.* represents significant different to 80% cell liability. 161
- Figure 4.37 Toxicity study on Caco-2 cells between different treatment groups; AA free, NLC blank, RSPNLC Blank, RSPcNLC Blank, AANLC RSPAANLC and RSPcAANLC. Toxicity study were conducted in equal of AA concentration at 100 μ M, 50 μ M, 25 μ M and 12.5 μ M. Error bars represent standard deviations of the mean based on three replicates. 162
- Figure 4.38 Cumulative drug transport of AA through Caco-2 cells between treatment groups of AA Free, AASLN, RSPAASLN, RSPcAANLC,

- AANLC RSPAANLC and RSPcAANLC. Error bars represent standard deviations of the mean based on three independent experiments were omitted to obtained clear image..... 164
- Figure 4.39 Permeability study on Caco-2 cells between different treatment groups: AA free, AASLN, AANLC, RSPAASLN, RSPcAASLN, RSPAANLC and RSPcAANLC. Error bars represent standard deviations of the mean based on three independent experiments.* represents significantly different ($p < 0.05$) to AA free group. ** represents significantly different to original lipid nanoparticles (AASLN and AANLC)..... 166
- Figure 4.40 Reverse ratio of AA free, AASLN, AANLC, RSPAASLN, RSPcAASLN, RSPAANLC and RSPcAANLC on Caco-2 cells. Error bars represent standard deviations of the mean based on three independent experiments. 167
- Figure 4.41 Uptake study on Caco-2 cells between different treatment groups; AA Free, AASLN, AANLC, RSPAASLN, RSPcAASLN, RSPAANLC and RSPcAANLC. Error bars represent standard deviations of the mean based on three independent experiments. 169
- Figure 4.42 Percentage of TEER change value on Caco-2 cell between different treatment groups. Error bars represent standard deviations of the mean based on three independent experiments..... 171
- Figure 4.43 Nanoaggregates size of redispersed spray dried powder of AASLN chitosan-based and spray dried powder of AANLC chitosan-based, before and after permeability study. Error bars represent standard deviations of the mean based on three replicates..... 172
- Figure 4.44 Zeta potential of redispersed spray dried powder of AASLN and AANLC chitosan-based, before and after permeability study. Error bars represent standard deviations of the mean based on three replicates. 174
- Figure 4.45 Confocal Laser Scanning Microscopy (CLSM) study of R6gSLN, RSPR6gSLN, RSPcR6gSLN, R6gNLC, RSPR6gNLC and RSPcR6gNLC on bEnd3 cells. Intracellular localization of R6g fluorescence was noted (arrow). 177
- Figure 4.46 Toxicity study on bEnd3 between different treatment groups; AA free, SLN, RSPSLN Blank, RSPcSLN Blank, AASLN, RSPAASLN and RSPcAASLN. Error bars represent standard deviations of the mean based on three replicates. 179

- Figure 4.47 Toxicity study on bEnd3 between different treatment groups; AA free, NLC blank, RSPNLC Blank, RSPcNLC Blank, AANLC RSPAANLC and RSPcAANLC. Error bars represent standard deviations of the mean based on three replicates..... 179
- Figure 4.48 Percentage transport of AA through bEnd3 cells cocultured with CTX-TNA2 between treatment groups of AA Free, AASLN, RSPAASLN, RSPcAANLC, AANLC, RSPAANLC and RSPcAANLC. Error bars represent standard deviations of the mean based on three independent experiments were omitted to obtained clear graph image. 181
- Figure 4.49 Permeability study of AA on bEnd3 cells cocultured with CTX-TNA2 between different treatment groups; AA Free, AASLN, RSP-AASLN chitosan-based, AANLC and RSP-AANLC chitosan-based. Error bars represent standard deviations of the mean based on three independent experiments.* represents significant different ($p < 0.05$) to AA Free group.** represents significant different to their original nanoparticles of AASLN and AANLC group..... 182
- Figure 4.50 Reverse ratio of between different treatment groups, AA free, AASLN, AANLC, RSPAASLN, RSPcAASLN, RSPAANLC and RSPcAANLC) on bEnd3 cells. Error bars represent standard deviations of the mean based on three independent experiments. 183
- Figure 4.51 Uptake AA after 6 h incubation between different treatment groups; AA free, AASLN, redispersed spray dried powder of AASLN chitosan-based (RSP-AASLN), AANLC and redispersed spray dried powder of AANLC chitosan-based (RSP-AANLC) by bEnd3 cells cocultured with CTX-TNA2. Error bars represent standard deviations of the mean based on three independent experiments. 184
- Figure 4.52 Percentage of TEER change value on bEnd3 cell between different treatment groups; AA free, AASLN, RSP-AASLN chitosan-based, AANLC and RSP-AANLC chitosan-based. Error bars represent standard deviations of the mean based on three independent experiments. 187

LIST OF TABLES

Table 3.1	Formulation composition of BMSLN and BMNLC	38
Table 3.2	Processing parameter and coded level of variables for experimental design.....	42
Table 3.3	Generated experimental design and responses of the design	44
Table 3.4	Formulation of AA loaded SLN/NLC.....	52
Table 3.5	Optimization of feed concentration of spray drying AASLN chitosan based.....	54
Table 4.1	Properties of SLN with low molecular weight chitosan, zeta potential and polydispersity (mean (n=5) \pm SD).....	70
Table 4.2	A rotatable central composite experimental design and responses; yield, nanoaggregatesize and moisture content of spray dried SLN in chitosan-based	72
Table 4.3	Statistical analysis of experimental design.....	75
Table 4.4	Analysis of variance (ANOVA) of linear model of product yield response	76
Table 4.5	Analysis of variance (ANOVA) of moisture content response	77
Table 4.6	Analysis of variance (ANOVA) of redispersed nanoaggregate size response	78
Table 4.7	Comparison of the observed and the predicted values	83
Table 4.8	Solution of optimum condition of spray drying	84
Table 4.9	Comparison of parameter of SLN and NLC system and their redispersed spray dried powder (mean (n=5) \pm SD)	94
Table 4.10	Spray dried BMSLN and BMNLC (mean (n=5)+SD).....	98
Table 4.11	Regression parameters of the linearity of system.....	104
Table 4.12	The size of SLN and NLC dispersion (mean \pm SD).....	109
Table 4.13	Nanoaggregate size of redispersed nanoggregates of SLN and NLC after spray drying, % yield and moisture content.....	112
Table 4.14	Product yield of obtained cAASLN powder by varying AASLN dispersion and amount of maltodextrin	121

Table 4.15	The size of AASLN and AANLC dispersion, and redispersed nanoaggregates AASLN and AANLC (mean (n=5)±SD).....	124
Table 4.16	Spray dried powder of AASLN (SPcAASLN) and SPcAANLC characterization (mean (n=5)±SD).....	127
Table 4.17	Regression parameters of the linearity of system.....	140
Table 4.18	The robustness test results of the method by varying pH.....	142
Table 4.19	The robustness test results of the method by varied the acetonitrile proportions in the mobile phase	143
Table 4.20	Drug entrapment efficiency (DEE) and drug retention (DR) (mean (n=5)±SD)	145



CHAPTER I

INTRODUCTION

Delivery drug to the brain is constrained by the strictest barrier of blood brain barrier (BBB). The BBB is a continuous endothelial monolayer cell associated with pericytes and astrocytes. The most physical barrier is due to the tighter junctions (zonulae occludens) surrounding the cell margin of the brain capillaries than other junction of other capillary endothelium (Butt et al. 1990). Furthermore, some drug efflux transporters, specifically the multidrug resistance transporter, p-glycoprotein, and various organic anion transporters, are present in this barrier in order to protect the brain from circulating toxins, xenobiotics and endogenous molecules (Sun et al. 2003; Smith and Gumbleton 2006).

Based on the circumstance in the BBB, only the tiny entities (<5000 Da), lipid-soluble substances, neutral molecules and weak bases are able to diffuse passively across to the BBB (Abraham et al. 1994). And oppositely the hydrophilic compounds, small proteins and charged molecules demonstrate limited permeation (Smith et al. 2004; Béduneau et al. 2007). Therefore, the lipophilic surface-drug and prodrugs were thus developed (Sinkula and Yalkowsky 1975) to across the BBB. On the other hand, active brain targeting strategies have been employed to macromolecules to outwit the BBB by endocytosis mechanism as an employable pathway similar to the brain gaining nutrient than other pathways (Smith and Gumbleton 2006).

Incorporating drug into lipid nanoparticles has emerged possibilities to interact with and pass BBB (Barbu et al. 2009).

However, hydrophobic surface properties of lipid nanoparticles, are proficiently coated by opsonins (plasma components), such as immunoglobulins (IgG), albumin, fibronectin, and then rapidly cleared from the blood stream by the phagocytic cells (Moghimi et al. 2001; Furumoto et al. 2004). In order to decrease the adsorption by opsonins in plasma and also for brain specific targeting, surface modification using several hydrophilic properties, such as Pluronic F68 or Poloxamer 188 (Borchard et al. 1994; Yang et al. 1999), poly-ethylene glycol (Brigger et al. 2002; Mistry et al. 2009) and polysorbate 80, have been employed in nanoparticles (Schröder and Sabel 1996; Kreuter et al. 1997; Alyautdin et al. 1998; Gulyaev et al. 1999; Olivier et al. 1999; Kreuter 2004; Sun et al. 2004; Sant et al. 2008; Wilson et al. 2008a, 2008b; Gelperina et al. 2010).

One of nanoparticles lipid based formulation is solid lipid nanoparticles (SLN) and the second generation of lipid nanoparticles is nanostructured lipid carrier (NLC). SLN has potentially advantages ie., widely application spectrum (dermal, oral, intravenous), lower toxicity, higher loading drug capacity, sterilization ability and best production scalability (Dingler and Gohla 2002; Blasi et al. 2007). NLC consists of solid lipid substances with liquid lipids resulting in a structure with more imperfections in crystal to facilitate the drug solubilization (Souto and Müller 2006). Lipid and surfactant were used in SLN or NLC to inhibit P-glycoprotein mediated efflux of drugs (Wong et al. 2006) and to enlarge drug

transport via intestinal lymphatic systems (Müller et al. 1997; Bargoni et al. 1998). According to these benefits, it is a big challenge to formulate SLN/NLC into oral formulation which not only can avoid first-pass metabolism thereby enhances bioavailability with longer-acting circulation in blood, but also has a specific target tissue.

Recently, using biopolymer of chitosan to modify nanoparticles surface has improved long-circulating and specific brain targeting of nanoparticles (Aktaş et al. 2005; Tosi et al. 2008; Sheng et al. 2009; Kong et al. 2010). Furthermore, chitosan, generally regarded as safe (GRAS) biodegradable polymer, has found its application in many areas of drug delivery (Kean and Thanou 2010). In addition, the positive charge of soluble chitosan allows its electrostatic interaction with negative charge of membrane intestinal cell or mucus and increases paracellular permeability via tight junction opening (Artursson et al. 1994; Illum et al. 1994; Schipper et al. 1997; Ranaldi et al. 2002). Considering the advantages of SLN/NLC and the tremendously promising of chitosan, formulating chitosan-based SLN systems might be approached to enhance the targeting drug to the brain in the application of oral administration.

Nevertheless, as an aqueous dispersion, SLN and also the second generation of lipid nanoparticles, NLC, exhibits long-term stability at 3 years only (Freitas et al. 1994) and over 3 years by optimizing condition storage (Freitas and Müller 1998; Freitas 1999). Transforming SLN or dispersion into dry product allows to prolong long-term stability (Freitas and Müller, 1998b). Moreover, SLN or NLC granulates or powders can be filled into

capsules, compressed into tablets or incorporated into pellets then applied through oral administration thereby increase patient's compliance and convenience (Pinto and Müller 1999).

The spray dry technique has been an important and widely applied technique in the pharmaceutical and biochemical fields to transform liquid dosage form into dry product (Freitas and Müller 1998; Mu and Feng 2001). The polymeric microsphere drug delivery systems produced by this technology have a potential to provide various types of administered routes, targeting systems and long acting parenteral systems (He et al. 1999). Recently, a new spray dryer that can produce lower particles size of resulting powder reaching submicron size has been developed (Li et al. 2010). Thus, developing spray dried SLN/NLC chitosan-based is highly expected to form microsphere particles which have easier powder handling and longer storage period.

Bromocriptine mesylate (BM) and Asiatic acid (AA) are two of water insoluble drugs which have neuroprotective effects to the brain. The activity of BM as anti Parkinson's disease (PD) due to its dopamine (DA) D2 agonist receptor which directly stimulates the dopamine receptors in the corpus striatum (Rascol et al. 1979; Rascol et al. 2002). And the triterpenoid-derivative compound of AA also has been shown neuroprotective properties both *in vitro* (cultured cells) and *in vivo* (Mook-Jung et al. 1999; Krishnamurthy et al. 2009; Xiong et al. 2009). According to their physical properties, these two drug models probably can pass BBB easily. However, in oral administration case, these drug models still have limitations on

delivery systems. So, incorporating both BM and AA can be used as model drugs to formulate dry powder of SLN/NLC chitosan-based formulations.

In this study, spray dried powder of SLN/NLC was developed as novel strategy to improve intestinal penetration, improve BBB crossing higher brain level and increase drug half-life. In order to evince this hypothesis, first, factors influencing spray dried powder of SLN/NLC chitosan-based are optimized using response surface methodology. Then, the nanoparticle morphology and other physicochemical properties were characterized. In vitro release and stability of BM or AA from SLN/NLC chitosan-based were also evaluated. Penetration and toxicity of BM or AA loaded SLN/NLC chitosan-based to intestinal cells model and to brain endothelial cell model were finally studied. The purposes of this study were:

1. To optimize the development of spray dried powder of lipid nanoparticles (SLN and NLC) chitosan-based using bromocriptine (BM) and asiatic acid (AA) as model drugs.
2. To characterize the physicochemical properties of lipid nanoparticles (SLN and NLC) chitosan-based containing bromocriptine (BM) and asiatic acid (AA) as model drugs.
3. To study the cytotoxicity and absorption of lipid nanoparticles (SLN and NLC) chitosan-based containing asiatic acid (AA) as model drugs on Caco-2 cells.

4. To study the cytotoxicity and absorption of lipid nanoparticles (SLN and NLC) containing asiatic acid as model drugs on mouse brain endothelial cells (bEnd3).



CHAPTER II

LITERATURE REVIEW

1. Blood Brain Barrier (BBB)

Blood Brain Barrier (BBB) was early discovered by Paul Ehrlich in 1885 and later confirmed by Edwin Goldmann in 1913 (Moody 2006). The BBB is a barrier situated along the blood capillaries in the cerebral cortex (Reese and Karnovsky 1967). The appearance of BBB in the brain becomes one of defensive mechanisms to protect the brain from substances which are neurotoxic in physiological concentrations (Ueno 2007). The components composing the BBB are brain microvascular endothelial cells, end feet astrocytes, basement membrane, pericytes and neurons that are physically similar to the endothelium (Persidsky et al. 2006) (Figure 2.1).

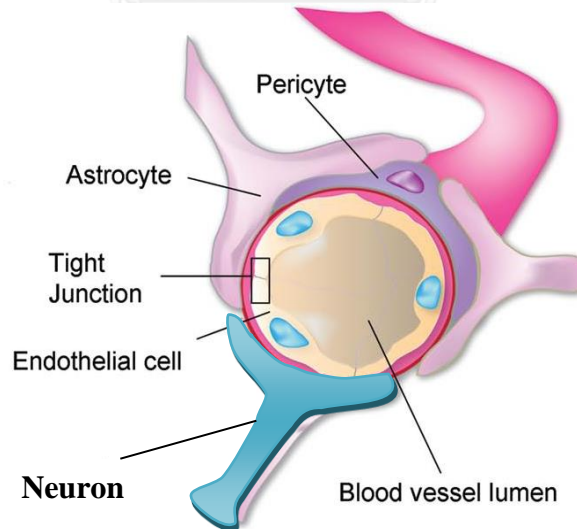


Figure 2.1 Illustration of blood brain barrier (modified from Benny and Pakneshan, 2009)

The permeability of BBB is controlled by biochemical properties of brain microvascular endothelial cells (BMVECs) (Pardridge 1999). The presence of BMVECs at the interface between blood and the brain consequently perform other biological functions, including regulate selective matrices from blood to brain and vice versa from the parenchyma back to the systemic circulation, transport of micronutrients and macronutrients, receptor-mediated signaling, leukocyte trafficking, and osmoregulation (Persidsky et al. 2006; Zheng et al. 2003).

The BMVECs differ from the most peripheral endothelial cells. The differences are shown first, the very tight junctions between endothelial cells which is 50-100 times tighter than other peripheral microvessels (Butt et al. 1990), second, uniform thickness of cytoplasm with lack fenestrations, low pinocytosis activity and continuous membrane-based (de Boer and Gaillard 2006; Goldstein 1988) and third, the huge number and volume of mitochondria (Persidsky et al. 2006) (Figure 2.2). Those differences cause impediment of the diffusion via paracellular pathway for hydrophilic solutes, transcellular pathway for hydrophobic solutes and provides more energy for enzymes to breakdown compound allowing active and selective transport nutrient and other compounds into and out of the brain, respectively (Abbott et al. 2006; de Boer and Gaillard 2006; Rubin and Staddon 1999). Therefore, Pardridge, *et al.*, (2003) suggested the small-molecule compound crossing the BBB should have the two molecular characteristics of: 1) molecular mass under a 400 to 500Da and 2) high lipid solubility. However, as similar as other membrane cells, the BMVECs have a negative surface charge that

repulse negatively charged compounds and attract positive charged compounds (de Boer and Gaillard 2006; Rojanasakul et al. 1992). This phenomena can be employed to modify the surface substance to enhance drug interaction.

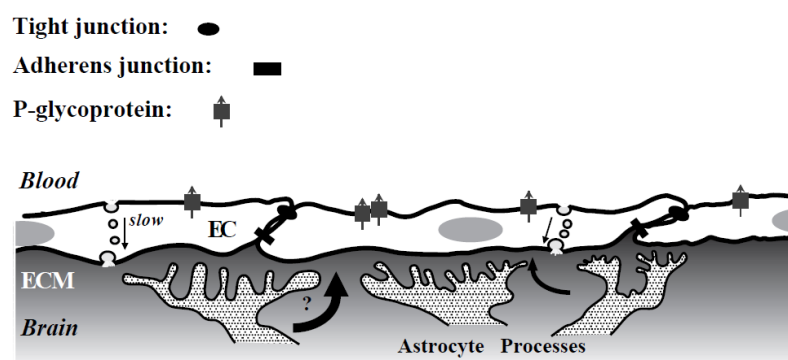


Figure 2.2 The illustration of the presences tight junctions and adherents junctions at BBB that causes limitation of paracellular penetration, and P-glycoprotein that effluxes the compound out from the brain and the presence of flattened end-feet astrocyte (Cardoso et al. 2010).

The tighter junctions of BMVECs are composed by tight junctions (TJ) and adherent junction (AD) (Persidsky et al. 2006) (Figure 2.2). The other unique properties of BBB that inhibit penetrating compound across the BBB are the presence of astrocytes (Figure 2.1 and Figure 2.2). Astrocytes are one type of glial cells that cover >99% of the BBB endothelium (Hawkins and Davis 2005). Interaction of astrocytes with BMVECs hugely enhanced endothelial cell TJ and reduced gap junctional area (Holash et al. 1993). In other words, astrocytes modulate the BBB phenotype involved in the physical BBB properties indirectly (Holash et al. 1993; Persidsky et al. 2006). Recently, the close relation of neuronal cell bodies to brain capillaries suggests that astrocyte–BMVEC interactions are essential to functionalize

neurovascular unit which their mutual induction helps to establish the differentiated phenotype of both the cells involved in the association, upregulating barrier properties in the endothelium, and specific features of the end feet astrocytes, including involved in ionic and water regulation (Abbott et al. 2006).

One of the BBB models are a cancer (cells-line) of mouse brain endothelial cells (bEnd3 cells). Except can internalize the acetylated low-density lipoprotein, bEnd3 cells also can maintain BBB characteristics after repeated passages, barrier functions and flexibility to numerous molecular interventions as well as low their cost effectiveness (Brown et al. 2007). Those advantages make bEnd3 cells become popular as a BBB model. Hu and colleagues (2009) have successfully used these cells as BBB model for their nanoparticles formulation uptake.

Transendothelial electrical resistance (TEER) value as an indicator of tightness junctional between endothelial is used to validate the dense structure of endothelia (Kuo and Wang 2010). A BBB model with satisfactory tight junction between brain-microvascular endothelial cells is a prerequisite to investigate the transport properties across the BBB (Chen et al. 2014). The electrical resistance and transport of solutes have a non-linear relationship because solute transport depends on the sum of transport across all junctional pathways, while TEER depends on areas with the lowest electrical resistance between single cells (Madara 1998). Gaillard and de Boer (2000) have determined a threshold TEER value of $131 \Omega\text{cm}^2$ on an *in vitro* BBB model. Meanwhile, Callahan et al (2004) concluded that TEER

value should be higher than $120 \Omega\text{cm}^2$ for proper brain delivery study. Then, there is a consensus that the *in vitro* BBB models should show a sufficiently high TEER of at least $150\text{--}200 \Omega\text{cm}^2$ (Gumbleton and Audus, 2001; Reichel et al. 2003).

Koto et al (2007) measured the TEER value of monoculture bEnd3 cells increased by days, reaching the maximum of $\sim 110 \Omega\text{cm}^2$ at day 8 and decreased afterwards. This TEER value is much smaller than the *in vivo* TEER value of brain parenchymal microvessel which is $\sim 1800 \Omega\text{cm}^2$ (Gumbleton and Audus 2001). In order to overcome the tightness junction on monoculture of bEnd3 cells, co-cultured with astrocytes could increase TEER value. Omidi et al (2003) found that bEnd3 cells-co-cultured with C6 glioma cell treated with cAMP elevators showed high TEER value averaging $130 \Omega\text{cm}^2$. Meanwhile, Li et al (2010) co-cultured bEnd3 with rat astrocytes on 12 Transwells™ using several basement membrant substitutes resulting increasing of TEER value up to 170% with base monoculture cells at $8.6 \Omega\text{cm}^2$. Chen et al (2014) used CTX-TNA2 as astrocytes cells to be co-cultured with bEnd3 cells on 12 Transwell™ displaying an adequate TEER value at $215 \Omega\text{cm}^2$. In this study, bEnd3 as endothelial cells were co-cultured with CTX-TNA2 as astrocytes cells using collagen type I as coating agent.

2. Human Colon Carcinoma Cell Line (Caco-2) Cells as Model for Intestinal Epithelial

Caco-2 cells grown on polycarbonate membranes were first used to predict intestinal drug transport in 1989 (Hidalgo and Borchardt 1990). Since

then, these cell monolayers have been applied to screen new therapeutic agents for their intestinal permeability (Artursson and Karlsson 1991), and to investigate intestinal drug absorption mechanisms (Hidalgo and Borchardt 1990; Ranaldi et al. 1992). Advantages associated with the use of Caco-2 cell monolayer include its human origin, which permits better correlation with clinical data.

When cultured on permeable inserts, confluent Caco-2 cells undergo differentiation, which leads to the formation of apical tight junctional complexes (Ophir et al. 1995) and the polarized distributions of membrane enzymes (Chantret et al. 1988), receptors, transport systems (Riley et al. 1991; Hidalgo and Borchardt 1990), ion channels (Thwaites et al. 1993) and lipid molecules (Simons and Fuller 1985) similar to those found in the human small intestinal enterocytes (Bailey et al. 1996). Compared with animal models, the Caco-2 cell culture model permits better control of experimental conditions, greater data reproducibility and the establishment of transport mechanisms (van de Waterbeemd and Gifford 2003)

Epithelial cell culture systems have been developed from cells with a low background expression of transporters, such as the LLC-PK1 (porcine kidney cells) and MDCK (Madin-Darby canine kidney) cells (Evers et al. 1998). LLC-PK1 and L-MDR1 cells monolayers require shorter culture time, approximately 3-7 days, to reach confluence compared to 21-25 days required by the Caco-2 cell monolayers, which makes it easier to generate cell culture systems for drug transport studies. In order to provide a more robust correlation in this project, the Caco-2 cell monolayers were used in

addition to the L-MDR1 and LLC-PK1 cells as in vitro cell models for P-gp mediated drug transport studies (van de Waterbeemd and Gifford 2003).

3. Alzheimer's Disease

Alzheimer's disease (AD) is characterized by advanced loss of memory and cerebral function (Figure 2.3). The cognitive degradation associated with AD extremely affects the social and behavioral skills of people living with this disease. In studies of mortality, the age-specific death rate of AD victims is two to four times that of individuals in the general population (Katzman and Saitoh 1991).

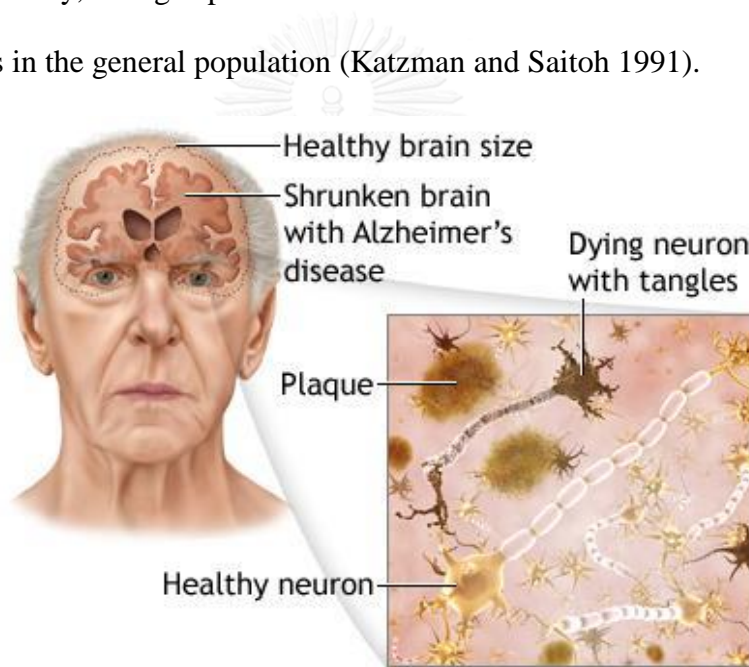


Figure 2.3 AD patient's brain (<https://www.premedhq.com/alzheimers-disease>)

Alzheimer's disease could be occurred by the deposition of the amyloid beta protein (senile plaques) into the extracellular synaptic spaces of the neocortex, particularly in the temporal and parietal lobes. Neurodegeneration affects the cognition function such as learning, abstraction, judgment, etc. The memory also have been affected with behavioral consequences such as aggression, depression, hallucination, delusion, anger and agitation (Olson and Shaw 1969). Pathologically, the enlargement of ventricular and atrophy of the hippocampus were occurred, and the cerebral cortex can be seen (Roney et al. 2005).

According to target site of Alzheimer's disease (Figure 2.3), the therapeutic strategies to inquiry the central nervous system (CNS) are limited by the high restriction of tight junctions at the endothelial cells of the blood brain barrier (BBB). To overcome the burdens of the BBB, polymeric biocompatible drug carriers have been applied to the central nervous system. Polymers are promising candidates in the investigation of AD because nanoparticles are capable of: opening tight junctions (Ranaldi et al. 2002), crossing the BBB (Barbu et al. 2009) and high drug loading capacity (Blasi et al. 2007). Lipid nanoparticles incorporated with brain targeting properties (biopolymers) can be promised as new strategy to overcome the barrier problem to deliver the drug for Alzheimer's disease.

4. Parkinson's Disease

Parkinson's disease (PD) is still the second most common neurodegenerative disease, after Alzheimer's disease (Chen and Tansey 2011)

and the most neurodegenerative movement (Schapira 2009). Parkinson's disease (PD) is characterized by a selective neurodegeneration of mesencephalic substantia nigra pars compacta, the origin of the dopaminergic nigrostriatal tract (Lang and Lozano 1998) causing the classic clinical motor features of Parkinson's disease i.e. latent tremor, slowed movement, unstable posture and rigidity of muscle (Figure 2.4) (Gelb et al. 1999). The secondary symptoms that might be included are depression and other emotional changes such as difficulty in speaking, chewing and swallowing; urinary problems or even constipation; skin problems; and sleep disruptions (Chen and Tansey 2011). In sporadic cases, the causes and etiology of PD are still largely uncertain, but some studies have found that there is a correlation between aging and oxidative stress neuron degradation in brain (Beal et al. 1998; Emerit et al. 2004; Imam and Ali 2001). For non-familial forms of PD, it is multiple causes such as genetic predispositions, environmental toxins, and aging are important factors in initiation and progression of the disease (Nagatsu and Sawada 2006). Recently, studies found that neuroinflammation and microglia activation also played important roles in PD pathogenesis (Chen and Tansey 2011; Hirsch and Hunot 2009; Tansey and Goldberg 2010).

PD prevalence is age-dependent, with an average onset age at 55 years old, only 4% cases being under 50 years, rapidly increases over the age of 60 years and increases to 4–5% in 85-year-olds. The rate of PD for men is 91% higher than women (Van Den Eeden et al. 2003). In industrialized countries, it is estimated at 0.3% of the entire population and about 1% people over

60 years of age (de Lau and Breteler 2006). Mortality of this disease is two to five times as high among affected persons and also a markedly reduction in life expectancy (Lang and Lozano 1998). In addition, De Lau and Brateler (2006) have consistently found that older age and smoking habits are the only risk factors for PD.

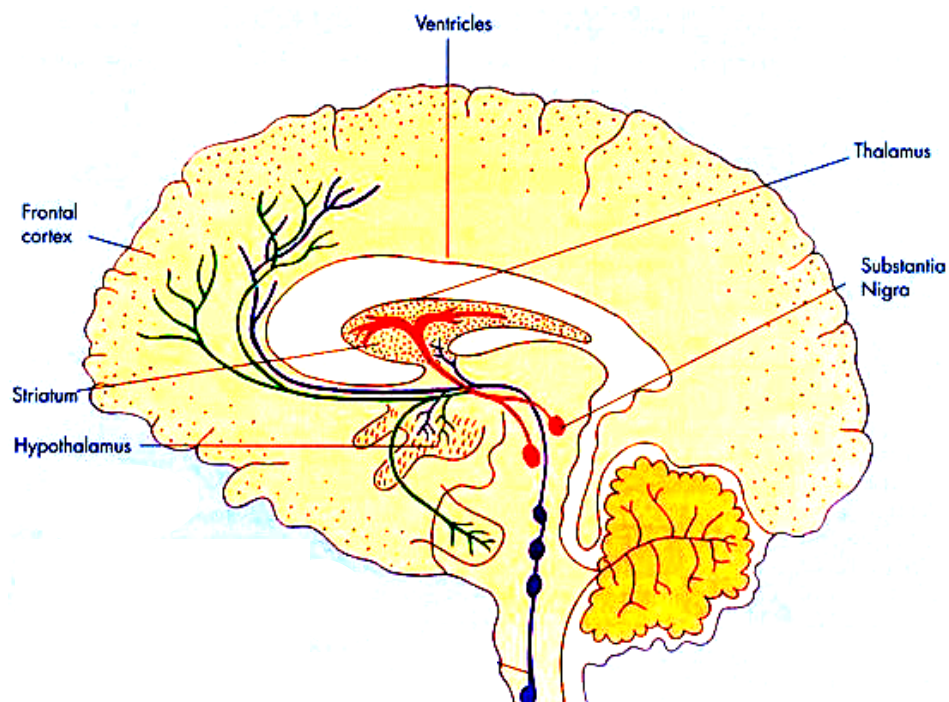


Figure 2.4 The sites of neurodegeneration and neurochemical pathway in Parkinson' disease (modified from Lang and Lozano, 1998)

The aim of symptomatic therapy on PD is to stimulate dopamine D2 in substantia nigra, using dopamine agonists including bromocriptine (ergot dopamine D2 receptor agonist) (Rascol et al. 2002) with the addition of L-DOPA for further symptomatic improvement (Kvernmo et al. 2006). Dopamine agonists restored the nigrostriatal pathway in by increasing neuroprogenitor cells (5-bromo-2'-deoxyuridine (BrdU)⁺ cells in Parkinson's diseases model) (Van Kampen and Eckman 2006). However, clinically

therapy on Parkinson's disease with dopamine D2 receptor cause some side-effects, such as motor fluctuations, dyskinesia and limits drug effectiveness during the treatment (Nutt et al. 2000). These side-effects, in particular dyskinesia, are alleged to be due to pulsatile DA receptor stimulation which strictly reflects plasmatic L-DOPA concentrations during advanced stages of the disease (Obeso et al. 2000). Therefore, stabilizing plasma concentration of L-DOPA or using longer-acting dopamine agonists. Thus, it is suggested to develop a novel formulate the dopamine receptor with longer activity or extend the half-life of the drug.

5. Bromocriptine

Bromocriptine (2-bromo α -ergocriptine) (BC) is a semi synthetic derivative of the natural peptide alkaloid α -ergocriptine (Figure 2.5) with molecular weight of 654.595 g/mol. BC was synthesized by the bromination of α -ergocriptine with different brominating agents (Schiff 2006). According to the structure, BC is water insoluble drug. Its mesylate (methanesulfonate) salt, introduced since 1975 (Brooks 2000), possesses a slightly of 0.8 mg/mL solubility in water (Florey 1979). The pKa value in methy cellulosol/water 8:2 (w/w was 4.90 ± 0.05). The partition coefficient between of pH 1.2 and n-octanol was 1:90 and between of pH 7.5 and n-octanol was 1:235 (Giron-Forest and Schonleber 1992). In a previous study, the solubility of BC mesylate (BM) had been increased 39 times when the BM was mixed with pluronic F-127 (Darwish et al. 2005). BM is an unstable in associated with light and heat which has no exactly melting point but it will melt in the range

of 180-230⁰C (Florey 1979). Analytically, 2.87 mg of BM is equivalent to 2.5 mg of its base form (Moro et al. 1991). BM is known in market as a tablet (2.5 mg) and a capsule (5 mg) under the name of Parlodel[®].

BM, as non-hydrogenated ergot alkaloid, an autooxidation both in solid and dissolved state is relatively occurred (Giron-Forest and Schonleber, 1992). In hydroxyl-containing solvents, non-hydrogenated ergot peptide alkaloids are easy to epimerized at C-8 to an equilibrated mixture of the lysergic and iso-lysergic series. The light-induced addition of water to the 9,10-double bond of bromocriptine to lumi-product. In slight acid condition, bromocriptine can form the corresponding 10 α -methoxy-lumi-derivative by proton-catalyzed addition of methanol (Giron-Forest and Schonleber, 1992). BM dosage forms, tablets and capsules have been proven stable at least 4 years at ambient temperature when store in amber glass bottles (Giron-Forest and Schonleber, 1992). BM in bulk form, is sensitive to heat and light but stable for up to 3 ears at ambient temperature when stored in sealed polyethylene bags contained in twist-off amber glass bottles. In solution, BM is rather labile in aqueous or alcoholic solution, particularly in the presence of acid, yielding mainly the equilibrated mixture with its 8-epimer and to smaller extent, its hydrolysis products 2-bromo-lysergamide and 2-bromo-lysergic acid and their 8 α -isomer, respectively. 2-bromolysergamide and 2-bromolysergic acid are listed by the British Pharmacopeia as impurities D and E in the monograph.

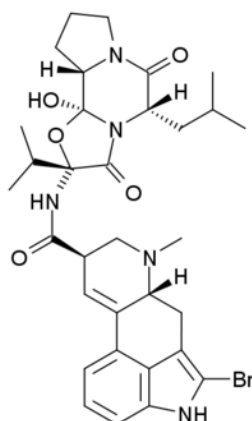


Figure 2.5 Chemical structure of bromocriptine (Siegel et al. 1999).

BM is the first dopamine D₂ agonist a semi-synthetic ergot alkaloid that used in treatment Parkinson's disease assisted with L-DOPA (Brooks 2000). Dopamine agonist can be categorized as ergot derived (bromocriptine, cabergoline and pergolide) and non-ergot derived (ropinirole and pramipexole) (Oda et al. 2008). Generally, a three times daily regime of BM has been employed with an initial dose of 2.5 mg daily then increased by increments of 2.5 mg every third day up to 40 mg daily (Lees et al. 1978). BM has slow onset of action (1–2 h) and prolonged half-life (3–5 h) (Kvernmo et al. 2006). This prolonged half-life explains the lower dyskinesogenic potential compared to L-DOPA (Pearce et al. 1998). In addition, BM is extensively metabolized with a first-pass effect that yields an oral bioavailability of only 4±2% (Cedarbaum 1987; Kvernmo et al. 2006).

The side effects of BM are most commonly nausea, vomiting, headache and dizziness. The adverse effects include gastrointestinal (GIT) troubles, slight absorption, broader liver metabolism and hypotension (Kopitar et al. 1991). The long-acting injectable form of BM has been

developed to improve the efficacy and tolerability of BM treatment (Defoort et al. 1987). BM has been used as a medication for the treatment of non-influent aphasia because of its physiological effect and its receptor distribution (Gold et al. 2000). BM is also the cornerstone in most of the treatment protocols of hyperprolactinemia for infertile women (Colao et al. 2006).

In order to avoid first pass metabolism by liver, the use of BM *via* parenteral approach was very limited. Alternatively, vaginal ring had been developed by Acartürk and Altug (2001) resulting effectively absorption and decreasing of plasma prolactin level in rabbits for ten days (Acartürk and Altug 2001). Vaginal tablet for BM has also been clinically successful for hyperprolactinemia treatment (Darwish et al. 2007; Darwish et al. 2005). However, it still remains inconveniences and compliances to patients. Thus, developing BM in oral dosage form with high bioavailability, better convenience and resulting high compliance is still being challenged to formulation scientists.

In addition, Esposito et al. (2008) was successfully formulated bromocriptine loaded SLN. *In vitro* release kinetics demonstrated that bromocriptine was released in a prolonged fashion for 48 h based on a dialysis method. This information confirmed that nanolipidic carriers encapsulation represent an effective strategy to prolong the half-life of bromocriptine.

underlying its protective effects may be related to prevent the mitochondrial dysfunction.

However, Asiatic acid has limitation to be explored as new drug for neurodegenerative disease due to its physical properties. One major problem associated with administration of AA is its low solubility in aqueous which may delay dissolution causing decreased bioavailability of the drug (Yonh-Liang et al. 2010). Thus, suitable formulation with pharmaceutical approach is needed to increase its bioavailability.

7. Solid Lipid Nanoparticles

Solid lipid nanoparticles (SLNs) introduced in 1991 are characterized as nanosphere particles made of lipid and being solid state in room and human body temperature (Hou et al. 2003; Müller et al. 2000). SLNs are unconventional drug delivery system to traditional polymeric nanoparticles (Mehnert and Mäder 2001), liposome (Müller et al. 2002b) and emulsion (Hu et al. 2004) for encapsulating lipophilic drug. SLNs are composed Nanoparticles are in the submicron size range (50–1000nm) and are composed of well body tolerated lipid components (Müller et al. 1995; Schwarz et al. 1994). In order to stabilize lipid aggregate, surfactants or polymers in a right concentration are employed (Müller et al. 2000). Surfactants also can modify release profile of entrapped drug in associated with lipid function and production parameters (eg. temperature) (Schwarz et al. 1994; zur Mühlen et al. 1998).

SLNs combine the advantages of polymeric nanoparticles, fat emulsions and liposomes (Mehnert and Mäder 2001). They can be produced on a large industrial scale by high-pressure homogenization (Dingler and Gohla 2002) and be safely sterilized through aseptic production filtration, γ -irradiation or heating (Mehnert and Mäder 2001). Moreover, they are less toxically acceptable like emulsions and liposomes, produce sustained release due to their solid matrix, similar to polymeric nanoparticles, and surface modification effectively target specific tissues after parenteral administration (Cavalli et al. 2003; Yang et al. 1999). In addition, due to their properties, SLNs are employed to enhance the absorption and bioavailability of poorly soluble drugs for oral administration (Hu et al. 2004).

The simple way and cost-effective technique to produce SLN in large scale is using high pressure homogenizer. Basically, there are two techniques covered in this method which are hot homogenization and cold homogenization technique. For both techniques the drug is dissolved or solubilized in the lipid being melted at approximately $5 \pm 10^\circ\text{C}$ above its melting point. For the hot homogenization technique the drug-containing melt is dispersed under stirring in a hot aqueous surfactant solution obtained pre-emulsion. The pre-emulsion is homogenized using hot high pressure homogenizer produced hot O/W nanoemulsion then cooled down to room temperature. The lipid recrystallizes and leads to solid lipid nanoparticles. For cold homogenization, melting lipid containing drug are dispersed in a cold surfactant solution yielding a pre-suspension. Then this pre-suspension is homogenized at or below room temperature, the cavitation forces are

strong enough to break the lipid microparticles directly to solid lipid nanoparticles. This technique is suitable for heat sensitive material and therefore can minimize loss of hydrophilic drugs to the water phase (Müller et al. 2000). And the alternative approach to produce large scale of SLN is via microemulsion. The microemulsion should be produced at a temperature above the melting point of the lipid. The lipid, a mixture of water, co-surfactant(s) and the surfactant is heated to the same temperature as the lipid and added under mild-stirring producing a clear dispersion. Then, it is dispersed in a cold aqueous medium under mild agitation until form solid lipid nanoparticles dispersion (Gasco and Antonelli 1993).

8. Nanostructure Lipid Carrier (NLC)

Nanostructured lipid carriers (NLC) is the second generation of lipid nanoparticles, consist of solid lipid matrices with spatially incompatible liquid lipids resulting in a structure with more imperfections in crystal to accommodate the drug (Souto et al. 2006). They combine the advantages of SLN and overcome their limitations, namely, limited drug loading, risk of gelation and drug leakage during storage caused by lipid polymorphism (Müller et al. 2002b).

The NLC has been considered as an alternative to liposomes and emulsions due to improved properties such as ease of manufacture, high drug loading, and more flexibility in modulating the drug release profile (Müller et al. 2002b, 2002a). Its features, high drug payload, avoidance or minimization of drug expulsion and enhancement of chemical and physical stability, has

been represented NLC as new promising colloidal carrier (Teeranachaideekul et al. 2007).

NLC as one of lipid nanoparticles can be categorized as suitable formulation for brain targeting drug formulation. Recent studies have been conducted to investigate this promising formulation. Zhang *et al.*, (2010) have studied that the pharmacokinetic and tissue distribution of DHA-NLC were higher than DHA solution after intravenous administration. Kasongo and colleagues (2011) also have evaluated the potential NLC to deliver didanosine to brain. They found that Tween® 80 has been shown to have the ability to facilitate the targeting of colloidal drug delivery systems to the brain (Kasongo et al. 2011). Other research results also concluded that incorporation vitamin E with NLC improved baicalein's stability and the ability of baicalein to penetrate the brain (Tsai et al. 2012). However, those NLC preparations are administered via intravenous which is less compliance to patient. So, it is a big challenge to develop NLC for brain targeting via oral administration.

9. Chitosan

Chitosan which derived from chitin is the most bountiful natural polysaccharide after cellulose in the amount produced annually by biosynthesis (Alves and Mano 2008) that supports numerous living organism (Figure 2.7). Chitin is synthesized via common pathway of polymerization of N-acetylglucosamine from the activated precursor UDP-GlcNAc (Kumar et al. 2004).

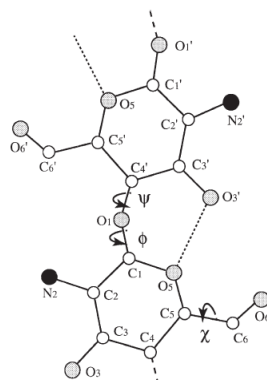


Figure 2.7 Chemical structure of chitosan (Agrawal et al. 2010)

The biocompatibility and the biodegradability of chitosan allows its interesting application in many filed such as exhibits interesting properties such as biomedicine, waste water treatment, functional membranes and flocculation (Kumar et al. 2004). Moreover, the non-toxic, non-immunogenic and non-carcinogenic of degradation products of chitosan is also offering potential applications on biomedical filed such as gene delivery, tissue engineering, wound healing (Ueno et al. 2001; Ueno et al. 1999), as well as for use in antimicrobial, antiviral and immune adjuvant strategies(Chirkov 2002; Singla and Chawla 2001). In addition, biocompatibility of chitosan and its ability to prolong residence time in the gastrointestinal tract through mucoadhesion and also its property to enhance absorption by increasing cellular permeability promises potential oral drug dosage forms (Bowman and Leong 2006). Moreover, based on its mucoadhesive, chitosans have also been found to enhance the nasal absorption of peptide (Illum et al. 1994), D-Arg-kyotorphin in rats (Tengamnuay et al. 2000), nanoemulsion of riperidone (Kumar et al. 2008) and tetramethyl pyrazine phosphate in rats (Mei et al.

2008). In addition, due to its biocompatibility, chitosan can be employed to modify surface has appeared improvement longer-circulating in blood (Kong et al. 2010; Sheng et al. 2009), specific brain targeting of nanoparticles (Aktaş et al. 2005; Tosi et al. 2008) and better drug retention (Kaasgaard and Keller 2010).

Based on the positive charged chitosan, it allows the chitosan to electrostatically interact with cell membranes which have negatively charges including intestinal cell (Artursson et al. 1994; Ranaldi et al. 2002). Moreover, chitosan solutions have been shown to increase paracellular permeability in a reversible which depends on the molecular weight and degree of deacetylation of the chitosan (Schipper et al. 1997). The mechanism action of increasing paracellular permeability is mediated by the positive charges on the chitosan, includes interactions with the tight junction proteins occludin and ZO-1, redistribution of F-actin, and slight destabilization of the plasma membrane (Smith et al. 2004). Thus, incorporating chitosan as a carrier to lipid nanoparticles (SLN/NLC) can enhance permeability the lipid nanoparticles across intestinal cells by paracellular pathway.

10. Spray Drying

Spray drying is common technique to transform liquid to solid. Spray drying also can be utilized to encapsulate oil or other active ingredient by entrapping it within inert material (Ré 1998). Moreover, formulation processes including encapsulation, complexes formation and even

polymerization can be accomplished in a single step (Gharsallaoui et al. 2007). Although it exhibits rapidly in process, modulation on physicochemical characteristics of the resulting powders potentially occurs along spray-drying process (Alamilla-Beltrán et al. 2005). In addition, spray-drying is cheaper and takes less time process than freeze drying (Broadhead et al. 1992; Oakley 1997).

The process of spray drying consists of three steps: (a) atomization through a spray nozzle, (b) contact of the sprayed feed with warm air, (c) dehydration of the droplets, and (c) collection of the powder (Figure 2.8). Practically, the liquid feed is atomized by an atomizer creating a spray of fine droplets into a chamber of heated air, from which the solvent quickly evaporates resulting in dried particles (Masters 1990). Resulted dry powders from spray drying processes can be inhaled as aerosols into the lung, delivered to the nose, filled into capsules, or pressed into tablets for oral applications, or even delivered transdermally (Vehring 2008).

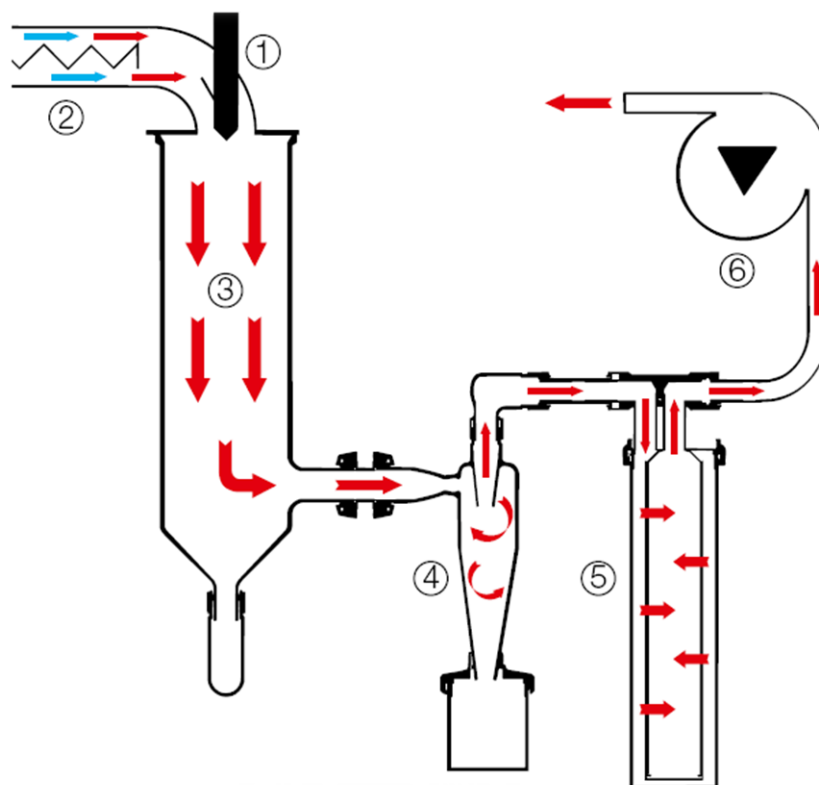


Figure 2.8 Mini Buchi Spray Dryer B-290

(<http://micro-encapsulation.eu/microencapsulation/manufacturing/spraydrying.html>)

Spray-drying process allows amorphous structures of drugs or biomolecules such as protein, peptide when they are prepared from solutions of pure compounds with the presence of sugars or maltodextrin as additional excipients. This additional excipient also can stabilize the biomolecules or drugs during the spray drying process and during subsequent storage (Saklatvala et al. 1999). In the case of pharmaceutical materials, especially for oral administration drug, the amorphous solids give many advantages, such as higher solubility and dissolution rate and sometimes better compression characteristics than the corresponding crystalline solids.

However, amorphous materials are more thermodynamically unstable than the crystalline form on storage (Singhal and Curatolo 2004).

Moreover, spray-drying requires particular attention in the process control because of limitations and the high number of parameters. These limitations include problems with low yield collection and instability to heat-sensitive materials. Each process variable is critical and reveals difficulties in spray-drying optimization attempts. The spray-drying process optimization involves the evaluation of parameters concerning both spray-dryer condition and feed formulation (Gharsallaoui et al. 2007).

The next generation of spray dryer is nanospray dryer. Nanospray dryer is based on a new spray drying concept. This device can produce higher yield powder with more uniform fine particles size. A complete diagram of the apparatus is illustrated in Figure 2.9. The liquid sample is fed to the spray head by a pump. Then the generation of droplets based on a piezoelectric driven actuator, vibrating around 60 kHz, perforated through stainless steel membrane (micron-sized holes; 4.0, 5.5 or 7.0 μm) in a small spray cap, ejecting millions of precisely sized droplets per second with a very narrow distribution. These fine droplets are dried into solid particles which are collected by electrostatic charging and are deflected to the collecting electrode. Finally the resulting powder is collected using a rubber spatula (Li, et al. 2010).

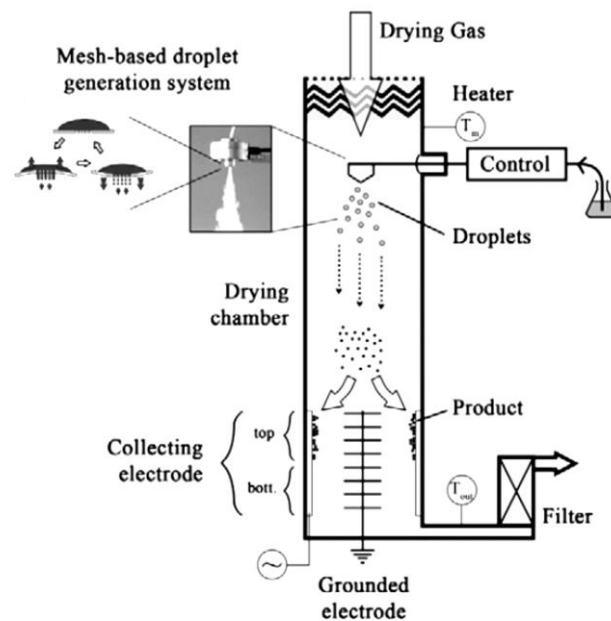


Figure 2.9 Schematic of the Nanospray Dryer (Li et al. 2010)

11. Response Surface Methodology and Central Composite Design

Response surface methodology, or RSM, is set of mathematical and statistical techniques to analyze and to form a model describing a response of interest influenced by several independent variables. RSM can be used to optimize and predict the response associated to the significant variables. Mathematically, the response can be expressed as following this equation,

$$y = f(x_1, x_2) + \epsilon \quad \text{Equation 2. 1}$$

where ϵ represents the noise or error observed, y is the response, x_1 and x_2 are the variables influenced the response. If the expected response of $f(x_1, x_2)$ is denoted as η , then η is called surface response which normally represented in 3D graphic as the function of combination of two variable.

The models of the relationship between response and independent variables are fitted using regression analysis. Determination coefficients (R^2)

and lack of fit testing are considered to determine the fitted model. Linear model (first-order model) and quadratic model (second-order model) are mostly used in RSM (Montgomery 2005).

According to fitting a second-order model, Box and Wilson in 1951 have introduced central composite design (CCD) as an efficient design of experiment and minimalist number of experimental runs considering the non-statistically lack of fit testing. This model, generally, consists of a 2^k factorial with nF runs, $2k$ axial or star runs and nC center point, geometrically shown in Figure 2.10.

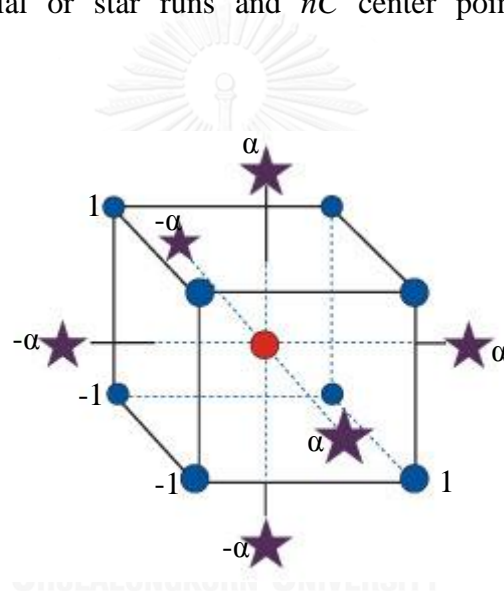


Figure 2.10 Central composite design with $k=3$ (Montgomery, 2005)

Billon *et al* (2000) used RSM to optimize the operating conditions to maximize production yields and minimize moisture contents of spray dried acetaminophen microparticles as responses. For the first screening to determine the significant independent variables, fractional factorial design was employed resulted that the most significant factors are inlet temperature, pump rate and their interaction for both formulations containing sodium carboxy methyl cellulose and feed rate and colloidal silica concentration for

the formulation containing microcrystalline cellulose to both of responses. Then, in order to estimate the optimized operating condition of spray drying, response surface methodology was used with central rotational composite design resulting adequate quadratic model for both of responses (Billon et al. 2000).

Tonon and co-workers (2008) also had employed RSM with central composite design to optimize the variables of inlet temperature, feed rate and maltodextrin concentration on moisture content, hygroscopicity, process yield and anthocyanin retention of açai (*Euterpe oleracea* Mart.) powder (Tonon et al. 2008). In this study, the response of hygroscopicity and process yield were significantly influenced by those independent variables which fitted-well with quadratic model. However, moisture content was significantly affected by the variable of inlet temperature and feed rate with which fitted-well with linear model whereas anthocyanin retention was only influenced by the inlet temperature but fitted well with quadratic model (Tonon et al. 2008).

Moreover, Ahn and colleagues (2008) used microencapsulation entrapment efficiency (MEE) of microencapsulated sunflower oil (MESO) as the response of four variables including SO concentration, proportion of milk protein isolates (MPI) to coating wall, soy lecithin concentration, and homogenizing pressure. RSM was employed by adopted central composite design resulting only 31 experimental runs with four variables which revealed quadratic model. In accordance with maximal MEE (94.6%)

observed in the MESO under optimized conditions displayed about 96.6% MEE. This result represents that the regression equation which exposed from was a suitable model to describe the response of the experimented parameters to the MEE of MESO. Thus, RSM with rotatable central composite design can be used in both of optimization feed formulation and of spray drying condition processes (Ahn et al. 2008).



CHAPTER III

MATERIALS AND METHODS

1. Materials

1.1 Chemicals

Acetic acid, Sigma-Aldrich, Germany

Asiatic Acid, Guangxi Changzhou Natural Product Development Co., Ltd,
China

Bromocriptine mesylate, lot SV-722210-01, Sigma Chemical Co, St Louis,
MO, USA

Chitosan, low molecular weight (50 kDa), Sigma-Aldrich, Germany

Ethylene oxide/propylene oxide block copolymer (Pluronic F-127), BASF,

Maltodextrin, Becthai, Thailand

Rhodamine-6g, Molecular Probes, Eugene, OR, USA

Sorbitane polyoxyethylene monooleate (Tween 80), VWR International Ltd.,
UK

Sorbitane monooleate (Span 80), Fluka Chemika, Germany

Tristearin, TCI, Japan

Trimyristin, TCI, Japan

Ultrapure water (Maxima Ultra Pure Water, Elga-Prima Corp, UK) with a
resistivity greater than 18 M Ω /cm was used to prepare all solutions

1.2 Cell culture

bEnd3 (ATCC® CRL-2999™), American Type Culture Collection, USA

Caco-2 cells, (ATCC® HTB-37™), American Type Culture Collection, USA

Collagen I, Rat Tail, Gibco®, Gibthai Co. Ltd., Thailand

CTX TNA2 (American Type Culture Collection® CRL-2006™), Gibthai Co. Ltd. Thailand

Dulbecco's modified Eagle medium (DMEM) high glucose with L-glutamine (GIBCO), Gibthai Co. Ltd., Thailand

Fetal bovine serum (FBS), Gibco®, Gibthai Co. Ltd., Thailand

Hank's buffered salt solution (HBSS), Gibco®, Gibthai Co. Ltd., Thailand

Non essential amino acids (NEAA), Gibco®, Gibthai Co. Ltd., Thailand

Penicillin–streptomycin liquid, Gibco Gibthai Co. Ltd., Thailand

Phosphate-buffered saline (PBS), Gibco®, Gibthai Co. Ltd., Thailand

Transwells™ permeable membrane inserts (six wells, 0.4µm pore size, 2.44 cm²) (SIGMA), ANH Scientific Co. Ltd, Thailand

Tissue culture flask, Corning T-15 cm² cell culture and Corning T-75 cm² cell culture, ANH Scientific Co. Ltd., Thailand

Trypsin– Ethylenediaminetetraacetic Acid (EDTA) 0.05%, Gibco®, Gibthai Co. Ltd., Thailand

Triton X-100 (SIGMA), Gibthai Co. Ltd., Thailand

2-[4-(2-Hydroxyethyl)-1-piperazinyl]-ethanesulfonic acid (HEPES), Gibco®, Gibthai Co. Ltd., Thailand

Chamber slide, 8-chambered Nunc® Lab-Tek II® - CC2™ slide, ANH Scientific, Co. Ltd., Thailand

1.3 Equipments

Centrifuge, Clay-Adams Safeguard, USA

Confocal Laser Scanning Microscope, Fluoview FV10i, Olympus, Japan

Differential Scanning Calorimetry (DSC), 2000A, Mettler TA, USA

Eppendorf Centrifuge 5810, Germany

FTS Dura Dry MP Microprocessor Controlled Corrosion, FTS System, USA

Mini Büchi Spray dryer B-290, Büchi, Switzerland

Nano Büchi spray dryer B-90, Büchi, Switzerland

High Performance Liquid Chromatography, Shimadzu model LC-8A, Japan

High pressure homogenizer, Emulsiflex-B3, Avestin inc., Canada

Inverted Microscope CKX31, Olympus, Japan

Laminar Cabinet HBB 2448, Holten, Thermo Scientific, Dreieich, Germany

Scanning Electron Microscope (SEM), Hitachi 5-4100, Japan

Transmission Electron Microscope (TEM), JSM-6700F, JEOL, USA

Ultra Turrax®, IKA-Werke, T50 digital, GmbH & Co., Staufen, Germany

VICTOR³™ Multilabel Counter, 1420-051, Perkin Elmer, USA

Vortex mixer vm-300, Gemmy, USA

Water Jacketed CO₂ Incubator, Thermo Forma Scientific 3158, UK

X-Ray Diffraction, SIEMENS D 5000, Germany

Zetasizer, Malvern Instruments, Malvern, UK

2. Methods

2.1 Preparation and Characterizations of Lipid Nanoparticles

2.1.1 Preparation of BMSLN

The formulations of BMSLN, shown in Table 3.1, were prepared from preliminary study by hot high homogenization technique. Briefly, lipid (tristearin and trimyristin for SLN) and span 80 were melted at 10°C above their melting points as lipid phase into which BM was then dissolved. The aqueous phase consisting of hot ultrapure water (80°C), tween 80 and pluronic F127 were added to lipid phase. Then, the mixture was homogenized using ultra Turrax at 10,000 rpm in 5 min to form emulsion (o/w). In order to form nanoemulsion, the resulting emulsion was homogenized using hot high homogenizer at the pressure of 1000 bar and 5 cycles (water bath temperature at 82.5 °C).

Table 3.1 Formulation composition of BMSLN and BMNLC

Ingredients	% Content (w/w)	
	SLN	NLC
BM	0.025	0.060
Lipid (tristearin:trimyristin=7:3)	1	-
Lipid (tristearin:trimyristin:castor oil=4:2:4)	-	1
Surfactant (tween 80: pluronic f127:span 80=2:1:1)	2	2
Purified water to make	100	100

2.1.2 Particle size and zeta potential measurement

The average particle size, polydispersity index (PI) and zeta potential of BMSLN were determined by a Nano-ZS zetasizer (Malvern Instruments, Malvern, UK) at 25 °C. Each measurement was taken in triplicate.

2.2 Preparation of Spray Dried SLN Chitosan-based

2.2.1 Preparation of SLN chitosan-based containing BM

Low molecular weight of chitosan was dissolved in 1% (v/v) acetic acid until resulted 1% (w/w) chitosan solution (pH 3.99) followed by mild agitation using magnetic stirrer at 50°C, 70 rpm over-night. The solution was then filtered to get rid of dust and other traces impurities and was used as a stock solution. The stock solution was then diluted in ultrapure water to form 0.5% (w/w) solution.

In order to see how to form SLN chitosan-based, 10 mL BMSLN dispersion was added consecutively drop wise to an equal volume (10 mL) of chitosan solution with varied concentration (0.5 and 1% w/w). Chitosan was let to coat the SLNs in 30-min incubation at room temperature (25°C). TEM characterization was employed to see the morphology of BMSLN chitosan-based following method in the next section 2.3.6.

In order to convert SLN chitosan-based into spray dried powder, SLN chitosan-based was prepared following the method above with 0.5% chitosan solution. Mini Büchi B290 spray dryer (Büchi, Switzerland) was employed to spray dry SLN chitosan-based by noticing three processing parameters conditions i.e. (i) temperature, (ii) feed concentration and (iii) pump rate. Maltodextrin was added and varied q.s as a filler to form spray dried powder

of SLN chitosan-based considering variation of feed concentration that would be designed. The powder was then stored in a humidity controlled cabinet for a 48 h-period prior to their characterization (Kho et al. 2010).

2.2.2 Experimental design

In order to optimize the spray dried SLN chitosan-based, response surface methodology was employed. A three factors, five-level central composite rotatable design 2^3 principal (Box et al. 1978) was selected to study the effect of 3 independent variables, inlet temperature (X_1), pump rate (X_2) and feed concentration (X_3). The responses used were the yield %, redispersion of nanoaggregate powder size and moisture content of the nanoaggregates powder. An initial 2^3 full factorial design was created, providing the upper (+1) and lower (-1) level values for each evaluated parameter (X_1 - X_3) (Table 3.2). A total of 8 experiments were obliged (factorial points, Table 3.3). Effects and interactions between factors were derived.

The 8 full factorial designs were expanded to a central composite design (CCD) by adding 12 “star” points (6 axial points and 6 replicated centre points, Table 3.2). This design was generated and analyzed by the statistical software package Design-Expert V. 8 (StatEase Inc., USA).

The studied experimental responses were the results of the individual influence and the interactions of the 3 independent variables following polynomial model:

$$\hat{Y} = b_0 + b_1x_1 + b_2x_2 + b_3x_3 + b_{11}x_1^2 + b_{22}x_2^2 + b_{33}x_3^2$$

$$+ b_{12}x_1x_2 + b_{13}x_1x_3 + b_{23}x_2x_3 \dots \dots \dots \text{Equation 3. 1}$$

$$+ b_{12}x_1x_2 + b_{13}x_1x_3 + b_{23}x_2x_3 \dots \dots \dots \text{Equation 3. 1}$$

Where \hat{Y} was the measured response, b_0 the intercept term, b_i 's (for $i = 1-3$) were the linear effects, b_{ii} 's were the quadratic effects, b_{ij} 's (for $i,j = 1-3$, $i < j$) were the interaction between the i and j variables. To perform the statistical data analysis, analysis of variance (ANOVA) was able to determine the significance of the factors and interactions between them.



Table 3.2 Processing parameter and coded level of variables for experimental design

Variable	Processing parameters				
	Low level (-)	Center point (0)	High level (+)	Low level of axial point (- α)	High level of axial point (+ α)
X_1 : Inlet temperature ($^{\circ}$ C)	115	137.5	160	100	175
X_2 : feed rate (%*)	16	24	32	10.6	37.4
X_3 : feed concentration (%)	10	20	30	3.2	36.8

* 1% of feed rate equal to 0.5 mL/min

In order to select the model equation, statistically significant at F ratio ($\alpha < 0.05$) and high R^2 were considering then associated with statistically insignificant lack of fit ($\alpha > 0.05$) (Asasutjarit et al. 2007). The criteria of optimization were determined by the minimum inlet temperature on maximum yield and minimum nanoaggregate size of powder redispersion.



Table 3.3 Generated experimental design and responses of the design

NO	Run	X ₁	X ₂	X ₃	Design	Inlet temperature (°C)	Feed rate (%)	Feed concentration (%)	Responses
1	3	-1	-1	-1	Factorial design	115	16	10	Yield (%) Moisture content(%) Nanoaggregate size (nm)
2	12	1	-1	-1	Factorial design	160	16	10	
3	9	-1	1	-1	Factorial design	115	32	10	
4	1	1	1	-1	Factorial design	160	32	10	
5	2	-1	-1	1	Factorial design	115	16	30	
6	6	1	-1	1	Factorial design	160	16	30	
7	10	-1	1	1	Factorial design	115	32	30	
8	4	1	1	1	Factorial design	160	32	30	
9	8	-1.68	0	0	Star design	100	24	20	
10	11	1.68	0	0	Star design	175	24	20	
11	5	0	-1.68	0	Star design	138	11	20	
12	7	0	1.68	0	Star design	138	38	20	
13	14	0	0	-1.68	Star design	138	24	3.2	
14	13	0	0	1.68	Star design	138	24	36.8	
15	18	0	0	0	Center points	138	24	20	
16	15	0	0	0	Center points	138	24	20	
17	17	0	0	0	Center points	138	24	20	
18	19	0	0	0	Center points	138	24	20	
19	20	0	0	0	Center points	138	24	20	
20	16	0	0	0	Center points	138	24	20	

2.3 Spray Dried Powder Characterization

The spray dried powder of BMSLN chitosan-based resulting from optimization of spray drying was characterized for their physical properties following methods.

2.3.1 % product yield.

The obtained sample was collected from the spray dryer collector chamber and weighed to get the mass of obtained product yield. The % product yield was calculated following this equation,

$$\% \text{ yield} = \frac{W_{\text{obtained}}}{W_{\text{initial solid content}}} \times 100\% \dots \dots \dots \text{Equation 3. 2}$$

where W_{obtained} was the mass of obtained product yield and $W_{\text{initial solid content}}$ was the mass of initial solid part in the sample.

2.3.2 Moisture content.

The obtained powder sample of 0.5g was weighed. The residual moisture content was determined via loss-on-drying using a Mettler Toledo Deluxe Halogen Moisture Analyzer HR83 (Mettler-Toledo, Belgium).

2.3.3 Size and zeta potential measurement of spray dried powder redispersion BMSLN chitosan-based (RSPcBMSLN).

The obtained powder sample of 0.3g was dispersed in 10 mL of water. After 5 min gentle agitation using vortex, nanoaggregate size and zeta potential were measured following method mentioned in section 2.1.2

2.3.4 Particle size measurement

The droplet size distribution of the spray dried powder was determined by a Scirocco 2000 dry powder system provided with a Mastersizer 2000 using laser diffraction (Malvern Mastersizer 2000, UK). The refractive index of lipid was 1.3300, the absorption value was 0.1 and the refractive index of maltodextrin was 1.4300. The droplet size distribution was determined by volume distribution and expressed as mean $[d(4,3)]$. The width of the powder size distribution was expressed by the SPAN value:

$$\text{SPAN} = \frac{d(v,0.9) - d(v,0.1)}{d(v,0.5)} \dots \text{Equation 3.3}$$

$d(0,9)$, $d(0,5)$ and $d(0,1)$ were the diameter of 90% volume distribution, diameter of 50% volume distribution (median) and diameter of 10% volume distribution, respectively.

2.3.5 Particles flowability determination

The Carr's compressibility index (CI), which used as the particle flowability characterization, was determined by following Equation 3.4. A bulk density of spray dried powders (ρ_{bulk}) was determined at tap volume (V_{bulk}) that was achieved by weighing 4 mL of the bulk of spray dried powder into a 10-mL measuring cylinder without tapping. Then, in order to determine (ρ_{tap}), the bulk was tapped using in-house densitometer until 1200 taps to measure V_{bulk} . CI values below 25 indicated free-flowing particles and values above 40 indicate poor flowability (Podczek, 1998).

$$CI = \frac{(\rho_{\text{tap}} - \rho_{\text{bulk}})}{\rho_{\text{tap}}} \times 100\% \dots \text{Equation 3.4}$$

2.3.6 TEM analysis

The nanoaggregate morphology was characterized using a transmission electron microscope (TEM) model JSM-6700F (JEOL, USA). The sample was prepared by dropping a formulation which was diluted 10-fold with ultrapure water on to a copper grid followed by negative staining with 1% phospho tungstic acid (Luo et al. 2011). In order to get rid of the water from the sample, desiccators were using for 2 h then the prepared sample were stored in a controlled humidity chamber until their characterization.

2.3.7 SEM analysis

The shape and surface morphology of the dry powder was examined with the scanning electron microscopy (SEM, Hitachi S-4100) after gold palladium coating onto the powder using an ion coater.

2.4 Development of Spray Dried Powder of BMNLC Chitosan-based (SPcBMNLC)

Nanostructured lipid carrier (NLC) as the second generation of lipid nanoparticles had some advantages to increase the stability of model drug (BM). The ability to avoid drug expulsion was interesting to explore NLC to be spray-dried (Müller et al. 2002b).

2.4.1 Preparation of BMNLC

BMNLC was generated following the method mentioned in section 2.1. The composition of NLC formulation was prepared following Table 3.1

in section 2.1. BMNLC was physically characterized by following method in section 2.1.2.

2.4.2 Spray drying of BMNLC chitosan-based (cBMNLC)

BMNLC chitosan-based was prepared following the method mentioned in section 2.2 in optimized condition which resulted from the experimental design. Spray dried BMNLC chitosan-based was physically characterized (% product yield, moisture content, nanoaggregate size, TEM, and SEM) following methods mentioned in section 2.3. (1-7) and then compared to spray dried powder of BMSLN chitosan-based.

2.5 Chemical Characterization of BMSLN, BMNLC, Spray Dried Powder of BMSLN Chitosan-based (SPcBMSLN) and Spray Dried Powder of BMNLC Chitosan-based (SPcBMNLC).

In this study, chemically characterization was hard experiment since the instability of BM as a model drug. In order to avoid degradation by light, all of experiments were conducted under low light condition.

2.5.1 HPLC procedure

The HPLC determinations were performed using a HPLC (Shimadzu model LC-8A, Japan) system consisting of a two plungers alternative pump (Shimadzu LC-20AD, Japan), a variable wavelength UV-detector (Shimadzu SPD-20A/AV, Japan), operating at 300nm and an injection with a 20 μ L loop. The BDS Hypersil C-18 reverse-phase column (25 \times 0.46cm) by Thermo Scientific, USA, packed with 5 μ m particles was used. The mobile phase used was a mixture of acetonitrile and buffer ammonium (70:30). The flow

rate was 1.0 mL min^{-1} and the column temperature was room temperature 25°C (Esposito et al. 2008). Linearity and robustness of BM assay were also conducted.

2.5.2 Drug Entrapment Efficiency (DEE)

Free BM (non-incorporated in the BMSLN or BMNLC) was separated by ultrafiltration centrifugation technique (Zhuang et al. 2010). Briefly, 1 mL of BMSLN or BMNLC was placed in the upper chamber of a centrifuge tube matched with an ultrafilter (Amicon ultra, Millipore Co., USA, MWCO 3 kDa) and centrifuged using Eppendorf 5810 from Germany for 30 min at 4000 rpm and the filtrate with free BM was obtained. The obtained filtrate was diluted with methanol and filtered through 0.45μ membrane filters. Afterwards, the resulting solution was analyzed by HPLC procedures mentioned in 2.5.2. The total drug content in BMSLN or BMNLC was determined as follows: aliquots of 1 mL BMSLN or BMNLC dispersion were diluted appropriately by methanol to dissolve the lipid ingredient. Then the obtaining suspension was filtrated through 0.45μ membrane filters and analyzed by HPLC procedures (section 2.5.2). The drug loading content was the ratio of incorporated drug to lipid (w/w). The encapsulation efficiency (EE) was calculated by the following equations, respectively:

$$DEE (\%) = \frac{W_{Total} - W_{Free}}{W_{Total}} \times 100\% \dots\dots\dots \text{Equation 3. 5}$$

W_{Total} , W_{Free} , were the weight of total drug in SLN or NLC and the weight of untrapped drug in ultra-filtrated part.

2.5.3 Drug retention (DR)

Retention of BM was determined by dispersing approximately 0.3g of spray dried BM-SLN/NLC chitosan-based powder in 10 mL of Milli-Q H₂O in capped glass vials. One mL of the redispersed of spray dried BM-SLN/NLC was diluted ad 5 mL of 1% Triton X-100 (dissolved in methanol) and incubated in shaker for 1 h (100 rpm, 25°C) to extract the drug from nanoaggregates of SLN/NLC. Then approximately 1.5 mL of sample was filtered into brown vial (2 mL) and determined using the HPLC method (mentioned in 2.5.1). The total drug content in spray dried BMSLN/BMNLC chitosan-based was determined by following the previous procedure mentioned in drug encapsulation part as well as determining of the amount of encapsulated BM before spray drying. Drug retention was calculated as the amount of BM in the spray dried powder relative to the amount of BM in the SLN/NLC before spray drying:

$$\text{Drug Retention}(\%) = \frac{(BM_{\text{inspraydriedpowder}})}{(BM_{\text{beforespraydrying}})} \times 100\% \dots \dots \dots \text{Equation 3. 6}$$

(Kaasgaard and Keller 2010).

2.6 Development and Comparison of Spray Drying BMSLN/BMNLC and Nanospray Drying BMSLN/BMNLC Chitosan-based

In order to reduce the nanoaggregates size, Nanospray Dryer B-90 that could produce submicron particles from solution or liquid dispersion was employed. The nanospray dried powder and their redispersed nanoaggregates were compared to those obtained spray dried powder and their redispersion powder. In order to match the condition of this spray dryer, the previous optimum condition was employed with some adjustments.

The feeding of both spray drying BMSLN or BMNLC chitosan-based and nanospray drying BMSLN or BMNLC chitosan-based was prepared by following the previous method mentioned in section (2.1, 2.2 and 2.3) with some adjustments. The feed of concentration was at 3% by reducing maltodextrin concentration. In order to decrease the viscosity, the concentration of chitosan was reduced from 0.5% to 0.1%. The hot homogenizing process was fixed on to 7 cycles to obtain smaller droplets of SLN/NLC. The spray dryer (Buchi B-290 Spray Drier) was set up in optimum condition (inlet temperature at 115° C, pump rate at 16% and gas flow rate at 350 L/min). The inlet temperature of Buchi Nanospray dryer B-90 was 115°C. The gas flow rate was at 350 L/min and the pump setting at 22% from the optimum condition (Li et al. 2010). The powder products were then characterized by their physical properties (product yield, particles size and SEM) following the previous methods (section 2.3.1 and 2.3.2).

2.6.1 FTIR analysis

In order to characterize the effects of the different apparatus spray drying on IR spectra of BM, maltodextrin, BM loaded nanospray dried SLN or NLC chitosan-based were evaluated by FTIR (Perkin Elmer), using KBr pellet disk technique. All samples were scanned in the IR range from 400 to 4000 cm^{-1} (Florey 1979). Those IR spectras were then compared to spray dried BMSLN and BMNLC chitosan-based.

2.6.2 Wide angle X- ray diffraction analysis

The nanospray dried samples (nanospray dried BMSLN and BMNLC chitosan-based) were characterized for their crystallography structure by powder XRD (Siemens 500 D, Germany) as well as maltodextrin, tristearin, trimyristin and pluronic f127 as lipid component and the spray dried of BMSLN and BMNLC chitosan-based were also characterized for comparison. A voltage of 40 kV and a current of 50 mA for the generator were applied with Cu as the tube anode material. The solids were exposed to a Cu-K radiation, over a range of 2θ angles from 5° to 30° , at an angular speed of $2^\circ (2\theta)/\text{min}$, a sampling interval of 0.001° (Suresh et al. 2007).

2.7 Development and Comparison of Spray Dried Powder of AASLN/AANLC Chitosan-based

2.7.1 Preparation of AALN/NLC

The concentration of the drug was increased to raise the dose of the drug in the formulation. From preliminary study, 60mg of AA was the optimum drug amount that could be dissolved in 1mg of meting lipid. Therefore, formulations of AA-loaded SLN/NLCs, shown in Table 3.4, were prepared as follows.

Table 3.4 Formulation of AA-loaded SLN/NLC

Ingredients	% Content (w/w)	
	SLN	NLC
AA	0.060	0.060
Lipid (tristearin:trimyristin=7:3)	1	-
Lipid (tristearin:trimyristin:castor oil=4:2:4)	-	1
Surfactant (tween 80: pluronic F127:span 80=2:1:1)	2	2
Purified water to make	100	100

AASLN and AANLC were prepared by following the method in section 2. 1. 1 with increasing cycles on hot pressure homogenization into 7 cycles (water bath temperature at 82.5 °C).

2.7.2 Spray drying of AASLN/AANLC chitosan-based

Spray dried AA-loaded SLN/NLCs chitosan-based were produced by following the method from optimized condition mentioned at section 2 with some adjustments. To optimize the concentration of drug in dried powder, the feed of concentration was increased by varying increasing the amount of AASLN dispersion and reducing the amount of maltodextrin. The experiments were set as follows Table 3.5. The volume of 0.5% chitosan (in 1% acetic acid) was also modified to reach equal volume of AASLN (10 mL, 25 mL and 40 mL). According to the previous results of spray drying BMSLN, the product yield was used as dependent variable which was

influenced by the feed concentration parameter. The appearance of the obtained powder was also considered.

Table 3.5 Optimization of feed concentration of spray drying AASLN chitosan-based

Solid (%)	AASLN (mL)		
	10	25	40
1	A	B	C
2	D	E	F
3	G	H	I

The optimized feed concentration of spray drying AASLN was employed to spray drying AANLC.

The dry products of AA-loaded SLN/NLC chitosan-based were then characterized their physical (yield, particles size of RSP, moisture content, powder particle size, flowability, SEM, TEM, FTIR, WXR) following the previous methods (section 2.3.1-7, 2.6.1 and 2.6.2) with some adjustments.

2.7.3 DSC analysis

The physical state of AA in powder samples was characterized by a differential scanning calorimeter (DSC 2000A, Mettler Toledo TA, USA) as well as, SPcAASLN and SPcAANLC, their physical mixtures and each solid component of formulation. About 5mg of the above samples were sealed in standard aluminum pans with lids. All samples were scanned at a temperature speed of 20° C/min with the heat flow from 25 to 350 °C and protected with pure dry nitrogen gas at 60 mL/min. Indium was used as the standard

reference material to calibrate the temperature and energy scale of the DSC instrument (Castelli et al. 2005).

In order to investigate solid state of AASLN and AANLC, the bulk of SLN and NLC, blank SLN and NLC and AASLN/AANLC samples were scanned at 5°C/min heating rate from 25 to 90 °C and -1°C/min cooling rate from 90 to 0°C. The DSC profile of the bulk lipid of SLN/NLC the lipid nanoparticles of SLN/NLC and the influence of AA existence were studied.

2.7.4 HPLC procedure

AA was determined using HPLC procedure following Günther and Wagner (1996) with minor modifications. The HPLC, pumps, detector and column that used were mentioned in section 2.1.4. The sample was detected at 210nm. The mobile phase used was a mixture of acetonitrile and 10 mM of buffer phosphate (pH 7.7) (28:72). The flow rate was 1.0 mL.min⁻¹ and the column temperature was room temperature 25°C and the run time was 15 min. Specificity, linearity, accuracy, limit of detection (LOD), limit of quantification (LOQ) and robustness of AA assay were also conducted.

2.7.5 Drug Entrapment Efficiency (DEE)

The entrapped drug in the AASLN or AANLC was separated by MobiSpin g-50 column (MoBi Tec GmbH & Co.KG, Germany). Briefly, 0.5 mL of AASLN or AANLC was placed in the column that had been supported by a 1.5 mL flip-flop tube and spin for 2 min at 2444 rpm. The sample which contained AASLN or AANLC (unentrapped in SLN or NLC) was collected into the bottom of supporting tube. The entrapped drug was determined as

follows the following method. Aliquots of 0.4 mL sample were diluted appropriately by methanol with 1% Triton X-100 to dissolve the lipid ingredient. Then the obtaining suspension was filtrated through 0.45 μ membrane filters. Afterwards, the resulting solution was analyzed by HPLC following method that mentioned in section 2.8.3. The total drug content in AASLN or AANLC was determined by following method as mentioned in the previous without separating the entrapped drug. Drug Entrapment Efficiency (DEE) was calculated by the following equation:

$$DEE (\%) = \frac{W_{entrapped\ drug}}{W_{Total}} \times 100\% \dots\dots\dots \text{Equation 3. 7}$$

2.7.6 Drug Retention (DR)

The spray dried powder was prepared by following the method in section 2.5.3. And then the sample was determined using HPLC by following the method section 2.7.4. Drug retention was calculated by following Eq. 5.

2.7.7 *In vitro* release profile

In order to examine the release profile of spray dried powder cAASLN and cAANLC, other 2 formulations without chitosan (SPAASLN and SPAANLC) were also conducted, and the original AASLN and AANLC formulations were compared. The method on *in vitro* release profile followed Esposito et al. 2008 with some modifications. 0.3g of spray dried powder of cAASLN and cAANLC (also SPAASLN and SPAANLC) samples were weighed and were filled in size '2' hard gelatin capsules and were placed it into a dialysis bag (MWCO 3.5 kDA) with 3 mL of water. 3 mL of AASLN

and AANLC sample were just placed in a dialysis bag (MWCO 3.5 kDA) and put at the bottom of the vessel for comparison. Prepared samples were then evaluated for *in vitro* release using USP XXIII apparatus II at 37 ± 0.5 °C, at 100 rpm in 500 mL buffer of pH 1.2 for 2 h then replaced the medium with the same amount buffer of pH 6.8 for both spray dried powder of AASLN and AANLC chitosan-based (SPcAASLN and SPcAANLC). During study, 1.5 mL of aliquots was removed at 0, 0.5, 1 and 2h from pH 1.2 medium; 4, 6 and 8 h from pH 6.8 medium and replaced with fresh buffer. Amount of drug released was diluted with methanol and determined using the developed HPLC method that mention in 2.7.4.

2.7.8 Stability studies

Chemical and physical stability of spray dried powder of AASLN (SPcAASLN) and AANLC chitosan-based (SPcAANLC) were assessed at 25 ± 2 °C/ 75 ± 5 % RH. The powder samples (SPAASLN, SPcAASLN, SPaaNLC and SPcAANLC) were weighed of 0.3g and filled in size '2' hard gelatin capsules, packed in aluminum strips and stored for 3 months. The liquid samples (AASLN and AANLC) were placed into amber bottle glass and stored in the equal condition as powder samples. Samples were analyzed at 0, 15, 30, 60 and 90 days for drug content, percentage of entrapped drug and nanoaggregate size (Borhade et al. 2008). Drug content was prepared by following the method that mentioned in section 2.5.3 and analyzed by following section 2.7.4 for HPLC analysis. Percentage of entrapped drug was prepared by following section 2.7.5 and analyzed by following section 2.7.4.

Nanoaggregate size and PDI measurement was determined following section 2.3.3.

2.8 *In vitro* Absorption Studies of Redispersed Spray Dried Powder of AASLN and AANLC Chitosan-based (RSPcAASLN and RSPcAANLC) on Caco-2 cells

In order to investigate the cytotoxicity and permeability of spray dried cAASLN/cAANLC as oral drug, Human Colon Carcinoma Cell Line Colon or Caco-2 cells which represents small intestinal cell model were utilized. The selected formulation which was spray dried AA-loaded SLN/NLC was chosen to be studied following the methods below.

2.8.1 Cell culture

Caco-2 cells (ATCC®) were grown at 37°C with 5% CO₂/ 95% air and 90% relative humidity in Dulbecco's modified Eagle medium (D-MEM) supplemented with 1% penicillin–streptomycin, 1% nonessential amino acids (NEAA), and 10% fetal bovine serum (FBS). Caco-2 cells were maintained in T-25-cm² flasks and were split (1:3) when reaching 80%–90% confluence using trypsin-ethylenediamine tetraacetic acid (EDTA). Then, Dulbecco's modified Eagle medium (DMEM) supplemented with 10% fetal bovine serum (FBS), 1% nonessential amino acid (NEAA), and 1% penicillin–streptomycin was added. Culture medium was changed every second day and cells were grown at a temperature of 37°C in an atmosphere of 85% relative humidity and 5% CO₂. For the transport assay, cells were seeded on top of Transwell inserts (pore size 0.4µm, 4.67cm²) at a density of ~1x10⁵cells/well. Transepithelial electrical resistance (TEER) was measured and only

monolayers with a TEER > 350 $\Omega \cdot \text{cm}^2$ and background subtracted, were used for transport studies. Cells were differentiated for 20–21 days before the initiation of the experiments (Sha et al. 2005).

2.8.2 Confocal laser scanning microscopy (CLSM)

The Caco-2 cells were cultured in 8-chambered Nunc[®] Lab-Tek II[®] - CC² slide until formed monolayers (7 days). The transport pathway of these fluorescent markers (Rhodamine 6g) across Caco-2 cell monolayers was visualized with CLSM. The monolayer cells were incubated with formulations containing Rhodamine 6g (R6g) (R6g-SLN/NLC and redispersed spray dried R6g-SLN/NLC chitosan-based and non-chitosan-based) in serum-free DMEM and kept in life-conditions (37⁰C and 5% CO₂). A control experiment was executed in the same way without adding formulations. An Olympus FV10i-LIV of Center of Nano Imaging, Faculty of Science, Mahidol University, Bangkok, Thailand, was used for confocal imaging. R6g were excited at a wavelength of 516-536nm. The confocal images of the monolayer cells were captured every 10 min for 2 h incubation.

2.8.3 Assessment of cell viability

The cell viability of Caco-2 cells was measured by the MTT assay for evaluation of the cytotoxicity of re-dispersed formulations following to Mosmann (1983) with minor modifications. Approximately 5×10^4 cells (in 100 μL of cell culture medium) were seeded into the well in 96-well tissue culture plate. The cells were subsequently cultured under the same condition as the monolayer preparation for 96 h before use. Just prior to the start of

each experiment, the medium was removed from the cells, and redispersed formulation (AA free, SLN blank, RSPSLN Blank, RSPcSLN Blank, AASLN, RSPAASLN, RSPcAASLN, NLC blank, RSPNLC, RSPcNLC, AANLC, RSPAANLC and RSPcAANLC) in Hank's buffered salt solution (HBSS) was added to each well with following various of dilution of formulation that contained of AA concentration from 12.5 μM to 100 μM . After 2 h treatment, 100 μL 0.5 mg/mL MTT solution was added to each well, and the cells were incubated for 4 h (37 °C). Then the solution was removed and in order to dissolve formazan crystals, 100 μL DMSO was added. The absorbance of formazan was measured at 570nm (Sha et al. 2005) using VICTOR³™ Multilabel Counter model 1420-051 (Perkin Elmer, USA). Cell viability was determined by comparing absorbance of solution from wells containing treated cells with that of untreated cells. Triple replicates were measured for each concentration.

2.8.4 Transport assay

Caco-2 cells in TranswellTM inserts (pore size 0.4 μm , 4.67 cm^2) at a density of 1×10^5 cells/well were used in this experiment (mentioned in 2.8.1). AA transport assays were performed in absorptive (apical to basolateral, A to B) and secretory (B to A) directions (Figure 3.1). To initiate the experiments, free AA, formulations (AA free, AASLN, AANLC, RSPAASLN, RSPAANLC, RSPcAASLN and RSPcAANLC) in buffer solution, Hanks' balanced salt solution (HBSS) containing 25 mM 2-[4-(2-Hydroxyethyl)-1-piperazinyl]-ethanesulfonic acid (HEPES) (pH 6.5 for A to B; pH 7.4 for B to

A; 37 °C), was added to the donor compartment, and 2-[4-(2-Hydroxyethyl)-1-piperazinyl]-ethanesulfonic acid (HEPES) (pH 6.5 for apical side; pH 7.4 for basolateral side) was added to the receiver compartment (2.5 mL). The A to B samples were collected from the receiver compartment by complete replacement of the receiver volume with fresh buffer solution (37 °C) at 0, 15, 30, 60, 120, 240 and 360 min. The 200 µL of B to A samples were collected at 0, 120 and 240 min. In order to calculate drug uptake, after each of incubation, the medium was removed and the uptake process was stopped by washing the cells three times with ice-cold PBS (pH 7.4). The cells were then trypsinized with trypsin/EDTA, and solubilized with 1% TritonX-100. Total drug (AA) was quantified following method as described previously in section 2.7.3 (HPLC) (Chattopadhyay, et al., 2008).

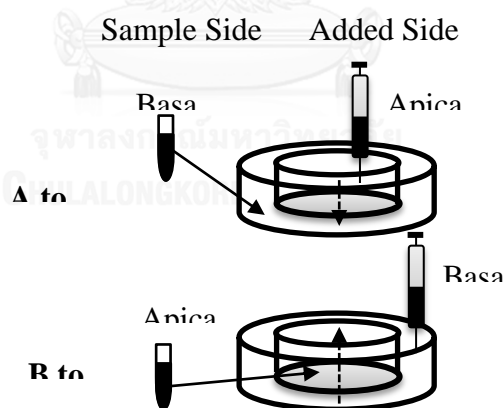


Figure 3.1 Schematic of dosing and sampling drug transport study (Wandel et al. 2002).

Flux was determined using receiver compartment compound steady-state permeability rate. Apparent permeability coefficient (P_{app}) (cm/s) across Caco-2 monolayers was calculated via the following equation

$$P_{app} = \frac{\Delta Q}{\Delta t A C_0} \dots\dots\dots \text{Equation 3. 8}$$

where $\Delta Q/\Delta t$ is a permeability rate ($\mu\text{g/s}$), C_0 is an initial concentration in the donor chamber ($\mu\text{g}/\text{cm}^3$), and A is a membrane surface area (cm^2).

Reverse ratio (RR) was computed as

$$RR = \frac{P_{app(B-A)}}{P_{app(A-B)}} \dots\dots\dots \text{Equation 3. 9}$$

where $P_{app(A-B)}$ is apparent permeability of Apical to Basolateral site and $P_{app(B-A)}$ is apparent permeability of Basolateral to Apical site (Buchanan et al. 2007).

2.8.5 Transepithelial electrical resistance (TEER) measurement

During the permeability experiment (section 2.8.4), the transepithelial resistance (TEER) was also studied. The resistance across the cell monolayers was measured at given intervals during experiment (0, 15, 30, 60, 120, 240 and 360 min) (Sha et al. 2005) to determine TEER value change using (Millicell®-ERS meter, Millipore, USA). The observed TEER values ($\Omega.\text{cm}^2$) were corrected with the blank filter resistance (Sirigul et al. 2015). The mean of TEER value of each group after treatment were statistically compared using ANOVA analysis and continued with post-hoc Bonferroni analysis.

2.8.6 Nanoaggregate size and zeta potential measurement of cAASLN/cAANLC redispersion (RSPcAASLN/RPScAANLC) before and after passing Caco-2 cells

In order to investigate the penetration of RSPcAASN/cAANLC through Caco-2 cells, measurement of nanoaggregate size of RSPcAASLN/RSPcAANLC and also their zeta potential before permeability study and after passing Caco-2 cells study was conducted. Before permeability study, RSPcAASLN and RSPcAANLC and their non-chitosan-based were measured for their average nanoaggregate size and zeta potential following procedure in section 2.3.3. In this experiment, monolayer Caco-2 cells were prepared in 6 TranswellsTM. One hundred μ L of RSPcAASLN and RSPcAANLC and their non-chitosan-based formulation (RSPAASLN and RSPAANLC) were placed on apical site of wells. After 2 h incubation, 1.5 mL of samples from basolateral site were taken then examined for their nanoaggregate size and zeta potential following method in section 2.3.3. The mean of nanoaggregate size and zeta potential was statistically compared using paired T-test analysis.

2.9 *In vitro* Absorption of cAASLN and cAANLC Redispersion (RSPcAASLN and RSPcAANLC) on bEnd3 Cells Cocultured with CTX-TNA2

In order to investigate the cytotoxicity, uptakes and permeability of drug model in the formulation through BBB, bEnd3 cells as a model of BBB were used. The procedure of this *in vitro* study followed the method below.

2.9.1 Cell culture

The bEnd3 (passage 33-34) (ATCC®) with density of 1×10^5 cells/cm² were seeded on a culture dish. Seeded bEnd3s were cultured with endothelial cell medium of Dulbecco's modified Eagle medium (DMEM) containing 10% fetal bovine serum (FBS), 1% endothelial cell growth supplement (Biocompare), 1% antibiotic penicillin-streptomycin solution (Sigma), 1% NEAA nonessential amino acid solution (Sigma), 1% l-glutamine (Sigma) and 1% sodium pyruvate (Sigma) in a humidified 5% CO₂ incubator at 37°C over 6 days (Chattopadhyay et al. 2008).

The bEnd3s were grown as a monolayer on 25cm² polystyrene cell culture flasks and 6 or 96 well plates. All cultures were maintained at 37°C in an atmosphere of 95% air and 5% CO₂. The culture medium was replaced on alternate days until the cells reached ~90% confluence. Confluent cultures were harvested by washing the cells with medium. The cells were then detached with a 0.25% trypsin-ethylenediamine tetraacetic acid (EDTA) solution for 3 min followed by reseeding in cultured flasks (Chattopadhyay et al. 2008).

2.9.2 Coculture of bEnd3 cells with CTX TNA2 cells

By following Li et al (2010), Chen et al. (2013) and Thongrangsalit et al (2015) methods, coculturing bEnd3 cell with CTX TNA2 cell as rat astrocytes cells were conducted. The bottom membrane filter of 6 Transwell™ (Corning Costar, USA) inserts (pore size 0.4µm, 4.67cm²) was coated with collagen type I (100 pg/filter) from Gibco®. Transwells™ filter

were incubated at 37 °C for 1 h to form gel. After that, the coated Transwells™ were placed in a laminar air flow cabinet and allowed to air dry.

CTX TNA2, a rat astrocytes cells, were seeded on the bottom of coated Transwells™ filter at density of 5×10^5 cells/filter. In the inverted position, the CTX TNA2 were allowed to adhere to the bottom of ≈ 1.5 h in an incubator (37°C) and then cultured upside position for 3 days before bEnd3 cells were seeded on top of filter. The bEnd3 were seeded at density of 5×10^5 cells/filter and cultured for over 6 days (Figure 3.2).

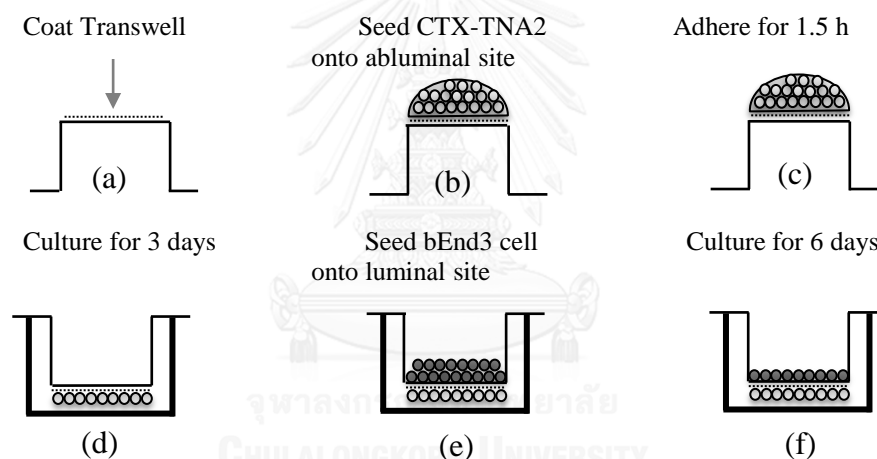


Figure 3.2 Coculturing of bEnd3 cells and CTX-TNA2 cells on different sides of the Transwell filter with $0.4 \mu\text{m}$ diameter pores. The Transwell filters were coated with rat tail collagen type I (a). CTX-TNA2 cells were seeded onto the abluminal side of the inverted Transwell™ filter at a density of 5×10^5 cells per filter, (b). allowed to adhere to 1.5 h, (c). filter was flipped back and the CTX-TNA2 were cultured for 3 days, (d). bEnd3 cells were seeded onto the luminal side of Transwell filter at a density of 5×10^5 cells per filter and (e). cocultured with astrocytes (CTX-TNA2) for an additional 6 days.

The bEnd3 and CTX TNA2 co-cultured cells were washed three times with HBSS and pre-treated with HBSS for 30 min at 37°C before the

experiments. TEER value was examined to investigate the tight junction and integrity of cells. High TEER value was required for transport properties across the BBB (Kuo and Wang 2010). A TEER value of BBB model for assessing drug delivery to the brain should be higher than $120 \Omega \cdot \text{cm}^2$ (Callahan et al. 2004).

2.9.3 Confocal Laser Scanning Microscopy (CLSM)

CLSM procedure of uptake and permeability studies of redispersed spray dried R6g loaded cSLN/cNLC followed the method as described previously in section 2.8.2. All of samples were obtained from the basolateral site of permeability study on Caco-2 cells. The penetration images of cR6gSLN/cR6gNLCs redispersion (RSPcR6gSLN/RSPcR6gNLC) in bEnd3 as brain blood barrier model were compared to their non-chitosan and R6gSLN and R6gNLC dispersion images.

2.9.4 Cell viability

Viability of bEnd3 cocultured with CTX-TNA2 cells in the presence or absence of free AA, blank as well as redispersed AASLN/AANLC in a period of 6 h was evaluated by a 3-[4,5-dimethylthiazol-2-yl]-2,5-diphenyl-tetrazoliumbromide (MTT) assay as previously described in section 2.9.3. One hundred μL of sample obtained from basolateral site of permeability study on section 2.8.4. of AA free, AASLN/AANLC, RSPAASLN/RSPAANLC and RSPcAASLN/RSPcAANLC were placed into 96 wells of bEnd3 cocultured with CTX-TNA2. The samples of blank group treatments, SLN/NLC blank, RSPSLN/RSPNLC blank, RSPcSLN/RSPcNLC

blank were obtained from similar technique to section 2.8.4. Cell viability in the presence of the various treatments was calculated as a percent of control cells by following calculation in section 2.8.3.

2.9.5 Permeability and uptake studies

Samples were collected from basolateral site of transport study of formulation on Caco-2 cells in section 2.8.4. AA loaded formulations (AA free, AASLN, AANLC, AASLN redispersion (RSPAASLN), cAASLNC redispersion (RSPcAASLN), AANLC redispersion (RSPAANLC) and cAANLC redispersion (RSPcAANLC) prepared in Hank's buffered salt solution (HBSS) was evaluated in confluent bEnd3 monolayer cocultured with CTX TNA2 cells. Cells were washed three times with Hank's buffered salt solution (HBSS) (pH 7.4, 37°C, 10 mM Hydroxyethyl-Piperazine Ethane sulfonic Acid (HEPES)) and pre-equilibrated in HBSS for 30 min. After the equilibration period, HBSS was removed and replaced with the mentioned previously above. Samples collecting, permeability calculating and drug accumulation in cells (drug uptake) were conducted following method that mentioned in section 2.8.4. TEER also was determined to evaluate TEER value change following method that mentioned in section 2.8.5. Results were reported as a mean \pm SD from a minimum of three independent experiments performed in monolayer cells pertaining to different passages. Differences among treatment group were considered significant at $p < 0.05$ using one way analysis of variance (ANOVA) with post-hoc Bonferroni analysis.

CHAPTER IV

RESULTS AND DISCUSSIONS

1. BMSLN, Chitosan and Non-Chitosan-based

Morphology of BMSLN under TEM (Figure 4.1a) illustrates that the SLN possessed spherical with some oblong shape and nanometer range diameter. Quite different surroundings of nanoparticles suggested the presence of polysorbates 80. This surfactant could be applied to modify the lipophilic surface of SLN into hydrophilic surface to avoid being coated by specific plasma components (opsonins), such as immunoglobulins (IgG), albumin, the elements of the complement system, fibronectin, and others, and then cleared from the blood stream by the phagocytic cells within minutes (Moghimi et al. 2001; Furumoto et al. 2004). After incubating SLN dispersion with 0.5% chitosan in 1% acetic acid, the surface of SLN became smoother and more be seen as a spherical structure (Figure 4.1b). Such bigger size droplet shown in Figure 4.1b was attributable to chitosan coating around SLN (cBMSLN) with hydrophilic surface of polysorbates 80. Aggregation might be possible occurred; the stickiness of the polymer may have contributed to the partial agglomeration (Sandri et al., 2010; Sarmiento et al., 2011; Fonte et al., 2011)

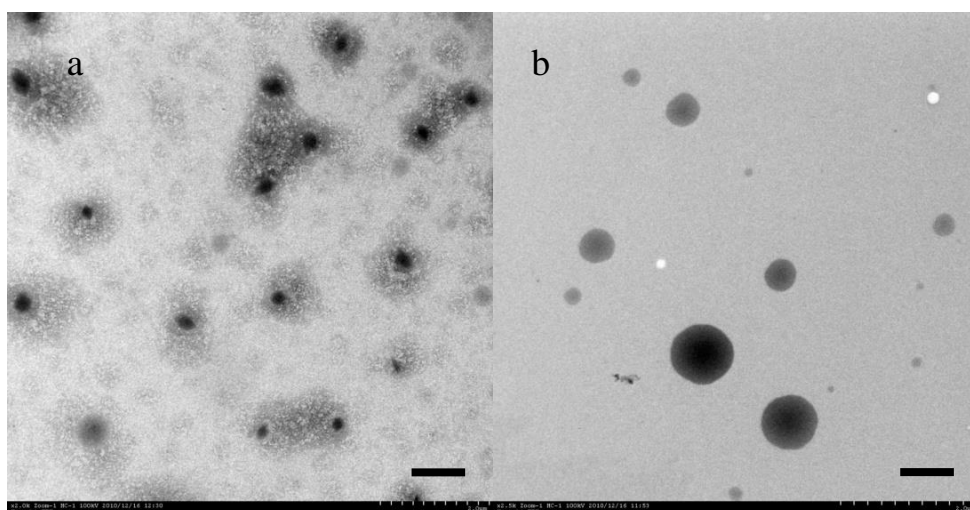


Figure 4.1 TEM characterization of a. SLN dispersion and b. SLN chitosan-based. Scale bars equal to 1.0 μ m.

In addition, the size of particles was noticeably larger. By nano-ZS zetasizer, the particle sizes of chitosan-based SLN (Table 4.1) were 110.5 ± 1.96 nm and 164.5 ± 2.23 nm for non-chitosan and 0.5% of chitosan-based SLN, respectively, (Table 4.1) corresponding to the photomicrographs. The zeta potential of chitosan coated SLN was changed to positive values due to the positive charge of chitosan which also consistently showed that chitosan was existed surrounding SLN (Table 4.1). According to Luo et al. (2011) findings, chitosan might adhere to polysorbate 80 and neutral lipid by hydrogen bonding. They found that chitosan oligo saccharide (COS) coated a neutral lipid of NLC (Compritol ATO 888, Miglyol 812 and Gelucire 44/14) by hydrogen bonding and hydrophobic interaction.

Table 4.1 Properties of SLN with low molecular weight chitosan, zeta potential and polydispersity (mean (n=5) \pm SD)

SLN system	Particles size (nm)	Zeta potential (mV)	PdI
SLN	110.51 \pm 1.96	-0.889 \pm 0.06	0.44 \pm 0.03
SLN + 0.5% chitosan	164.54 \pm 2.23	20.04 \pm 1.69	0.49 \pm 0.02

2. Experimental Design

In this work, a central rotatable composite design was chosen to describe the effects of variables in the spray drying of chitosan coated SLN (Box et al. 1978) using three factors of independent variables. This design offers an ease of investigation a high number of variables at different level with a limited number of experiments (Ahn et al. 2008). The levels of each factor were determined based on preliminary experiments (Table 3.2) The design containing 20 runs; i.e., 8 factorial points, six star points and six center points as shown in Table 4.2 was generated and analyzed by the statistical software package Design-Expert V. 8 (Stat Ease Inc., USA). Table 3.2 also shows experimental results the concerning three dependent variables ranged 31.00% to 85.56% by weight of yield, 254.6nm to 1586nm by size of redispersed nanoaggregates and 3.18% to 8.32% by weight of moisture content. Response surface methodology (RSM) was used to form a model depicting those responses of interest influenced by several significant independent variables.

The fitted models of equation chosen were based on the result statistical analysis shown in Table 4.2. The significant F ratio ($\alpha < 0.05$) of model p value and non-statistically significant lack of fit ($\alpha > 0.05$) of three models indicate that the model equations fitted the data well. The yield of product, moisture content and average nanoaggregate size of redispersed spray dried powder of cBMSLN responses were fitted with linear, quadratic and quadratic models, described in Equation 4.1, 4.2 and 4.3,

$$\text{Product yield} = 83.76 + 0.009 * X_1 - 0.48 * X_2 - 1.48 * X_3 \dots\dots\dots \text{Equation 4. 1}$$

$$\begin{aligned} \text{Moisture content} = & 30.15 - 0.42 * X_1 + 0.41 * X_2 - 0.04 * X_3 + 0.001 * X_1 X_2 \\ & + 0.01 * X_1 X_3 - 0.01 * X_2 X_3 + 0.001 * X_1^2 - 0.007 * X_2^2 \\ & + 0.002 * X_3^2 \dots\dots\dots \text{Equation 4. 2} \end{aligned}$$

$$\begin{aligned} \text{Nanoaggregate size} = & -6253.31 + 73.48 * X_1 + 42.91 * X_2 + 169.03 * X_1 X_2 \\ & - 0.01 * X_1 X_3 - 0.29 * X_2 X_3 - 0.31 * X_1^2 - 2.75 * X_2^2 \\ & - 3.30 * X_3^2 \dots\dots\dots \text{Equation 4. 3} \end{aligned}$$

where X_1 , X_2 and X_3 were inlet temperature, pump rate and feed concentration, respectively.

Results of optimization spray drying processes were likewise similar reported by Oomah and Mazza (2001). The second-order polynomial equation in terms of coded units the following equations were generated by the application of response surface methodology to obtain the empirical relationship between the experimental results on the basis of central composite design. In general, proceeding with exploration and optimization using a fitted response surface may produce unreliable results unless the model exhibits an adequate fit (Omwamba and Hu 2009).

Table 4.2 A rotatable central composite experimental design and responses; yield, nanoaggregatesize and moisture content of spray dried SLN in chitosan-based

Standard order	Run	X ₁	X ₂	X ₃	Design	Inlet Temperature (°C)	Feed rate (%)	Feed concentration (%)	Yield (%)	Average of Nanoaggregates size (nm)	Moisture content (%)
12	1	0	0	0	Center point	137.5	24.0	20.0	55.20	1448	4.09
3	2	-1	1	1	Factorial	115.0	32.0	10.0	61.30	311	8.32
9	3	0	0	0	Center point	137.5	24.0	20.0	55.80	1586	5.42
1	4	-1	-1	-1	Factorial	115.0	16.0	10.0	73.70	254.6	5.13
2	5	1	-1	-1	Factorial	160.0	16.0	10.0	77.80	282.2	5.38

Continue

Standard order	Run	X ₁	X ₂	X ₃	Design	Inlet Temperature (°C)	Feed rate (%)	Feed concentration (%)	Yield (%)	Average of Nanoaggregates size (nm)	Moisture content (%)
6	6	1	-1	1	Factorial	160.0	16.0	30.0	42.67	886.7	5.40
10	7	0	0	0	Center point	137.5	24.0	20.0	55.80	1445	5.15
4	8	1	1	-1	Factorial	160.0	32.0	10.0	64.80	293.7	4.86
8	9	1	1	1	Factorial	160.0	32.0	30.0	38.93	1297	5.92
11	10	0	0	0	Center point	137.5	24.0	20.0	53.10	1220	6.86
5	11	-1	-1	1	Factorial	115.0	16.0	30.0	40.50	1365	8.07
7	12	-1	1	1	Factorial	115.0	32.0	30.0	31.00	834.6	3.74
14	13	1.68	0	0	Star axial	175.3	24.0	20.0	60.15	1378	7.13

Continue

Standard order	Run	X ₁	X ₂	X ₃	Design	Inlet Temperature (°C)	Feed rate (%)	Feed concentration (%)	Yield (%)	Average of Nanoaggregates size (nm)	Moisture content (%)
6	6	1	-1	1	Factorial	160.0	16.0	30.0	42.67	886.7	5.40
10	7	0	0	0	Center point	137.5	24.0	20.0	55.80	1445	5.15
4	8	1	1	-1	Factorial	160.0	32.0	10.0	64.80	293.7	4.86
8	9	1	1	1	Factorial	160.0	32.0	30.0	38.93	1297	5.92
11	10	0	0	0	Center point	137.5	24.0	20.0	53.10	1220	6.86
5	11	-1	-1	1	Factorial	115.0	16.0	30.0	40.50	1365	8.07
7	12	-1	1	1	Factorial	115.0	32.0	30.0	31.00	834.6	3.74
14	13	1.68	0	0	Star axial	175.3	24.0	20.0	60.15	1378	7.13

Table 4.3 summarized the ANOVA analyses of the model of each response. All of model p values were significant on linear, quadratic and quadratic models that representation of product yield, moisture content and average nanoaggregate size model, respectively. And all the lack of fit test p value of each response also showed insignificance value.

Table 4.3 Statistical analysis of experimental design

Responses	Sources			
	Model p value	R^2	Lack of fit test p value	Model equation
Product yield	<0.0001	0.9668	0.0837	Linear
Moisture content	0.0400	0.7437	0.5463	quadratic
Nano aggregate size	0.0108	0.8208	0.0501	quadratic

The analysis of variance (ANOVA) of a linear model of product yield response was given in Table 4.4. The significance of each coefficient of the parameter was determined by F value and p value indicating that model terms were significant. The model F value of <0.0001 implied a significantly model. Inlet temperature (X_1), pump rate (X_2) and feed of concentration were significant model terms ($p < 0.05$). The significance of model p value ($p < 0.05$), the insignificant lack of fit model value ($p > 0.05$) and the high value of the R^2 (0.9668) indicated that the model was acceptable and fit with the experimental data (Table 4.4).

Table 4.4 Analysis of variance (ANOVA) of linear model of product yield response

Source	Sum of Squares	Df	Mean Square	F Value	p-value Prob > F
Block	83.62998	2	41.8149875		
x_1 -Inlet Temperature	61.08881	1	61.08880958	7.649921363	0.0152
x_2 -pump rate	199.949	1	199.9490043	25.03886014	0.0002
x_3 -feed concentration	2993.794	1	2993.7941	374.9015506	< 0.0001
Residual	111.7977	14	7.985547392		
Pure Error	4.87625	3	1.625416667		
Cor Total	3450.26	19			

Table 4.5 shows that the model was significant model ($p < 0.05$). The model F value of 0.0400 implied a significant model ($p < 0.05$) (Table 4.5). However, only interaction of pump rate and feed concentration (x_2x_3) and the x_1^2 were significant model terms ($p < 0.05$). Other were found to be insignificant ($p > 0.005$). The significant of model p value of 0.400 ($p < 0.05$) and the insignificant lack of fit model value of 0.5463 ($p > 0.05$) shown in Table 4.5, indicated that the model was acceptable and fit with the experimental data.

Table 4.5 Analysis of variance (ANOVA) of moisture content response

Source	Sum of Squares	Df	Mean Square	F Value	p-value Prob > F
Block	10.57670333	2	5.288351667		
x_1 -Inlet Temperature	0.71653217	1	0.71653217	0.9243	0.3645
x_2 -pump rate	0.129960479	1	0.129960479	0.167644	0.6930
x_3 -feed concentration	0.404204193	1	0.404204193	0.521408	0.4908
$x_1 x_2$	0.16245	1	0.16245	0.209554	0.6593
$x_1 x_3$	0.9248	1	0.9248	1.192957	0.3065
$x_2 x_3$	5.2488	1	5.2488	6.770754	0.0315
x_1^2	6.416831432	1	6.416831432	8.277471	0.0206
x_2^2	2.409168527	1	2.409168527	3.107737	0.1159
x_3^2	0.839916161	1	0.839916161	1.08346	0.3284
Residual	6.20173139	8	0.775216424		
Pure Error	2.3707	3	0.790233333		
Cor Total	34.77172	19			

The model F value of <0.0108 implied a significant model ($p<0.05$) (Table 4.6). Only feed of concentration (x_3) and its x_3^2 were significant model terms ($p<0.05$). Inlet temperature (x_1) and pump rate (x_2) were found to be

insignificant ($p>0.05$). However, the significant model p value of 0.0108 and the insignificant lack of fit model value 0.0501 ($p>0.05$) shown in Table 4.6, indicated that the model was acceptable and fit with the experimental data.

Table 4.6 Analysis of variance (ANOVA) of redispersed nanoaggregate size response

Source	Sum of Squares	Df	Mean Square	F Value	P value Prob > F
Block	49475.51	2	24737.75433		
x_1 -Inlet Temperature	84082.43	1	84082.43075	0.912222	0.3675
x_2 -pump rate	81585.54	1	81585.54175	0.885133	0.3743
x_3 -feed concentration	1061834	1	1061834.446	11.51999	0.0094
$x_1 x_2$	100307.2	1	100307.205	1.088247	0.3274
$x_1 x_3$	85.805	1	85.805	0.000931	0.9764
$x_2 x_3$	4418	1	4418	0.047931	0.8322
x_1^2	349506.8	1	349506.7555	3.791847	0.0874
x_2^2	447659	1	447658.9621	4.856714	0.0586
x_3^2	1570401	1	1570401.283	17.0375	0.0033
Residual	737385.8	8	92173.22418		
Pure Error	46084.5	3	15361.5		
Cor Total	4164871	19			

2.1 Validation of Model Equations

In order to validate the models, the following diagnostic plots were employed to confirm the fit models: 1) normal probability plot of studentized residuals, 2) studentized versus predicted values and 3) Cook's distance of run number, generated by Design Expert V.8. 05.

The plot of studentized residual versus normal % probability all of model described straight line indicating normally distribution residual (Figure 4.2). The unrevealed any pattern of the plot of studentized residuals versus predicted values of three models and the less than ± 3 value that shown in Figure 4.3, indicated that models were correct and the assumptions to build the models were satisfied (Montgomery 2005).

Cook's distance plots of all responses shown in Figure 4.4 were less than 1.00 indicating that run number did not influence the data response (Asasutjarit et al. 2007). Other diagnostic graphs (residual vs run, DFBETAS for intercept vs run and Box-Cox plot)) also show that the models were valid (see Appendix A). Therefore, these models of three responses generated from response surface methodology with the rotatable central composite design were applicable for following prediction of optimum condition set for spray drying BM-loaded SLN chitosan-based.

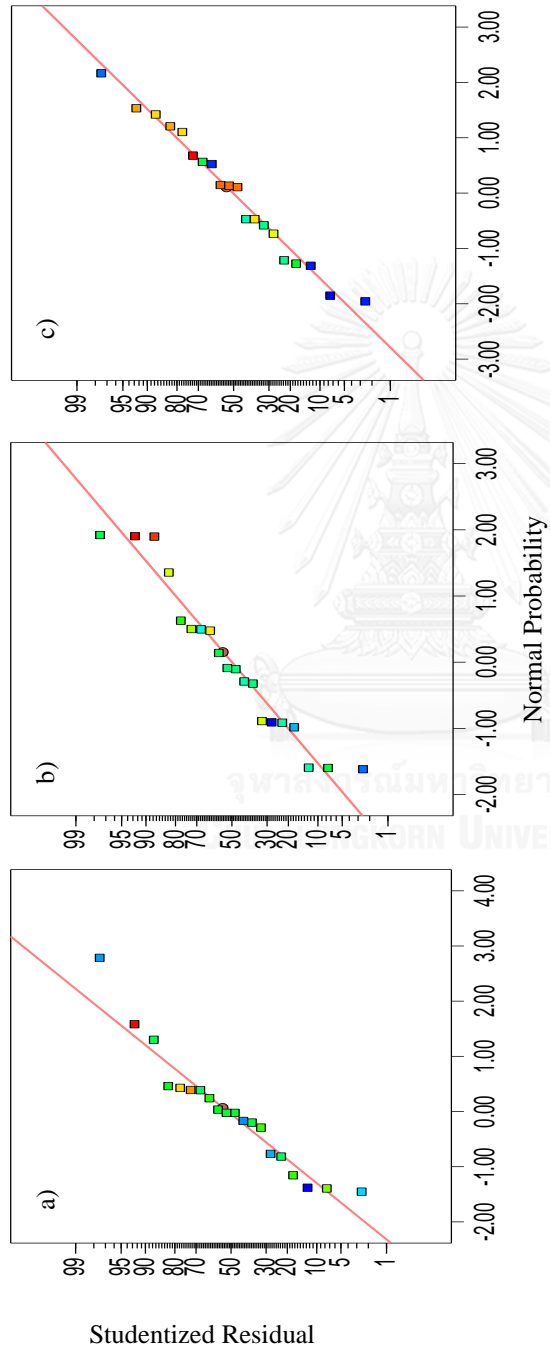


Figure 4.2 Normal % probability plot of model equation for a) Yield of product, b) moisture content and c) redispersed nanoaggregate size of spray dried powder cBMSLN

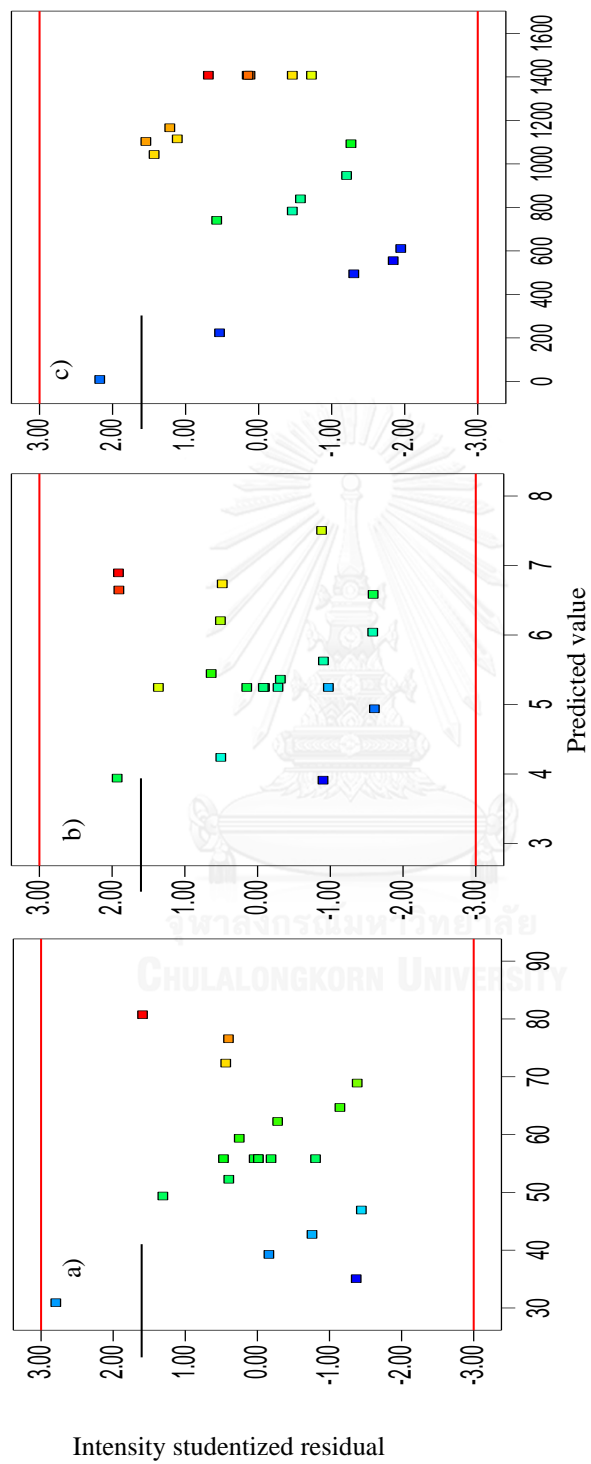


Figure 4.3 Plots of predicted values versus studentized residual; a) yield, b) moisture content and c) redispersed nanoaggregate size of spray dried powder cBMSLN

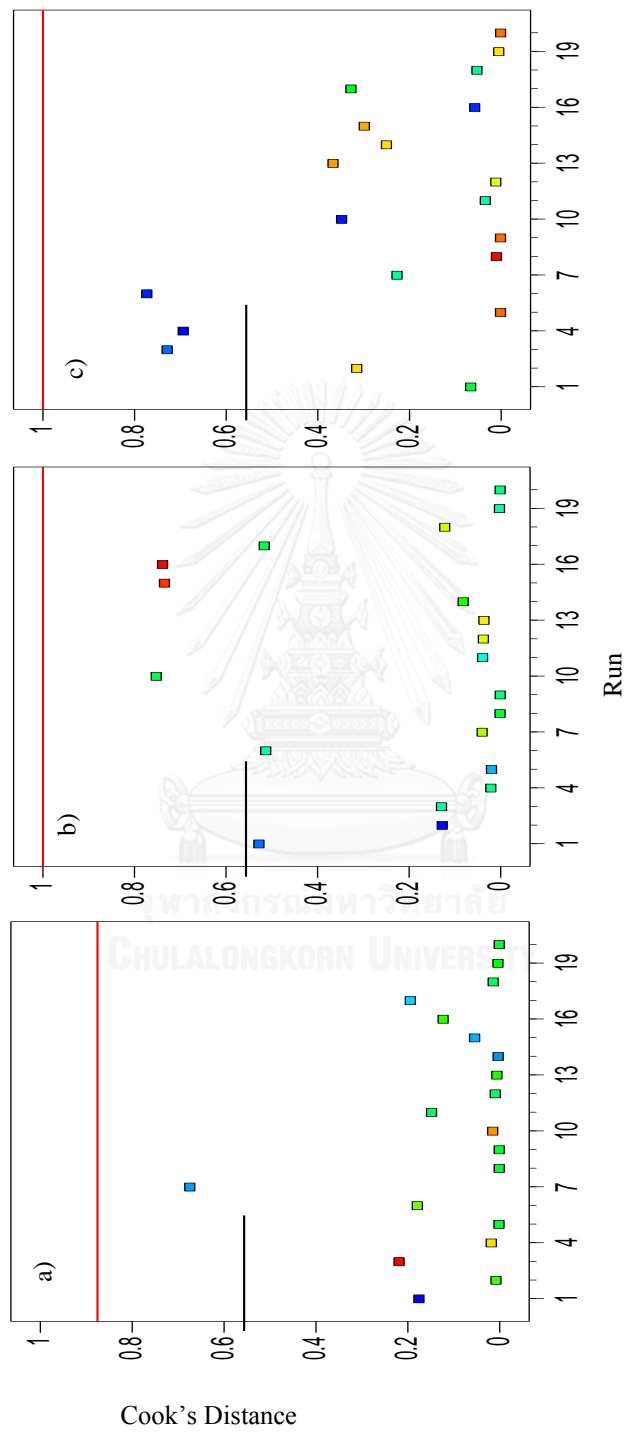


Figure 4.4 Cook's distance plots of three models; a) yield, b) moisture content and c). redispersed nanoaggregates size

In addition, an experiment was run to prove the prediction response values using these models. Table 4.7 comprises the experimental results and the prediction values. The observed values of redispersed nanoaggregate size and moisture content were correct with bias $\leq 5.0\%$.

Table 4.7 Comparison of the observed and the predicted values

Variables	Values	Response variables	Predicted value	Observed value	Bias (%)
Inlet temperature ($^{\circ}\text{C}$)	101	Product yield result (%)	54.12	56.85	5.0
Feed rate (%)	23	Moisture content (%)	7.43	7.11	4.3
Feed concentration (%)	19	Redispersed nanoaggregates (nm)	866.43	825.33	4.7

2.2 Selection of Optimum Formulation

With considering responses and variable condition, the criteria used to select optimized conditions of spray drying were the maximum product yield and minimum inlet temperature, pump rate, feed concentration, average size of nanoaggregates and moisture content. The Design Expert.V.8.05 generated some solutions to meet those criteria shown in Table 4.8. The ten solutions were presented in Table 4.8, the optimum parameters i.e. inlet temperature, pump rate and feed concentration ranged 115 to 118.68 $^{\circ}\text{C}$, 16-16.21% and 10-10.56%, respectively. These optimum conditions could be carried out to produce spray dried powder of containing BM loaded SLN chitosan-based.

Table 4.8 Solution of optimum condition of spray drying

No	Inlet temperature (°C)	Feed rate (%)	Feed concentration (%)	Yield of product (%)	Average of nanoaggregate size (nm)	Moisture content (%)	Desirability
1	115.00	16.00	10.00	72.1126	548.946	5.39274	0.833066
2	115.35	16.00	10.00	72.1452	553.242	5.36139	0.833006
3	116.06	16.00	10.00	72.2127	561.914	5.29738	0.832783
4	115.64	16.01	10.00	72.1691	557.002	5.33657	0.832759
5	116.65	16.00	10.00	72.2677	568.738	5.24628	0.832507
6	118.68	16.00	10.00	72.4585	590.798	5.07585	0.830938
7	115.00	16.00	10.16	71.8716	564.607	5.39529	0.828887
8	115.16	16.21	10.00	72.0271	555.736	5.41963	0.828269
9	115.77	16.00	10.56	71.3571	611.423	5.33352	0.818431

Continue

No	Inlet temperature (°C)	Feed rate (%)	Feed concentration (%)	Yield of product (%)	Average of nanoaggregate size (nm)	Moisture content (%)	Desirability
10	128.13	16.00	10.00	73.3465	660.107	4.42586	0.813381
11	130.51	16.00	10.00	73.5703	668.851	4.29928	0.806677
12	115.00	17.74	10.00	71.2827	581.184	5.71687	0.794536
13	144.34	16.00	10.00	74.8709	650.893	3.85896	0.74467
14	119.13	24.52	10.00	68.4277	616.316	6.28927	0.661601

3. Effects of Inlet Temperature, Pump Rate and Feed Concentration on Responses

In order to observe the influence of each parameter to response surface, The p value of coefficients of the regression fitting model design from Table 4.4, Table 4.5 and Table 4.6; and also the value of each coefficient in Equation 4.1, 4.2 and 4.3 were depicted. **Error! Reference source not found.** displays the 3D graphs generated from Design Expert V.8.05 to obtain the influence of process (inlet temperature and pump rate) and feed concentration.

3.1 Effects on % Product Yield

Table 4.4 shows significant ($p < 0.05$) linear impact of 3 parameters of spray drying (inlet temperature, pump rate and feed concentration). The value of coefficient number (Equation 4.1) showed the positive effect of inlet temperature and negative effect of pump rate and feed concentration.

Error! Reference source not found..1a and **Error! Reference source not found..1b** show increasing inlet temperature increased the product yield. The positive effect of inlet temperature showed that increased temperature led to a slight increase in product yield both at low and high level feed concentration or pump rate. This positive effect might be caused by increasing of the heat efficiency and mass transfer as showed in the following equation

$$q = h_s A (T_a - T_s) \dots\dots\dots \text{Equation 4. 4}$$

where q is the heat transfer rate in J s^{-1} , h_s is the surface heat-transfer coefficient $\text{J.m}^2.\text{s}^{-1}.\text{°C}^{-1}$, A is the area through which heat flow is taking place, m^2 , T_a is the air temperature and T_s is the temperature of the surface which is drying, (°C). The rate of the heat transfer was affected by air temperature. Air temperature can be increased by increasing inlet temperature. The adiabatic air drying efficiency (η) was defined by

$$\eta = (T_1 - T_2)/(T_1 - T_a) \dots\dots\dots \text{Equation 4. 5}$$

where T_1 is the inlet (high) air temperature into the dryer, T_2 is the outlet air temperature from the dryer, and T_a is the ambient air temperature. The numerator, the gap between T_1 and T_2 , is a major factor in the efficiency.

If the air drying is more efficient at high temperature, the potential pressure and concentration difference are also increasing. The rate of mass transfer is proportional to the potential difference as showed in the following equation

$$dw/dt = k'_g A dY \dots\dots\dots \text{Equation 4. 6}$$

where w is the mass being transferred kg s^{-1} , A is the area through which the transfer is taking place, k'_g is the mass-transfer coefficient in this case in units $\text{kg m}^{-2} \text{s}^{-1}$, and dY is the humidity difference in $\text{kg (of water). kg}^{-1}$ (of material).

Moreover, the lower of product loss with exhausted air and residue accumulation also were observed in the higher inlet temperature resulting higher product yield (Goula et al. 2003). This was consistent to the results

from Tonon et al. (2008) and Rocchia et al. (2014) that the inlet temperature was a positive and significant factor to affect product yield of spray drying natural oil.

Error! Reference source not found..1b and **Error! Reference source not found..1c** show the negative effect of the pump rate. Increasing pump rate resulted in lower product yield at low and high of inlet temperature and of feed concentration. Increasing pump rate caused ineffectiveness heat and mass transfer resulting in lower product. Lowering pump rate allowed to complete evaporation and decreasing the probability of dispersion condensation on the chamber wall, thus giving better product yield (Gallo et al. 2011). This finding was also consistently similar to Toneli et al (2010) that working with spray drying of inulin.

Error! Reference source not found..1a shows the effect of the negative effect on increasing of the amount of maltodextrin in the feed which resulted in lower product yield both at low and high level temperature. In this variable, the increasing feed concentration might be related to an increasing mixture viscosity which can decrease the effectiveness of drying process then resulted in lower product yield (Cai et al. 2000). The negative effect of feed concentration could be seen in Figure 4.5.1c which increasing feed concentration resulted in lower product yield at low and high pump rate.

3.2 Effects on Moisture Content

According to Equation 4.2, pump rate had a positive effect to moisture content, while inlet temperature and feed concentration had the

opposite effect. However, Table 4.5 shows that 3 spray drying parameters did not linearly significantly affect to moisture content of spray dried powder of BMSLN chitosan-based. Only the interaction of feed concentration and pump rate, and quadratic inlet temperature contributed significant effect to moisture content response.

Error! Reference source not found..2 shows a positive effect of feed concentration on moisture content in low pump rate and negative effect in high pump rate. This figure also illustrated that in low feed concentration, pump rate had a positive effect while in high feed concentration condition and pump rate had negative effect. The negative effect of interaction between feed concentration and pump rate might be related to ineffectiveness of the drying process which occurred in high concentration of feed and also time contact of feed and heat which is shorter contact lead less evaporation then resulting higher moisture content. (Hong and Choi 2007).

3.3 Effect on Nanoaggregate Size

Table 4.6 shows that only feed concentration and temperature had a significant effect on nanoaggregate size of RSPBMSLN chitosan-based, linear and quadratic, respectively. **Error! Reference source not found..3a** shows that increasing the concentration of maltodextrin in the feed had a markedly positive effect on average nanoaggregates size both in low and high level temperature. Lower feed concentration led to less amount of dried substance, thus less cohesion or agglomeration on the drying chamber after atomization causing smaller redispersed nanoaggregate size (Mosén et al.

2005). The effect of temperature on size was only slight opposed to the effect of feed concentration. Elevated temperature led to slightly larger size. The effect of pump rate on nanoaggregates size of redispersed spray dried powder showed a negative effect. The smaller size would be obtained when the pump rate increased both in low and high level temperature. It was probably assumed that the faster pump rate might cause higher collision of particles and avoid the formation of bigger mean diameter of nanoaggregates resulting in smaller nanoaggregate size.

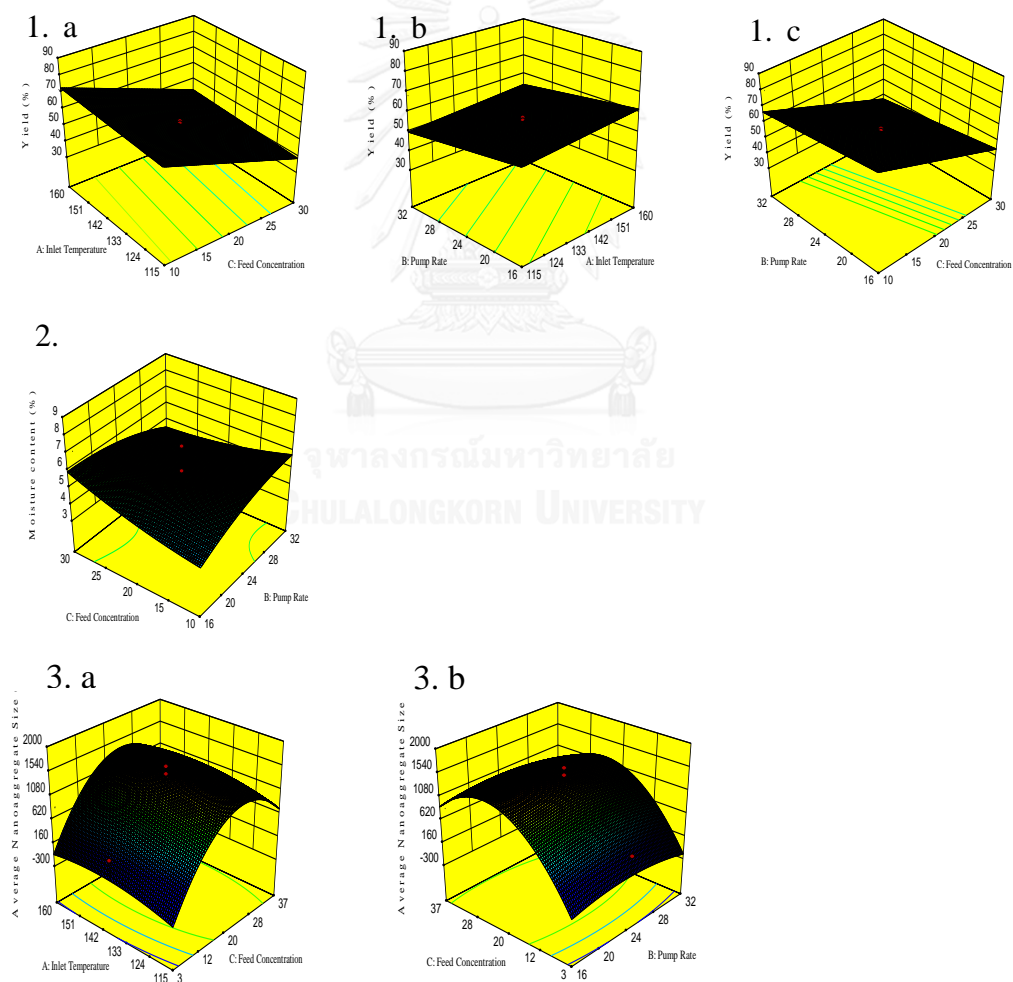


Figure 4.5 Response surface for 1. product yield of cBMSLN powder; a. effects of inlet temperature and feed concentration, b. effects of feed rate and inlet temperature, c. effects of inlet temperature and feed rate, 2. A. effect of feed concentration and feed rate on moisture content, 3. nanoaggregate size of RSPcBMSLN; a. effect of inlet temperature and feed concentration, b. effect of feed concentration and feed rate.



In order to see clearly the effect those three independents (inlet temperature, feed concentration and feed rate) on nanoaggregate size of redispersed spray dried BM-SLN chitosan-based, 2D response graphs also can be depicted (see Appendix B).

4. Characterization of Spray Dried Powder of cBMSLN and cBMNLC

4.1 Physical Characterizations

4.1.1 Size, moisture and product yield characterizations

Table 4.9 shows the characterization between spray dried powder of SLN and NLC loaded BM. Using the same ratio of lipid (Table 3.1) and process as SLN production, NLC droplets showed smaller size than SLN droplets. The smaller size of BMNLC than BMSLN might be caused by the easier of surfactant properties in contact with the present oil (liquid lipid) in NLC replacing the molten solid lipid than with the only molten lipid in SLN. However, according to PDI value (Table 4.9), SLN dispersion is more uniform size (0.44 ± 0.03) than NLC dispersion (0.53 ± 0.10). The more uniform in BMSLN may be due to the less of BM loading than in BMNLC. Zeta potential value of SLN showed small negative charge at -0.89 ± 0.32 mV indicating that SLN would have slightly less stable dispersion system than NLC which has higher positive charge at 5.37 ± 0.82 mV. These differences zeta potential might be caused by the difference charge of the lipid components. The Adding 0.5% chitosan on both of BMSLN and BMNLC dispersion resulted bigger size of nanoparticles than their original size (164nm and 158nm vs 112nm and 101nm). Size of redispersed of spray dried

powder of BMSLN (RSPBMSLN) and cBMSLN (RSPcBMSLN) was bigger than the size of redispersed spray dried powder of BMNLC (RSPBMNLC) and cBMNLC (RSPcBMNLC) might be contributed by bigger size of BMSLN droplets at $112.70 \pm 3.56 \text{ nm}$ vs BMNLC at 101 nm . The positive charge of both RSPcBMSLN and RSPcBMNLC caused by the positively charged of chitosan that deposited at their nanoaggregate surface. Higher positively charged of nanoaggregates can lead to rapid electrostatic interaction with negatively charged mucin on small intestinal membrane (Artursson et al. 1994; Ranaldi et al. 2002). The high number of zeta potential over than 20 mV also indicated that the redispersion of spray dried powder of both cBMSLN and cBMNLC was potentially stable size (Müller and Jacobs 2002). The PDI value of RSPcBMSLN (0.41 ± 0.09) was slightly less than the spray dried BMNLC value (0.46 ± 0.16) stating that RSPcBMSLN was less uniform than RSPcBMNLC.

Table 4.9 Comparison of parameter of SLN and NLC system and their redispersed spray dried powder (mean (n=5) \pm SD)

Formulation	Prepared lipid Nanosystem				Redispersed nanoaggregates			
	Size (nm) \pm SD	ZP (mV) \pm SD	PdI \pm SD	DEE (%) \pm SD	Size (nm) \pm SD	ZP (mV) \pm SD	PdI \pm SD	DR (%) \pm SD
BMSLN	112.70 \pm 3.56	-0.89 \pm 0.32	0.44 \pm 0.03	86.33 \pm 0.07	569.10 \pm 19.50	-7.37 \pm 0.31	0.37 \pm 0.07	22.87 \pm 0.61
cBMSLN	164.5 \pm 2.23	20.0 \pm 1.69	0.49 \pm 0.02	63.87 \pm 0.59	662.71 \pm 94.79	19.37 \pm 3.80	0.41 \pm 0.09	47.44 \pm 0.55
BMNLC	101.62 \pm 5.26	5.37 \pm 0.82	0.53 \pm 0.09	90.09 \pm 4.96	468.70 \pm 21.13	-9.41 \pm 1.57	0.41 \pm 0.11	46.12 \pm 1.38
cBMNLC	158.7 \pm 3.89	18.4 \pm 1.23	0.55 \pm 0.10	64.80 \pm 0.38	594.96 \pm 63.83	14.84 \pm 1.23	0.46 \pm 0.16	62.44 \pm 0.76

Figure 4.6 shows the log-normal volume distribution of nanolipidic systems and the nanoaggregates of their powder redispersions. Both the nanoaggregate size of BMSLN and BMNLC redispersion systems show increasing size compared to the original size of their BMSLN and BMNLC (Figure 4.6 and Figure 4.7). Figure 4.6 shows that majority of redispersed BMSLN and cBMSLN powder formed nanoaggregates have peak size at 412nm for redispersed of BMSLN powder and 477nm for redispersed of cBMSLN powder. However, even nanosize distribution that disclosed to the origin of their nanolipidic size also could be observed with and without chitosan. It is indicated that spray drying BMSLN and cBMSLN can be partially redispersible and reach nanosize distribution. Similar results also can be observed in log-normal of volume distribution of BMNLC systems

(Figure 4.7). Nanosize distribution peak was observed in the original size of nanoparticles (BMNLC) verifying that spray dried powder of BMNLC could be partially redispersed. Compared to redispersed of BMSLN systems, redispersed of BMNLC systems have better volume distribution of redispersible fraction (Figure 4.7) with smaller size of nanoaggregate particles, 265nm for redispersed of BMNLC and 412nm for redispersed of cBMNLC.

The increasing size after spray drying might be due to the heat involved in the drying process. The inlet temperature was 115°C and the outlet temperature was 50-60°C. This temperature was possible to melt SLN and NLC droplets containing lipids i.e. tristearin which has a melting point at 54.5°C (α), 64.3°C (β^*) and 73.1°C (β), trimyristin at 32.0°C (α^*), 44.0°C (β^*) and 55.5°C (β) (Lutton 1945). The small size of nanoparticles fused to bigger droplets and made aggregates. The aggregation of SLN or NLC during spray drying might occur from removal water that switched the properties of surfactant layer coating (Lee et al. 2003) and might reduce its repulsion and stabilization effects to their dry powder redispersion (Tewa-Tagne et al. 2007a).

If we compared the amount percent of volume distribution of BMSLN systems (Figure 4.6) to BMNLC systems (Figure 4.6), it was observed that SLN systems showed a higher amount of percent volume distribution than NLC systems. The difference lipid composition between BMSLN and BMNLC may be due to the particles density of obtained powder

which affected to amount percent of volume distribution when they were redispersed (Chen 2004). Figure 4.6 and Figure 4.7 show that the percent volume distribution of RSPcBMSLN and RSPcBMNLC was less than the percent volume distribution of RSPBMSLN (1.3% and 19.5% vs 0.7% and 19.2%) and RSPBMNLC (5.8% and 18.6% vs 3.7% and 17.8%). The stickiness of chitosan may contribute to the loss of product yield resulting in less amount of percent volume distribution of chitosan-based spray dried powder of BMSLN and also of BMNLC.

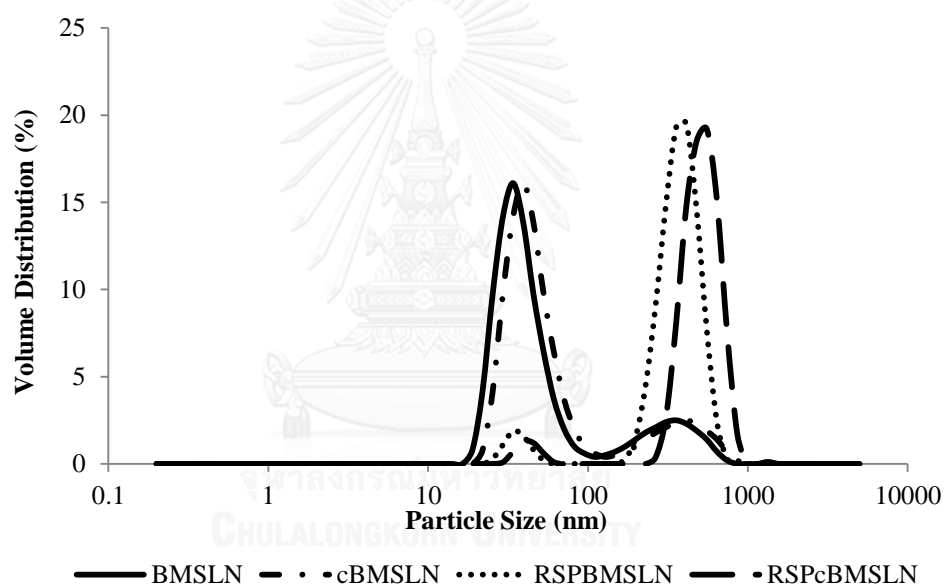


Figure 4.6 Normal size distributions by volume of BMSLN systems

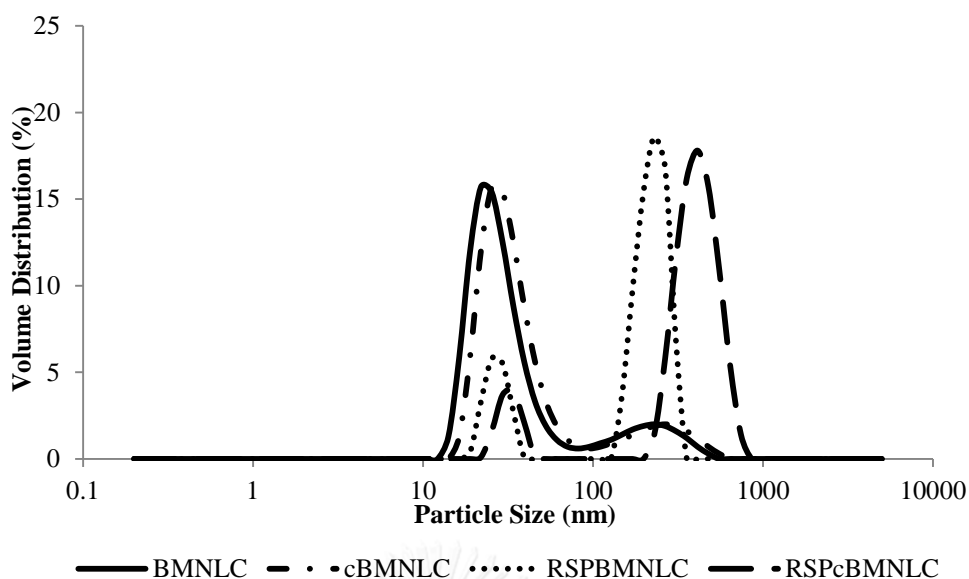


Figure 4.7 Normal size distributions by volume of BMNLC systems

Table 4.10 shows spray dried powder characterization of SPBMSLN and SPBMNLC with and without chitosan as base. Incorporating chitosan on either BMSLN or BMNLC increased the size of powder. The mean ($d(4,3)$) and the median ($d(0.5)$) of cBMSLN and cBMNLC powder showed micron size at $4.99\mu\text{m}$ and $5.09\mu\text{m}$ while the BMSLN and BMNLC powder were smaller at $4.74\mu\text{m}$ and $4.77\mu\text{m}$, respectively. As explained previously that incorporation chitosan into BMSLN or BMNLC also increased the nanoparticles size (Table 4.9), this cause also can explain the increasing size on spray drying cBMSLN and cBMNLC.

Adding chitosan to both systems (BMSLN and BMNLC) gave significantly less yield product. The adhesive effect of chitosan might contribute to less yield product. The adhesive effect also affected the flowability of the powder. The higher CI of SPBMSLN/SPBMNLC chitosan-based than their non-chitosan-based indicated that incorporating chitosan

giving less powder flowability. According to CI number, all spray dried powder still have good flowability (less than 40) (Podczeck 1998) but for comparison, spray dried powder of BMNLC system showed higher CI number indicating less flowability than spray dried powder of BMSLN systems. The liquid lipid involved in BMNLC lipid nanoparticles might contribute to this different flowability characteristic. The moisture content of both systems showed no significantly different ($p>0.05$). According to the percentage yield of the result indicated that spray drying process on BMSLN is more effective than on BMNLC.

Table 4.10 Spray dried BMSLN and BMNLC (mean (n=5)+SD)

Formulation	Yield (%)	Moisture Content (%)	SPAN	d(4,3)	Uniformity	d(v,0.5)	CI (%)
SPBMSLN	70.61 ±0.56	5.04 ±0.20	1.43 ±0.02	4.74 ±0.09	0.46 ±0.01	4.34 ±0.06	23.33 ±3.81
SPcBMSLN	68.21 ±0.78	5.40 ±0.27	1.44 ±0.05	4.99 ±0.24	0.47 ±0.03	4.52 ±0.14	26.67 ±3.81
SPBMNLC	68.45 ±2.26	5.17 ±0.82	1.44 ±0.06	4.77 ±0.07	0.45 ±0.02	4.38 ±0.09	25.00 ±2.5
SPcBMNLC	65.30 ±1.01	5.21 ±0.41	1.38 ±0.04	5.09 ±0.12	0.44 ±0.01	4.68 ±0.11	28.75 ±3.31

4.1.2 SEM analysis

It is important to see how the formulation and condition of drying process effect on the surface morphology. Examination of SEM micrographs showed that particles size of spray dried powder of BM-SLN and NLC powder ranged

powder ranged from 0.3 μ m to 2 μ m approximately. The outer topography of spray spray dried capsules was affected and differentiated by wall composition of SLN or SLN or NLC (

Figure 4.8.1-4b).

The SEM photomicrographs of the spray dried samples from optimum conditions of optimum conditions of temperature at 115⁰C, 16% pump rate and 10% feed concentration are shown in

Figure 4.8.1-4b. After spray drying, cBMSLN and cBMNLC might undergo aggregation to larger size and with maltodextrin formed micron size particles. However, SPcBMNLC (

Figure 4.8.4b) showed a smoother surface than the one of SPcBMSLN (

Figure 4.8.2b). The liquid lipid in NLC particles could be more soften and round up on powder formation during spray drying process leading to a smoother surface of surface of microspheres. Incorporated chitosan into SLN and NLC systems resulted in resulted in rough, less porous but larger powder (

Figure 4.8.2b and

Figure 4.8.4b) than the unincorporated one (

Figure 4.8.1b and

Figure 4.8.3b) due to increasing viscosity of BMSLN and BMNLC (Mi et al. 1999).

The microsphere-shaped powder contributes the flowability which affecting consistency weight in filling into capsule or tableting process (Gonnissen et al. 2007).

al. 2007). In addition, spray dried powders with positively charged chitosan also also showed significantly higher zeta potential than those without chitosan. All

All powders had a spherical shape with quite narrow bimodal volume distribution size distribution size according to the spraying droplet (

Figure 4.8.1-4a).

All powders had a spherical shape with quite narrow bimodal volume distribution size according to the spraying droplet (

Figure 4.8.1-4a). The volume distribution of spray dried powder of BMNLC systems (SPBMNLC and SPcBMNLC) was narrower volume distribution than BMCLN systems (

Figure 4.8.3a and

Figure 4.8.4a vs

Figure 4.8.1a and

Figure 4.8.2a). It is indicated that spray dried powder BMNLC systems were more uniform than spray dried powder of BMSLN systems. The data at Table 4.10 also show the less number of uniformity value of spray dried powder of BMNLC systems than BMSLN systems with and without chitosan (0.45 and 0.44 vs 0.46 and 0.47). Less SPAN value of spray dried powder cBMNLC as Table 4.10 (1.38) indicated that the spray dried cBMNLC showed better homogeneity than other systems.

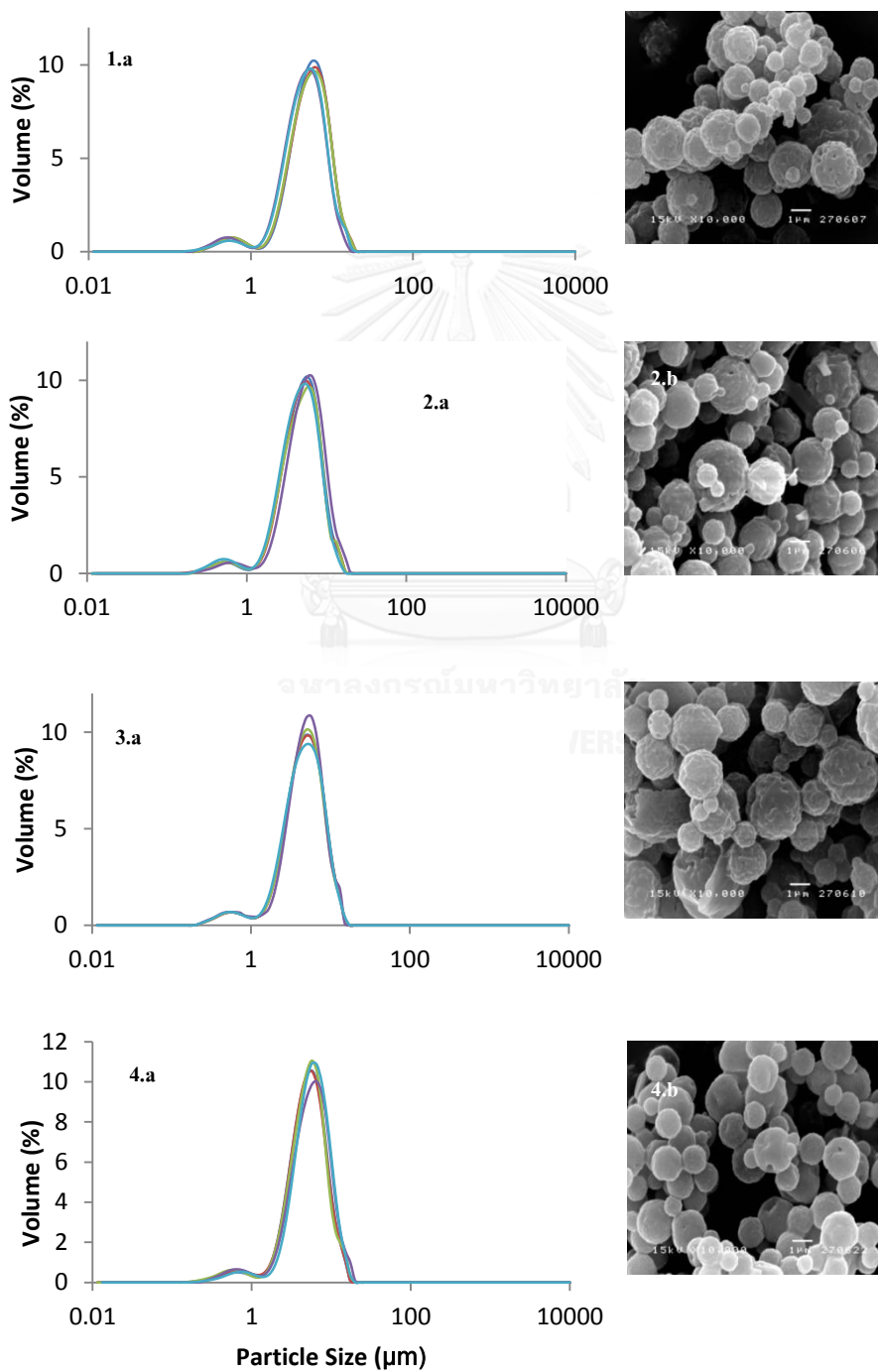


Figure 4.8 Log-normal size distribution by volume graph (a) and SEM characterization (b) of spray dried nanosystems of : 1) BMSLN, 2) cBMSLN, 3) BMNLC, 4) cBMNLC.



4.1.3 TEM analysis

Morphology of BMSLN and BMNLC under TEM (Figure 4.9.1a and Figure 4.9.2a) illustrates that both of BMSLN and BMNLC had spherical with some oblong shape and nanometer range diameter. The presence of polysorbate 80 to modify the surface into hydrophilic surface was shown in Figure 4.9.1a and Figure 4.9.2a. This surface modification was intended to avoid BMSLN and BMNLC from being coated by specific plasma components (opsonins) and then cleared from the blood stream by the phagocytic cells within minutes (Moghimi et al. 2001; Furumoto et al. 2004). The presence of chitosan as a cationic polymer and mucoadhesion properties was also seen in Figure 4.9.1b and Figure 4.9.2b.

The redispersed nanoaggregates of spray dried BMSLN chitosan-based (Figure 4.9.1d) had a smoother and rounder surface than of non-chitosan-based (Figure 4.9.1c) followed by those of spray dried BMNLC chitosan-based (Figure 4.9.2c) and non-chitosan-based (Figure 4.9.2b), respectively. The nanoaggregates of both former systems showed more dense solid aggregation of appearance than latter systems indicating of possibly less stability of later systems than the formers. However, all 4 systems still showed round surface which might give positive effect on dissolution and permeation (Mosharraf and Nyström 1995). Chithrani and Chan (2007) also found that the uptake spherical nanoparticles were higher than nanorods shape particles. It indicated that the shape of nanoparticles affected on permeability and also drug uptake.

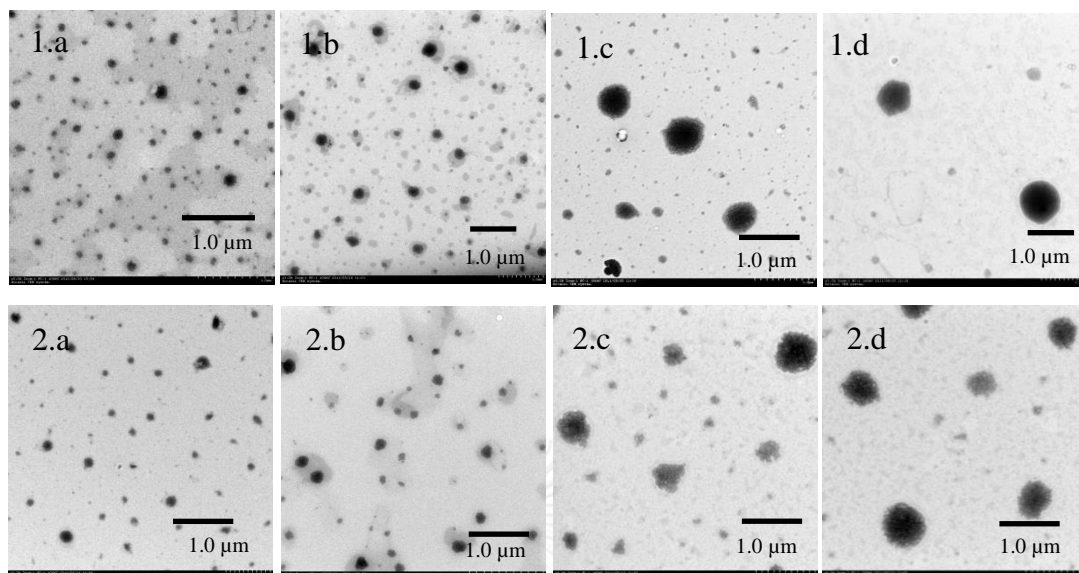


Figure 4.9 TEM characterization of 1.a, BMSLN dispersion 1.b redispersed spray dried of BMSLN (RSPBMSLN) 1.c redispersed spray dried of cBMSLN (RSPcBMSLN) and 2.a BMNLC dispersion, 2.b redispersed spray dried of BMNLC (RSPBMNLC) 2.c redispersed spray dried of cBMNLC. (RSPcBMNLC)

4.2 Chemical Properties Characterization

4.2.1 BM assay method

Specificity The chromatogram of BM was free of interference from excipients. The peak of BM was symmetrical (Figure 4.10). The retention time of the peak was reached at 6.19 to 6.298 min. The observation indicated the assay had adequate specificity.

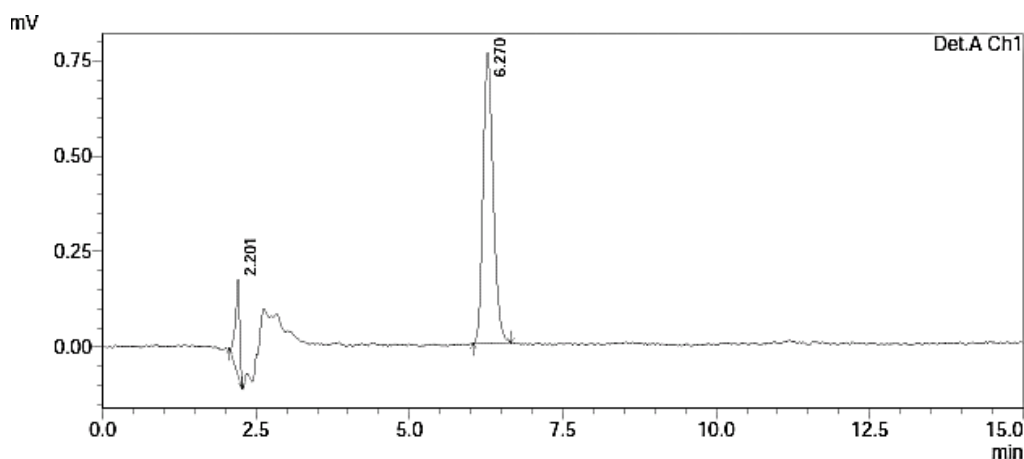


Figure 4.10 Chromatogram of bromocriptine mesylate (HPLC condition of acetonitrile: 10 mM buffer ammonium = 70:30, v/v, flow rate 1.0 mL/min, detected 300nm).

Linearity Calibration of BM was linear in range 2 – 10 $\mu\text{g/mL}$. The standard curve of concentrations ($\mu\text{g/mL}$) against AUC (area under curve) was $y = 10609x + 4410.20$ with $r = 0.9982$ ($n=5$), where x was concentration ($\mu\text{g/mL}$) and y was AUC (Figure 4.11). The regression parameters of the linearity of the method were reported in Table 4.11.

Table 4.11 Regression parameters of the linearity of system

Regression Parameters	Day 1	Day 2	Day 3	Mean \pm SD
Slope	10609	10252	10629	10496.67 \pm 212.12
Y-intercept	4410.20	4401.9	4477	4429.7 \pm 41.17
Correlation coefficient (r^2)	0.9982	0.9989	0.9983	0.9985 \pm 0.0004

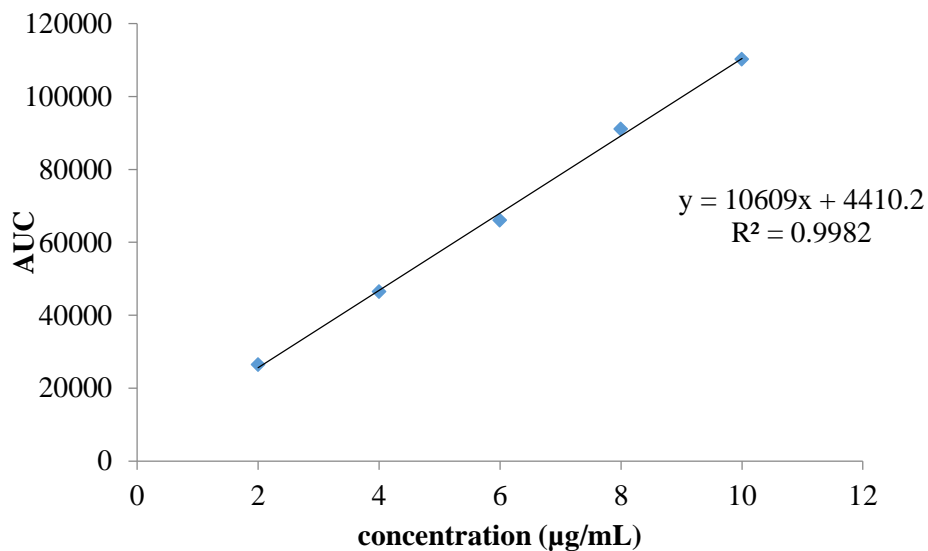


Figure 4.11 Standard Curve of BM (HPLC condition of acetonitrile: 10 mM buffer ammonium = 70:30, v/v, flow rate 1.0 mL/min, detected 300nm).

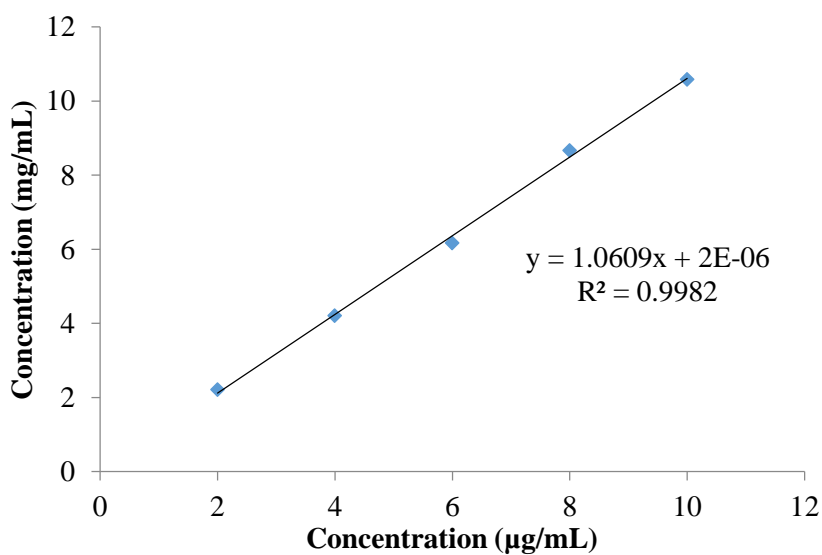


Figure 4.12 The calibration curve was shown the linearity of the method (HPLC condition of acetonitrile: 10 mM buffer ammonium = 70:30, v/v, flow rate 1.0 mL/min, detected 300nm).

4.2.2 Drug Entrapment Efficiency (DEE)

The drug entrapment efficiency (DEE) of dry powder of SLN loaded BM was $86.33 \pm 0.07\%$ and the DEE of BM loaded NLC was $90.09 \pm 4.96\%$ (Table 4.9). It is indicated that in the process of both lipid nanoparticles could make the drug (BM) be well-entrapped into the lipid nanoparticles. It might be caused by the more soluble BM in the lipophilic phase of NLC which contained solid matrix and liquid lipid than in SLN which only contained solid lipids. As it also had been reported by Jennings et al. (2000) that addition of liquid lipid to the lipophilic phase combined the advantages of the solid matrix prevented drug leakage, and of the liquid regions (oily compartments) also showed comparatively high solubility for lipophilic drugs (Jennings et al. 2000). During the cooling process after homogenization, solubility of drug was decreased. Reducing drug solubility leads to drug expulsion from lipid nanoparticles. Solubility of various drugs in liquid lipids is higher than in solid lipids. So, BMNLC which consisted of solid and liquid lipid had higher DEE value than BMSLN.

4.2.3 Drug retention

The drug retention of SPBMSLN with and without chitosan-based were $47.44 \pm 0.55\%$ and $22.87 \pm 0.61\%$, respectively, while those from NLC systems, with and without chitosan-based were $62.44 \pm 0.76\%$ and $46.12 \pm 1.38\%$, respectively, as listed in Table 4.10. Chitosan as biopolymer has gel property which is important in the protection of encapsulated drug from degradation during spray drying process by forming a skin around the

droplets which absorbs most of the heat and thus could prevent drug degradation (Zhang et al. 2008). Except to control the nanoaggregates size, the gel properties of chitosan could avoid the deformation of SLN/NLC that might happen during spray drying (Mosén et al. 2005). This deformation of SLN and NLC also could lead to drug release or drug expulsion. In addition, the comparison result between SLN and NLC systems showed that after spray drying processes NLC system which has higher entrapment efficiency could protect BM from expulsion during spray drying processes.

During spray drying the small size of nanoparticles might fuse to bigger droplets and made aggregates. This condition not only led increasing mean diameter of nanoaggregate size as mentioned previously but also releasing some drug out from droplets. NLC which has liquid lipid (oil) component in it, the lipid nanoparticles might be fused more smooth and did not cause drug expulsion than SLN which only has solid lipid. Meanwhile, BM itself is unstable in associated with light and heat which has not exactly melting point but it will melt in the range of 180-230 °C (Florey 1979). In the condition of spray drying with inlet temperature 115⁰C and outlet temperature 50-60°C, it is possible that un-entrapped BM and the expelled drug from lipid droplet underwent degradation during spray drying.

6. Development and Comparison of Spray Drying and Nanospray Drying BMSLN and BMNLC Chitosan-based

Another limitation of spray drying BMSLN and BMNLC was the big size of redispersed nanoaggregates. A novel technology of spray dryer was introduced by Buchi Company in order to reduce the nanoaggregates size of redispersed spray dried powder of BMSLN and BMNLC chitosan.

6.1 Characterization and Comparison of Spray Drying and Nanospray Drying of BMSLN and BMNLC Chitosan-based

6.1.1 Size, zeta potential and polydispersity characterization

Adjustments to BMSLN and BMNLC production to acquire smaller BMSLN and BMNLC droplets than the previous displayed in Table 4.9 were successfully shown in Table 4.12. The BMSLN was significantly larger than BMNLC ($p < 0.05$). Smaller initial size of BMSLN and BMNLC for this study was caused by the increasing cycles on hot high pressure homogenizing process. Unlike as expected, the PDI value of SLN was also higher than PDI value of NLC that indicating the BMSLN has broader size distribution than BMNLC. The zeta potential of both systems was positive on both systems, BMSLN and BMNLC but still counted as low value of zeta potential. Zeta potential is important information to predict the size stability during storage (Thode et al. 2000). The well-stabilized nanoparticles have zeta potential in the range of -15-30 mV (Kesisoglou et al. 2007).

Table 4.12 The size of SLN and NLC dispersion (mean±SD)

Formula	Particles size (nm)	Zeta potensial (mV)	Polydispersity Index (PdI)
BMSLN	89.85±1.87	6.59±0.50	0.54±0.01
Lipid Nanoparticles			
BMNLC	84.66±1.63	3.16±0.58	0.42±0.04

After spray drying, SLN and NLC size underwent aggregation which led to increasing average size. Table 4.13 shows the different size of redispersed nanoaggregates between two kinds of nanoparticles systems (BMSLN and BMNLC) and different apparatus of spray dryer. From Figure 4.13, it can be seen that incorporating BMSLN and BMNLC systems with chitosan as basis showed significantly higher average size than non-chitosan both in using a spray dryer and a nanospray dryer ($p < 0.05$). However, there were some interesting findings, different type of nanoparticles showed different nanoaggregate size. BMSLN which had larger droplet size produced significant ($p < 0.05$) larger nanoaggregate size than BMNLC. Interestingly, using nanospray dryer produced significantly smaller size of nanoaggregates only on BMSLN system. On BMNLC system, using nanospray dryer produced non-significant ($p > 0.05$) smaller nanoaggregate size (Appendix G). According to produce smaller nanoaggregate size, the different type of nanoparticles (SLN and NLC) is more significant to give effect than the type of apparatus of spray dryer that used. The different type of lipid that used in

the initial nanoparticles might behave differently producing different redispersion powder.

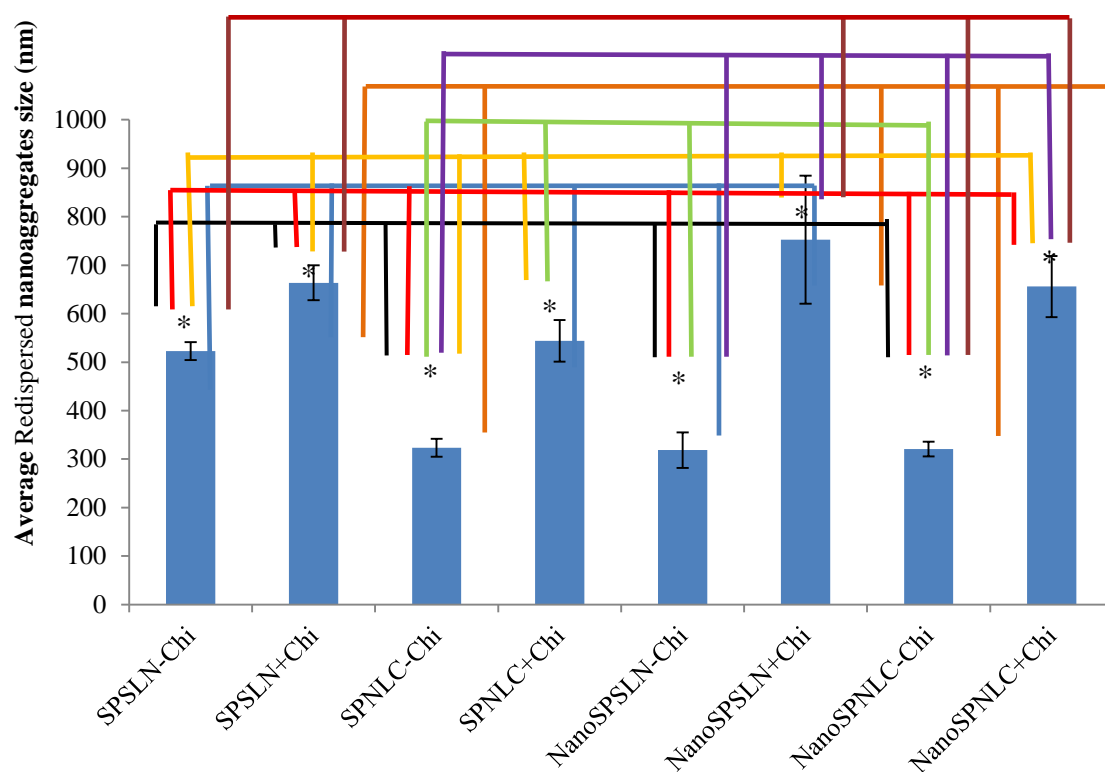


Figure 4.13 Significance difference of average nanoaggregate size of spray and nanospray dried powder. * = significant at $p < 0.05$.

6.1.2 SEM characterization

There were 4 types of morphologies observed: (a) smooth spherical, (b) smooth-collapsed, (c) porous spherical and (d) semi-hollow spherical (Figure 4.19). Smoother surface of spray/nanospray dried in BM-SLN or NLC was obtained from formulations with added chitosan. The collapsed surfaces tend to be seen on using spray dryer rather than nanospray dryer. Less concentration of maltodextrin than the previous experiments (spray

dried cBMSLN and spray dried cBMNLC with 10% solid) showed slightly porous surface (Figure 4.19d, 4.19g and 4.19h). It might be also related to higher stability of the drug since it was reported by Wagner and Warthesen (1995) that higher concentration of maltodextrins provided protection against to the core of oxidation. Using biopolymer of chitosan is not just giving advantage on chemical properties but also on physical properties such as surface smoother topography. The incorporated BMSLN or BMNLC with chitosan especially in nanospray dried powder showed less porous than the unincorporated ones.



Table 4.13 Nanoaggregate size of redispersed nanoggregates of SLN and NLC after spray drying, % yield and moisture content

Formula	Spray Dry			Nano Spray dry		
	Nanoggregates size mean±SD (nm)	Yield (%)	Moisture content (%)	Nanoggregates size mean ±SD(nm)	Yield (%)	Moisture content (%)
SLN	in chitosan-based	60.32	5.03	632.6±35.79	53.82	4.01
	non-chitosan based	58.45	5.12	370.08±36.53	55.60	4.23
NLC	In chitosan-based	75.43	5.20	491.68±42.73	87.07	4.89
	Non chitosan	72.60	5.30	308.1±18.38	83.01	5.01

Figure 4.14 shows the different surface between two kinds of spray dried of BM loaded lipid nanoparticles systems (SLN and NLC). The dried product of SLN system showed smoother rounded-surface than in NLC systems. The physical properties similarity of each lipid that involved in SLN system might lead to the smoother surface than NLC systems. The evaporation characteristics that exhibited on micrograph of dry powder were determined by the composition of the preparation. The components of these two formulations can be differentiated by the difference of lipid composition. The lipid compositions of SLN were only solid lipid (stearin and trimyristin) whereas castor oil was involved in the NLC preparation. During drying, feed that contains lipid nanoparticles droplets undergoes atomization. The droplets have a tendency to expand, others collapse, disintegrate or even aggregate. In the spray drying process of BM loaded SLN and NLC with chitosan and without chitosan, aggregation between droplets was occurred. It was confirmed by the increasing size of redispersed powder (Table 4.13). The aggregation or disintegration might lead to porous or irregularly shaped particles (Masters 1990).

Spray dried SLN system with and without chitosan showed that the particles were undergone collapse during spray drying and showed irregular shape. After atomized droplets contact the drying air, the evaporation takes place from their surface and develops a significant gradient concentration. The droplets and other additives tend to migrate from the edge to center minimize the concentration gradient, and this flow is function of the droplet

viscosity and the vapor diffusion (Tewa-Tagne et al. 2007a; Tewa-Tagne et al. 2007b). SLN with all solid lipid components which have higher viscosity than NLC might be difficult to migrate and then lead irregular formation aggregates. And then formed unrounded shape, after evaporation occurs (Figure 4.14a and Figure 4.14c). Both SLN or NLC systems using spray dryer or nanospray dryer showed that incorporated chitosan of lipid nanoparticles (SLN and NLC) formed more uniformed shape and size than the unincorporated one. It is indicated that the existence of chitosan during spray drying plays role in maintaining the uniform aggregation during spray drying.

Porosity in the surface was less seen in the SLN system than NLC system using spray dryer or nanospray dryer. The incorporated chitosan also showed less porous than the unincorporated one. It is indicated that the component of lipid nanoparticles that involved in the formulation (lipid and chitosan) is important on porosity formation.

Nanospray dryer apparatus seemed to producing smaller size and more uniformed shape (Figure 4.14e and Figure 4.14g) than using a spray dryer (Figure 4.14a and Figure 4.14c). Vibrated membrane mesh in nanospray dryer which spray dryer does not have, might work to keep the uniform and smaller dried powder. However, smaller size on the obtained dried powder from nanospray dryer was confirmed by statistically significant of redispersed nanoaggregate size only for SLN systems (Table 4.13).

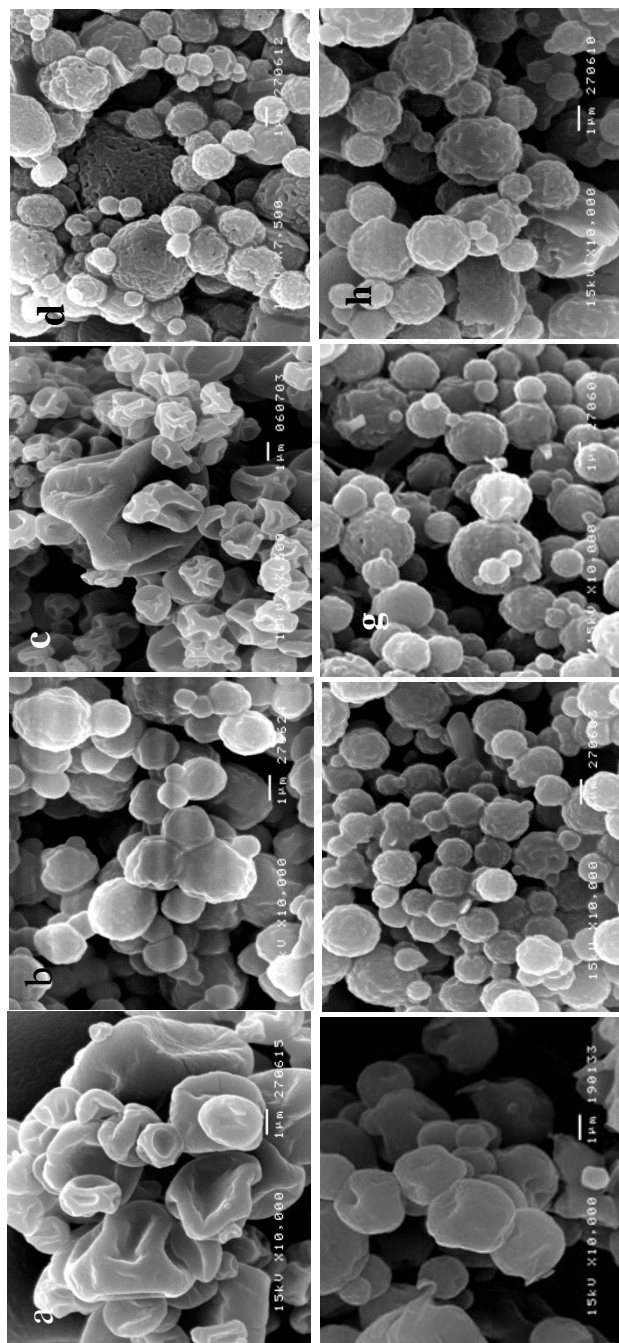


Figure 4.14 SEM characterization: a. spray dried powder of SLN in chitosan –based, b. spray dried powder of NLC in chitosan –based, c. spray dried powder of SLN non chitosan-based, d. spray dried powder of NLC non chitosan-based, e. nanospray dried powder of SLN in chitosan based, f. nanospray dried powder of NLC in chitosan based, g. nanospray dried powder of SLN non-chitosan based and h. nanospray dried powder of NLC non-chitosan based.

6.1.3 TEM characterization

The TEM micrograph (Figure 4.20) confirmed the different size characterization between redispersed nanoaggregates SLN and NLC chitosan-based and non-chitosan-based using nano-zetasizer which was mentioned in Figure 4.15. Figure 4.15 shows that incorporation SLN or NLC with chitosan significantly increase the nanoaggregate size (Table 4.13). Figures of nanospray dried powder cBMSLN and cBMNLC redispersion (Figure 4.15a and Figure 4.15b) show the clearly different surrounding nanoparticles compared to nanospray dried powder of BMSLN and BMNLC (Figure 4.15c and Figure 4.15d). The different surrounding nanoparticles was attributable to the chitosan coated the nanoaggregates. Chitosan coating of BMSLN was regular and rounded coating than in BMNLC. Shape of nanoaggregates of BMSLN and BMNLC might affect on chitosan coating because compared to BMNLC systems. It shows that the nanoaggregates of BMSLN systems (BMSLN and cBMSLN redispersion) were more rounded than BMNLC systems.

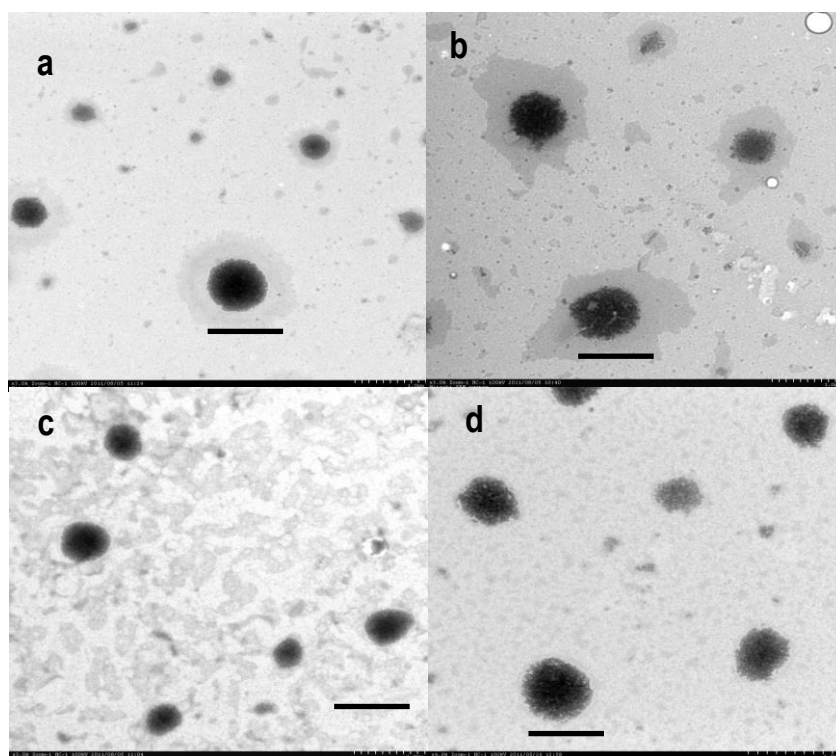


Figure 4.15 TEM characterization of redispersed of dried powder containing lipid nanoparticles (BM-SLN/NLC): a. nanospray dried SLN in chitosan-based, b. nanospray dried NLC in chitosan-based, c. nanospray dried SLN non chitosan-based and d. nanospray dried NLC non chitosan-based. Bars scale equal to 1.0 μ m length.

6.1.4 FTIR characterization

FTIR characterization was employed to investigate whether the interaction between ingredient during spray drying occurs or not. Comparing with other ingredients, the ratio between drug and other component was very low (1:49). So, it is very difficult to recognize the different spectra of BM in the formulation. However, there is something interesting among 4 figures shown in Figure 4.16c shows that spray dried SLN using spray dryer significant decreased peak on 1643 cm^{-1} which associated with C=O. It is indicated that the drying process might allow the excipients to interact with functional group of C=O in BM. Sharp peaks on 2959.38 cm^{-1} and

2698.14 cm^{-1} which represent C-H aliphatic asymmetric and C-H aliphatic symmetric, respectively, also were decreased.

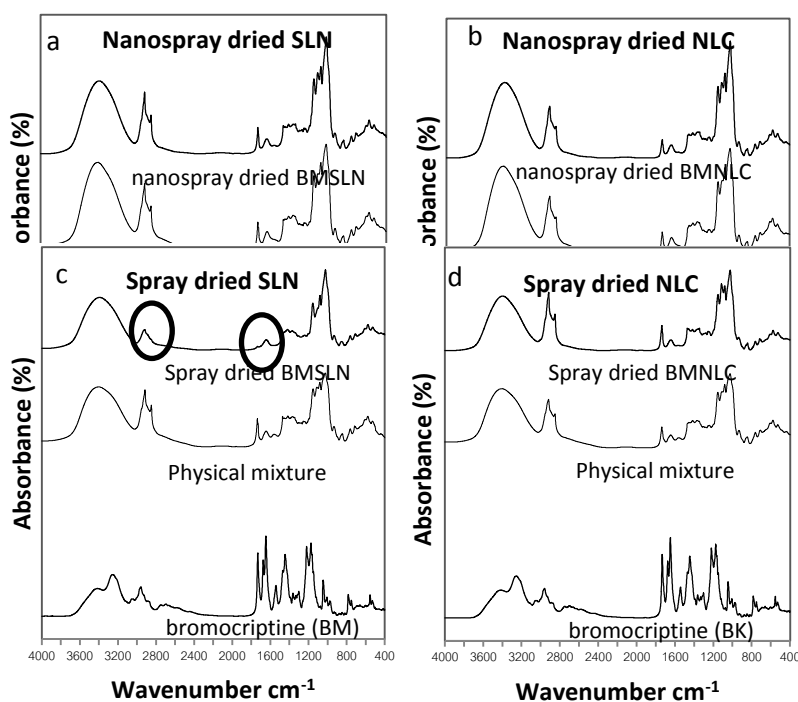


Figure 4.16 FTIR characterization of spray dried of SLN and NLC systems compared to bromocriptine (BM) a. nanospray dried BM-SLN chitosan-based, b. nanospray dried BM-NLC chitosan-based, c. spray dried BM-SLN chitosan-based and d. spray dried BM-NLC chitosan-based

6.1.5 WXR D characterization

The WXR D characterization showed that the spray dried SLN systems were more dispersed amorphously than their nanospray dried systems (Figure 4.17). Spray dried product of NLC systems showed that the sharp peaks from lipid were still appeared both using spray drier and nanospray drier apparatus (Figure 4.18). Involving heat in the process of spray drying might be contributed to crystalline peaks that shown at

nanospray dried BMSLN and BMNLC. In the nanospray drier apparatus (B-90 Nanospray drier), the dispersion was fed to the spray head by a pump and flow to vibrating membrane to reach nanofine particles. According to those processes which tend to size reduction targeting, it seems that maltodextrin as amorphous agent was not to be well-functionalized. It is indicated that using nanospray dryer giving fewer advantages to improve the stability of drug. Moreover, this process was equally time-consuming.

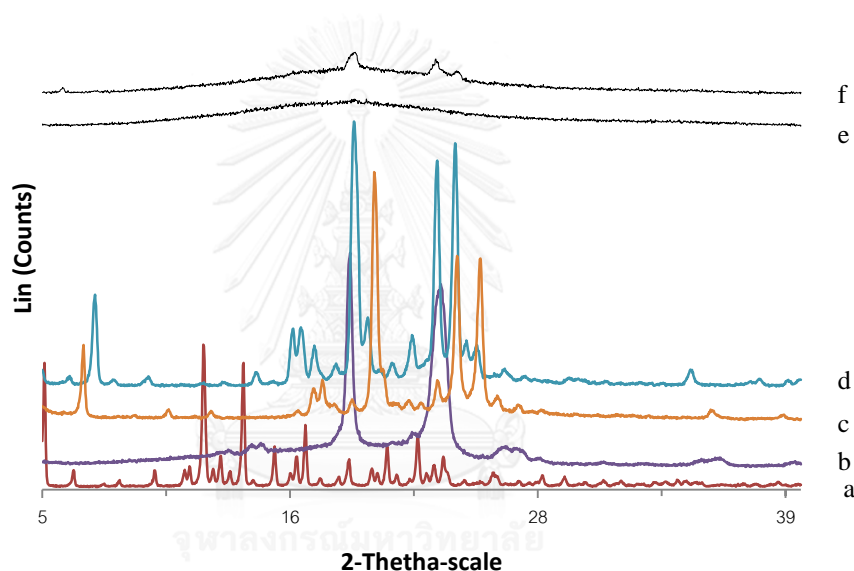


Figure 4.17 WXR D characterization of spray dried SLN systems; a. bromocriptine, mesylate, b. pluronic f127, c. tristearin, d. trimyristin, e. spray dried powder of BMSLN chitosan-based and f. nanospray dried powder of BMSLN chitosan-based

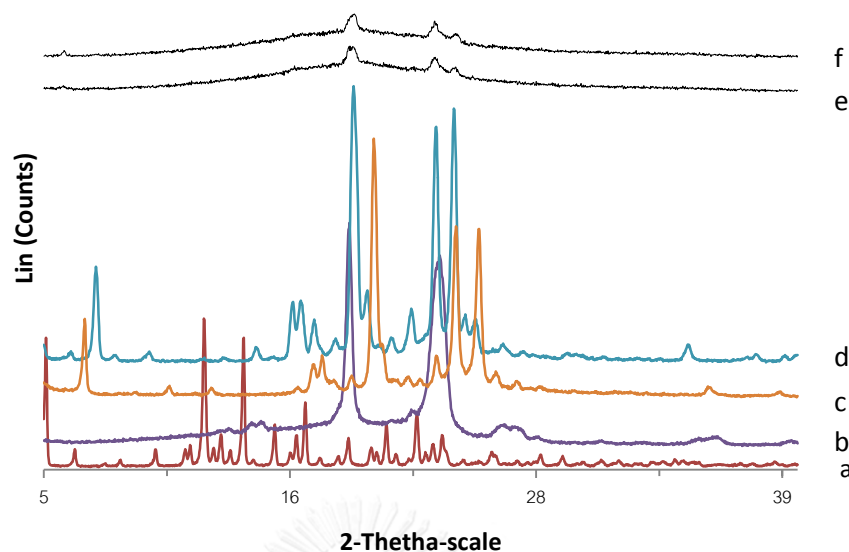


Figure 4.18 WXR D characterization of spray dried NLC systems; a. bromocriptine, mesylate, b. pluronic f127, c. tristearin, d. trimyristin, e. spray dried powder of BMNLC chitosan-based and f. nanospray dried powder of BMNLC chitosan-based

7. Development and Comparison of Spray Dried Nanoaggregates Containing Asiatic Acid SLN and NLC Chitosan-based

Converting water dispersion formulation to dry product has shown better chemically and physically stability to the active ingredient. In the previous study, in spray dried powder chitosan-based formulation, BM as drug model did not show a good stability during storage in the formulation. Some experiments also have been carried out to improve the stability of BM, but the instability of BM cannot be overcome. However, comparing to the water dispersion, the dried powder still showed better chemical stability (data not shown). In this study, Asiatic acid as one of the brain targeted drug was chosen to replace BM as a drug model to develop the brain targeted delivery

formulation via the oral route. With some adjustments, the optimized formulation of BMSLN and BMNLC and also the spray drying condition as reference was employed to the formulation of spray dried powder of cAASLN and cAANLC.

In order to increase the dose of drug in dried powder, sixty mg of Asiatic acid was dissolved in 1 mL of ethanol 95% to improve the solubility in melted lipid during SLN/NLC production. The initial dose of the obtained powder was also increased by increasing the AASLN or AANLC dispersion into the feed and reducing the amount of maltodextrin. Table 4.14 shows in the product yield of the obtained powder from experiment set in Table 3.5. The highest product yield was formulation G which contained 10 mL of AASLN dispersion with 10 mL of 0.5% chitosan (dissolved in 1% of acetic acid) and total 2% of solid content included maltodextrin as filler. However, the total dose of AA in formulation G was less than formulation H which contained 25 mL of AASLN added 25 mL of 0.5% chitosan (dissolved in 1% acetic acid) and total 3% of solid content (included maltodextrin). Thus, formulation H was selected for this study. This formulation was further employed to spray drying AANLC chitosan-based as comparison for this study.

Table 4.14 Product yield of obtained cAASLN powder by varying AASLN dispersion and amount of maltodextrin

Formulation	Product Yield (%)	Appearance
-------------	-------------------	------------

A	72.21	-
B	69.25	-
C	65.32	Sticky
D	74.82	-
E	71.87	-
F	67.87	Sticky
G	78.65	-
H	77.92	-
I	72.14	Sticky

7.1 Size, Zeta Potential and Yield Characterization

Similar to BM formulation, after spray drying, AASLN and AANLC size also underwent aggregation which lead an augmenting the size. Incorporating on spray drying AASLN and AANLC with chitosan as base showed significantly higher zeta potential value on their redispersed powder. Increasing zeta potential of redispersed spray dried powder of both AASLN and AANLC chitosan-based also confirmed the deposition of positively charged chitosan to AASLN and AANLC surface.

Table 4.15 shows the size characterization of AASLN, AANLC and their redispersed spray dried powder in chitosan base. The AASLN and AANLC seem has bigger size than BMSLN or even BMNLC, with size of $123.33 \pm 3.30 \text{nm}$ and $124.7 \pm 3.50 \text{nm}$, respectively. Increasing the drug loading

into the lipid phase from 0.025mg of BM to 0.060mg of AA was responsible for this increasing size. Between AASLN and AANLC, there is not any statistically significant different size ($p>0.05$). The different size was also shown between RSPcAASLN and RSPcAANLC which smaller size of RSPcAASLN than RSPcAANLC at $527.40\pm 45.83\text{nm}$ and $584.60\pm 58.63\text{nm}$, respectively but still not statistically different ($p>0.05$). The different solubility of the drug into the lipid phase might contribute to the different size of nanoparticles.

AASLN or AANLC dispersion shows negative charge zeta potential. Then addition of chitosan on spray drying AASLN or AANLC increased the zeta potential up to 41.64 ± 1.42 mV for RSPcAASLN and 33.22 ± 2.32 mV. The greater zeta potential value is the possibility at the hydrodynamic shear plane and determined from the particle mobility under an applied field. The greater zeta potential value gave better stability of nanoparticulate system due to repulsion effect between charged nanoparticles (Thode et al. 2000). Reversely, smaller zeta potential value can lead agglomeration, drug expulsion and eventually breaking the particles during storage (Wissing et al. 2004).

Although spray drying process increased the redispersed nanoparticle size, but it is interesting that PdI value of redispersed of cAASLN and cAANLC was decreased from 0.41 to 0.36 and 0.48 to 0.46, respectively. PdI is a measure of dispersion homogeneity, the smaller PdI value the more homogenous dispersion. Decreasing PdI value allowed the nanoparticulate systems to be less heterogeneity.

Table 4.15 Size of AASLN and AANLC dispersion, and redispersed nanoaggregates AASLN and AANLC (mean (n=5)±SD)

Formulation	Prepared lipid Nanosystem			Redispersed nanoaggregates chitosan-based		
	Size (nm)	ZP (mV)	PdI	Size (nm)	ZP (mV)	PdI
AASLN	123.42 ±5.59	-6.37 ±0.54	0.41 ±0.03	527.40 ±45.83	41.64 ±1.42	0.36 ±0.03
AANLC	124.73 ±3.50	-6.16 ±0.60	0.48 ±0.01	584.60 ±58.63	33.22 ±2.32	0.46 ±0.08

Figure 4.19a shows the log-normal size distribution of AASLN and redispersed spray dried powder of AASLN and cAASLN (RSPAASLN and RSPcAASLN). The redispersed spray dried powder of both AASLN with and without chitosan was distributed in a bimodal peak. The small peak of RSPAASLN and RSPcAASLN associated with the original peak of AASLN indicating after spray drying, small part of AASLN was still in their original size 123nm and most of AASLN form nanoaggregates with bigger size 527nm.

Figure 4.19b shows a normal volume particle size distribution of redispersed nanoaggregates of AANLC of bigger size than redispersed nanoaggregates of AASLN at 584nm. Bimodal peak was also depicted from the Figure 4.19b. Both of redispersed spray dried powder of AASLN (RSPcAASLN) and AANLC (RSPcAANLC) showed increasing size compared to the original size of their AASLN or AANLC (Table 4.15). The

aggregation of SLN or NLC during spray drying might be due to removal of water that changed the properties of the surfactant layer coating (Lee 2003). In the dry state, surfactants have no longer effective repulsion and stabilization properties as observed in water, so that in the spray drying process, aggregation between particles might occur, and increasing the size of nanoparticles.

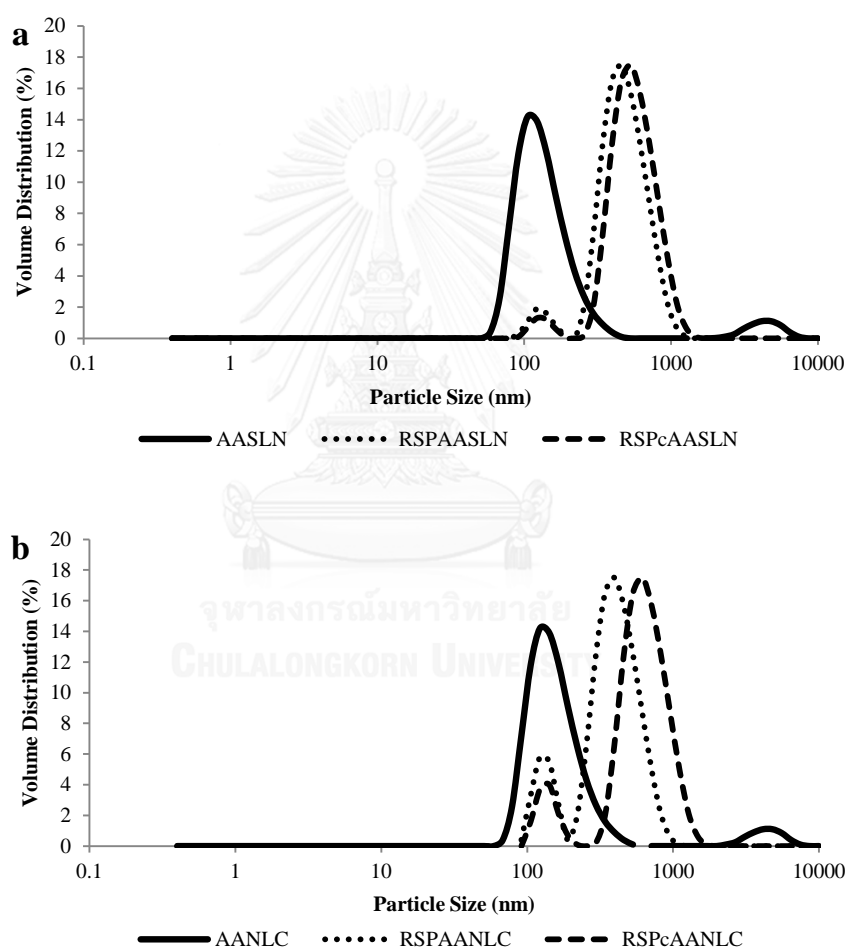


Figure 4.19 Log distribution size by volume of a. AASLN systems and b. AANLC systems

Table 4.16 shows spray dried powder characterization of spray dried powder of AASLN chitosan-based (SPcAASLN) and spray dried powder of

AANLC chitosan-based (SPcAANLC). According to higher product yield of SPcAASLN at 77.46% than SPcAANLC at 74.40%, it is indicated that spray drying process on AASLN is more effective than on AANLC. All liquid lipid of lipid component in AANLC might contribute to stickiness of spray dried powder then resulting in less product yield than AASLN. The more moist dry powder of SPcAANLC might be also caused by the liquid lipid component in AANLC. The moisture content also related to flowability of the powder that giving higher CI value than SPcAASLN. However, according to Podczek (1998), all spray dried powder still showed good flowability (less than 40). According to SPAN, $d(4.3)$ and $d(v,0.5)$, it can be observed that the SPcAASLN is smaller but less uniform than SPcAANLC. The smaller size of AASLN than AANLC might contribute to the smaller size of SPcAASLN than SPcAANLC. Figure 4.20 shows in the distribution size of spray dried powder of both cAASLN and cAANLC. Both of SPcAASLN and SPcAANLC showed slight bimodal peak distribution. The broader peak of SPcAANLC (Figure 4.20b) indicates that the more heterogeneity of dispersion than the narrower peak SPcAASLN (Figure 4.20a). The different number of uniformity of (Table 4.16) was also consistent with a log-normal volume distribution graph of dried powder (Figure 4.20a and Figure 4.20b).

Table 4.16 Spray dried powder of AASLN (SPcAASLN) and SPcAANLC characterization (mean (n=5) \pm SD)

Formulation	Yield (%)	Moisture Content (%)	SPAN	d(4,3)	Uniformity	d(v,0.5)	CI (%)
SPcAASLN	77.56 \pm 1.23	5.23 \pm 0.17	1.32 \pm 0.10	5.42 \pm 0.09	0.48 \pm 0.03	4.87 \pm 0.08	25.83 \pm 5.20
SPcAANLC	74.40 \pm 2.10	5.41 \pm 0.34	1.54 \pm 0.11	5.12 \pm 0.38	0.40 \pm 0.03	4.57 \pm 0.19	26.67 \pm 3.81

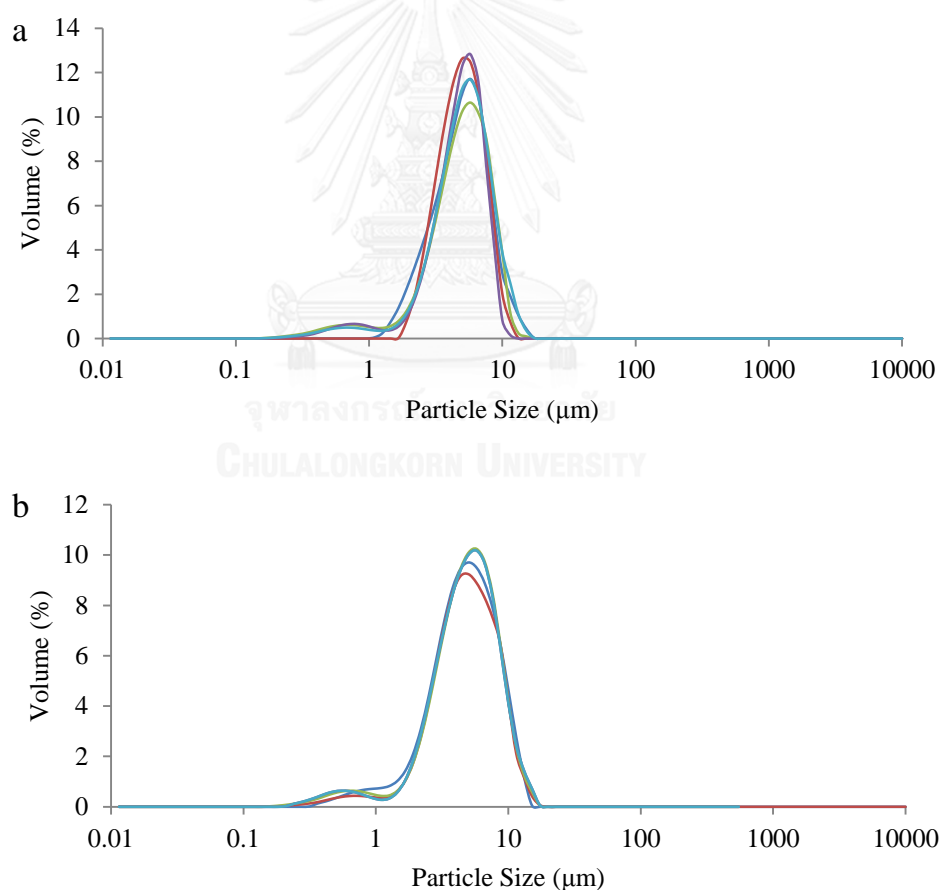


Figure 4.20 Log-normal size distribution by volume graph of a. SPcAASLN and b. SPcAANLC

7.2 SEM Characterization

Figure 4.21 is shown that the dried product of AASLN chitosan-based was smoother rounded-surface than dried product of AANLC systems. Spray dried AANLC systems showed more uniform than the AASLN. According to SEM analyses and the TEM analysis that redispersed SLN seem more rounded and solid (Figure 4.21) but the pores were also shown in indicating that all solid lipid might tend to aggregate irregularly during spray drying. Related to the characteristic of SLN that all lipid components were solid and can be melted, the heat that involved in the spray drying process might contribute to deformation of SLN resulted the less uniformity and the pores formation of spray dried AASLN systems. Less uniformity observation on SEM micrograph also was seen in powder measurement using Malvern Mastersizer 2000 (Table 4.16). Compared to BMSLN systems (

Figure 4.8.2b), it is shown that reducing the amount of maltodextrin (from 10 to 3% solid) gave less collapsed shape and a more rounded shape on the dried powder.

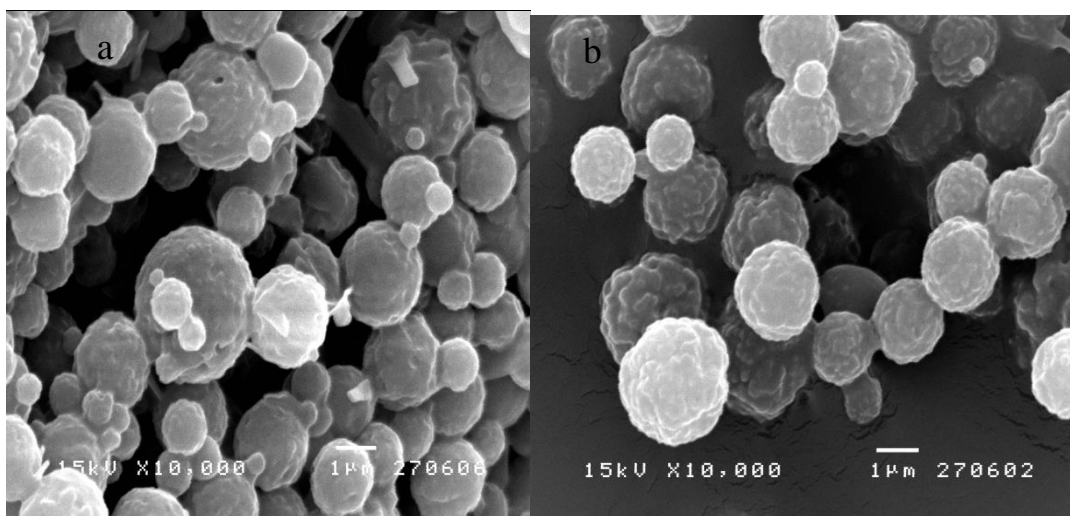


Figure 4.21 SEM characterization: a. spray dried SLN loaded AA chitosan-based (SPcAASLN) and b. spray dried NLC loaded AA chitosan-based (SPcAANLC)

7.3 TEM Characterization

Figure 4.22 is shown that aggregation of AASLN or AANLC were occurred during spray drying process. The redispersed nanoaggregates of AASLN showed rounded shape than AANLC. Similar to BM's systems results, the solid lipid components that involved in SLN systems might contribute to a more rounded and smoother shape of redispersed nanoaggregates of AASLN. The different shape of redispersed of spray dried powder of cAASLN (Figure 4.22d) than the cAANLC (Figure 4.22b) might be caused by the difference of interaction between surfactant and lipid component in both of the initial lipid nanoparticles (SLN and NLC).

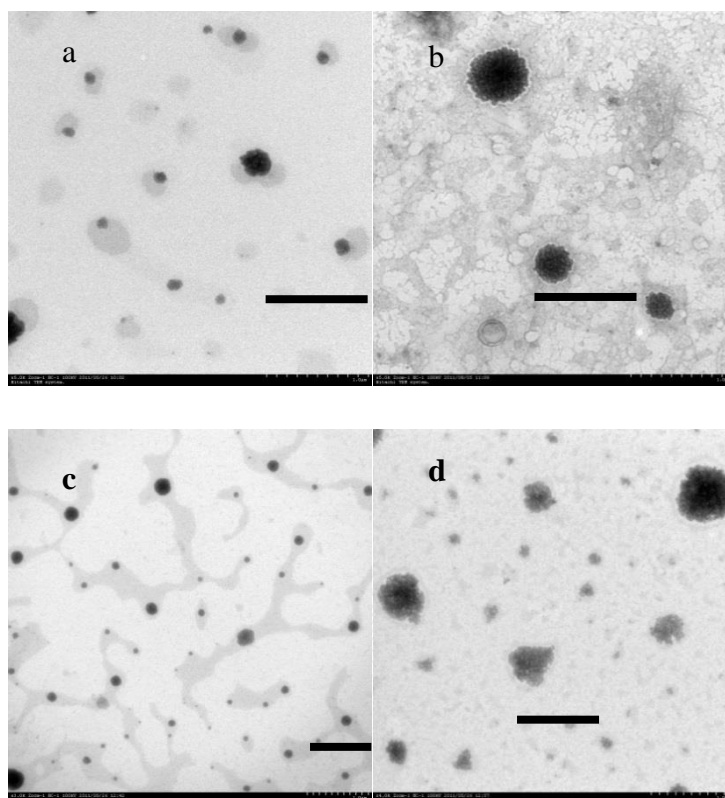


Figure 4.22 TEM characterization: a. SLN loaded AA, b. Redispersed spray dried SLN chitosan-based loaded AA c. NLC loaded AA and d. Redispersed spray dried NLC chitosan-based loaded AA. Scale bars equal to 1.0 μm .

7.4 FTIR Characterization

A mid-infrared region of 400 and 4000 cm^{-1} were used to exhibit the infrared bands. The position and intensity of a vibrational band were the characteristic of specific molecular motion and consequently of the atom participating in chemical bond, their conformation, and their immediate environment. Thus, a certain submolecular group produces bands in a characteristic spectral region (Bunaciu et al. 2010). Shifting, decreasing or disappearing of vibrational peak also can be indicated a chemical interaction between the active ingredient with excipients.

Figure 4.23 illustrates the FTIR spectra of Asiatic acid, physical mixture of powder SLN and NLC, spray dried powder of AASLN chitosan-based and spray dried powder of AANLC chitosan-based. IR spectrum of Asiatic acid (Figure 4.23a) was characterized by principal absorption peaks at 2926.14 cm^{-1} (C-H aliphatic asymmetric), 2869.57 cm^{-1} (C-H aliphatic symmetric), 1694.12 cm^{-1} (C=O), 3404.61 cm^{-1} (O-H), 1049.28 cm^{-1} (C-O) (see Appendix C). In IR spectra of physical mixture (Figure 4.23b and Figure 4.23d), all of the peaks appeared with decreased intensity. The IR spectra of spray dried powder of AASLN chitosan-based and spray dried powder of AANLC chitosan-based (Figure 4.23c and Figure 4.23e) show that there was no significant difference with their physical mixture spectra indicating that there was no chemical interaction between AA and the excipients during spray drying of AASLN and AANLC with chitosan-based.

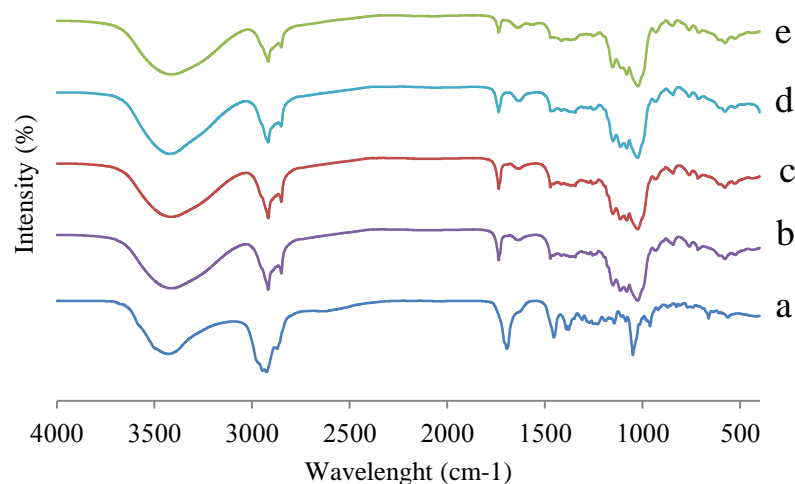


Figure 4.23 FTIR characterization of AASLN systems; a. Asiatic acid (AA), b. physical mixture of AASLN, c. spray dried powder of AASLN chitosan-based

(SPcAASLN), d. physical mixture of AANLC and e. spray dried powder of AANLC chitosan-based (SPcAANLC).

7.5 DSC Characterization

DSC characterization is used for investigating crystallinity the formulation and differentiation between amorphous solids and liquids (Westesen et al. 1997). The incorporation lipid with amorphous component-maltodextrin was suggested to increase bioavailability of drug. On the other hands, maltodextrin is also highly sensitive to water uptake which it would plasticize amorphous carbohydrates (Kilburn et al. 2004).

Figure 4.24.1 and Figure 4.24.2 show the DSC curves of heating and cooling process represent the heating and cooling on AASLN and AANLC production. Relatively sharp peaks were observed in heating of bulk lipid of SLN and NLC (Figure 4.24.1a and Figure 4.24.2a). The broader peaks of SLN Blank and NLC Blank indicating of the less pronounced polymorphic forms (smaller maxima and shoulder) was attributable to surfactant incorporated in particles and the dispersed state of lipid (Figure 4.24.1b and Figure 4.24.2b). Incorporation of drug reduced the peak area (decreased melting enthalpy) (Figure 4.24.1c and Figure 4.24.2c).

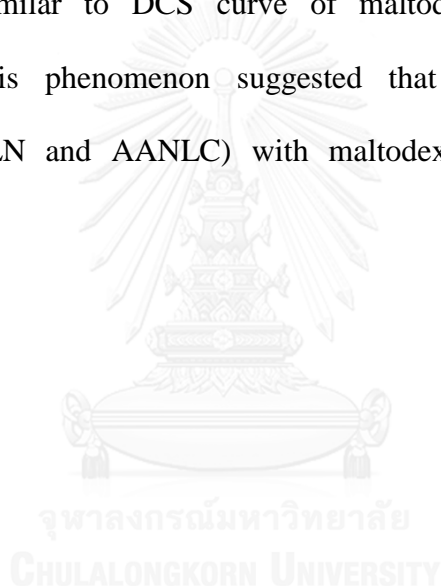
In order to investigate the solid state of AASLN and AANLC after cooling process, DSC curves were observed at 1 °C/min cooling rate represent the cooling process after AASLN and AANLC production. On DSC curves of bulk lipid of SLN and NLC, two peaks were observed at 48.08 °C and 34.47 °C for SLN bulk attributed to tristearin and trimyristin respectively and one peak at 46.83 °C for NLC bulk (Figure 4.24.1a and

Figure 4.24.2a). On cooling of SLN and NLC blank, the solidifications were occurred at 48.82 °C and 44.12 °C for SLN blank, at 48.48 °C and 45.00 °C for NLC blank indicating that SLN and NLC without drug were in the solid state at room temperature (25 °C) or even in body temperature (37 °C) (Figure 4.24.1b and Figure 4.24.2b). The nanosize and incorporation of lipid with surfactant on SLN and NLC production did not change the lipid behavior. On DSC curves of cooling AASLN and AANLC, two peaks were observed at 48.01°C and 44.17 °C for AASLN and 48.01 °C and 44.17 °C for AANLC indicating that incorporation of drug (AA) into SLN and NLC did give significant effect to lipid behavior (Figure 4.24.1c and Figure 4.24.2c). These results were consistent with Bunjes et al works (1996) that addition of longer chain triglycerides such as tristearin in lipid nanoparticles preparation overcome solidification problems of triglycerides nanoparticles.

Figure 4.24.3 shows that the crystalline of AA displayed large broad exothermic peak at 28.33-53.33°C and a small sharp endothermic peak at 205.33°C and sharp exothermic peak at 332.67°C (see Appendix D). The crystalline components of formulation, tristearin, trimyristin, pluronic f127 each showed an exothermic peak at 75.67°C, 60.33°C and 59.67°C respectively (Figure 4.24.3b, Figure 4.24.3c and Figure 4.24.3d). As an amorphous compound, maltodextrin showed a very large broad exothermic band from 32.67 to 211.67°C (Figure 4.24.3e). The physical mixture of SPcAASLN and SPcAANLC (Figure 4.24.3f and Figure 4.24.3h), all components in the formulation (i.e. tristearin, trimyristin, pluronic F127 and maltodextrin) still showed a sharp exothermic peak at 71.33°C and two

exothermic peaks at 55.33°C, 46.33°C which associated with the shifted peaks of tristearin, trimyristin and pluronic F127, respectively.

For comparison, SPcAASLN peaks were less appeared than the peaks of SPcAANLC. It is indicating that SPcAASLN was less crystalline ordered structure than SPcAANLC. The next WXRd data was used to confirm these differences. The DCS system of SpcAASLN and SpcAANLC showed that the exothermic peaks of the crystalline components were broader and the curve was more similar to DCS curve of maltodextrin (Figure 4.24.3g and Figure 4.24.3i). This phenomenon suggested that the spray dried of lipid nanoparticles (AASLN and AANLC) with maltodextrin as filler existed in an amorphous state.



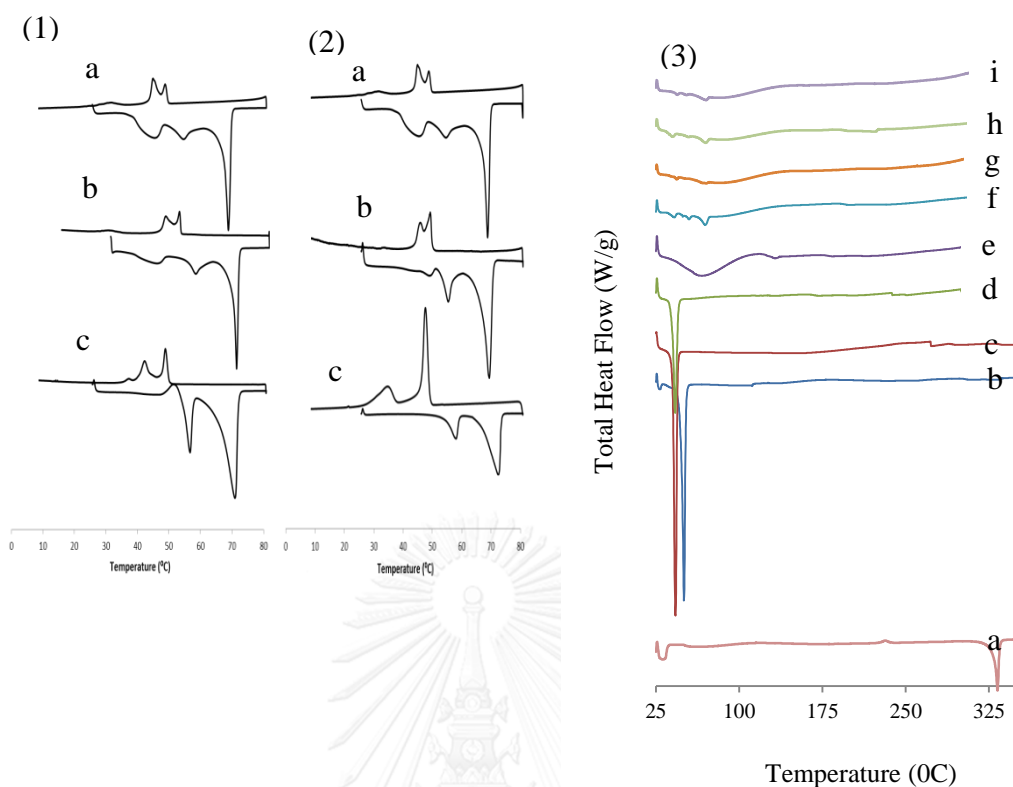


Figure 4.24 DSC characterization, (1) Heating (5°C/min) and cooling (1°C/min) of SLN; a. Bulk SLN lipid (tristearin:trimyristin=7:3) after tempering, b. SLN Blank and c. AASLN, (2) Heating (5°C/min) and cooling (1°C/min) of NLC a. Bulk NLC lipid (tristearin:trimyristin:castor oil=2:1:2) after tempering and c. AANLC, (3) Heating (5°C/min) of a. BM, b. tristearin, c. trimyristin, d. pluronic F127, e. Maltodextrin, f. Physical mixture of AASLN (PMAASLN), g. spray dried powder of cAASLN (SPcAASLN), h. physical mixture powder BMNLC (PMAANLC) and i. spray dried powder of cAANLC (SPcAANLC).

7.6 WXR Characterization

X-ray diffraction was conducted for the study of crystallinity and polymorphism of lipid nanoparticles (Bunjés et al. 1996). Therefore, these measurements were performed in order to compare the crystalline nature of the investigated lipid particles of spray dried powder of AASLN and

AANLC. Figure 4.25 shows the X-ray diffractograms of spray dried powder AASLN and AANLC chitosan-based compared to their lipid particles components, solid surfactant and also their physical mixture.

Figure 4.25, AA itself (Figure 4.25a), the solid lipid components (tristearin, trimyristin) and also the surfactant (pluronic F127) were shown as crystalline components. Numerous sharp peaks were shown in those spectra (Figure 4.25b, Figure 4.25c and Figure 4.25d) (see Appendix E). On the other hands, maltodextrine that used as filler in the spray drying of AASLN and AANLC was shown as amorphous component (Figure 4.25e). Physical mixtures on both systems (SPcAASLN and SPcAANLC) were shown that the sharp peaks were decreased significantly (Figure 4.25f and Figure 4.25h). If we compared, on the diffraction pattern of physical mixture on SLN system (Figure 4.25f), those peaks seemed more appeared than on NLC systems (Figure 4.25g). It is indicating that the crystalline components give stronger effect in physical mixture of SLN system than in NLC systems. However, peaks in physical mixture were broader and weaker than in bulk material indicating that adding maltodextrin also can reduce the crystallinity of dispersion.

Figure 4.25g and Figure 4.25i shows the diffraction pattern of spray dried powder of cAASLN (SPcAASLN) and spray dried powder of cAANLC (SPcAANLC). As expected the crystalline character of lipids was more decreasing than the physical mixture more similar to maltodextrin pattern. The characteristic of β^* / β modification of tristearin and trimyristin (arrows) were appeared on both SPcAASLN and SPcAANLC, but SPcAASLN was

weaker than SPcAANLC. The differences of crystalline character between SPcAASLN and SPcAANLC might be due to less ordered structure of SLN than NLC which also confirmed by DSC data. According to these results, the expulsion of oil might be occurred during shelf life of spray dried powder of AANLC. However, in both types of spray dried powder of lipid nanoparticles (AASLN and AANLC) chitosan-based, using maltodextrin as filler decreased crystallinity of the lipid matrix and tends to amorphous system which is easier to disperse.



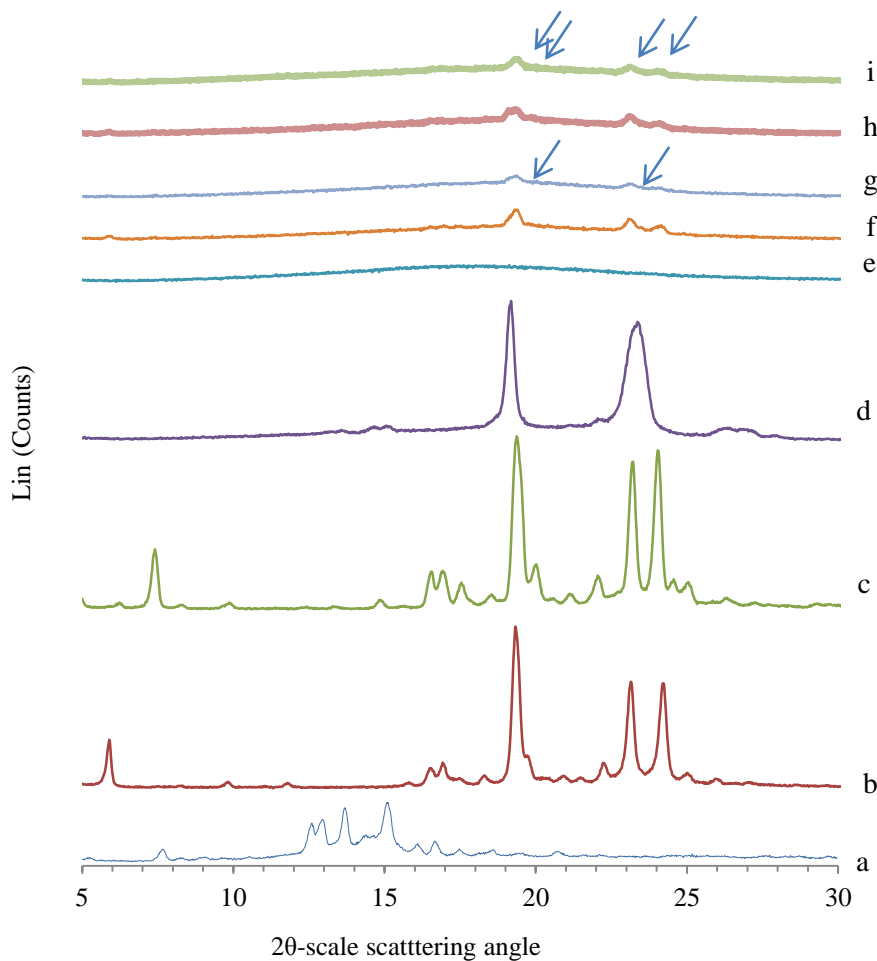


Figure 4.25 WXR D characterization of spray dried AASLN and AANLC chitosan-based; a. AA, b. tristearin, c. trimyristin, d. pluronic F127, e maltodextrin, f. physical mixture AASLN chitosan-based, g. spray dried powder of AASLN chitosan-based (SPcAASLN), h. physical mixture AANLC chitosan-based and i. spray dried powder of AANLC chitosan-based (SPcAANLC).

7.7 Chemical Properties Characterization

7.7.1 AA assay

Specificity The peak of AA was indicated by a symmetrical single peak (Figure 4.26). The retention time of the peak was at 12.166 to 12.562

min. This observation showed an adequate specificity of the assay. This result was different from the previous study by Günther and Wagner (1996) that found the retention time of AA at 24.4 min. Different condition of HPLC such as different column, different mobile phase (including ratio) suggested the different results.

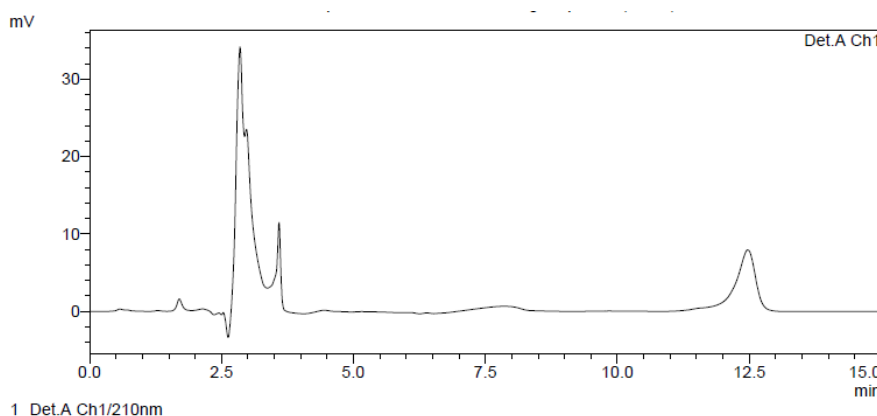


Figure 4.26 Chromatogram of Asiatic acid (AA) (HPLC condition of acetonitrile: 10 mM buffer phosphate = 28:72, v/v, pH 7.7, flow rate 1.0 mL/min, detected 210nm).

Linearity, Calibration of BM was linear in range 0.4 – 8.0 $\mu\text{g/mL}$. The standard curve of concentrations (mg/mL) against AUC (area under curve) was $y = 3869x + 167.96$ with $r=0.9989$ ($n=5$), where x was concentration ($\mu\text{g/mL}$) and y was AUC (Figure 4.27). The regression parameters of the linearity of the system was reported in Table 4.17.

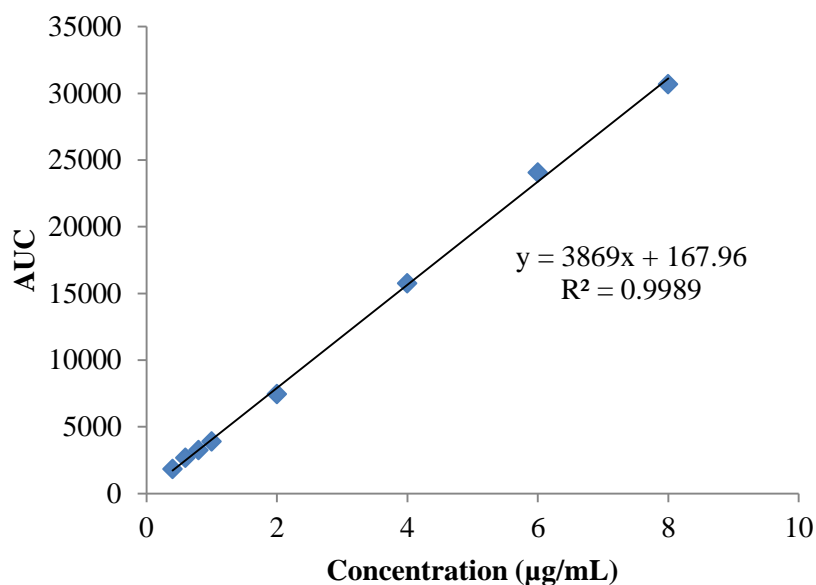


Figure 4.27 The calibration curve was shown the linearity of systems on the range of concentration 0. 4-8 µg/mL of AA (HPLC condition of acetonitrile: 10 mM buffer phosphate = 28:72, v/v, pH 7.7, flow rate 1.0 mL/min, detected 210nm).

Table 4.17 Regression parameters of the linearity of system

Regression Parameters	Day 1	Day 2	Day 3	Mean ±SD
Slope	3869	4311.5	3943.2	4050.23±227.50
Y-intercept	167.96	165.96	169.55	167.82±1.80
Correlation coefficient (r^2)	0.9989	0.9994	0.9994	0.9992±0.0003

Linearity of the method was revealed a linear correlation between concentration added and concentration found from the accuracy test and was reported in Figure 4.28.

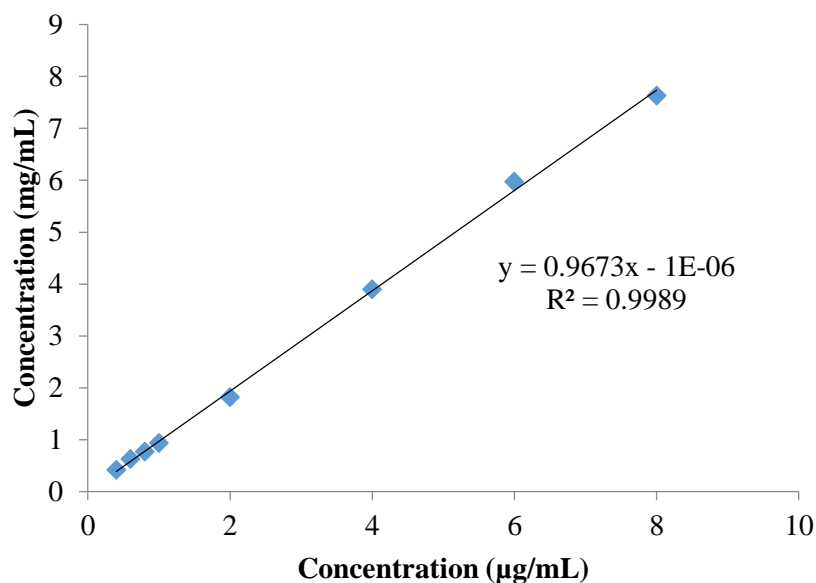


Figure 4.28 Calibration curve was shown the linearity of the method (HPLC condition consisting of acetonitrile: 10 mM buffer phosphate = 28:72 v/v, pH 7.7, flow rate 1.0 mL/min, detected at 210nm).

Robustness In order to evaluate robustness of the method, one chromatographic parameter was changed while the other parameters remained unchanged. The method robustness was tested after changing the final pH of mobile phase (7.6 to 8.0). The results revealed that the method was robust for these small changes at final pH. In addition the effect of the percent of organic solution on retention time and peak area was studied by varying acetonitrile proportion from 26 to 30%. The results showed that the variation of pH of the mobile phase of ± 0.2 units and organic strength of the mobile phase of $\pm 2\%$ did not have a significant effect to retention time and peak area (AUC) (% RSD ≤ 2.0) illustrating the robustness of the method (Table 4.18 and Table 4.19).

Table 4.18 The robustness test results of the method by varying pH

pH of Mobile Phase	RT (min)	Peak
7.5	12.230	15400
7.6	12.340	15580
7.7	12.341	15900
7.8	12.452	15800
7.9	12.454	15780
Average	12.363	15692
SD	0.09	200.30
% RSD	0.76	1.28

Table 4.19 The robustness test results of the method by varied the acetonitrile proportions in the mobile phase

Acetonitrile proportion (v/v)	RT (min)	Peak
26	12.110	15570
27	12.280	15632
28	12.441	15700
29	12.460	15300
30	12.542	14600
Average	12.367	15450.40
SD	0.17	294.84
% RSD	1.39	1.91

7.7.2 Drug entrapment efficiency

Drug entrapment efficiency (DEE) of AASLN and AANLC was $57.17 \pm 2.37\%$ and $62.08 \pm 1.79\%$, respectively (Table 4.20). Compared to BM results (Table 4.9), drug entrapment efficiency of AA in SLN and NLC was lower. Since the solubility of BM and AA in water is similar at 0.1 mg/mL (Florey 1979; Kim et al. 1997), the lower DEE of AA might be contributed by the less solubility of AA in the lipid phase than the solubility of BM in lipid phase. The solubility of drug in lipid (melted lipid) and also in water affected to the entrapment drug in lipid phase of nanoparticles.

Entrapment efficiency will contribute to stability of the drug. According to result (Table 4.20), the higher DEE of AA in NLC indicated that process and ingredients of the formulation of NLC were more able to keep AA to be entrapped in lipid and avoid degradation.

7.7.3 Drug retention

The drug entrapment efficiency of AA in SLN and NLC also affects the total drug content (Table 4.20). It was shown that the drug retention of AANLC was higher ($91.39\pm 0.23\%$) than the drug retention of AASLN ($66.42\pm 0.61\%$). The lipid components of NLC on AANLC which is consisted of liquid and solid lipid could be the drug expulsion. This result was consistent to DEE result, which the higher DEE will contribute on stability of drug then resulting high drug retention. Therefore, preventing the drug from water reduced the degradation drug (Oppenheim 1981).

In spray drying process, drug retention of SLN and NLC systems showed different results. The drug retention of SPcAANLC was higher ($98.07\pm 0.93\%$) than drug retention of SPcAASLN ($82.16\pm 0.17\%$). These results also were consistent with the DEE results, that higher DEE increased the stability of drug resulting higher drug retention. Since the drug lost might be occurred on the untrapped drug, the role of the NLC formulation on keeping the drug from expulsion leads the higher drug retention of SPcAANLC than SPcAASLN. The high drug retention consequence of both systems indicated that the spray drying process could maintain the stability of AA.

Comparing to BM results (Table 4.9), these results were significantly higher than the previous study on BM. Since the DEE of BM in SLN and NLC was similar to DEE of AA in SLN and NLC, the higher drug expulsion of BM during spray drying of SLN and NLC might tend to firmly occurred than in AA. Easier drug expulsion leads to the easier drug to be degraded. Since using the same lipid component, so the crystalline behavior of the drug its self might contribute to the expulsion and the stability during spray drying.

Table 4.20 Drug entrapment efficiency (DEE) and drug retention (DR) (mean (n=5)±SD)

Parameter	Drug Entrapment efficiency (%)	Drug retention (%)
AASLN	57.17±2.37	66.42±0.61
AANLC	62.08±1.79	91.39±0.23
SPcAASLN	-	82.16±0.17
SPcAANLC	-	98.07±0.93

7.7.4 *In vitro* release study profile

Figure 4.29 shows the release profile of AA from AASLN and AANLC showed controlled drug release. In SLN or NLC, drug release was controlled by the surrounding lipid barrier during a long time release study (Müller et al. 2000). At pH 1.2 which conducted for 2 h, only 2.80% of AA could be released from SLN and 2.2% of AA from NLC. The slower release

of AA from NLC might be caused by the high solubility of AA in the lipid phase of NLC resulting prolonged release drug. Interactions between drug–lipid molecules, between surfactant lipid molecules and solubility of the drug in the molten and solid lipid, play a major role on drug release. The difference of the melting point of lipid was considered as important parameters determining the structure of the SLN and also NLC matrix which would be contributed on releasing drug from droplets (zur Mühlen et al. 1998). After 2 h, the medium was changed to pH 6.8 mimicking intestinal condition. In pH 6.8, the release profile of the drug also showed controlled release profile. After 8 h, 16.89% of the drug was released from SLN and 14.31% from NLC. The weak acid of AA may be responsible for its increasing dissolution in higher pH condition (pH 6.8).

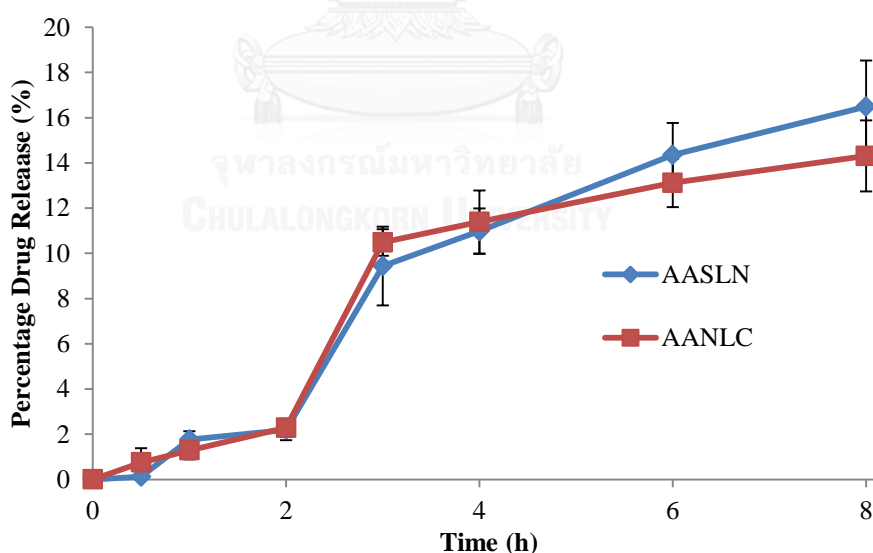


Figure 4.29 *In vitro* release of AA of SLN and NLC in situ pH change. AA were released from AASLN and AANLC at pH 1.2 for 2 h then replaced to medium to pH 6.8 for 6 h. Error bars represent standard deviations of the mean based on three replicates.

Figure 4.30 shows the in vitro release profile of spray dried powder of AASLN (SPAASLN) and spray dried powder of AANLC (SPAANLC). Figure 4. 30 shows a controlled release on both SPAASLN and SPAANLC. After 2 h, only 2.87% of AA that could be released from NLC and 4.58% could be released from SLN. It is consistent with the released-AA from AASLN and AANLC (Figure 4.30) that AA was easier to release from SLN system than from NLC. After 8 h from beginning or 6 h in pH 6.8 media, the controlled release was also shown and released 35.48% AA of SPAASLN and 31.94% AA of SPAANLC. This prolonged release of AA was expected since as brain drug targeted should have stable plasmatic drug levels and prolong drug action. Previous research by Brodaty et al. (2005) found that the prolonged release Galantamine demonstrated a safe and effective treatment for mild and moderate Alzheimer's disease (AD). Compared to AASLN and AANLC, the spray dried powder of them showed greater drug released than their SLN and NLC dispersion. Spray dried with maltodextrin as filler has been involved to change the crystallinity of lipid into the amorphous state causing a faster dissolution (Figure 4.24 and Figure 4.25).

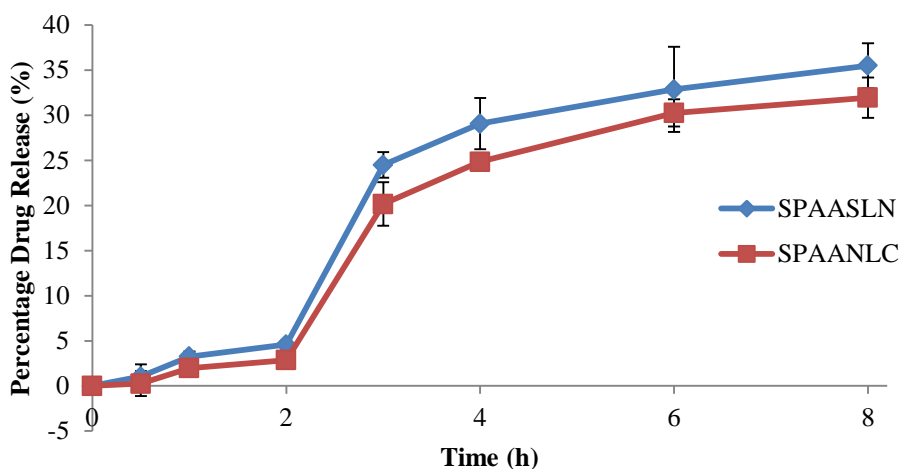


Figure 4.30 *In vitro* released of Asiatic acid of SPAASLN and SPAANLC in situ pH change. AA from SPAASLN and SPAANLC were released at pH 1.2 for 2 h then replaced to medium to pH 6.8 for 6 h. Error bars represent standard deviations of the mean based on three replicates.

Figure 4.31 shows *in vitro* release profile of spray dried AASLN chitosan-based (SPcAASLN) and spray dried powder of AANLC chitosan-based (SPcAANLC). The profile release of AA was similar to release profile of AASLN and AANLC, but at 8 h, 23.69% AA-released from SPcAASLN and 19.79% AA-released from SPcAANLC. The smaller AA-released of SPcAASLN and SPcAANLC than the unincorporated one (SPAASLN and SPAANLC) might be caused by the presence of chitosan. The mucoadhesive chitosan played a key role in the release of drug suggested a matrix like system resulting from the mechanical interlocking of the long polymer chains, with the potential for hydrogen bond formation between hydroxyl group of chitosan and SLN and NLC's surfactant (Learoyd et al. 2007). This physical mechanism is the so-called 'interdiffusion'. The slower AA-release from SPcAASLN and SPcAANLC supported the objective of this study to

form prolonged AA-released since the prolong AA was needed to brain delivery (Esposito et al. 2008).

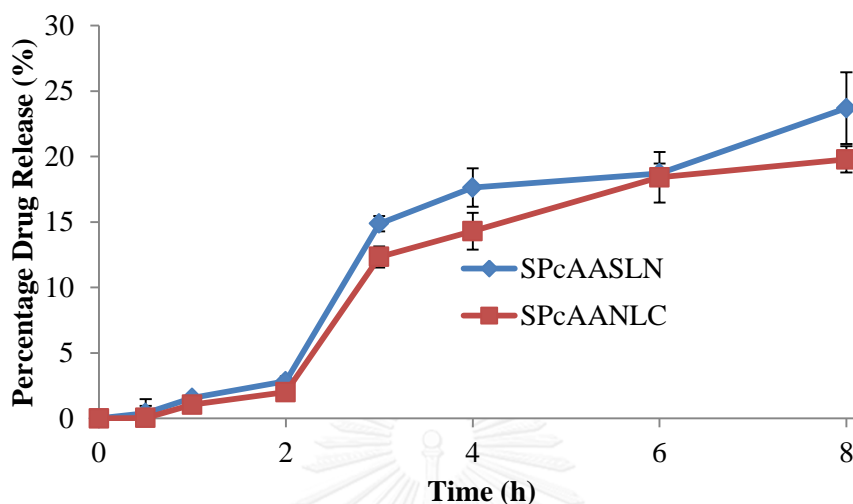


Figure 4.31 *In vitro* released of AA of SPAAcSLN and SPcAANLC in situ pH change. AA from SPcAASLN and SPcAANLC were released at pH 1.2 for 2 h then replaced to medium to pH 6.8 for 6 h. Error bars represent standard deviations of the mean based on three replicates.

7.8 Stability Study

7.8.1 Chemical stability of drug content

Oppenheim (1981) has stated that if the drug degrades in an aqueous environment. The time of contact with water will influence the amount of drug incorporated into the nanoparticles. The manufacturing procedure should minimize the time over which degradation may occur. This study was aimed to figure out the stability of drug content during storage under room temperature (25°C).

Figure 4.32a shows the stability of AASLN compared to SPAASLN. After 90 days storage, the drug content of AA in SPAASLN was 82.36%

whereas in AASLN was 71.25% from initial drug content. It is indicated that removing water minimized the drug degradation. Dehydration reduced the hydrolysis that might be occurred on AA.

After 90 days storage, the percentage of drug content in SPcAASLN was 97.73% which was significantly higher than without chitosan. It is indicated that chitosan reduced the AA degradation. The lower pH condition might be responsible to increase the stability of AA since AA is a weak organic acid which more tends to be nonionized in lower pH condition. The nonionized entity of AA facilitates drug to stay in a lipid base and reduced the possibility of drug degradation.

Comparing to AANLC systems, AANLC systems shows better stability than AASLN systems (Figure 4.32b). But, the similar phenomenon also was shown between AANLC, SPAANLC and SPcAANLC formulation which the dried powder of cAANLC was better than the water dispersion of AANLC. After 90 days storage, the drug content was 86.76%, 98.06% and 74.91% for SpAANLC, SPcAANLC and AANLC, respectively (Figure 4.32b). The drug was easier to undergo the degradation when the drug was released from nanoparticles. Better stability of AANLC systems was contributed by the higher DEE in initial AANLC than in AASLN which is affected to the solubility of drug in lipid phase of nanoparticles. More solubility drug in NLC lipid phase played important role to reduce drug expulsion during storage which could reducing drug degradation (Wissing et al. 2004).

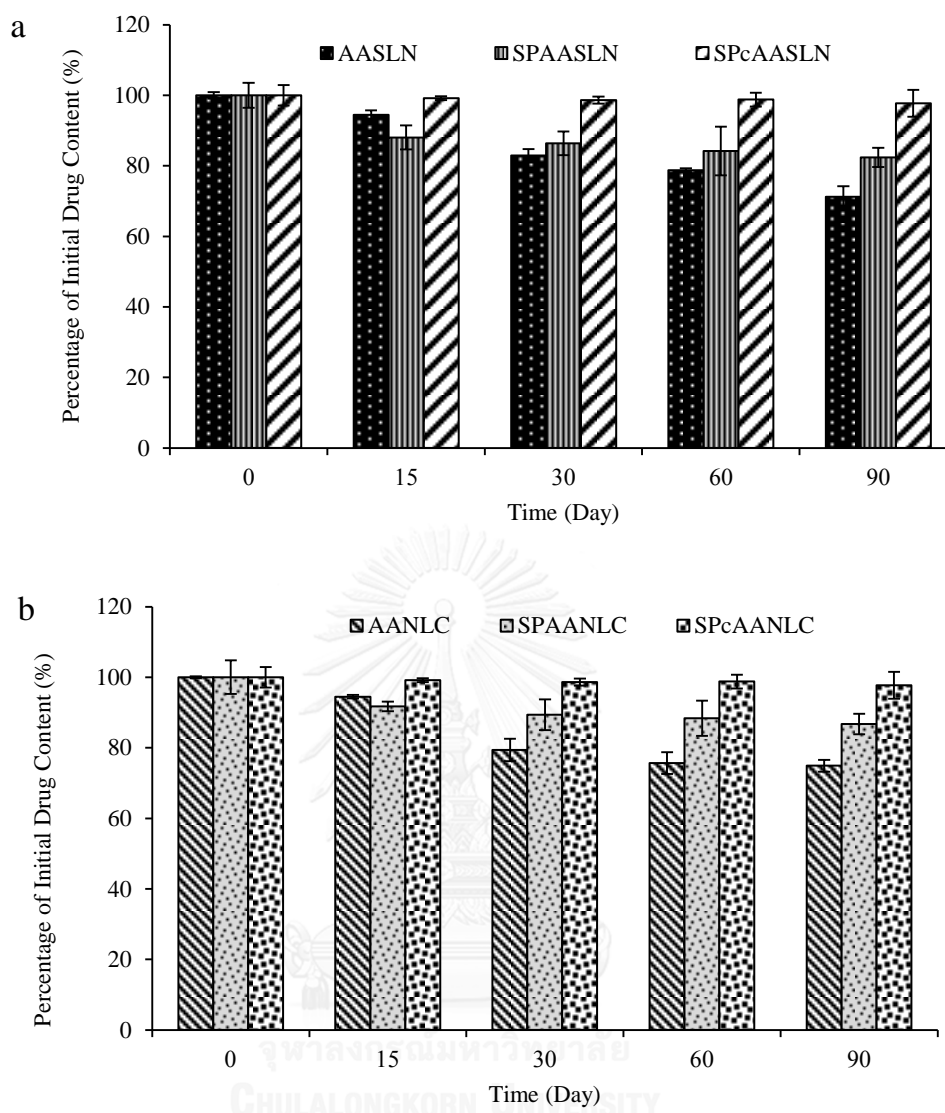


Figure 4.32 Comparison of stability of drug content (AA) in nanoparticles dispersion and in their dry powder; a). Content of AA in AASLN and spray dried powder of SLN (SPcAASLN) and b). Content AA in AANLC and spray dried powder of NLC (SPcAALNC). Error bars represent standard deviations of the mean based on three replicates

7.8.2 Chemical stability of entrapped drug

Chemical integrity of drugs entrapped in nanoparticles is another fundamental aspect of the overall stability evaluation of this study. It is important in order to analyze not only the particle size but also the eventual leaking of the drug from the carrier during storage. This study was conducted to evaluate the stability of entrapped drug during storage.

Figure 4.33a and Figure 4.33b show the entrapped drug of spray dried powder of AASLN (SPAASLN) and AANLC (SPAANLC) was more stable than the water dispersion of AASLN and AANLC. After 90 days storage, the entrapped drug in SPAASLN and SPAANLC were 78.91 and 83.50% whereas in the water dispersion of AASLN and AANLC were 67.56% and 73.73%. It is indicated that removing water from the environment reduced the drug leaking.

Figure 4.33 shows percent of drug entrapped in droplet comparing to drug content. It is surprising that the trend of those graphs after 15 days showed that the entrapped of the spray dried powder chitosan-based (SPcAASLN and SPcAANLC) compared to drug content was more stable than the other formulations (AASLN, SPAASLN, AANLC and SPAANLC). It is indicated that chitosan contributed to reducing the drug leaking from droplets. Chitosan was dissolved in 1% acetic acid which resulted in lower pH condition (pH 5.55). This lower pH condition reduced the aqueous solubility of AA which increased the partition coefficient of AA and kept the drug entrapped in nanoparticles. Furthermore, the hydrogen bond between the hydroxyl group of chitosan and AASLN or AANLC's surfactant might

form a mechanical interlocking of long polymer chains that played a role on impairing drug leaking of SPaAASLN and SPcAANLC (Learoyd et al. 2008). It is suggested to concern about increasing drug entrapment efficiency during SLN and NLC production to increase the stability of the drug during storage.

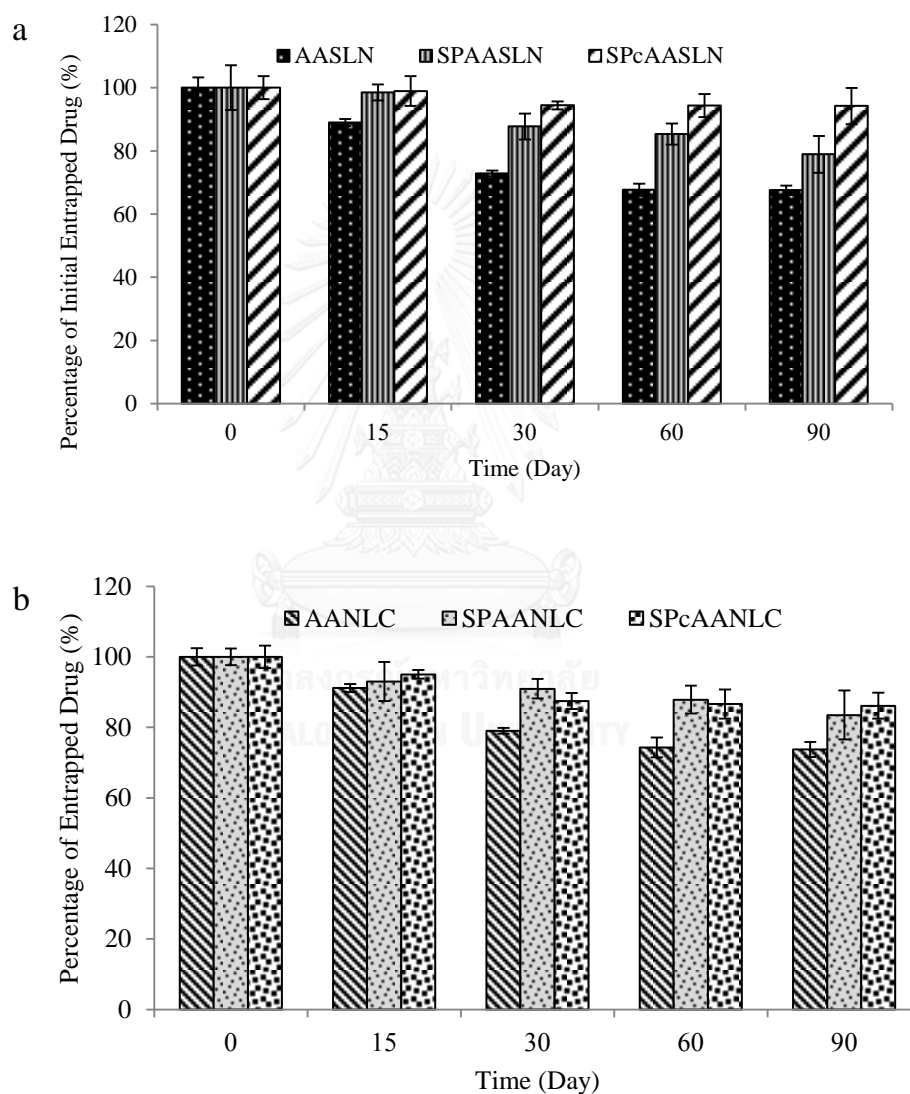


Figure 4.33 Drug entrapment efficiency stability; a. SLN and spray dried powder of SLN chitosan-based and b. NLC and spray dried powder of NLC chitosan-based. Error bars represent standard deviations of the mean based on three replicates.

7.8.3 Stability size and polydispersity index

Figure 4.34a and Figure 4.34b displayed the stable size of AASLN and AANLC and redispersed spray dried powder of AASLN and AANLC (RSPAASLN, RSPcAASLN, RSPAANLC and RSPcAANLC). Both graphs show that AASLN and AANLC significantly changed to bigger size during storage ($p < 0.005$) (see Appendix G). After 90 days storage, the size of original AASLN and AANLC was increased from 122.96 to 160.74nm for AASLN and from 124.60 to 163.00nm for AANLC. As mentioned previously, low zeta potential of both initial AASLN and AANLC played the role of instability size during storage. These results also confirmed the stability sizes prediction from zeta potential value (Table 4.15).

However, PDI of both AASLN and AANLC systems was more stable than PDI of redispersion powder of AASLN and AANLC, RSPcAASLN and RSPcAANLC. The polydispersity Index (PDI) value explained about the uniformity. The lower PDI value of AASLN and AANLC shows consistency result with stable droplets size during storage than the redispersed nanoaggregates size of cAASLN and cAANLC. The graphs show that PDI values of SLN systems have a tendency to increase indicating that the trend of uniformity of the size was become less during storage. This condition might be caused instability of droplet size can lead agglomeration and also drug expulsion following by degradation drug (Lee 2003). Meanwhile, the PDI values of AANLC systems seem not to reveal any trend and tend to a constant value, indicating that the uniformity size on AANLC systems was more stable than AASLN systems then also related to chemical stability.

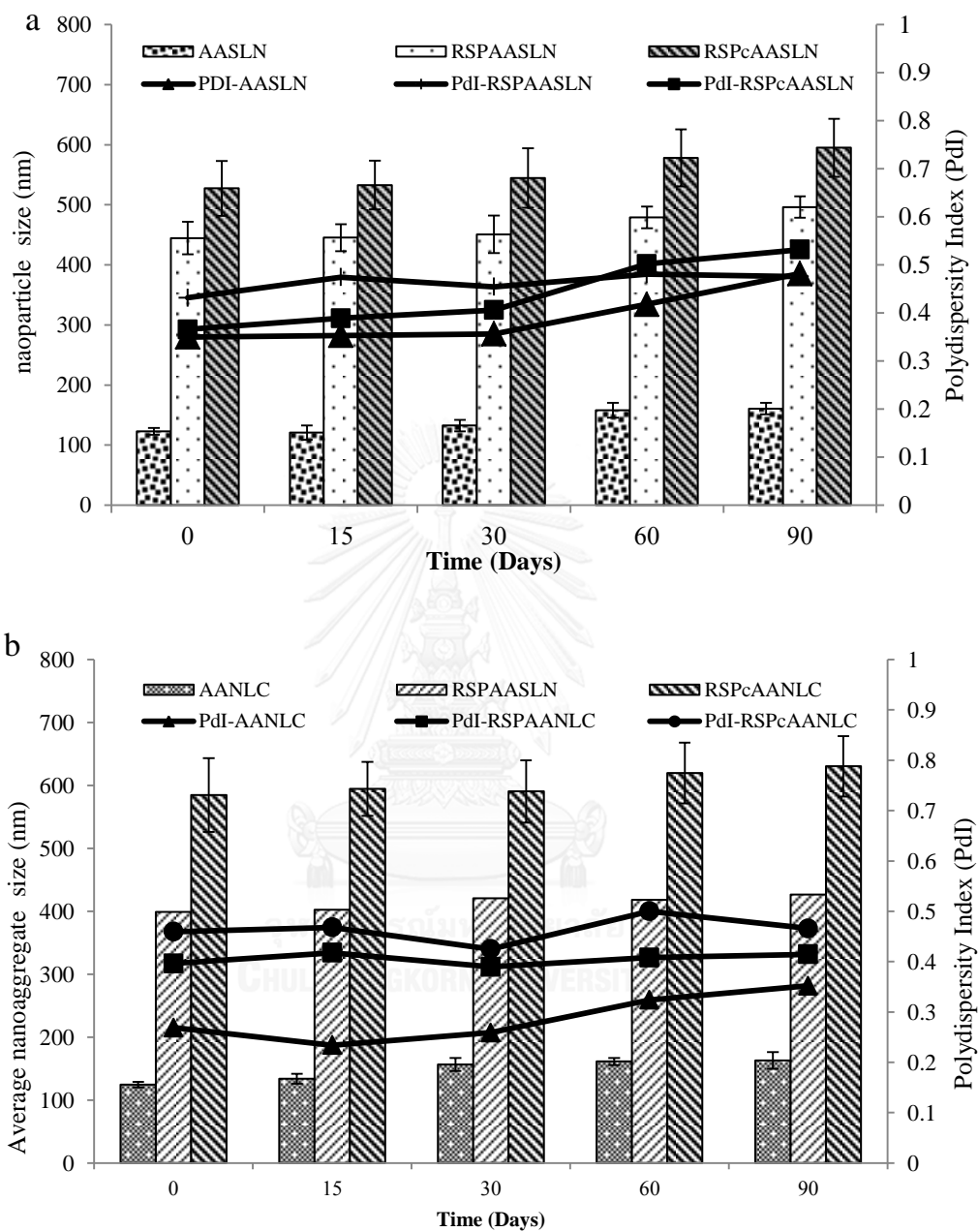


Figure 4.34 Comparison of size stability (average size and polydispersity index (PdI) value); a. AASLN system with their RSPcAASLN and b. AANLC system with their RSPc AANLC.

7.9 Permeability Study of Redispersed Spray Dried Powder of AASLN and AANLC Chitosan-based on Caco-2 Cells

7.9.1 Confocal Laser Scanning Microscopy (CLSM) study

Confocal laser scanning microscopy (CLSM) study was conducted to observe penetration of RSPcAASLN and RSPcAANLC through Caco-2 cells. Rhodamine 6G (R6g) was utilized to replace AA in SLN and NLC formulations, then also in the spray dried product of them with and without chitosan as base. Our finding obtained from confocal microphotographs of monolayer Caco-2 cells treated by R6gSLN, RSPR6gSLN, RSPcR6gSLN, R6gNLC, RSPR6gNLC and RSPcR6gNLC demonstrated paracellular localization (extracellular) (Figure 4.35). Fluorescent-cells image of the group treated with chitosan-based showed higher intensity than without chitosan indicating chitosan could enhance uptake and penetration of SLN and NLC through Caco-2 cells. The positive charge of chitosan might contribute on cell uptake since membrane cell has a negative charge revealed an easy uptake reflected by high intensity of the fluorescent image in cells.

Figure 4.35 also shows the different rate of permeability of various treatment group formulations. It was shown that the R6gSLN and R6gNLC tend to have slower penetration than redispersed spray dried powder of cR6gSLN (RSPcR6gSLN and RSPcR6gNLC) since the strong intensity was started at 30 min and the group of redispersed spray dried powder, the strong intensity was started at 10 min. It was proven that the existence of a positive charge of chitosan could increase the interaction between the RSPcAASLN and RSPcAANLC with the negative charge of the cell membrane. The

mucoadhesive properties of chitosan played the important role of the more drug uptake (van der Lubben, et al., 2001). Smith et al. 2004 found that chitosan-mediated tight junction disruption on epithelial cells by the positive charges on the chitosan included interactions with the tight junction proteins occludin and ZO-1, redistribution of F-actin, and slight destabilization of the plasma membrane. Thus, incorporating chitosan as a carrier to lipid nanoparticles (SLN/NLC) can enhance permeability the lipid nanoparticles across intestinal cells by paracellular pathway.

The possible mechanisms for the particles to pass through the gastrointestinal (and other physiological) barriers could be paracellular passage particles “kneading” between intestinal epithelial cells for extremely small size (<50nm), endocytotic uptake particles which absorbed by intestinal enterocytes through endocytosis if the particles size \approx 500nm and also lymphatic uptake particles adsorbed by M cells of the Peyer’s patches for bigger particle (particle size <5mm) (Florence 2004). According to this, the possible mechanism for all formulation is following endocytosis pathway since the particle size of all formulation from 100nm to 600nm. However, according to the PDI value of each formulation that indicated broad distribution size, it is still possible that any small particles from the all formulation to penetrate through Caco-2 by paracellular pathway, especially when the tight junction was opened. Polysorbate 80 also which able to modify the lipophilic surface into hydrophilic compound also can lead paracellular pathway uptake. It can be proposed that both redispersed spray dried of AASLN (RSPcAASLN) and redispersed spray dried powder of

AANLC chitosan-based (RSPcAANLC) penetrated Caco-2 cells by paracellular pathway.



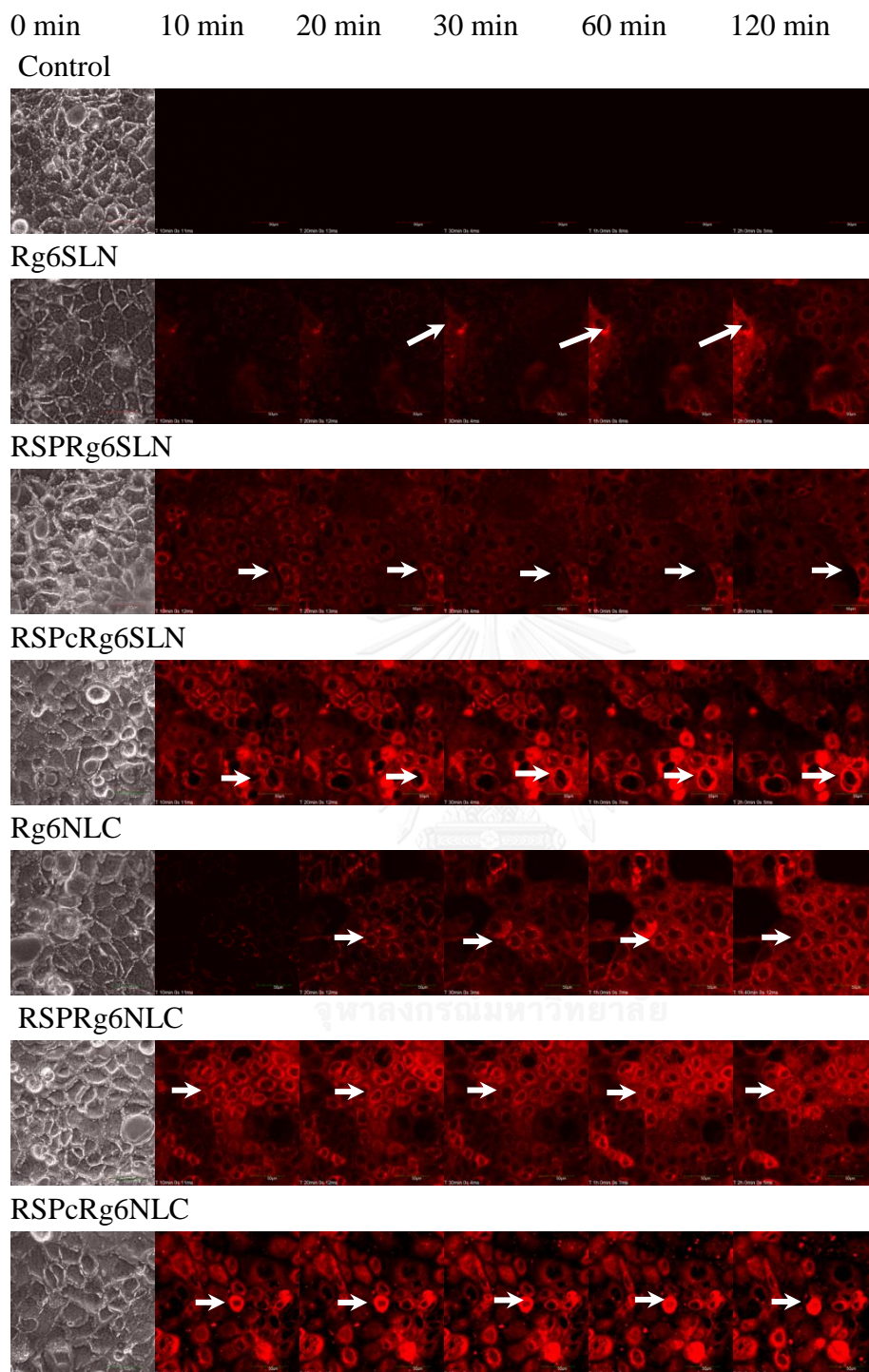


Figure 4.35 Confocal Laser Scanning Microscopy (CLSM) study of R6gSLN, RSPR6gSLN, RSPcR6gSLN, R6gNLC, RSPR6gNLC and RSPcR6gNLC on Caco-2 cells for 2 h incubation. Paracellular localization of R6g fluorescence was noted (arrow).

7.9.2 Toxicity Study on Caco-2 cells

One of major requirements for drug formulation should be non-toxic. MTT assay were to carry out toxicity of RSPcAASLN and RSPcAANLC on Caco-2 cells viability shown in Figure 4.36 and Figure 4.37. Comparing to 80% cell viability of control group, only RSPcSLN blank that significantly decreased until 63.82% ($p < 0.05$) (see Appendix H). Meanwhile, RSPcAASLN and RSPcAANLC did not show toxicity in the highest concentration (100 μM). It is indicated that the existence of AA itself also has a positive effect on cell viability.

The toxic RSPcSLN blank might be also caused by the interaction of chitosan with cells more intensely than other formulations. Although chitosan was generally regarded as safe (GRAS) biodegradable polymer and also had been found its application in many areas of drug delivery (Kean and Thanou 2010), Schipper et al. (1997) observed some toxic effect of certain chitosan in Caco-2 cells. Except chitosan, the other component of formulations also contributed to toxicity of the formulation. It can be seen that the cell viability tend to increase with the diluting formulation from equal to 100 μM to 12.5 μM of AA.

Even though the other formulations did not show toxicity effect on Caco-2 cells on concentration 100 μM (biggest concentration) with no significant difference from 80% of cell viability, which is indicated safe formulation (Sha et al. 2005), the cells viability of SLN systems (Figure 4.41) were lower than NLC systems (Figure 4.42) (63.72-88.62% vs 73.71-89.88%). Since AA also contributed on cell viability, the higher cell viability

of NLC systems treatment might be due to the ease of AA-released from NLC systems than from SLN systems. The ease AA-released from NLC systems then could reduce killing the cells.

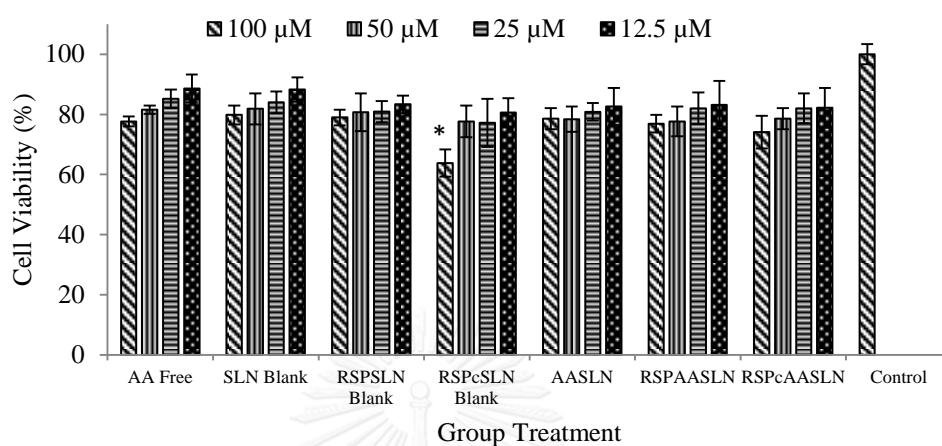


Figure 4.36 Toxicity study on Caco-2 cells between different treatment groups; AA free, SLN blank, RPSLN blank, RSPcSLN blank, AASLN, RSPAASLN and RSPcAASLN. Toxicity study were conducted in equal concentration of AA concentration at 100 μ M, 50 μ M, 25 μ M and 12.5 μ M. Error bars represent standard deviations of the mean based on three replicates.* represents significantly different to 80% cell liability.

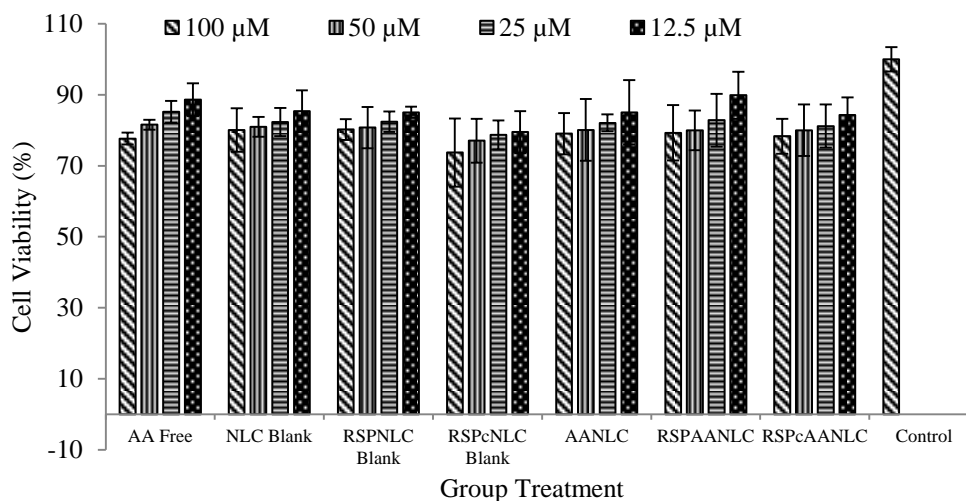


Figure 4.37 Toxicity study on Caco-2 cells between different treatment groups; AA free, NLC blank, RSPNLC blank, RSPcNLC blank, AANLC RSPAANLC and RSPcAANLC. Toxicity study were conducted in equal of AA concentration at 100 μM , 50 μM , 25 μM and 12.5 μM . Error bars represent standard deviations of the mean based on three replicates.

7.9.3 Permeability on Caco-2 cells

Figure 4.38 shows that after 2 h incubation, cumulative drug transport became relatively constant in many groups treatment. Comparing to AA free, AA in SLN or NLC and also in their spray dried powder with and without chitosan showed higher drug transport. Since paracellular and endocytosis pathway are the possible pathways of those formulations, the hydrophilic surface of those formulations (AASLN, AANLC, RSPAASLN, RSPcAASLN, RSPAANLC and RSPcAANLC) might role on higher paracellular transport resulting higher drug transport. After 2 h incubation, the cumulative drug of the group with chitosan (RSPcAASLN and RSPcAANLC) treatment showed the significant highest percentage of drug transport at 49.40% and 42.90% ($p < 0.05$) (see Appendix I). Chitosan with its positive charge and mucoadhesive properties might play the role on opening tight junction resulting high

drug transport through Caco-2 cells. These results were comparable with Fonte et al. (2011) that found their coating SLN with chitosan significantly increased the cumulative transport of insulin.

For comparison of drug transport of AASLN and AANLC vs the redispersed powder of AASLN and AANLC with and without chitosan, it seems that the smallest size of particles did not show the higher drug transport. These results were supported by Yin Win and Feng (2004) found that the nanoparticles with 500nm size were able to be uptake by Caco-2 cells by 1.8 folds greater than the nanoparticles with 50nm size.

Comparison between AASLN systems and AANLC systems, it is shown that the AASLN showed higher drug transport than AANLC systems. After 6 h incubation 53.66% of drug was transported from RSPcAASLN, while only 46.45% of drug was transported from RSPcAANLC. Non chitosan groups also were shown the similar trend which after 6 h incubation, 38.39% of drug was transported from RSPAASLN and 34.91% from RSPAANLC (Figure 4.38).

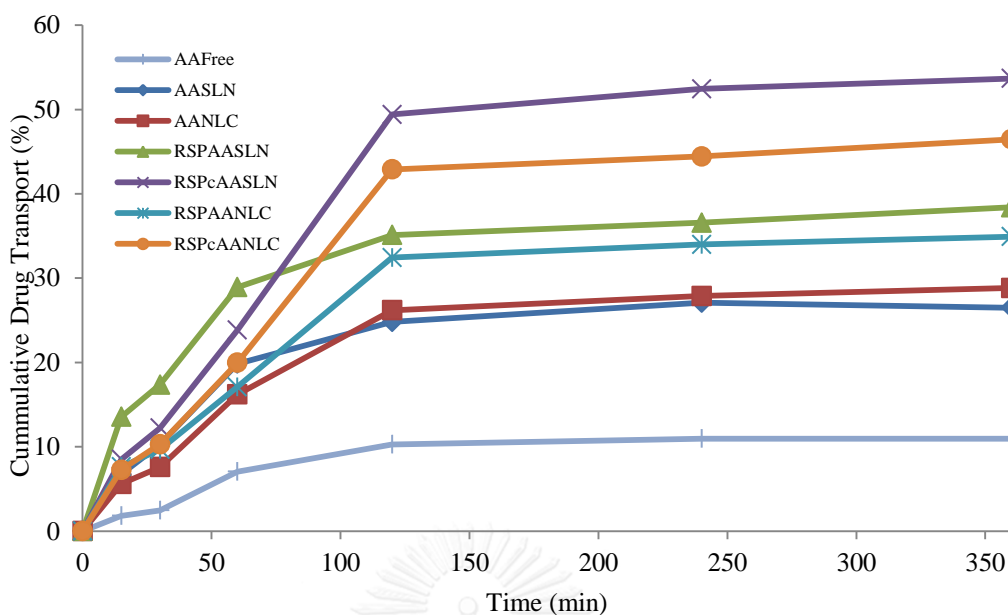


Figure 4.38 Cumulative drug transport of AA through Caco-2 cells between treatment groups of AA Free, AASLN, RSPAASLN, RSPcAANLC, AANLC RSPAANLC and RSPcAANLC. Error bars represent standard deviations of the mean based on three independent experiments were omitted to obtained clear image.

Since after 2 h incubation, the amount of drug transport was in relatively constant drug cumulative, apparent permeability (P_{app}) of this study was calculated at 2 h incubation. Relatively constant of drug indicated a steady state condition. Figure 4.39 shows that after 2 h incubation, the absorptive flux (apical-to-basolateral, A-to-B) was found to be statistically significant difference for any treatment groups (AASLN, AANLC, RSPAASLN, RSPcAASLN, RSPAANLC and RSPcAANLC) compared to the media control (AA free) (see Appendix I). Groups with RSPcAASLN and RSPcAANLC treatment also showed significantly ($p < 0.05$) higher permeability (2.46×10^{-5} cm/s and 2.19×10^{-5} cm/s) than a group of AASLN, AANLC, RSPAASLN and RSPAANLC indicating that the AA from

RSPcAASLN and RSPcAANLC system could permeate Caco-2 cell in significant higher amount ($p < 0.05$) than AA in water dispersion of AASLN, AANLC and AA free. This result showed that incorporation AASLN and AANLC with chitosan and also adding maltodextrin and then spray drying them, gave positive contribution in permeability process. The positive charge of chitosan not only increased the electrostatically interaction between nanoaggregates and Caco-2 cell membrane (Ranaldi et al. 1992) but also had mucoadhesive property that allowed much more nanoaggregates of AASLN or AANLC attached and easy to permeate (van der Lubben et al. 2001) either paracellular or transcellular pathway (Fonte et al. 2011). The graph in Figure 4.44 also shows that RSPcAANLC had significant lower permeability than the RSPcAASLN ($p < 0.05$), the castor oil as liquid lipid component of NLC might lead less interaction between lipid nanoparticles and the cell membrane so AA in RSPcAANLC could not penetrate as easy and rapid as in RSPcAASLN.

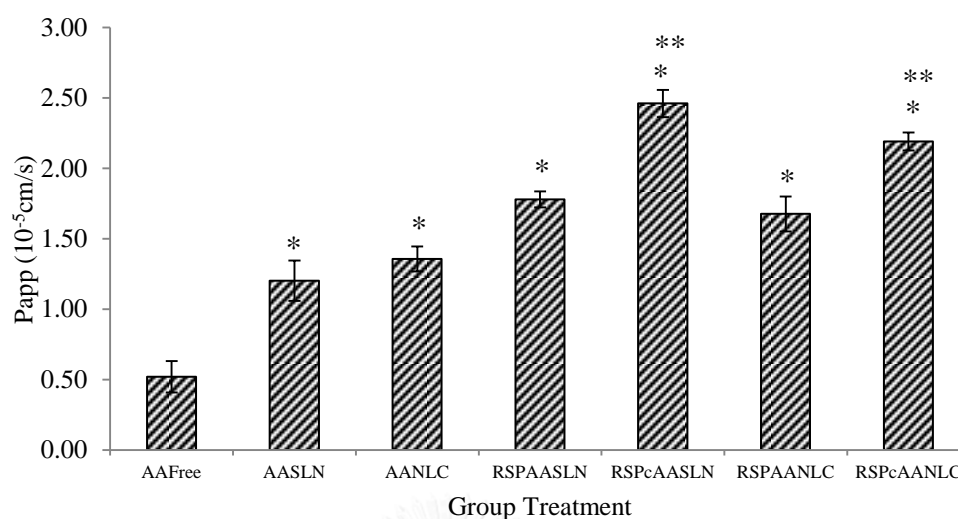


Figure 4.39 Permeability study on Caco-2 cells between different treatment groups: AA free, AASLN, AANLC, RSPAASLN, RSPcAASLN, RSPAANLC and RSPcAANLC. Error bars represent standard deviations of the mean based on three independent experiments.* represents significantly different ($p < 0.05$) to AA free group. ** represents significantly different to original lipid nanoparticles (AASLN and AANLC)

Figure 4.40 shows that all formulations did not show drug reverse ratio (< 2.00). RSPAASLN treatment group showed the smallest reverse ratio (0.38), indicated that this formulation less tendency to reverse the drug (AA) from Caco-2 cells (Mensch et al. 2010). It is concluded that lipid nanoparticles especially AANLC, redispersed spray dried powder of AASLN and redispersed spray dried powder of AANLC chitosan-based could improve the permeability in the small intestine.

It is interesting that the redispersed spray dried powder of AASLN and AANLC showed less reverse ratio than their original AASLN and AANLC (0.38 and 0.51 vs 0.59 and 0.54). As known that surfactants also played role increase the modulator of drug efflux (Göppert et al. 2005, Huang et al 2008) the dehydration

during spray drying process might alter the surfactant properties (Lee 2003) which might reduce their modulator effect on drug reverse. It is not satisfied that incorporation of chitosan into spray drying AASLN and AANLC increase the drug reverse (0.41 and 0.65). The mucoadhesion chitosan might play a role the residence time of the drug on the cell surface that not only increase permeability but also increase the interaction between drug and drug efflux transporters. However, the increasing drug reverse ratio is still less than 2.00 which considered as moderate reverse drug.

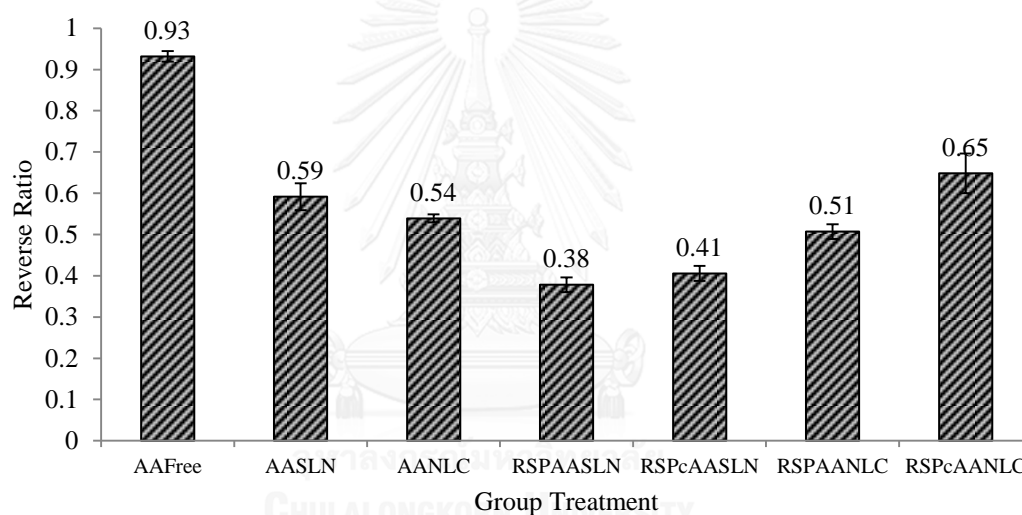


Figure 4.40 Reverse ratio of AA free, AASLN, AANLC, RSPAASLN, RSPcAASLN, RSPAANLC and RSPcAANLC on Caco-2 cells. Error bars represent standard deviations of the mean based on three independent experiments.

7.9.4 Uptake study on Caco-2 cells

Figure 4.41 shows the association of drug with cells during permeability study. It is shown that the groups that treated by incorporated AA in SLN and NLC and also spray dried in chitosan-based increased permeability compared to AA free. Chitosan incorporation increases

significantly to the uptake drug by Caco-2 cells. Positive charge of chitosan also indicated not only rapid electrostatically interaction but easier association which led high drug uptake amount. In addition, mucoadhesion of biopolymer-chitosan also provide mucus layer (Kawashima and York 2008; Cui et al. 2009; Fonte et al. 2011) that could improve nanoaggregates of AASLN and AANLC form RSPcAAASLN and RSPcAANLC interface on Caco-2 cells and oral absorption (Bowman and Leong 2006). These results also highlighted the misconception that the smaller nanoparticle size, the better the cellular can be resulted. Yin Win and Feng (2004) found that there is an optimum size range of particles that shows the best cellular uptake.

From Figure 4.41, it was shown that NLC systems (AANLC, RSPAANLC and RSPcAANLC) seemed easier to associate to Caco-2 cells than SLN systems (AASLN, RSPAASLN and RSPcAASLN). As colloidal drug carrier, NLC systems which contain solid and liquid lipid provided flexible form to achieve higher drug uptake in Caco-2 cells than SLN systems which contained solid lipid only (Müller et al. 2002a). This uptake drug result was consistent with confocal laser scanning microscopy study (Figure 4.35).

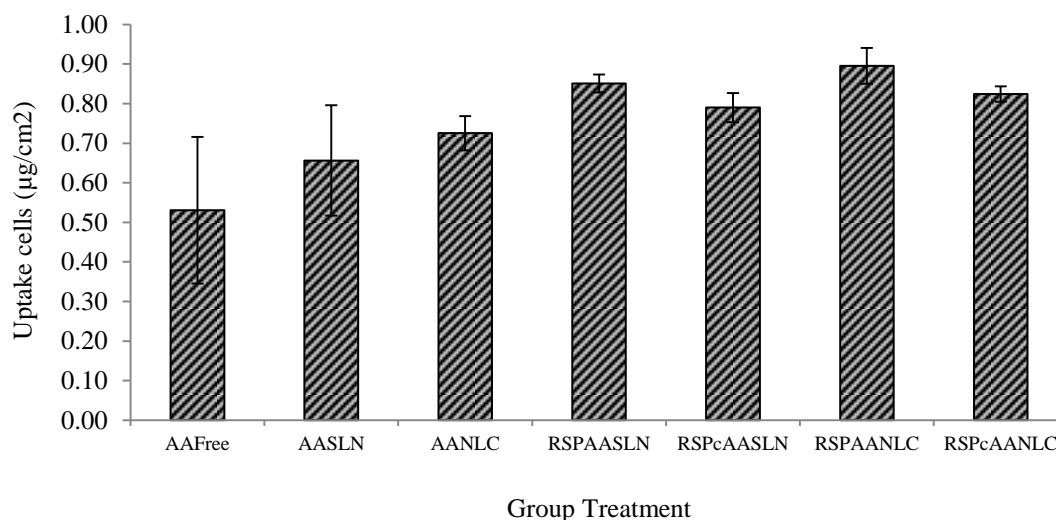


Figure 4.41 Uptake study on Caco-2 cells between different treatment groups; AA Free, AASLN, AANLC, RSPAASLN, RSPcAASLN, RSPAANLC and RSPcAANLC. Error bars represent standard deviations of the mean based on three independent experiments.

7.9.5 TEER study on Caco-2 cells

Transepithelial electrical resistance (TEER) reflects the impedance to the passage of small ions through the physiological barrier and is recognized as one of the most accurate and sensitive measures of epithelial cells integrity (Rutten et al. 1987). Results of the TEER experiments are expressed as percentage of the initial resistance value of the monolayer, which was $401.30 \pm 50.44 \Omega \cdot \text{cm}^2$ ($n = 24$).

Figure 4.42 shows TEER value on Caco-2 cells by experiment. After 2 h incubation, TEER value become in constant value. Except control group (without treatment), all group treatment underwent significant TEER decreasing ($p < 0.05$) at 39.25-93.74% (see appendix J). Decreasing of TEER value reflected loss of barrier function of epithelial cells and also opening of

the tight junction. However, decreasing TEER value that can open tight junction should over than 50% decrease (Briske-Anderson et al. 1997). In this observation, only RSPcAASLN and RSPcAANLC that showed decreasing TEER value until $39.25\pm 4.32\%$ and $47.19\pm 5.37\%$ which are over than 50% decrease indicating opening tight junction. The incorporating AASLN and AANLC with chitosan decreased TEER value. The positive charge of chitosan might play a role on reversible effect on TEER value (Sha et al. 2005). Ranaldi et al. (2002) also found that chitosan was the only cationic polymer that displayed an irreversible effect on the tight junction at 0.01%. It can be possible to conclude that incorporating chitosan on spray drying AASLN and AANLC could open the tight junction of Caco-2 cells (0.0125%).

The TEER value after incubation of RSPcAASLN and RSPcAANLC groups was observed in the next 24 h and the value reached almost the same TEER value before incubation at $388.15\pm 38.12 \Omega\cdot\text{cm}^2$ or 96.67% back, indicating that after removing the integrity of cells recover. This result also indicated that chitosan in the formulation had recovery properties tendency and also showed a quite safe polymer to Caco-2 cells as a model of epithelial cells.

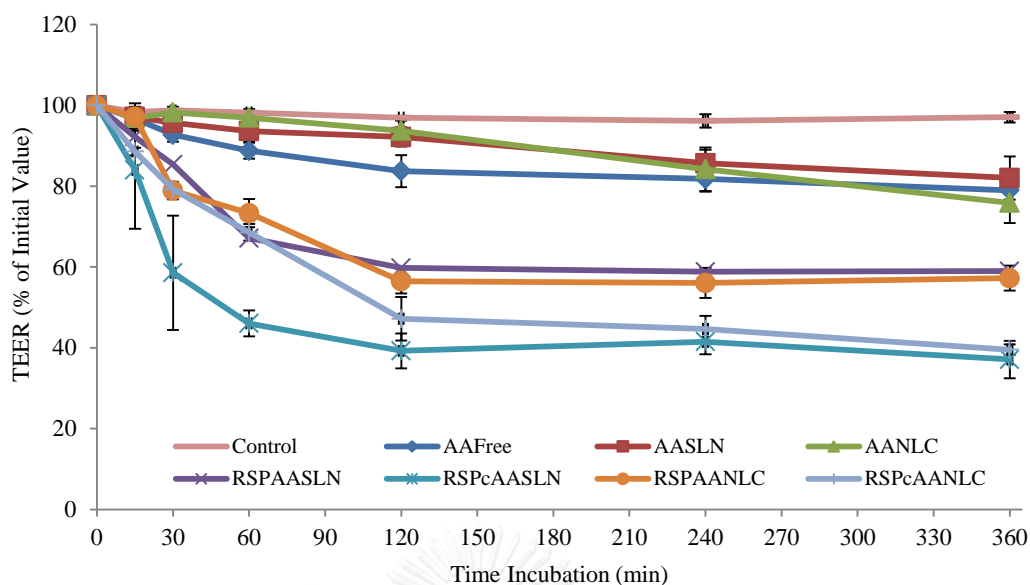


Figure 4.42 Percentage of TEER change value on Caco-2 cell between different treatment groups. Error bars represent standard deviations of the mean based on three independent experiments.

7.9.6 Size and zeta potential behavior in permeability study on Caco-2 cells

Figure 4.43 shows nanoaggregates measured after passing Caco-2 cells compared to before passing Caco-2 cell on permeability study. After passing Caco-2 cells (2 h incubation), the average nanoaggregate size of all formulations was significantly decreased. Before passing Caco-2 cells, average nanoaggregate size of redispersed spray dried powder of AASLN and AANLC in apical site was measured 444.28nm and 399.78nm, respectively. After passing Caco-2 cell, the size of RSPAASLN was 326.12nm and 344.28nm for RSPAANLC. Size of RSPcAASLN before passing Caco-2 cells was 527.40nm then after passing Caco-2 cells became 448.70nm and for RSPcAANLC was 584.60nm then became 480.78nm. Since from CLSM images confirmed that the nanoparticles penetrate Caco-2

cells via paracellular pathway, the significant decreasing size after passing Caco-2 cell suggesting disaggregation of nanoparticles generating smaller nanoparticles on endocytosis pathway. The mean diameter number of all groups was found a small number less than 50nm (data not shown). These small particles might penetrate through Caco-2 cells by paracellular pathway.

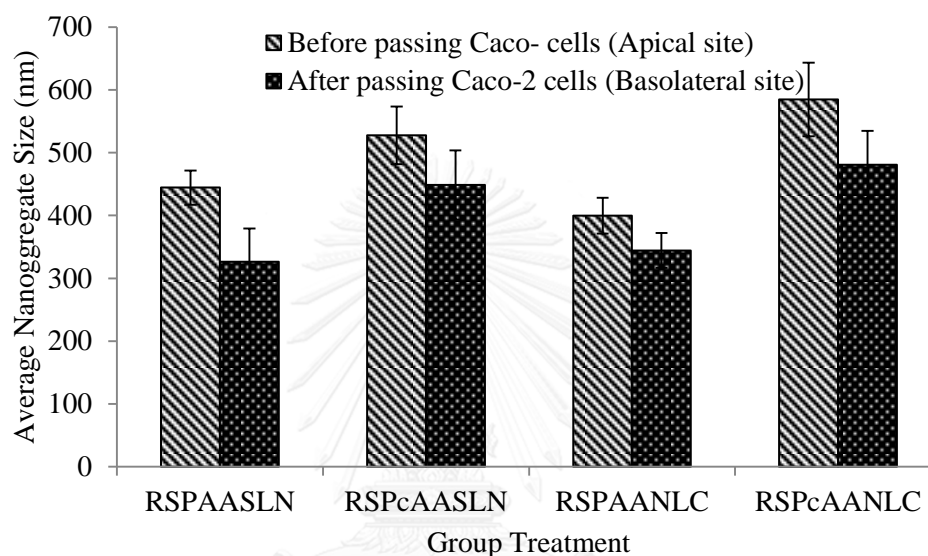


Figure 4.43 Nanoaggregates size of redispersed spray dried powder of AASLN chitosan-based and spray dried powder of AANLC chitosan-based, before and after permeability study. Error bars represent standard deviations of the mean based on three replicates.

Figure 4.44 shows the change of zeta potential value of redispersed spray dried powder of cAASLN (RSPcAASLN), cAANLC (RSPcAANLC) and RSPAASLN, RSPAANLC for comparison. Zeta potential as an indicator of surface charge of nanoparticles was important to facilitate nanoparticles to be uptake by epithelial cells in intestinal mucus which has a negative charge. Most of zeta potential value of nanoparticles is attributed to their surfactant or other charged component nanoparticles. Zeta potential values of

RSPAASLN and RSPAANLC before passing Caco-2 cells were -16.92 mV then became -9.17 mV after passing Caco-2 cells. The milieu of the apical site of transwell brings the negative surface charge. The increasing zeta potential of nanoaggregates from RSPAASLN and RSPAANLC might be caused by reducing surfactant surrounding their nanoaggregates during penetration. Zeta potential of RSPcAASLN was 41.64 mV then after passing Caco-2 cells became -9.24 mV. The decreasing zeta potential was also occurred in RSPAASLN from -16.70 to -12.61 and RSPcAANLC from 33.22 mV to 1.72 mV after passing Caco-2 cells. The negative charge of RSPAASLN might be attributed to the milieu of the apical site of transwell which the bEnd3 were seeded on. On RSPcAANLC, changing zeta potential value from positive value to negative value was caused by the interaction of chitosan with the epithelial cells to facilitate the cells uptake nanoparticles or nanoaggregates via paracellular pathway. The standard deviation of this group was higher than the mean because of the different charge of zeta potential value of each sample (see Appendix K). The nanoparticles or nanoaggregates permeated Caco-2 cells only surrounded by surfactant which had a negative charge. Meanwhile, on RSPcAANLC, some nanoparticles or nanoaggregates might still be surrounded by small amount of chitosan resulting slight positive charge of zeta potential. The nanoparticles or nanoaggregates were only surrounded by surfactants (Tween 80, Span 80 and pluronic F127) would be contributed on surface hydrophilicity of nanoaggregates. The hydrophilic surface could avoid the nanoaggregates

from disappearance in the blood stream by phagocytic cells (Moghimi et al. 2001; Furumoto et al. 2004).

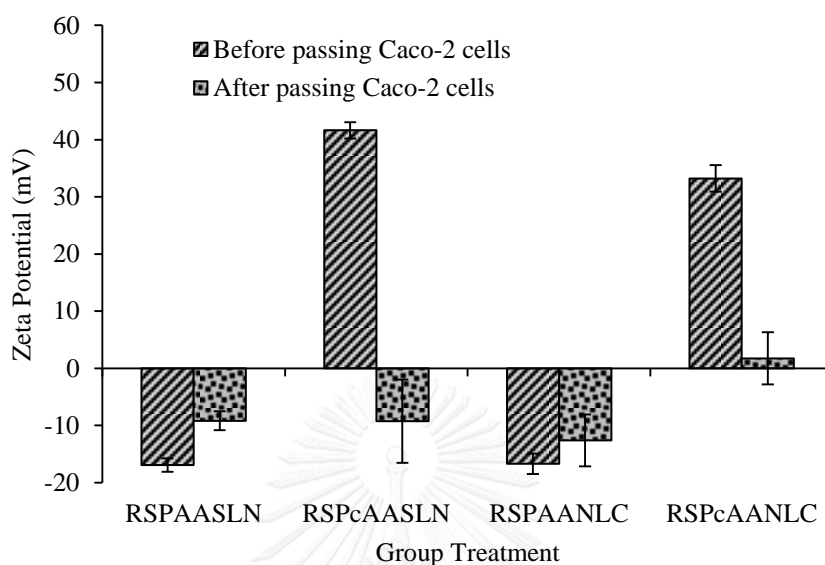


Figure 4.44 Zeta potential of redispersed spray dried powder of AASLN and AANLC chitosan-based, before and after permeability study. Error bars represent standard deviations of the mean based on three replicates.

7.10 Permeability Study on bEnd3 Cells Cocultured with CTX-TNA2 Cells

7.10.1 Confocal Laser Scanning Microscopy (CLSM) study

bEnd3 cells are immortalized mouse brain endothelial cell line exhibiting endothelial properties. It expresses von Willebrand factor, vascular endothelial growth factor receptors and can internalize acetylated low-density lipoprotein (Pepper et al. 1997). Due to their rapid growth, ease of maintenance over repeated passages, formation of functional barriers and amenability to numerous molecular interventions, bEnd3 cells are interesting

BBB model (Brown et al. 2007). So, in this study, bEnd3 was selected as BBB model.

Confocal microscopy study was conducted to observe penetration and distribution of the formulation in bEnd3 monolayer.

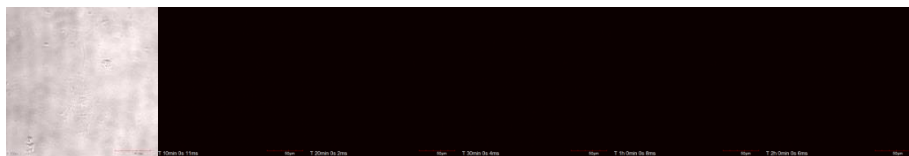
Figure 4.45 illustrates confocal microphotographs of bEnd3 cells treated with the penetration and distribution of the formulation from basolateral site of Caco-2 cell permeability study which dyed with rhodamine 6g (R6g) in bEnd3 cells (clear images (clear images can be seen in Appendix I).

Figure 4.45 shows the fluorescence of R6g from all of formulations (SLN, RSPSLN, RScSLN, NLC, RSPNLC and RSPcNLC) was internalized within cells and was localized in cytoplasmic compartments. Therefore, it is concluded that AASLN, RSPAASLN, RSPcAASLN, AANLC, RSPAANLC and RSPcAANLC penetrated bEnd3 monolayer through cells by intracellularly pathway. In previous study, it was found that the lipid nanoparticles across BBB via passive diffusion (Abraham et al. 1994), endocytosis pathway (Smith and Gumbleton 2006). Meanwhile, Kaili et al. 2009 found that the uptake lactoferin-nanoparticles loaded Coumarin-6 by bEnd3 cells were time-, temperature- and concentration-dependent and suggested active endocytosis mechanism. In addition, Martins et al. 2012 also found that SLN stabilized with polysorbate 60 and 80 are internalized by glioma cell lines by an energy dependent mechanism.

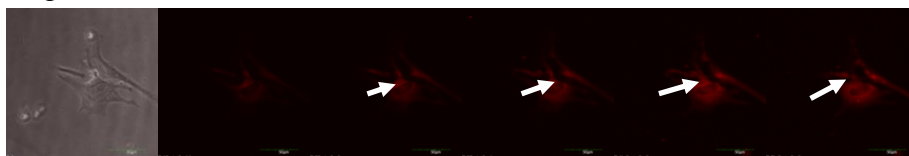
Figure 4.45 shows that incorporating chitosan on spray dried powder of Rh6gSLN or R6gNLC increased the rate of penetration. The R6gSLN and

R6gNLC nanoaggregates from RSPcRR6gSLN and RSPcR6gNLC penetrated slower than the spray dried of R6gSLN and R6gNLC with and without chitosan. The group of spray dried R6gSLN and R6gNLC, fluorescent cells picture could be seen at 10 min of incubation while in a group of R6gSLN and R6gNLC, and fluorescent cells were seen after 20 min of incubation. Intensity of fluorescent cells that were outlined by chitosan incorporated groups (RSPcR6gSLN and RSPcR6gNLC) also increased than without chitosan group (RSPR6gSLN and RSPR6gNLC). The mucoadhesion of chitosan might play a role to increase the drug uptake by increasing the residence time of the drug on the cell surface (Kotzé et al. 1999). It is indicated that although the mechanism has not been fully understood, by which spray dried of cR6gSLN and cR6gNLC delivery systems can be developed for more efficient delivery to brain targeted drug.

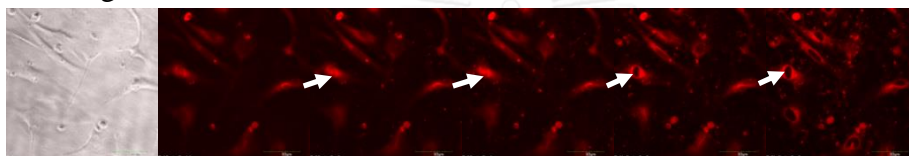
0 min 10 min 20 min 30 min 60 min 120 min
Control



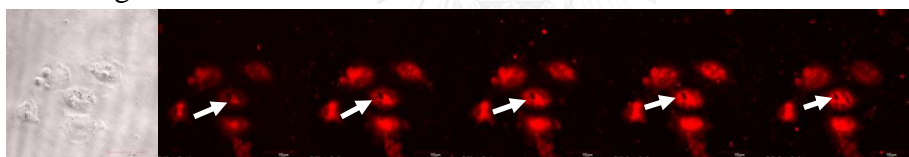
R6gSLN



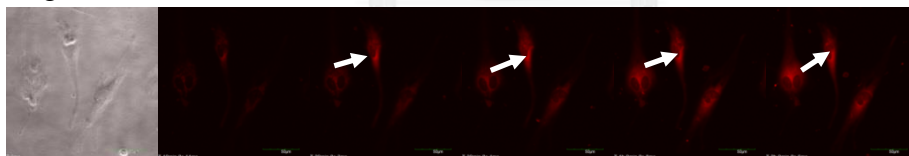
RSPR6gSLN



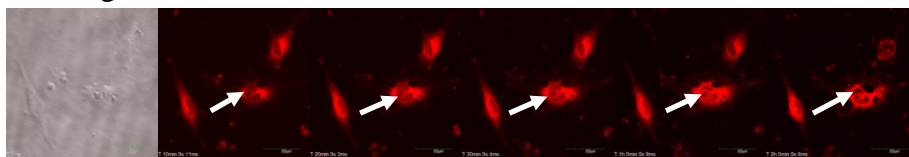
RSPcR6gSLN



R6gNLC



RSPR6gNLC



RSPcR6gNLC

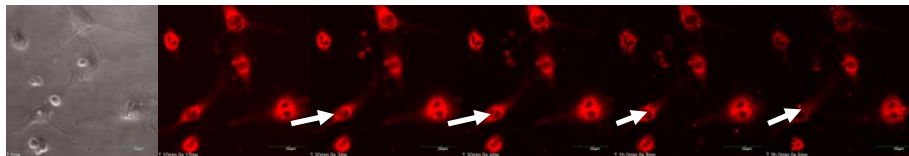


Figure 4.45 Confocal Laser Scanning Microscopy (CLSM) study of R6gSLN, RSPR6gSLN, RSPcR6gSLN, R6gNLC, RSPR6gNLC and RSPcR6gNLC on bEnd3 cells. Intracellular localization of R6g fluorescence was noted (arrow).

7.10.2 Toxicity study on bEnd3 cells cocultured with CTX-TNA2

To evaluate the potential of oral formulation of AA loaded RSPcSLN and RSPcNLC to be delivered across BBB, cell viability study was carried out using MTT assay with bEnd3 as the model cell line. MTT is added to a cell culture and is modified into a dye by enzymes associated metabolic activity in a live cell (formazan forming). The cell viability of placebo-SLN, NLC, RSPSLN, RSPNLC, RSPcSLN, RSPcNLC and AA free treatment groups were also tested for comparison.

Figure 4.46 and Figure 4.47 show the formulation effect on percent cells viability. In this experiment, the concentrations of AA in each formulation were not exactly determined because formulations of all treatment groups were collected from basolateral site of permeability study on Caco-2. Concentrations of AA in each formulation cells were correlated to drug transport from the permeability study on Caco-2 cells (Figure 4.38).

According to percent cells viability that not less than 80% (Sha et al. 2005), it could be seen that all formulation, including the Blank SLN and NLC, free AA, SLNAA-SLN, AA-NLC, redispersed nanoaggregates of AASLN and AANLC chitosan-based did not show toxicity effect (>80%). Figure 4.46 and Figure 4.47 show that blank SLN and blank NLC affected in less cell viability than drug without formulation (AA free). It might be caused by surfactant that involved in SLN or NLC, but still considered as safe

surfactant. So, it was prudent to use the formulation for further permeability study on bEnd3 without dilution. And all these results demonstrated that AA loaded RSPcSLN and RSPcNLC as a potential tool to cross BBB via oral administration.

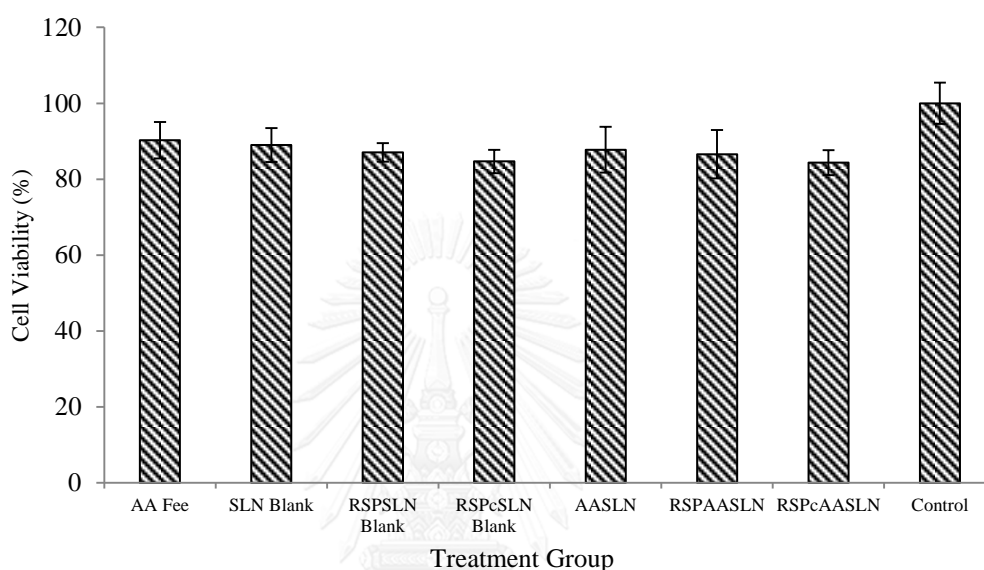


Figure 4.46 Toxicity study on bEnd3 between different treatment groups; AA free, SLN, RSPSLN Blank, RSPcSLN Blank, AASLN, RSPAASLN and RSPcAASLN. Error bars represent standard deviations of the mean based on three replicates.

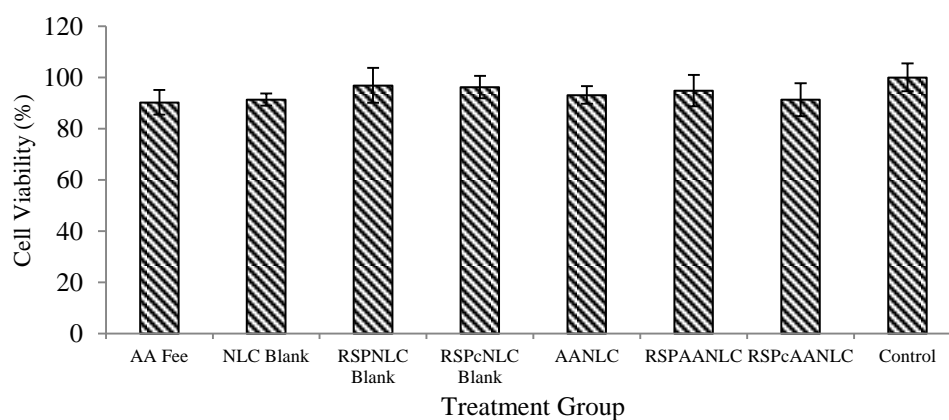


Figure 4.47 Toxicity study on bEnd3 between different treatment groups; AA free, NLC blank, RSPNLC Blank, RSPcNLC Blank, AANLC RSPAANLC and

RSPcAANLC. Error bars represent standard deviations of the mean based on three replicates.

7.10.3 Permeability study on bEnd3 cells cocultured with CTX-TNA2

Monolayer bEnd3 cells cocultured with CTX-TNA2 were treated by several formulations taken from basolateral site of transport study of Caco-2 cells. After 2 h incubation, all of the treatment group were significantly different with media control (AA Free). The percentage of all group treatments showed higher percent transport (32.64-56.64%) than the control group (AA free) (24.44%) (Figure 4.48). The lipid nanoparticles of AASLN, AANLC, RSPAASLN, RSPcAASLN, RSPAANLC and RSPcAANLC treatment group which prior passed Caco-2 cells were easier to penetrate bEnd3 cells by intracellular pathway than the free drug. The powder redispersion of both AASLN and AANLC with and without chitosan showed higher drug transport than the original AASLN and AANLC. It is indicated adding maltodextrin on spray drying showed improve permeability on bEnd3 cells cocultured with CTX-TNA2 which prior passed Caco-2 cells. The redispersion of spray dried AANLC groups (with and without chitosan) showed slightly better drug transport than the spray dried of AASLN group. The nanoparticles might be changed their behavior during passing Caco-2 cells.

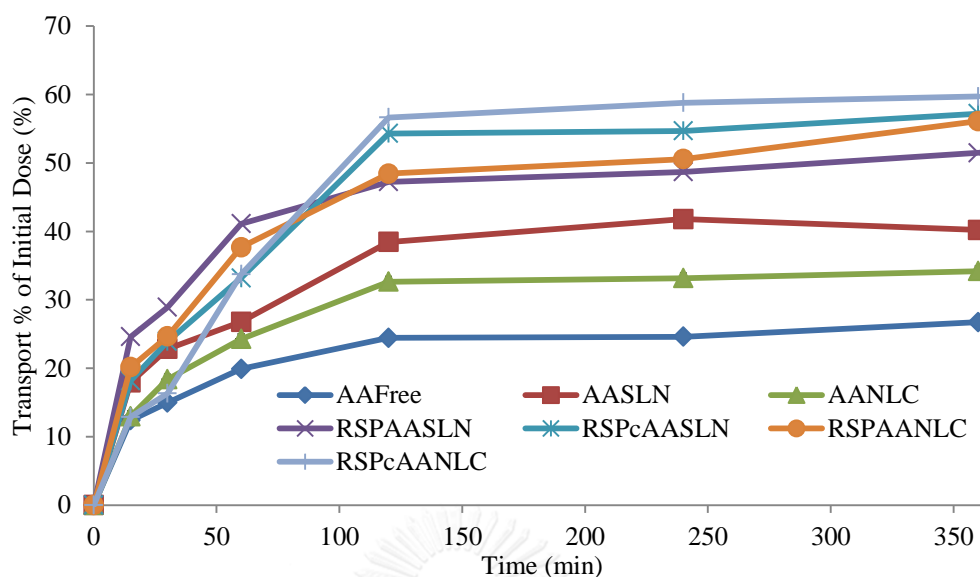


Figure 4.48 Percentage transport of AA through bEnd3 cells cocultured with CTX-TNA2 between treatment groups of AA Free, AASLN, RSPAASLN, RSPcAANLC, AANLC, RSPAANLC and RSPcAANLC. Error bars represent standard deviations of the mean based on three independent experiments were omitted to obtained clear graph image.

Figure 4.49 shows that after 2 h incubation, except the AANLC group, all treatment groups show higher permeability than the control group (free AA). RSPcAANLC group showed the highest permeability than other groups but did not significantly higher compared to RScAASLN ($p > 0.05$) (see Appendix I). The highest permeability of RSPcAANLC group might be caused by the presence of small amount of chitosan surrounding their nanoaggregates. As known before, RSPcAANLC after passing Caco-2 cells still a had positive charge (Figure 4.44). The positively charged of nanoaggregates increased the electrostatic interaction between the nanoaggregates and endothelial cells. According to the zeta potential measurement from Figure 4.44, other groups (RSPAASLN, RSPcAASLN,

and RSPAANLC) which consisted of only nanoparticles or nanoaggregates of lipid stabilized by surfactant could not interact with bEnd3 cells as fast as RSPcAANLC resulting lower apparent permeability.

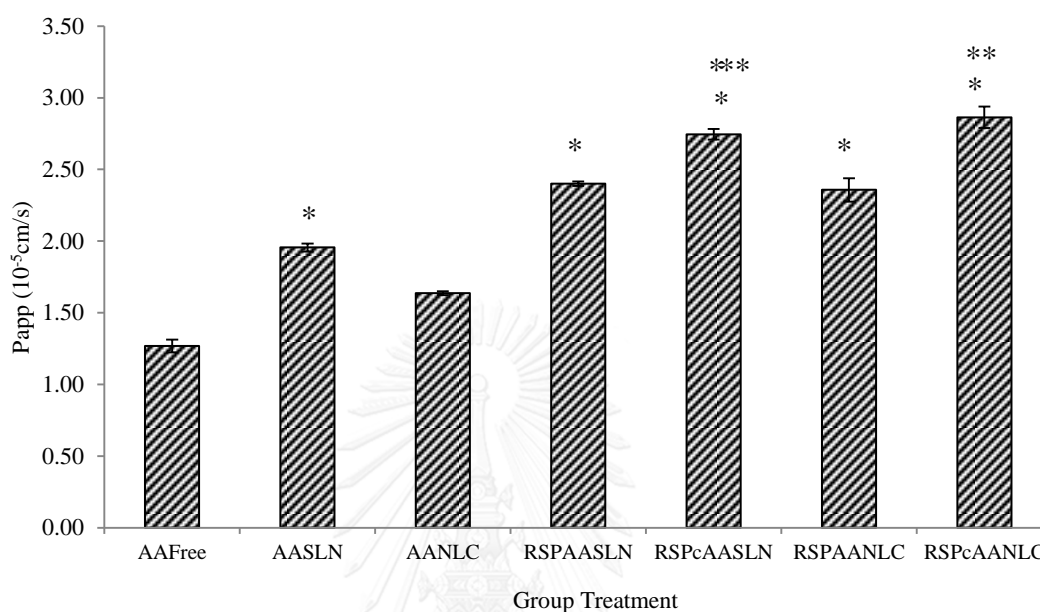


Figure 4.49 Permeability study of AA on bEnd3 cells cocultured with CTX-TNA2 between different treatment groups; AA Free, AASLN, RSP-AASLN chitosan-based, AANLC and RSP-AANLC chitosan-based. Error bars represent standard deviations of the mean based on three independent experiments.* represents significantly different ($p < 0.05$) to AA Free group.** represents significantly different to their original nanoparticles of AASLN and AANLC group.

Figure 4.50 shows that there was no treatment showing drug reverse ratio value over than 2.00. The lower drug reverse ratio drug ratio (Mensch et al. 2010) was satisfying the possibility of the hypothesis that the SPcAASLN and SPcAANLC could be employed as an oral drug, could permeate BBB then could be targeted to brain delivery.

The smallest drug reverse ratio value of RSPcAANLC group indicated that this in this formulation the drug underwent the less reverse than other groups. The

smallest drug reverse ratio of this also explained the high percentage drug transport in the RSPcAANLC group (Figure 4.48).

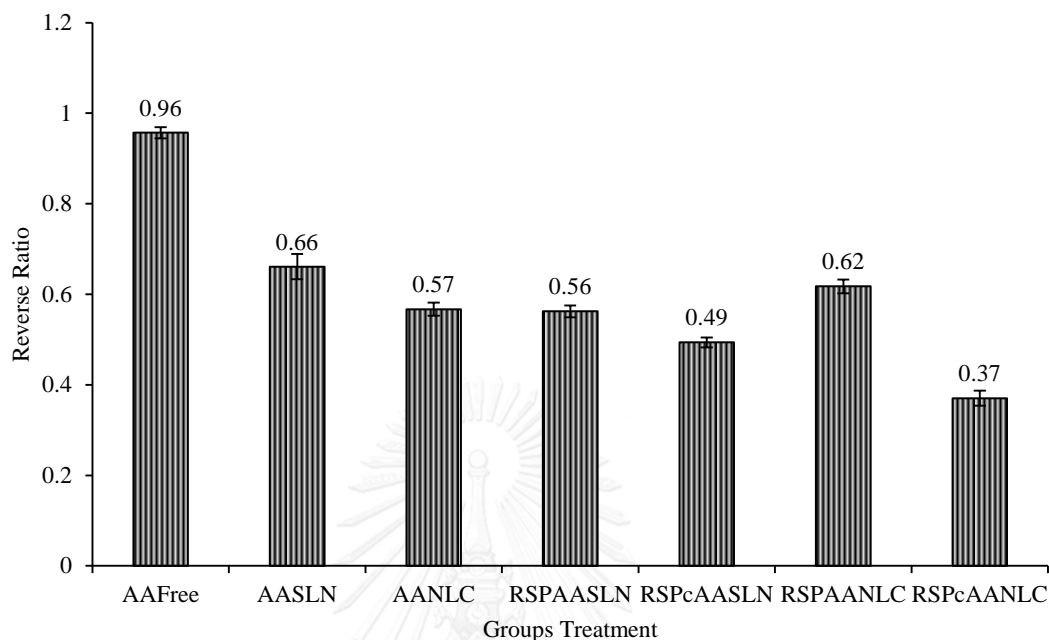


Figure 4.50 Reverse ratio of between different treatment groups, AA free, AASLN, AANLC, RSPAASLN, RSPcAASLN, RSPAANLC and RSPcAANLC) on bEnd3 cells. Error bars represent standard deviations of the mean based on three independent experiments.

7.10.4 Uptake study on bEnd3 cells cocultured with CTX-TNA2

Figure 4.51 shows the association of drug during permeability study. It was shown that the AASLN had the lowest uptake drug compared to other treatments groups. More intensity on picture of AANLC and RSPcAANLC from CSLM study also confirmed the higher uptake drug (

Figure 4.45). The more flexibility of lipid behavior of AANLC and RSPcAANLC might be one of the factors to increase drug uptake to bEnd3 cells. Figure 4.51 also shows the drug was easier to be uptake by cells in

RSPcAASLN and RSPcAANLC chitosan-based groups than only on AASLN and AANLC groups. The positive charge of chitosan might involve in faster attaching then easier to nanoaggregate to be uptaken. Mucoadhesive property of chitosan made the redispersed spray dried powder of AASLN chitosan-based (RSPcAASLN) and redispersed spray dried powder of AANLC chitosan-based (RSP-AANLC) were faster and easier to be uptake by cells than AASLN and AANLC (van der Lubben et al. 2001). The remained of surfactant coated also contributed to the enhancement of drug uptake by binding the nanogreegates to the inner endothelial lining of the brain capillaries and subsequently, particles deliver drugs to the brain by providing a large concentration gradient, thus enhancing the passive diffusion; brain endothelial uptake by phagocytosis (Alyautdin et al. 1998).

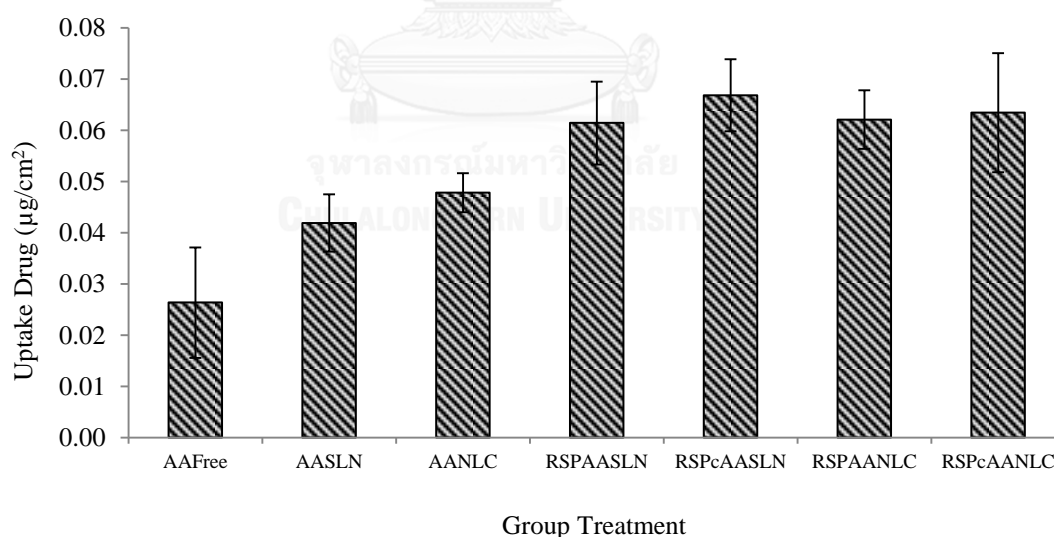


Figure 4.51 Uptake AA after 6 h incubation between different treatment groups; AA free, AASLN, redispersed spray dried powder of AASLN chitosan-based (RSP-AASLN), AANLC and redispersed spray dried powder of AANLC chitosan-based (RSP-AANLC) by bEnd3 cells cocultured with CTX-TNA2. Error bars represent standard deviations of the mean based on three independent experiments.

7.10.5 TEER study on bEnd3 cells cocultured with CTX-TNA2

Transendothelial electricity resistance (TEER) study using the mouse endothelial cell line, bEnd3 cocultured with rat astrocyte cells, CTX TNA2, was conducted to explore the mechanism penetration of oral administration of RSPcAASLN and RSPcAANLC through BBB for brain delivery. Coculturing the endothelial cells (bEnd3) with astrocyte cell (CTX-TNA2) was conducted to increase TEER. Using Corning Transwell™ membrane with diameter size of 4.67 cm², TEER value of bEnd3 alone was 139.13±4.44 Ω.cm². Meanwhile, TEER value of bEnd3 cocultured with CTX-TNA2 revealed 3.7 times higher than in bEND3 alone at 515.33±66.67 Ω.cm². The higher TEER value of the cell model is important to represent the tight junction of BBB. This TEER value also is significantly higher than TEER value of Caco-2 cell which is only 401.29±50.44 Ω.cm². This different TEER value Caco-2 cells and bEND3 cell cocultured with CTX-TNA2 cells represent enough to be used together as the small intestine and BBB model.

The TEER study (Figure 4.52) shows that the TEER values of all group treatment were significantly decreased after 2 h incubation. Except the group of RSPAANLC and RSPcAANLC, the decreasing of TEER values was about 84.80-92.12% (Appendix I). Even the decreasing of TEER value reflected on loss of barrier function, if the decreasing was less than 20% the integrity of bEnd3 cells were always maintained in a safe condition (Fonte et al. 2011). On group of RSPAANLC and RSPcAANLC, after 2 h incubation, TEER values were decreased at 79.76±0.44% and 66.32±9.11%. The decreasing TEER value of RSPAANLC group was quite high but did not

significantly different from 20% decrease, so it is still considered the barrier function of cells is still safely maintained. The quite high decreasing of TEER value of RSPcAANLC was 34%, which is over than 20%, might be indicated by losing cells integrity which reflected on increasing permeability coefficient (Figure 4.49). According to zeta potential determination passing Caco-2 cells, it is indicated that some chitosan might be existed of RSPcAANLC group then contributed on decreasing of TEER value. However, this decreasing did not indicate the opening of the tight junction because the threshold of opening tight junction is over 50% decrease (Briske-Anderson et al. 1997). According to these TEER value changes, it is indicated that RSPcAASLN and RSPcAANLC could not open the tight junction of BBB model. These results also confirmed RSPcAASLN and RSPcAANLC penetrated BBB by intracellular pathway. It can be studied further the mechanism of penetration whether by passive diffusion or endocytosis pathway as other researchers found that the lipid nanoparticles across BBB via passive diffusion (Abraham et al. 1994), endocytosis pathway (Smith and Gumbleton 2006).

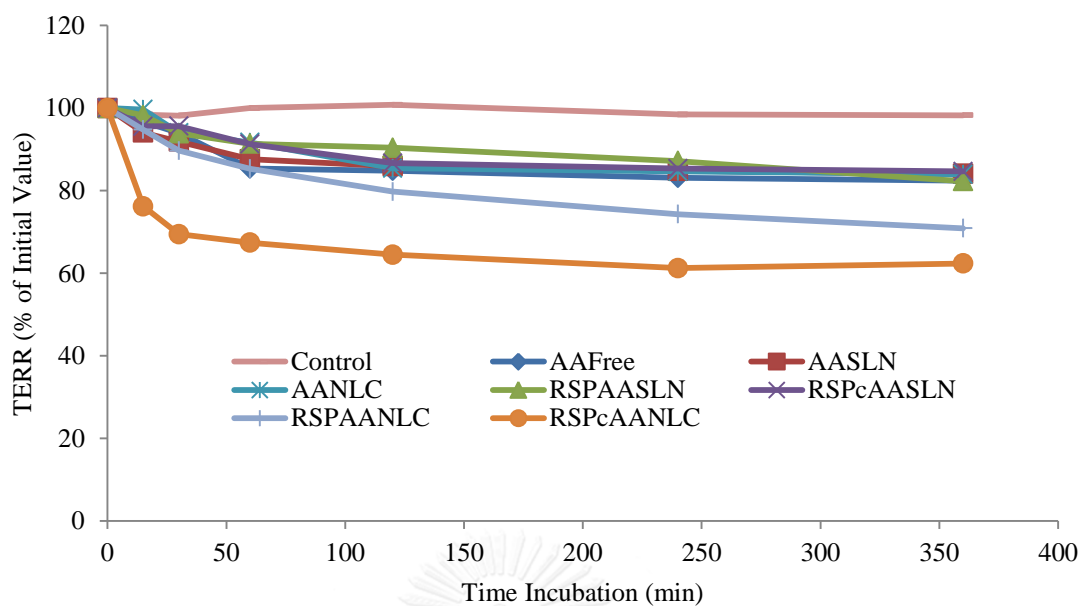


Figure 4.52 Percentage of TEER change value on bEnd3 cell between different treatment groups; AA free, AASLN, RSP-AASLN chitosan-based, AANLC and RSP-AANLC chitosan-based. Error bars represent standard deviations of the mean based on three independent experiments.

CHAPTER V

CONCLUSIONS

Response surface methodology could be employed to optimize spray drying process and feed concentration of spray dried SLN chitosan-based. Temperature had a positive influence on product yield, nanoaggregates size and moisture content. Feed rate had a negative influence to product yield and nanoaggregates, but positive response to moisture content. Feed concentration showed a negative response to product yield and moisture content in high temperature, but a positive response to nanoaggregate size.

The models of product yield, redispersed nanoaggregate size and moisture content of dry powder were fitted well with the linear, quadratic and quadratic equation model, respectively. The optimum conditions suggested from the program also could be applied for NLC as promising lipid nanoparticles. Spray drying SLN and NLC containing model drug could produce spherical shape particles and have a tendency to form an amorphous dispersion. Spray dried powder of SLN and NLC containing drug model can be redispersed into nanoaggregate of SLN and NLC particles. Nanospray drying also could produce a more rounded and smaller spherical microparticles powder and smaller redispersed nanoaggregate particles.

The model drug can be entrapped better in NLC more than SLN. The high entrapment efficiency of NLC containing modal drug lead better stability of dried powder NLC containing model drug was better than the dried powder SLN.

Converting the water dispersion of SLN and NLC and adding chitosan as based into dried powder prolong the drug release than the SLN and NLC dispersion.

Spray dried powder of SLN and NLC increase the drug transport, drug uptake and the apparent permeability of model drug both through Caco-2 cell and bEnd3 cell cocultured with CTX-TNA2. Thus, it is concluded that spray dried powder of AASLN and AANLC were a potential vehicle for AA oral delivery application tend to paracellular pathway penetration on Caco-2 cells and intracellular pathway on bEnd3 cell cocultured with CTX-TNA2. Incorporating chitosan on spray drying AASLN and AANLC could enhance permeability by opening the tight junction of Caco-2 cells.

Permeability test on bEnd3 as represent blood brain barrier also showed higher permeability on group of RSPcAASLN and RSPcAANLC. The confocal study and TEER showed that RSPcAASLN and RSPcAANLC are inclined to more intracellular penetration pathway. From those findings, it was concluded that SPcAASLN and SPcAANLC chitosan-based can be employed to oral administration for brain delivery.

REFERENCES

- Abbott, N. J., L. Ronnback, and E. Hansson. 2006. Astrocyte-endothelial interactions at the blood-brain barrier. *Nat Rev Neurosci* 7 (1):41-53.
- Abraham, M. H., H. S. Chadha, and R. C. Mitchell. 1994. Factors that influence the distribution of solutes between blood and brain. *Journal of Pharmaceutical Sciences* 83 (9):1257-1268.
- Acartürk, F., and N. Altug. 2001. In-vitro and in-vivo evaluation of a matrix-controlled bromocriptine mesilate-releasing vaginal ring. *Journal of Pharmacy and Pharmacology* 53 (12):1721-1726.
- Agrawal, P., G. J. Strijkers, and K. Nicolay. 2010. Chitosan-based systems for molecular imaging. *Advanced Drug Delivery Reviews* 62 (1):42-58.
- Ahn, J.-H., Y.-P. Kim, Y.-M. Lee, E.-M. Seo, K.-W. Lee, and H.-S. Kim. 2008. Optimization of microencapsulation of seed oil by response surface methodology. *Food Chemistry* 107 (1):98-105.
- Aktaş, Y., M. Yemisci, K. Andrieux, R. N. Gürsoy, M. J. Alonso, E. Fernandez-Megia, R. Novoa-Carballal, E. Quiñoá, R. Riguera, M. F. Sargon, H. H. Çelik, A. S. Demir, A. A. Hincal, T. Dalkara, Y. Çapan, and P. Couvreur. 2005. Development and brain delivery of Chitosan-PEG nanoparticles functionalized with the monoclonal antibody OX26. *Bioconjugate Chemistry* 16 (6):1503-1511.
- Alamilla-Beltrán, L., J. J. Chanona-Pérez, A. R. Jiménez-Aparicio, and G. F. Gutiérrez-López. 2005. Description of morphological changes of particles along spray drying. *Journal of Food Engineering* 67 (1-2):179-184.
- Albhar, K. G., V. S. Wagh, and B. B. Chavan. 2012. Effect of HPMC K4M, HPMC K15M, sodium alginate and carbopol 934 in the formulation of carbonyl iron capsule. *Der Pharmacia Lettre* 4:367-394.
- Alves, N. M., and J. F. Mano. 2008. Chitosan derivatives obtained by chemical modifications for biomedical and environmental applications. *International Journal of Biological Macromolecules* 43 (5):401-414.
- Alyautdin, R. N., E. B. Tezikov, P. Ramge, D. A. Kharkevich, D. J. Begley, and J. Kreuter. 1998. Significant entry of tubocurarine into the brain of rats by adsorption to polysorbate 80-coated polybutylcyanoacrylate nanoparticles: An in situ brain perfusion study. *Journal of Microencapsulation* 15 (1):67-74.
- Artursson, P., and J. Karlsson. 1991. Correlation between oral drug absorption in humans and apparent drug permeability coefficients in human intestinal epithelial (Caco-2) cells. *Biochemical and Biophysical Research Communications* 175 (3):880-885.
- Artursson, P., T. Lindmark, S. S. Davis, and L. Illum. 1994. Effect of chitosan on the permeability of monolayers of intestinal epithelial cells (Caco-2). *Pharmaceutical Research* 11 (9):1358-1361.
- Asasutjarit, R., S.-I. Lorenzen, S. Sirivichayakul, K. Ruxrungtham, U. Ruktanonchai, and G. Ritthidej. 2007. Effect of solid lipid nanoparticles formulation compositions on their size, zeta potential and potential for in vitro pHIS-HIV-hugag transfection. *Pharmaceutical Research* 24 (6):1098-1107.

- Bailey, C. A., P. Bryla, and A. W. Malick. 1996. The use of the intestinal epithelial cell culture model, Caco-2, in pharmaceutical development. *Advanced Drug Delivery Reviews* 22 (1-2):85-103.
- Barbu, E., É. Molnár, J. Tsibouklis, and D. C. Górecki. 2009. The potential for nanoparticle-based drug delivery to the brain: overcoming the blood–brain barrier. *Expert Opinion on Drug Delivery* 6 (6):553-565.
- Bargoni, A., R. Cavalli, O. Caputo, A. Fundarò, M. R. Gasco, and G. P. Zara. 1998. Solid Lipid Nanoparticles in Lymph and Plasma After Duodenal Administration to Rats. *Pharmaceutical Research* 15 (5):745-750.
- Beal, M. F., R. T. Matthews, A. Tieleman, and C. W. Shults. 1998. Coenzyme Q10 attenuates the 1-methyl-4-phenyl-1,2,3,6-tetrahydropyridine (MPTP) induced loss of striatal dopamine and dopaminergic axons in aged mice. *Brain Research* 783 (1):109-114.
- Béduneau, A., P. Saulnier, and J. P. Benoit. 2007. Active targeting of brain tumors using nanocarriers. *Biomaterials* 28 (33):4947-4967.
- Billon, A., B. Bataille, G. Cassanas, and M. Jacob. 2000. Development of spray-dried acetaminophen microparticles using experimental designs. *International Journal of Pharmaceutics* 203 (1-2):159-168.
- Blasi, P., S. Giovagnoli, A. Schoubben, M. Ricci, and C. Rossi. 2007. Solid lipid nanoparticles for targeted brain drug delivery. *Advanced Drug Delivery Reviews* 59 (6):454-477.
- Borchard, G., K. L. Audus, F. Shi, and J. Kreuter. 1994. Uptake of surfactant-coated poly(methyl methacrylate)-nanoparticles by bovine brain microvessel endothelial cell monolayers. *International Journal of Pharmaceutics* 110 (1):29-35.
- Borhade, V., H. Nair, and D. Hegde. 2008. Design and evaluation of self-microemulsifying drug delivery system (SMEDDS) of tacrolimus. *AAPS PharmSciTech* 9 (1):13-21.
- Bowman, K., and K. W. Leong. 2006. Chitosan nanoparticles for oral drug and gene delivery. *International Journal of Nanomedicine* 1(2):117–128.
- Box, G. E. P., W. G. Hunter, and J. S. Hunter. 1978. *Statistics for experimenters: An introduction to design, data analysis and model building*. New York: Wiley.
- Brigger, I., J. Morizet, G. Aubert, H. Chacun, M. J. Terrier-Lacombe, P. Couvreur, and G. Vassal. 2002. Poly(ethylene glycol)-coated hexadecylcyanoacrylate nanospheres display a combined effect for brain tumor targeting. *Journal Pharmacological Experimental Therapeutics* 303 (928–936).
- Briske-Anderson, M. J., J. W. Finley, and S. M. Newman. 1997. The influence of culture time and passage number on the morphological and physiological development of Caco-2 cells. *Experimental Biology and Medicine* 214 (3):248-257.
- Broadhead, J., S. K. Edmond Rouan, and C. T. Rhodes. 1992. The spray drying of pharmaceuticals. *Drug Development and Industrial Pharmacy* 18 (11-12):1169-1206.
- Brodaty, H., J. Corey-Bloom, F. C. V. Potocnik, L. Truyen, M. Gold, and C. R. V. Damaraju. 2005. Galantamine prolonged-release formulation in the treatment of mild to moderate Alzheimer's disease. *Dementia and Geriatric Cognitive Disorders* 20 (2-3):120-132.

- Brooks, D. J. 2000. Dopamine agonists: their role in the treatment of Parkinson's disease. *Journal of Neurology, Neurosurgery & Psychiatry* 68 (6):685-689.
- Brown, R. C., A. P. Morris, and R. G. O'Neil. 2007. Tight junction protein expression and barrier properties of immortalized mouse brain microvessel endothelial cells. *Brain Research* 1130 (0):17-30.
- Buchanan, C. M., N. L. Buchanan, K. J. Edgar, J. L. Little, M. G. Ramsey, K. M. Ruble, V. J. Wachter, and M. F. Wempe. 2007. Pharmacokinetics of saquinavir after intravenous and oral dosing of saquinavir: Hydroxybutenyl- β -cyclodextrin formulations. *Biomacromolecules* 9 (1):305-313.
- Bunaciu, A. A., H. Y. Aboul-Enein, and S. Fleschin. 2010. Application of fourier transform infrared spectrophotometry in pharmaceutical drugs analysis. *Applied Spectroscopy Reviews* 45 (3):206-219.
- Bunjes, H., K. Westesen, and M. H. J. Koch. 1996. Crystallization tendency and polymorphic transitions in triglyceride nanoparticles. *International Journal of Pharmaceutics* 129 (1-2):159-173.
- Butt, A. M., H. C. Jones, and N. J. Abbott. 1990. Electrical resistance across the blood-brain barrier in anaesthetized rats: a developmental study. *The Journal of Physiology* 429 (1):47-62.
- Cai, Y. Z., and H. Corke. 2000. Production and properties of spray-dried *Amaranthus betacyanin* pigments. *Journal of Food Science* 65 (7):1248-1252.
- Callahan, M. K., K. A. Williams, P. Kivisäkk, D. Pearce, M. F. Stins, and R. M. Ransohoff. 2004. CXCR3 marks CD4+ memory T lymphocytes that are competent to migrate across a human brain microvascular endothelial cell layer. *Journal of Neuroimmunology* 153 (1-2):150-157.
- Cardoso, F. L., D. Brites, and M. A. Brito. 2010. Looking at the blood-brain barrier: Molecular anatomy and possible investigation approaches. *Brain Research Reviews* 64 (2):328-363.
- Castelli, F., C. Puglia, M. G. Sarpietro, L. Rizza, and F. Bonina. 2005. Characterization of indomethacin-loaded lipid nanoparticles by differential scanning calorimetry. *International Journal of Pharmaceutics* 304 (1-2):231-238.
- Cavalli, R., A. Bargoni, V. Podio, E. Muntoni, G. P. Zara, and M. R. Gasco. 2003. Duodenal administration of solid lipid nanoparticles loaded with different percentages of tobramycin. *Journal of Pharmaceutical Sciences* 92 (5):1085-1094.
- Cedarbaum, J. M. 1987. Clinical pharmacokinetics of anti-Parkinsonian drugs. *Clinical Pharmacokinetics* 13 (3):141-178.
- Chantret, I., A. Barbat, E. Dussaulx, M. G. Brattain, and A. Zweibaum. 1988. Epithelial polarity, villin expression, and enterocytic differentiation of cultured human colon carcinoma cells: A survey of twenty cell lines. *Cancer Research* 48 (7):1936-1942.
- Chaubal, M., and C. Popescu. 2008. Conversion of nanosuspensions into dry Powders by spray drying: A case study. *Pharmaceutical Research* 25 (10):2302-2308.
- Chattopadhyay, N., J. Zastre, H.-L. Wong, X. Wu, and R. Bendayan. 2008. Solid lipid nanoparticles enhance the delivery of the HIV protease inhibitor, atazanavir, by a human brain endothelial cell line. *Pharmaceutical Research* 25 (10):2262-2271.

- Chen, X. D. 2004. Heat-Mass Transfer and Structure Formation During Drying of Single Food Droplets. *Drying Technology* 22 (1-2):179-190.
- Chen, X., and M. G. Tansey. 2011. The role of neuroinflammation in Parkinson's disease. In *neuroinflammation*. London: Elsevier, 403-421.
- Chen, Y.-C., C.-F. Chiang, L.-F. Chen, P.-C. Liang, W.-Y. Hsieh, and W.-L. Lin. 2014. Polymersomes conjugated with des-octanoyl ghrelin and folate as a BBB-penetrating cancer cell-targeting delivery system. *Biomaterials* 35 (13):4066-4081.
- Chirkov, S. N. 2002. The antiviral activity of chitosan (review). *Applied Biochemistry and Microbiology* 38 (1):1-8.
- Chithrani, B. D., and W. C. W. Chan. 2007. Elucidating the Mechanism of Cellular Uptake and Removal of Protein-Coated Gold Nanoparticles of Different Sizes and Shapes. *Nano Letters* 7 (6):1542-1550.
- Colao, A., A. Di Sarno, E. Guerra, M. De Leo, A. Mentone, and G. Lombardi. 2006. Drug insight: cabergoline and bromocriptine in the treatment of hyperprolactinemia in men and women. *Nature Clinical Practice Endocrinology Metabolism* 2 (4):200-210.
- Cui, J., B. Yu, Y. Zhao, W. Zhu, H. Li, H. Lou, and G. Zhai. 2009. Enhancement of oral absorption of curcumin by self-microemulsifying drug delivery systems. *International Journal of Pharmaceutics* 371 (1-2):148-155.
- Darwish, A. M., E. Farah, W. A. Gadallah, and I. I. Mohammad. 2007. Superiority of newly developed vaginal suppositories over vaginal use of commercial bromocriptine tablets: A randomized controlled clinical trial. *Reproductive Sciences* 14 (3):280-285.
- Darwish, A. M., E. Hafez, I. El-Gebali, and S. B. Hassan. 2005. Evaluation of a novel vaginal bromocriptine mesylate formulation: A pilot study. *Fertility and Sterility* 83 (4):1053-1055.
- de Boer, A. G., and P. J. Gaillard. 2006. Blood-brain barrier dysfunction and recovery. *Journal of Neural Transmission* 113 (4):455-462.
- de Lau, L. M. L., and M. M. B. Breteler. 2006. Epidemiology of Parkinson's disease. *The Lancet Neurology* 5 (6):525-535.
- Defoort, P., M. Thiery, G. Baele, D. Clement, and M. Dhont. 1987. Bromocriptine in an injectable retard form for puerperal lactation suppression: Comparison with estandron prolongatum. *Obstetrics & Gynecology* 70 (6):866-869.
- Dey, S., and K. Dora. 2011. Suitability of chitosan as cryoprotectant on croaker fish (*Johnius gangeticus*) surimi during frozen storage. *Journal of Food Science and Technology* 48 (6):699-705.
- Dingler, A., and S. Gohla. 2002. Production of solid lipid nanoparticles (SLN): scaling up feasibilities. *Journal of Microencapsulation* 19 (1):11-16.
- Emerit, J., M. Edeas, and F. Bricaire. 2004. Neurodegenerative diseases and oxidative stress. *Biomedicine & Pharmacotherapy* 58 (1):39-46.
- Esposito, E., M. Fantin, M. Marti, M. Drechsler, L. Paccamiccio, P. Mariani, E. Sivieri, F. Lain, E. Menegatti, M. Morari, and R. Cortesi. 2008. Solid lipid nanoparticles as delivery systems for bromocriptine. *Pharmaceutical Research* 25 (7):1521-1530.
- Esposito, E., P. Mariani, L. Ravani, C. Contado, M. Volta, S. Bido, M. Drechsler, S. Mazzoni, E. Menegatti, M. Morari, and R. Cortesi. 2012. Nanoparticulate lipid

- dispersions for bromocriptine delivery: Characterization and in vivo study. *European Journal of Pharmaceutics and Biopharmaceutics* 80 (2):306-314.
- Evers, R., M. Kool, L. van Deemter, H. Janssen, J. Calafat, L. C. Oomen, C. C. Paulusma, R. P. Oude Elferink, F. Baas, A. H. Schinkel, and P. Borst. 1998. Drug export activity of the human canalicular multispecific organic anion transporter in polarized kidney MDCK cells expressing cMOAT (MRP2) cDNA. *Journal of Clinical Investigation* 101 (7):1310-1319.
- Florence, A. T. 2004. Issues in Oral Nanoparticle Drug Carrier Uptake and Targeting. *Journal of Drug Targeting* 12 (2):65-70.
- Florey, K. 1979. *Analytical profiles of drug substances, excipients and related methodology*. 8 vols. New York: Academic Press.
- Fonte, P., T. Nogueira, C. Gehm, D. Ferreira, and B. Sarmiento. 2011. Chitosan-coated solid lipid nanoparticles enhance the oral absorption of insulin. *Drug Delivery and Translational Research* 1 (4):299-308.
- Freitas, C. 1999. Stability determination of solid lipid nanoparticles (SLN TM) in aqueous dispersion after addition of electrolyte. *Journal of Microencapsulation* 16 (1):59-71.
- Freitas, C., J. Luckas, and R. Müller. 1994. P238 effect of storage conditions on long-term stability of "solid lipid nanoparticles"(SLN) in aqueous dispersion. *European Journal of Pharmaceutical Sciences* 2 (1):178.
- Freitas, C., and R. H. Müller. 1998. Spray-drying of solid lipid nanoparticles (SLNTM). *European Journal of Pharmaceutics and Biopharmaceutics* 46 (2):145-151.
- Furumoto, K., S. Nagayama, K.-i. Ogawara, Y. Takakura, M. Hashida, K. Higaki, and T. Kimura. 2004. Hepatic uptake of negatively charged particles in rats: possible involvement of serum proteins in recognition by scavenger receptor. *Journal of Controlled Release* 97 (1):133-141.
- Gallo, L., J. M. Llabot, D. Allemandi, V. Bucalá, and J. Piña. 2011. Influence of spray-drying operating conditions on Rhamnus purshiana (Cáscara sagrada) extract powder physical properties. *Powder Technology* 208 (1):205-214.
- Gasco, M. R., and L. P. Antonelli. 1993. Method for producing solid lipid nanoparticles having narrow size distribution, edited by U. S. Patent. US.
- Gelb, D. J., E. Oliver, and S. Gilman. 1999. Diagnostic criteria for Parkinson disease. *Archives of Neurology* 56 (1):33-39.
- Gelperina, S., O. Maksimenko, A. Khalansky, L. Vanchugova, E. Shipulo, K. Abbasova, R. Berdiev, S. Wohlfart, N. Chepurnova, and J. Kreuter. 2010. Drug delivery to the brain using surfactant-coated poly(lactide-co-glycolide) nanoparticles: Influence of the formulation parameters. *European Journal of Pharmaceutics and Biopharmaceutics* 74 (2):157-163.
- Gharsallaoui, A., G. Roudaut, O. Chambin, A. Voilley, and R. Saurel. 2007. Applications of spray-drying in microencapsulation of food ingredients: An overview. *Food Research International* 40 (9):1107-1121.
- Giron-Forest D. A., and Schanleber W. B. 1992. *Analytical Profiles of Drug Substances*. New York: Academic Press.
- Gold, M., D. VanDam, and E. R. Silliman. 2000. An open-label trial of bromocriptine in nonfluent aphasia: A qualitative analysis of word storage and retrieval. *Brain and Language* 74 (2):141-156.

- Goldstein, G. W. 1988. Endothelial cell-astrocyte interactions. *Annals of the New York Academy of Sciences* 529 (1):31-39.
- Gonissen, Y., J. P. Remon, and C. Vervaet. 2007. Development of directly compressible powders via co-spray drying. *European Journal of Pharmaceutics and Biopharmaceutics* 67 (1):220-226.
- Gulyaev, A. E., S. E. Gelperina, I. N. Skidan, A. S. Antropov, G. Y. Kivman, and J. Kreuter. 1999. Significant transport of doxorubicin into the brain with polysorbate 80-coated nanoparticles. *Pharmaceutical Research* 16 (10):1564-1569.
- Gumbleton, M., and K. L. Audus. 2001. Progress and limitations in the use of in vitro cell cultures to serve as a permeability screen for the blood-brain barrier. *Journal of Pharmaceutical Sciences* 90 (11):1681-1698.
- Günther, B., and H. Wagner. 1996. Quantitative determination of triterpenes in extracts and phytopreparations of *Centella asiatica* (L.) urban. *Phytomedicine* 3 (1):59-65.
- Hawkins, B. T., and T. P. Davis. 2005. The blood-brain barrier/neurovascular unit in health and disease. *Pharmacological Reviews* 57 (2):173-185.
- He, P., S. S. Davis, and L. Illum. 1999. Chitosan microspheres prepared by spray drying. *International Journal of Pharmaceutics* 187 (1):53-65.
- Hidalgo, I. J., and R. T. Borchardt. 1990. Transport of a large neutral amino acid (phenylalanine) in a human intestinal epithelial cell line: Caco-2. *Biochimica et Biophysica Acta (BBA) - Biomembranes* 1028 (1):25-30.
- Hirsch, E. C., and S. Hunot. 2009. Neuroinflammation in Parkinson's disease: a target for neuroprotection? *The Lancet Neurology* 8 (4):382-397.
- Holash, J. A., D. M. Noden, and P. A. Stewart. 1993. Re-evaluating the role of astrocytes in blood-brain barrier induction. *American Journal of Anatomy* 197 (1):14-25.
- Hong, J. H., and Y. H. Choi. 2007. Physico-chemical properties of protein-bound polysaccharide from *Agaricus blazei* Murill prepared by ultrafiltration and spray drying process. *International Journal of Food Science & Technology* 42 (1):1-8.
- Hou, D., C. Xie, K. Huang, and C. Zhu. 2003. The production and characteristics of solid lipid nanoparticles (SLNs). *Biomaterials* 24 (10):1781-1785.
- [Http://micro-encapsulation.eu/microencapsulation/manufacturing/spraydrying.html](http://micro-encapsulation.eu/microencapsulation/manufacturing/spraydrying.html)
- [Https://www.premedhq.com/alzheimers-disease](https://www.premedhq.com/alzheimers-disease)
- Hu, K., J. Li, Y. Shen, W. Lu, X. Gao, Q. Zhang, and X. Jiang. 2009. Lactoferrin-conjugated PEG-PLA nanoparticles with improved brain delivery: In vitro and in vivo evaluations. *Journal of Controlled Release* 134 (1):55-61.
- Hu, L., X. Tang, and F. Cui. 2004. Solid lipid nanoparticles (SLNs) to improve oral bioavailability of poorly soluble drugs. *Journal of Pharmacy and Pharmacology* 56 (12):1527-1535.
- Huang, J., L. Si, L. Jiang, Z. Fan, J. Qiu, and G. Li. 2008. Effect of pluronic F68 block copolymer on P-glycoprotein transport and CYP3A4 metabolism. *International Journal of Pharmaceutics* 356 (1-2):351-353.
- Huang, S.-S., C.-S. Chiu, H.-J. Chen, W.-C. Hou, M.-J. Sheu, Y.-C. Lin, P.-H. Shie, and G.-J. Huang. 2011. Antinociceptive activities and the mechanisms of anti-

- inflammation of asiatic acid in mice. *Evidence-Based Complementary and Alternative Medicine* 2011:10.
- Illum, L., N. F. Farraj, and S. S. Davis. 1994. Chitosan as a novel nasal delivery system for peptide drugs. *Pharmaceutical Research* 11 (8):1186-1189.
- Imam, S. Z., and S. F. Ali. 2001. Aging increases the susceptibility to methamphetamine-induced dopaminergic neurotoxicity in rats: correlation with peroxynitrite production and hyperthermia. *Journal of Neurochemistry* 78 (5):952-959.
- Jaruszewski, K. M., S. Ramakrishnan, J. F. Poduslo, and K. K. Kandimalla. 2012. Chitosan enhances the stability and targeting of immuno-nanovehicles to cerebro-vascular deposits of Alzheimer's disease amyloid protein. *Nanomedicine: Nanotechnology, Biology and Medicine* 8 (2):250-260.
- Jenning, V., A. F. Thünemann, and S. H. Gohla. 2000. Characterisation of a novel solid lipid nanoparticle carrier system based on binary mixtures of liquid and solid lipids. *International Journal of Pharmaceutics* 199 (2):167-177.
- Kaasgaard, T., and D. Keller. 2010. Chitosan Coating Improves Retention and redispersibility of freeze-dried flavor oil emulsions. *Journal of Agricultural and Food Chemistry* 58 (4):2446-2454.
- Kasongo, K. W., M. Jansch, R. H. Müller, and R. B. Walker. 2011. Evaluation of the in vitro differential protein adsorption patterns of didanosine-loaded nanostructured lipid carriers (NLCs) for potential targeting to the brain. *Journal of Liposome Research* 21 (3):245-254.
- Katzman, R., and T. Saitoh. 1991. Advances in Alzheimer's disease. *The FASEB Journal* 5 (3):278-286.
- Kavitha, C. V., C. Agarwal, R. Agarwal, and G. Deep. 2011. Asiatic acid inhibits pro-angiogenic effects of VEGF and human gliomas in endothelial cell culture models. *PLoS ONE* 6 (8):e22745.
- Kawashima, Y., and P. York. 2008. Drug delivery applications of supercritical fluid technology. *Advanced Drug Delivery Reviews* 60 (3):297-298.
- Kean, T., and M. Thanou. 2010. Biodegradation, biodistribution and toxicity of chitosan. *Advanced Drug Delivery Reviews* 62 (1):3-11.
- Kesisoglou, F., S. Panmai, and Y. Wu. 2007. Nanosizing — Oral formulation development and biopharmaceutical evaluation. *Advanced Drug Delivery Reviews* 59 (7):631-644.
- Kho, K., W. S. Cheow, R. H. Lie, and K. Hadinoto. 2010. Aqueous re-dispersibility of spray-dried antibiotic-loaded polycaprolactone nanoparticle aggregates for inhaled anti-biofilm therapy. *Powder Technology* 203 (3):432-439.
- Kilburn, D., J. Claude, R. Mezzenga, G. Dlubek, A. Alam, and J. Ubbink. 2004. Water in glassy carbohydrates: Opening it up at the nanolevel. *The Journal of Physical Chemistry B* 108 (33):12436-12441.
- Kim, C.-K., J.-H. Kim, K.-M. Park, K.-H. Oh, U. Oh, and S.-J. Hwang. 1997. Preparation and evaluation of a titrated extract of *Centella asiatica* injection in the form of an extemporaneous micellar solution. *International Journal of Pharmaceutics* 146 (1):63-70.
- Kong, X., X. Li, X. Wang, T. Liu, Y. Gu, G. Guo, F. Luo, X. Zhao, Y. Wei, and Z. Qian. 2010. Synthesis and characterization of a novel MPEG-chitosan diblock

- copolymer and self-assembly of nanoparticles. *Carbohydrate Polymers* 79 (1):170-175.
- Kopitar, Z., B. Vrhovac, L. Povšić, F. Plavšić, I. Francetić, and J. Urbančič. 1991. The effect of food and metoclopramide on the pharmacokinetics and side effects of bromocriptine. *European Journal of Drug Metabolism and Pharmacokinetics* 16 (3):177-181.
- Koto, T., K. Takubo, S. Ishida, H. Shinoda, M. Inoue, K. Tsubota, Y. Okada, and E. Ikeda. 2007. Hypoxia disrupts the barrier function of neural blood vessels through changes in the expression of Claudin-5 in endothelial cells. *The American Journal of Pathology* 170 (4):1389-1397.
- Kotzé, A. F., H. L. Lueßen, A. G. de Boer, J. C. Verhoef, and H. E. Junginger. 1999. Chitosan for enhanced intestinal permeability: Prospects for derivatives soluble in neutral and basic environments. *European Journal of Pharmaceutical Sciences* 7 (2):145-151.
- Kreuter, J. 2004. Influence of the surface properties on nanoparticle-mediated transport of drugs to the brain. *Journal of Nanoscience and Nanotechnology* 4 (5):484-488.
- Kreuter, J., V. E. Petrov, D. A. Kharkevich, and R. N. Alyautdin. 1997. Influence of the type of surfactant on the analgesic effects induced by the peptide dalargin after its delivery across the blood-brain barrier using surfactant-coated nanoparticles. *Journal of Controlled Release* 49 (1):81-87.
- Krishnamurthy, R. G., M.-C. Senut, D. Zemke, J. Min, M. B. Frenkel, E. J. Greenberg, S.-W. Yu, N. Ahn, J. Goudreau, M. Kassab, K. S. Panickar, and A. Majid. 2009. Asiatic acid, a pentacyclic triterpene from *Centella asiatica*, is neuroprotective in a mouse model of focal cerebral ischemia. *Journal of Neuroscience Research* 87 (11):2541-2550.
- Kumar, M., A. Misra, A. K. Babbar, A. K. Mishra, P. Mishra, and K. Pathak. 2008. Intranasal nanoemulsion based brain targeting drug delivery system of risperidone. *International Journal of Pharmaceutics* 358 (1-2):285-291.
- Kumar, M. N. V. R., R. A. A. Muzzarelli, C. Muzzarelli, H. Sashiwa, and A. J. Domb. 2004. Chitosan chemistry and pharmaceutical perspectives. *Chemical Reviews* 104 (12):6017-6084.
- Kvernmo, T., S. Härtter, and E. Burger. 2006. A review of the receptor-binding and pharmacokinetic properties of dopamine agonists. *Clinical Therapeutics* 28 (8):1065-1078.
- Lang, A. E., and A. M. Lozano. 1998. Parkinson's disease. *New England Journal of Medicine* 339 (15):1044-1053.
- Learoyd, T. P., J. L. Burrows, E. French, and P. C. Seville. 2008. Chitosan-based spray-dried respirable powders for sustained delivery of terbutaline sulfate. *European Journal of Pharmaceutics and Biopharmaceutics* 68 (2):224-234.
- Lee, J. 2003. Drug nano- and microparticles processed into solid dosage forms: physical properties. *Journal of Pharmaceutical Sciences* 92 (10):2057-2068.
- Lee, K. E., S. H. Cho, H. B. Lee, S. Y. Jeong, and S. H. Yuk. 2003. Microencapsulation of lipid nanoparticles containing lipophilic drug. *Journal of Microencapsulation* 20 (4):489-496.
- Lee, K. Y., O.-N. Bae, K. Serfozo, S. Hejajian, A. Moussa, M. Reeves, W. Rumbelha, S. D. Fitzgerald, G. Stein, S.-H. Baek, J. Goudreau, M. Kassab,

- and A. Majid. 2012. Asiatic acid attenuates infarct volume, mitochondrial dysfunction, and matrix metalloproteinase-9 induction after focal cerebral ischemia. *Stroke* 43 (6):1632-1638.
- Lees, A. J., S. Haddad, K. M. Shaw, L. J. Kohout, and G. M. Stern. 1978. Bromocriptine in Parkinsonism: A Long-term Study. *Arch Neurol* 35 (8):503-505.
- Li, G., M. Simon, L. Cancel, Z.-D. Shi, X. Ji, J. Tarbell, B. Morrison, and B. Fu. 2010. Permeability of Endothelial and Astrocyte Cocultures: In Vitro Blood–Brain Barrier Models for Drug Delivery Studies. *Annals of Biomedical Engineering* 38 (8):2499-2511.
- Li, X., N. Anton, C. Arpagaus, F. Belleteix, and T. F. Vandamme. 2010. Nanoparticles by spray drying using innovative new technology: The Büchi Nano Spray Dryer B-90. *Journal of Controlled Release* 147 (2):304-310.
- Luo, Q., J. Zhao, X. Zhang, and W. Pan. 2011. Nanostructured lipid carrier (NLC) coated with Chitosan Oligosaccharides and its potential use in ocular drug delivery system. *International Journal of Pharmaceutics* 403 (1-2):185-191.
- Lutton, E. S. 1945. The polymorphism of tristearin and some of its homologs. *Journal of the American Chemical Society* 67 (4):524-527.
- Madara, J. L. 1998. Regulation of the movement of solutes across tight junctions. *Annual Review of Physiology* 60 (1):143-159.
- Martins, S., S. Costa-Lima, T. Carneiro, A. Cordeiro-da-Silva, E. B. Souto, and D. C. Ferreira. 2012. Solid lipid nanoparticles as intracellular drug transporters: An investigation of the uptake mechanism and pathway. *International Journal of Pharmaceutics* 430 (1–2):216-227.
- Masters, K. 1990. *Spray Drying Handbook*. New York: Longman Scientific and Technical.
- Mehnert, W., and K. Mäder. 2001. Solid lipid nanoparticles: Production, characterization and applications. *Advanced Drug Delivery Reviews* 47 (2-3):165-196.
- Mei, D., S. Mao, W. Sun, Y. Wang, and T. Kissel. 2008. Effect of chitosan structure properties and molecular weight on the intranasal absorption of tetramethylpyrazine phosphate in rats. *European Journal of Pharmaceutics and Biopharmaceutics* 70 (3):874-881.
- Mensch, J., L. J. L. W. Sanderson, A. Melis, C. Mackie, G. Verreck, M. E. Brewster, and P. Augustijns. 2010. Application of PAMPA-models to predict BBB permeability including efflux ratio, plasma protein binding and physicochemical parameters. *International Journal of Pharmaceutics* 395 (1–2):182-197.
- Mi, F.-L., T.-B. Wong, S.-S. Shyu, and S.-F. Chang. 1999. Chitosan microspheres: modification of polymeric chem-physical properties of spray-dried microspheres to control the release of antibiotic drug. *Journal of Applied Polymer Science* 71 (5):747-759.
- Mistry, A., S. Stolnik, and L. Illum. 2009. Nanoparticles for direct nose-to-brain delivery of drugs. *International Journal of Pharmaceutics* 379 (1-2):146-157.
- Moghimi, S. M., A. C. Hunter, and J. C. Murray. 2001. Long-circulating and target-specific nanoparticles: Theory to practice. *Pharmacological Reviews* 53 (2):283-318.

- Montgomery, D. C. 2005. *Design and analysis of experiments*. Sixth ed. Tempe: John Wiley & Sons.
- Moody, D. M. 2006. The blood-brain barrier and blood-cerebral spinal fluid barrier. *Seminars in Cardiothoracic and Vascular Anesthesia* 10 (2):128-131.
- Mook-Jung, I., J.-E. Shin, S. H. Yun, K. Huh, J. Y. Koh, H. K. Park, S.-S. Jew, and M. W. Jung. 1999. Protective effects of asiaticoside derivatives against beta-amyloid neurotoxicity. *Journal of Neuroscience Research* 58 (3):417-425.
- Moro, L., A. Fiori, and A. Natali. 1991. Processes for the preparation of pharmaceutical compositions containing bromocriptine having high stability and related products, edited by U. S. P. Office. United State of America: Poli Industria Chimica S.p A.
- Mosén, K., K. Bäckström, K. Thalberg, T. Schaefer, H. G. Kristensen, and A. Axelsson. 2005. Particle formation and capture during spray drying of inhalable particles. *Pharmaceutical Development and Technology* 9 (4):409-417.
- Mosmann, T. 1983. Rapid colorimetric assay for cellular growth and survival: Application to proliferation and cytotoxicity assays. *Journal of Immunological Methods* 65 (1-2):55-63.
- Mu, L., and S. S. Feng. 2001. Fabrication, characterization and in vitro release of paclitaxel (Taxol®) loaded poly (lactic-co-glycolic acid) microspheres prepared by spray drying technique with lipid/cholesterol emulsifiers. *Journal of Controlled Release* 76 (3):239-254.
- Müller, R. H., S. Maassen, C. Schwarz, and W. Mehnert. 1997. Solid lipid nanoparticles (SLN) as potential carrier for human use: interaction with human granulocytes. *Journal of Controlled Release* 47 (3):261-269.
- Müller, R. H., K. Mäder, and S. Gohla. 2000. Solid lipid nanoparticles (SLN) for controlled drug delivery - a review of the state of the art. *European Journal of Pharmaceutics and Biopharmaceutics* 50 (1):161-177.
- Müller, R. H., W. Mehnert, J. S. Lucks, C. Schwarz, A. Zur Mühlen, H. Meyhers, C. Freitas, and D. Rühl. 1995. Solid lipid nanoparticles (SLN) : an alternative colloidal carrier system for controlled drug delivery. *European Journal of Pharmaceutics and Biopharmaceutics* 41 (1):62-69.
- Müller, R. H., and C. Jacobs. 2002. Buparvaquone mucoadhesive nanosuspension: preparation, optimisation and long-term stability. *International Journal of Pharmaceutics* 237 (1-2):151-161.
- Müller, R. H., R. D. Petersen, A. Hommos, and J. Pardeike. 2007. Nanostructured lipid carriers (NLC) in cosmetic dermal products. *Advanced Drug Delivery Reviews* 59 (6):522-530.
- Müller, R. H., M. Radtke, and S. A. Wissing. 2002a. Nanostructured lipid matrices for improved microencapsulation of drugs. *International Journal of Pharmaceutics* 242 (1-2):121-128.
- . 2002b. Solid lipid nanoparticles (SLN) and nanostructured lipid carriers (NLC) in cosmetic and dermatological preparations. *Advanced Drug Delivery Reviews* 54, Supplement (0):S131-S155.
- Nagatsu, T., and M. Sawada. 2006. Cellular and molecular mechanisms of Parkinson's disease: Neurotoxins, causative genes, and inflammatory cytokines. *Cellular and Molecular Neurobiology* 26 (4):779-800.

- Nutt, J. G., J. A. Obeso, and F. Stocchi. 2000. Continuous dopamine-receptor stimulation in advanced Parkinson's disease. *Trends in Neurosciences* 23 (Supplement 1):S109-S115.
- Oakley, D. E. 1997. Produce uniform particles by spray-drying. *Chemical Engineering Progress* 93 (10):48-54.
- Obeso, J. A., C. W. Olanow, and J. G. Nutt. 2000. Levodopa motor complications in Parkinson's disease. *Trends in Neurosciences* 23 (Supplement 1):S2-S7.
- Oda, T., T. Kume, Y. Izumi, Y. Takada-Takatori, T. Niidome, and A. Akaike. 2008. Bromocriptine, a dopamine D2 receptor agonist with the structure of the amino acid ergot alkaloids, induces neurite outgrowth in PC12 cells. *European Journal of Pharmacology* 598 (1-3):27-31.
- Okhamafe, A. O., B. Amsden, W. Chu, and M. F. A. Goosen. 1996. Modulation of protein release from chitosan-alginate microcapsules using the pH-sensitive polymer hydroxypropyl methylcellulose acetate succinate. *Journal of Microencapsulation* 13 (5):497-508.
- Olivier, J.-C., L. Fenart, R. Chauvet, C. Pariat, R. Cecchelli, and W. Couet. 1999. Indirect evidence that drug brain targeting using polysorbate 80-coated polybutylcyanoacrylate nanoparticles is related to toxicity. *Pharmaceutical Research* 16 (12):1836-1842.
- Olson, M. I., and C.-M. Shaw. 1969. Presenile Dementia and Alzheimer's disease in Mongolism. *Brain* 92 (1):147-156.
- Omidi, Y., L. Campbell, J. Barar, D. Connell, S. Akhtar, and M. Gumbleton. 2003. Evaluation of the immortalised mouse brain capillary endothelial cell line, b.End3, as an in vitro blood-brain barrier model for drug uptake and transport studies. *Brain Research* 990 (1-2):95-112.
- Omwamba, M., and Q. Hu. 2009. Antioxidant capacity and antioxidative compounds in barley (*Hordeum vulgare* L.) grain optimized using response surface methodology in hot air roasting. *European Food Research and Technology* 229 (6):907-914.
- Oomah, B. D., and G. Mazza. 2001. Optimization of a spray drying process for flaxseed gum. *International Journal of Food Science & Technology* 36 (2):135-143.
- Ophir, I., E. Cohen, and Y. Ben Shaul. 1995. Apical polarity in human colon carcinoma cell lines. *Tissue and Cell* 27 (6):659-666.
- Oppenheim, R. C. 1981. Solid colloidal drug delivery systems: Nanoparticles. *International Journal of Pharmaceutics* 8 (3):217-234.
- Pardridge, W. M. 1999. Blood-brain barrier biology and methodology. *Journal of Neurovirology* 5 (6):556-569.
- Pearce, R. K. B., T. Banerji, P. Jenner, and C. David Marsden. 1998. De novo administration of ropinirole and bromocriptine induces less dyskinesia than L-dopa in the MPTP-treated marmoset. *Movement Disorders* 13 (2):234-241.
- Pepper, M. S., F. Tacchini-Cottier, T. K. Sabapathy, R. Montesano, and E. F. Wagner. 1997. Endothelial cells transformed by polyoma virus middle T oncogene: a model for hemangiomas and other vascular tumors. *Tumour angiogenesis. Oxford University Press, Oxford, United Kingdom*:309-331.

- Persidsky, Y., S. H. Ramirez, J. Haorah, and G. D. Kanmogne. 2006. Blood-brain barrier: Structural components and function under physiologic and pathologic conditions. *Journal of Neuroimmune Pharmacology* 1 (3):223-236.
- Pinto, J. F., and R. H. Müller. 1999. Pellets as carriers of solid lipid nanoparticles (SLN) for oral administration of drugs. *Pharmazie* 54 (7):506-509.
- Podczec, F. 1998. *Particle-particle adhesion in pharmaceutical powder handling*: World Scientific.
- Ranaldi, G., K. Islam, and Y. Sambuy. 1992. Epithelial cells in culture as a model for the intestinal transport of antimicrobial agents. *Antimicrobial Agents and Chemotherapy* 36 (7):1374-1381.
- Ranaldi, G., I. Marigliano, I. Vespignani, G. Perozzi, and Y. Sambuy. 2002. The effect of chitosan and other polycations on tight junction permeability in the human intestinal Caco-2 cell line. *The Journal of Nutritional Biochemistry* 13 (3):157-167.
- Rascol, A., B. Guiraud, J. L. Montastruc, J. David, and M. Clanet. 1979. Long-term treatment of Parkinson's disease with bromocriptine. *Journal of Neurology, Neurosurgery & Psychiatry* 42 (2):143-150.
- Rascol, O., C. Goetz, W. Koller, W. Poewe, and C. Sampaio. 2002. Treatment interventions for Parkinson's disease: an evidence based assessment. *The Lancet* 359 (9317):1589-1598.
- Ré, M. I. 1998. Microencapsulation by spray drying. *Drying Technology: An International Journal* 16 (6):1195 - 1236.
- Reese, T. S., and M. J. Karnovsky. 1967. Fine structural localization of a blood-brain barrier to exogenous peroxidase. *The Journal of Cell Biology* 34 (1):207-217.
- Reichel, A., D. Begley, and N. J. Abbott. 2003. An Overview of In Vitro Techniques for Blood-Brain Barrier Studies. In *The Blood-Brain Barrier*, edited by S. Nag: Humana Press, 307-324.
- Ribeiro, A. J., R. J. Neufeld, P. Arnaud, and J. C. Chaumeil. 1999. Microencapsulation of lipophilic drugs in chitosan-coated alginate microspheres. *International Journal of Pharmaceutics* 187 (1):115-123.
- Riley, S. A., G. Warhurst, P. T. Crowe, and L. A. Turnberg. 1991. Active hexose transport across cultured human Caco-2 cells: characterisation and influence of culture conditions. *Biochimica et Biophysica Acta (BBA) - Biomembranes* 1066 (2):175-182.
- Roccia, P., M. L. Martínez, J. M. Llabot, and P. D. Ribotta. 2014. Influence of spray-drying operating conditions on sunflower oil powder qualities. *Powder Technology* 254 (0):307-313.
- Rojanasakul, Y., L.-Y. Wang, M. Bhat, D. D. Glover, C. J. Malanga, and J. K. H. Ma. 1992. The transport barrier of epithelia: A comparative study on membrane permeability and charge selectivity in the rabbit. *Pharmaceutical Research* 9 (8):1029-1034.
- Roney, C., P. Kulkarni, V. Arora, P. Antich, F. Bonte, A. Wu, N. N. Mallikarjuana, S. Manohar, H.-F. Liang, A. R. Kulkarni, H.-W. Sung, M. Sairam, and T. M. Aminabhavi. 2005. Targeted nanoparticles for drug delivery through the blood-brain barrier for Alzheimer's disease. *Journal of Controlled Release* 108 (2-3):193-214.

- Rubin, L. L., and J. M. Staddon. 1999. The cell biology of the blood-brain barrier. *Annual Review of Neuroscience* 22 (1):11-28.
- Rutten, M. J., R. L. Hoover, and M. J. Karnovsky. 1987. Electrical resistance and macromolecular permeability of brain endothelial monolayer cultures. *Brain Research* 425 (2):301-310.
- Saklatvala, R., P. G. Royall, and D. Q. M. Craig. 1999. The detection of amorphous material in a nominally crystalline drug using modulated temperature DSC--a case study. *International Journal of Pharmaceutics* 192 (1):55-62.
- Sant, S., S. Poulin, and P. Hildgen. 2008. Effect of polymer architecture on surface properties, plasma protein adsorption, and cellular interactions of pegylated nanoparticles. *Journal of Biomedical Materials Research - Part A* 87 (4):885-895.
- Sarmento, B., D. Mazzaglia, M. C. Bonferoni, A. P. Neto, M. do Céu Monteiro, and V. Seabra. 2011. Effect of chitosan coating in overcoming the phagocytosis of insulin loaded solid lipid nanoparticles by mononuclear phagocyte system. *Carbohydrate Polymers* 84 (3):919-925.
- Sandri, G., M. C. Bonferoni, E. H. Gökçe, F. Ferrari, S. Rossi, M. Patrini, and C. Caramella. 2010. Chitosan-associated SLN: in vitro and ex vivo characterization of cyclosporine A loaded ophthalmic systems. *Journal of Microencapsulation* 27 (8):735-746.
- Schapira, A. H. V. 2009. Neurobiology and treatment of Parkinson's disease. *Trends in Pharmacological Sciences* 30 (1):41-47.
- Schiff, P. L. 2006. Ergot and its alkaloids. *American Journal of Pharmaceutical Education* 70 (5):1-10.
- Schipper, N. G. M., S. Olsson, J. A. Hoogstraate, A. G. DeBoer, K. M. Vårum, and P. Artursson. 1997. Chitosans as absorption enhancers for poorly absorbable drugs 2: Mechanism of absorption enhancement. *Pharmaceutical Research* 14 (7):923-929.
- Schröder, U., and B. A. Sabel. 1996. Nanoparticles, a drug carrier system to pass the blood-brain barrier, permit central analgesic effects of i.v. dalargin injections. *Brain Research* 710 (1-2):121-124.
- Schwarz, C., W. Mehnert, J. S. Lucks, and R. H. Müller. 1994. Solid lipid nanoparticles (SLN) for controlled drug delivery. I. Production, characterization and sterilization. *Journal of Controlled Release* 30 (1):83-96.
- Sha, X., G. Yan, Y. Wu, J. Li, and X. Fang. 2005. Effect of self-microemulsifying drug delivery systems containing Labrasol on tight junctions in Caco-2 cells. *European Journal of Pharmaceutical Sciences* 24 (5):477-486.
- Sheng, Y., C. Liu, Y. Yuan, X. Tao, F. Yang, X. Shan, H. Zhou, and F. Xu. 2009. Long-circulating polymeric nanoparticles bearing a combinatorial coating of PEG and water-soluble chitosan. *Biomaterials* 30 (12):2340-2348.
- Siegel, G. J., B. W. Agranoff, R. W. Albers, S. K. Fisher, and M. D. Uhler. 1999. *Basic neurochemistry: molecular, cellular, and medical aspects*. 6th ed. Vol. 1. Philadelphia: Lippincott-Raven.
- Simons, K., and S. D. Fuller. 1985. Cell surface polarity in epithelia. *Annual Review of Cell Biology* 1 (1):243-288.
- Singhal, D., and W. Curatolo. 2004. Drug polymorphism and dosage form design: a practical perspective. *Advanced Drug Delivery Reviews* 56 (3):335-347.

- Singla, A. K., and M. Chawla. 2001. Chitosan: some pharmaceutical and biological aspects - an update. *Journal of Pharmacy and Pharmacology* 53 (8):1047-1067.
- Sinkula, A. A., and S. H. Yalkowsky. 1975. Rationale for design of biologically reversible drug derivatives: prodrugs. *Journal of Pharmaceutical Sciences* 64 (2):181-210.
- Smith, J., E. Wood, and M. Dornish. 2004. Effect of Chitosan on epithelial cell tight junctions. *Pharmaceutical Research* 21 (1):43-49.
- Smith, M. W., and M. Gumbleton. 2006. Endocytosis at the blood-brain barrier: From basic understanding to drug delivery strategies. *Journal of Drug Targeting* 14 (4):191-214.
- Souto, E. B., W. Mehnert, and R. H. Müller. 2006. Polymorphic behaviour of Compritol®888 ATO as bulk lipid and as SLN and NLC. *Journal of Microencapsulation* 23 (4):417-433.
- Souto, E. B., and R. H. Müller. 2006. Investigation of the factors influencing the incorporation of clotrimazole in SLN and NLC prepared by hot high-pressure homogenization. *Journal of Microencapsulation* 23 (4):377-388.
- Stockwell, A. F., S. S. Davis, and S. E. Walker. 1986. In vitro evaluation of alginate gel systems as sustained release drug delivery systems. *Journal of Controlled Release* 3 (1-4):167-175.
- Sun, H., H. Dai, N. Shaik, and W. F. Elmquist. 2003. Drug efflux transporters in the CNS. *Advanced Drug Delivery Reviews* 55 (1):83-105.
- Sun, W., C. Xie, H. Wang, and Y. Hu. 2004. Specific role of polysorbate 80 coating on the targeting of nanoparticles to the brain. *Biomaterials* 25 (15):3065-3071.
- Suresh, G., K. Manjunath, V. Venkateswarlu, and V. Satyanarayana. 2007. Preparation, characterization, and in vitro and in vivo evaluation of lovastatin solid lipid nanoparticles. *AAPS PharmSciTech* 8 (1):E162-E170.
- Tansey, M. G., and M. S. Goldberg. 2010. Neuroinflammation in Parkinson's disease: Its role in neuronal death and implications for therapeutic intervention. *Neurobiology of Disease* 37 (3):510-518.
- Teeranachaideekul, V., R. H. Müller, and V. B. Junyaprasert. 2007. Encapsulation of ascorbyl palmitate in nanostructured lipid carriers (NLC)—Effects of formulation parameters on physicochemical stability. *International Journal of Pharmaceutics* 340 (1-2):198-206.
- Tengamnuay, P., A. Sahamethapat, A. Sailasuta, and A. K. Mitra. 2000. Chitosans as nasal absorption enhancers of peptides: comparison between free amine chitosans and soluble salts. *International Journal of Pharmaceutics* 197 (1-2):53-67.
- Tewa-Tagne, P., S. Briançon, and H. Fessi. 2007a. Preparation of redispersible dry nanocapsules by means of spray-drying: Development and characterisation. *European Journal of Pharmaceutical Sciences* 30 (2):124-135.
- Tewa-Tagne, P., G. Degobert, S. Briançon, C. Bordes, J.-Y. Gauvrit, P. Lanteri, and H. Fessi. 2007b. Spray-drying nanocapsules in presence of colloidal silica as drying auxiliary agent: Formulation and process variables optimization using experimental designs. *Pharmaceutical Research* 24 (4):650-661.
- Thode, K., R. H. Müller, and M. Kresse. 2000. Two-time window and multiangle photon correlation spectroscopy size and zeta potential analysis—

- Highly sensitive rapid assay for dispersion stability. *Journal of Pharmaceutical Sciences* 89 (10):1317-1324.
- Thongrangsalit, S., T. Phaechamud, V. Lipipun, and G. C. Ritthidej. 2015. Bromocriptine tablet of self-microemulsifying system adsorbed onto porous carrier to stimulate lipoproteins secretion for brain cellular uptake. *Colloids and Surfaces B: Biointerfaces* 131 (0):162-169.
- Thwaites, D. T., C. D. Brown, B. H. Hirst, and N. L. Simmons. 1993. Transepithelial glycy sarcosine transport in intestinal Caco-2 cells mediated by expression of H(+)-coupled carriers at both apical and basal membranes. *Journal of Biological Chemistry* 268 (11):7640-7642.
- Toneli, J., K. Park, A. Negreiros, and F. Murr. 2010. Spray-Drying Process Optimization of Chicory Root Inulin. *Drying Technology* 28 (3):369-379.
- Tonon, R. V., C. Brabet, and M. D. Hubinger. 2008. Influence of process conditions on the physicochemical properties of açai (*Euterpe oleracea* Mart.) powder produced by spray drying. *Journal of Food Engineering* 88 (3):411-418.
- Tosi, G., L. Costantino, B. Ruozi, F. Forni, and M. A. Vandelli. 2008. Polymeric nanoparticles for the drug delivery to the central nervous system. *Expert Opinion on Drug Delivery* 5 (2):155-174.
- Tracy, H. H., F. C. F. I. Pang, and N. Y. Ip. 2008. Recent development in the search for effective antidepressants using traditional Chinese medicine *Central Nervous System Agents in Medicinal Chemistry* 8 (1):64-71.
- Tsai, M.-J., P.-C. Wu, Y.-B. Huang, J.-S. Chang, C.-L. Lin, Y.-H. Tsai, and J.-Y. Fang. 2012. Baicalein loaded in tocol nanostructured lipid carriers (tocol NLCs) for enhanced stability and brain targeting. *International Journal of Pharmaceutics* 423 (2):461-470.
- Ueno, H., T. Mori, and T. Fujinaga. 2001. Topical formulations and wound healing applications of chitosan. *Advanced Drug Delivery Reviews* 52 (2):105-115.
- Ueno, H., H. Yamada, I. Tanaka, N. Kaba, M. Matsuura, M. Okumura, T. Kadosawa, and T. Fujinaga. 1999. Accelerating effects of chitosan for healing at early phase of experimental open wound in dogs. *Biomaterials* 20 (15):1407-1414.
- Ueno, M. 2007. Molecular anatomy of the brain endothelial barrier: An overview of the distributional features. *Current Medicinal Chemistry* 14 (11):1199-1206.
- van de Waterbeemd, H., and E. Gifford. 2003. ADMET in silico modelling: towards prediction paradise? *Nature Reviews Drug Discovery* 2 (3):192-204.
- Van Den Eeden, S. K., C. M. Tanner, A. L. Bernstein, R. D. Fross, A. Leimpeter, D. A. Bloch, and L. M. Nelson. 2003. Incidence of Parkinson's disease: Variation by age, gender, and race/ethnicity. *American Journal of Epidemiology* 157 (11):1015-1022.
- van der Lubben, I. M., J. C. Verhoef, G. Borchard, and H. E. Junginger. 2001. Chitosan and its derivatives in mucosal drug and vaccine delivery. *European Journal of Pharmaceutical Sciences* 14 (3):201-207.
- Van Kampen, J. M., and C. B. Eckman. 2006. Dopamine D3 receptor agonist delivery to a model of Parkinson's disease restores the nigrostriatal pathway and improves locomotor behavior. *Journal of Neurosciences* 26 (27):7272-7280.
- Vehring, R. 2008. Pharmaceutical particle engineering via spray drying. *Pharmaceutical Research* 25 (5):999-1022.

- Wagner, L. A., and J. J. Warthesen. 1995. Stability of spray-dried encapsulated carrot carotenes. *Journal of Food Science* 60 (5):1048-1053.
- Wandel, C., R. Kim, M. Wood, and A. Wood. 2002. Interaction of morphine, fentanyl, sufentanil, alfentanil, and loperamide with the efflux drug transporter p-glycoprotein. *Anesthesiology* 96 (4):913-920.
- Westesen, K., and H. Bunjes. 1995. Do nanoparticles prepared from lipids solid at room temperature always possess a solid lipid matrix? *International Journal of Pharmaceutics* 115 (1):129-131.
- Westesen, K., H. Bunjes, and M. Koch. 1997. Physicochemical characterization of lipid nanoparticles and evaluation of their drug loading capacity and sustained release potential. *Journal of Controlled Release* 48 (2):223-236.
- Williams, N. A., and G. P. Polli. 1984. The lyophilization of pharmaceuticals: A literature review. *PDA Journal of Pharmaceutical Science and Technology* 38 (2):48-60.
- Wilson, B., M. K. Samanta, K. Santhi, K. P. S. Kumar, N. Paramakrishnan, and B. Suresh. 2008a. Poly(n-butylcyanoacrylate) nanoparticles coated with polysorbate 80 for the targeted delivery of rivastigmine into the brain to treat Alzheimer's disease. *Brain Research* 1200:159-168.
- . 2008b. Targeted delivery of tacrine into the brain with polysorbate 80-coated poly(n-butylcyanoacrylate) nanoparticles. *European Journal of Pharmaceutics and Biopharmaceutics* 70 (1):75-84.
- Wissing, S. A., O. Kayser, and R. H. Müller. 2004. Solid lipid nanoparticles for parenteral drug delivery. *Advanced Drug Delivery Reviews* 56 (9):1257-1272.
- Wong, H. L., R. Bendayan, A. M. Rauth, and X. Y. Wu. 2006. Simultaneous delivery of doxorubicin and GG918 (Elacridar) by new Polymer-Lipid Hybrid Nanoparticles (PLN) for enhanced treatment of multidrug-resistant breast cancer. *Journal of Controlled Release* 116 (3):275-284.
- Wu, H., K. Hu, and X. Jiang. 2008. From nose to brain: understanding transport capacity and transport rate of drugs. *Expert Opinion on Drug Delivery* 5 (10):1159-1168.
- Xiong, Y., H. Ding, M. Xu, and J. Gao. 2009. Protective effects of asiatic acid on rotenone- or H₂O₂-induced injury in SH-SY5Y cells. *Neurochemical Research* 34 (4):746-754.
- Yang, S., J. Zhu, Y. Lu, B. Liang, and C. Yang. 1999. Body distribution of camptothecin solid lipid nanoparticles after oral administration. *Pharmaceutical Research* 16 (5):751-757.
- Yin Win, K., and S.-S. Feng. 2005. Effects of particle size and surface coating on cellular uptake of polymeric nanoparticles for oral delivery of anticancer drugs. *Biomaterials* 26 (15):2713-2722.
- Yonh-Liang, Z., W. Hai, Z. Hong-Hao, G. Zhen, W. Yu-Shun, Z. Dong-Hao, and Z. Jun. 2010. Enhancing water-solubility of poorly soluble drug, asiatic acid with hydroxypropyl- β -cyclodextrin. *Digest Journal of Nanomaterials & Biostructures (DJNB)* 5 (2):419-425.
- Zhang, L., L. Liu, Y. Qian, and Y. Chen. 2008. The effects of cryoprotectants on the freeze-drying of ibuprofen-loaded solid lipid microparticles (SLM). *European Journal of Pharmaceutics and Biopharmaceutics* 69 (2):750-759.

- Zhang, X., J. Wu, Y. Dou, B. Xia, W. Rong, G. Rimbach, and Y. Lou. 2012. Asiatic acid protects primary neurons against C2-ceramide-induced apoptosis. *European Journal of Pharmacology* 679 (1–3):51-59.
- Zheng, W., M. Aschner, and J.-F. Gherzi-Egea. 2003. Brain barrier systems: a new frontier in metal neurotoxicological research. *Toxicology and Applied Pharmacology* 192 (1):1-11.
- Zhuang, C.-Y., N. Li, M. Wang, X.-N. Zhang, W.-S. Pan, J.-J. Peng, Y.-S. Pan, and X. Tang. 2010. Preparation and characterization of vinpocetine loaded nanostructured lipid carriers (NLC) for improved oral bioavailability. *International Journal of Pharmaceutics* 394 (1-2):179-185.
- zur Mühlen, A., C. Schwarz, and W. Mehnert. 1998. Solid lipid nanoparticles (SLN) for controlled drug delivery - Drug release and release mechanism. *European Journal of Pharmaceutics and Biopharmaceutics* 45 (2):149-155.



APPENDIX

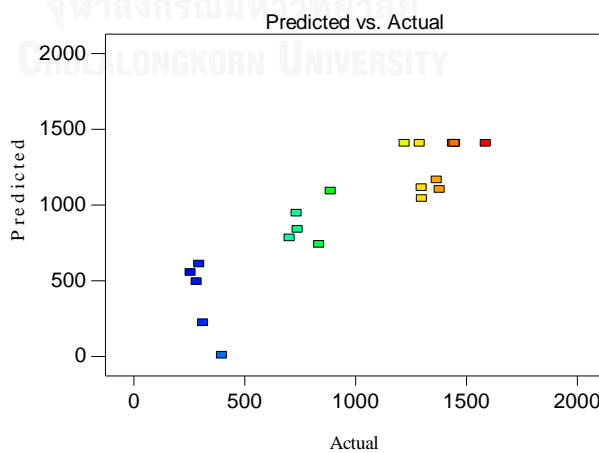
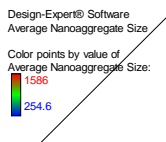
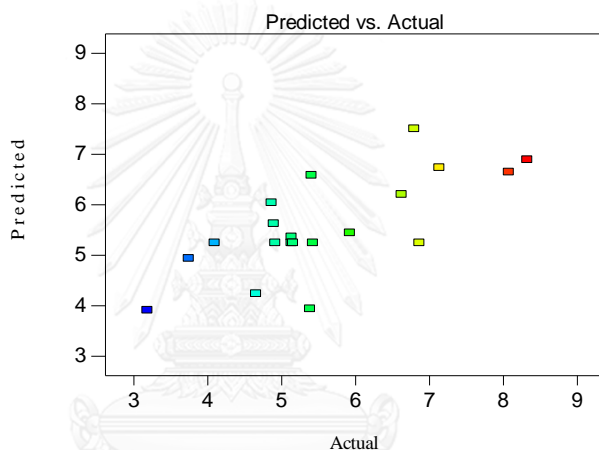
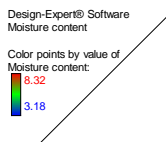
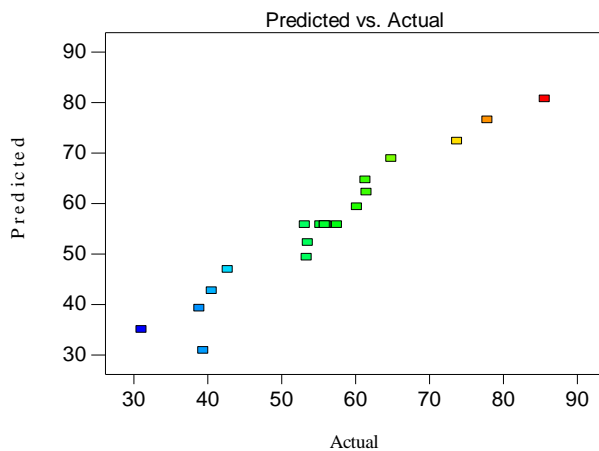
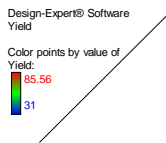


จุฬาลงกรณ์มหาวิทยาลัย
CHULALONGKORN UNIVERSITY

APPENDIX A

DIAGNOSTIC GRAPHS





Design-Expert® Software
Yield

Lambda
Current = 1
Best = 0.76
Low C.I. = 0.09
High C.I. = 1.47

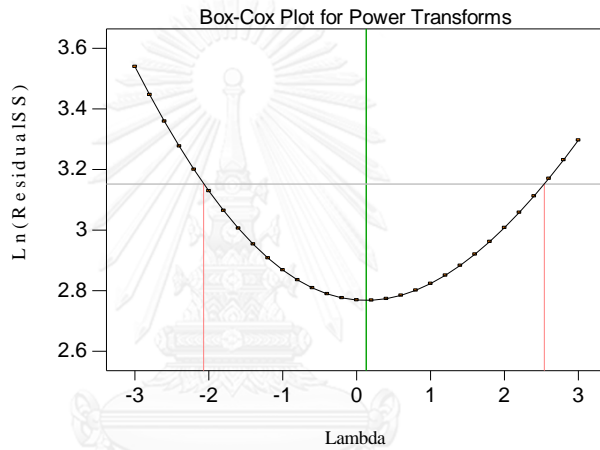
Recommend transform:
None
(Lambda = 1)



Design-Expert® Software
Moisture content

Lambda
Current = 1
Best = 0.13
Low C.I. = -2.07
High C.I. = 2.54

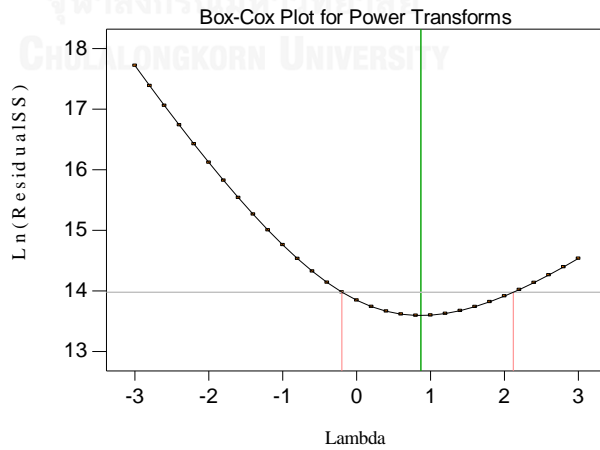
Recommend transform:
None
(Lambda = 1)



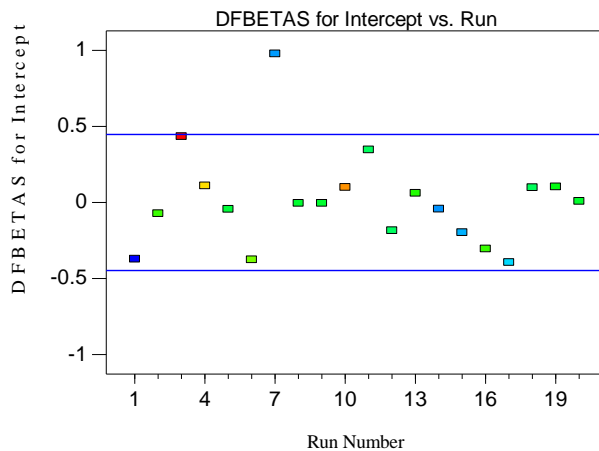
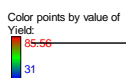
Design-Expert® Software
Average Nanoaggregate Size

Lambda
Current = 1
Best = 0.87
Low C.I. = -0.2
High C.I. = 2.12

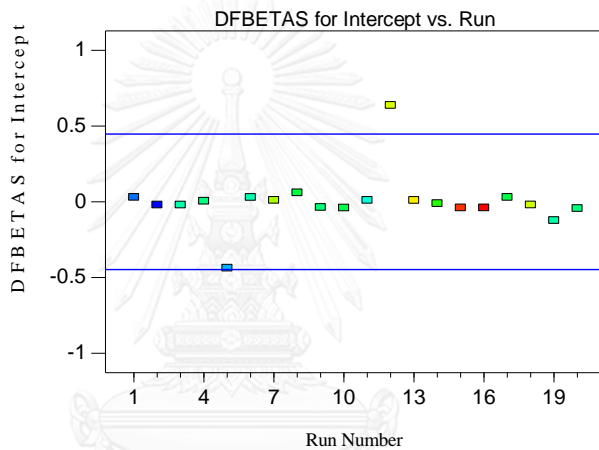
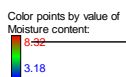
Recommend transform:
None
(Lambda = 1)



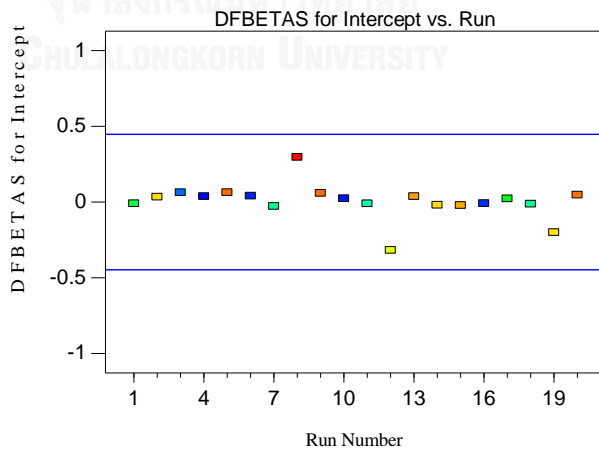
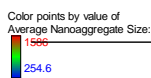
Design-Expert® Software
Yield



Design-Expert® Software
Moisture content

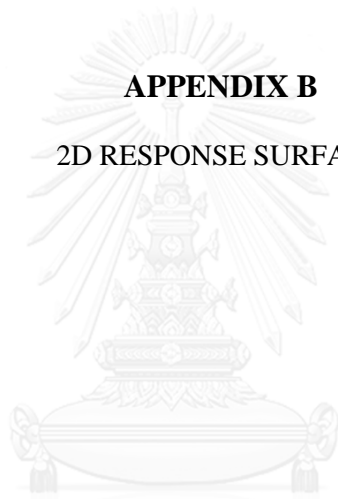


Design-Expert® Software
Average Nanoaggregate Size



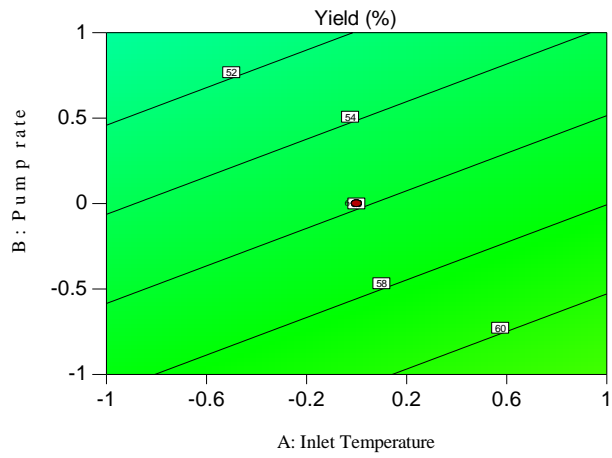
APPENDIX B

2D RESPONSE SURFACE

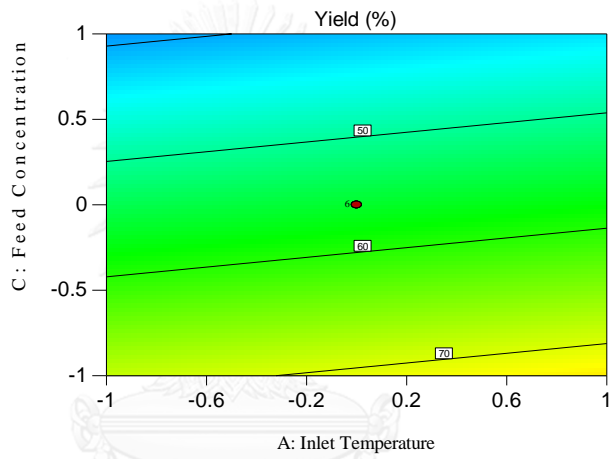


จุฬาลงกรณ์มหาวิทยาลัย
CHULALONGKORN UNIVERSITY

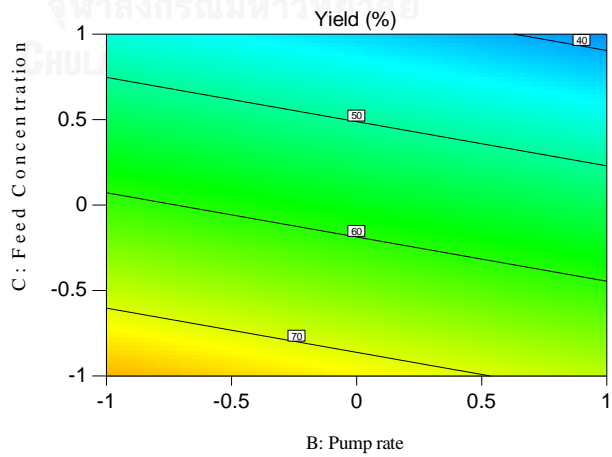
Design-Expert® Software
 Factor Coding: Coded
 Yield (%)
 ● Design Points
 85.56
 31
 X1 = A: Inlet Temperature
 X2 = B: Pump rate
 Coded Factor
 C: Feed Concentration = 0.000



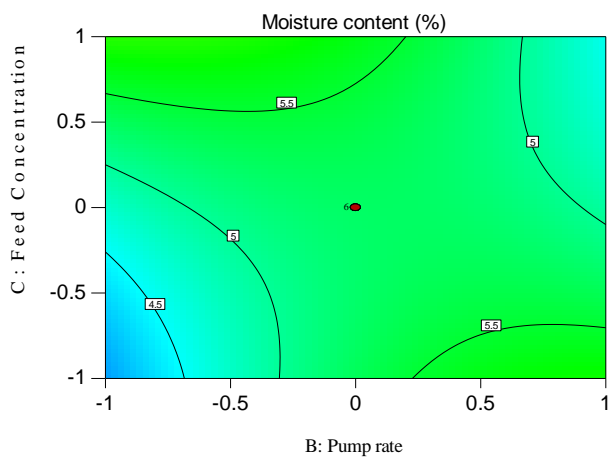
Design-Expert® Software
 Factor Coding: Coded
 Yield (%)
 ● Design Points
 85.56
 31
 X1 = A: Inlet Temperature
 X2 = C: Feed Concentration
 Coded Factor
 B: Pump rate = 0.000



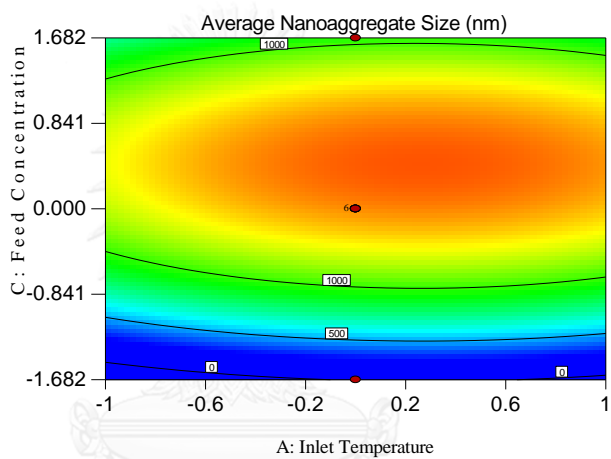
Design-Expert® Software
 Factor Coding: Coded
 Yield (%)
 ● Design Points
 85.56
 31
 X1 = B: Pump rate
 X2 = C: Feed Concentration
 Coded Factor
 A: Inlet Temperature = 0.649



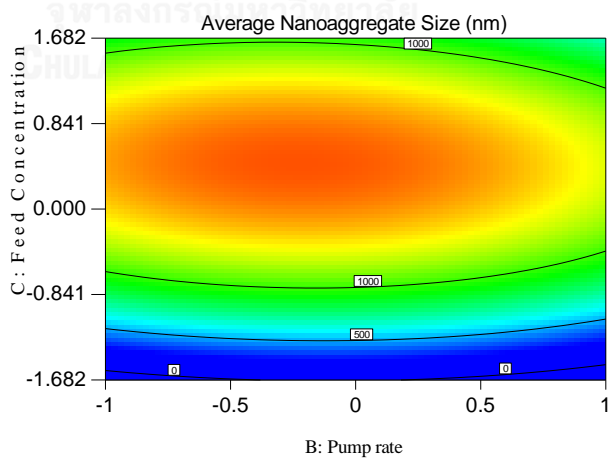
Design-Expert® Software
 Factor Coding: Coded
 Moisture content (%)
 ● Design Points
 8.32
 3.18
 X1 = B: Pump rate
 X2 = C: Feed Concentration
 Coded Factor
 A: Inlet Temperature = 0.000



Design-Expert® Software
 Factor Coding: Coded
 Average Nanoaggregate Size (nm)
 ● Design Points
 1586
 254.6
 X1 = A: Inlet Temperature
 X2 = C: Feed Concentration
 Coded Factor
 B: Pump rate = 0.000



Design-Expert® Software
 Factor Coding: Coded
 Average Nanoaggregate Size (nm)
 ● Design Points
 1586
 254.6
 X1 = B: Pump rate
 X2 = C: Feed Concentration
 Coded Factor
 A: Inlet Temperature = 0.026





APPENDIX C

FOURIER TRANSFORM INFRARED CHARACTERIZATION

จุฬาลงกรณ์มหาวิทยาลัย
CHULALONGKORN UNIVERSITY

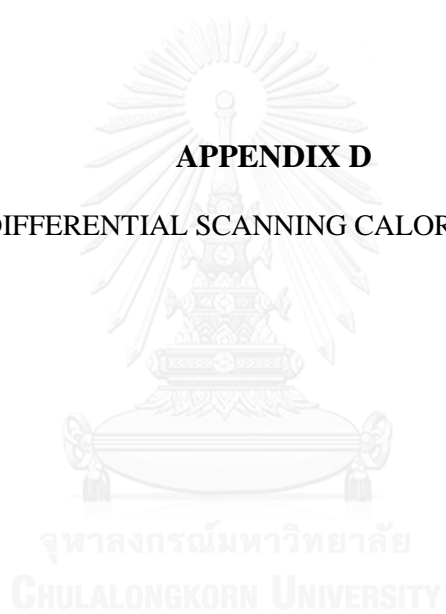
Bromocriptine

Peak Wavelength (cm ⁻¹)	Functional Group
3253.91	H-bonded OH groups, NH ₂ stretching
2959.38	C-H aliphatic asymmetric
2698.14	C-H aliphatic symmetric
1732.96	C=O stretching (carbonic acid)
1647.74	NH ₂ bending, C=O, C=N stretching (Amide I and II)
1445.83	C-H deformation in aliphatics
1220.27	C-O stretching
1174.74	C-O stretching (phenolic hydroxyl groups)
1047.64	C-O deformation (methoxyl group)

Asiatic acid

Peak Wavelength (cm ⁻¹)	Functional Group
3404.61	Stretching vibration in O-H
2926.14	C-H aliphatic asymmetric
2869.57	C-H aliphatic symmetric
1694.12	C=O stretching of carboxylic acid
1049.28	C-O deformation (methoxyl group)

APPENDIX D
DIFFERENTIAL SCANNING CALORIMETRY



DCS Characterization

Sample	Temperature ($^{\circ}\text{C}$)	ΔH (W/g)
Bromocriptine	215.33	-10.8243
	219.67	113.703
Tristearin	76.67	-9.66284
Trimyristin	60.33	-13.60140
Pluronic f127	59.67	-5.83034
Maltodextrin	32.67 - 211.67	-0.22403 – (-1.24714)

Differential Scanning Calorimetry

Sample	Temperature ($^{\circ}\text{C}$)	ΔH (W/g)
Asiatic Acid	28..33-53.33	-0.03133 – (-0.00312)
	205.33	0.09498
	332.67	-0.21358
Physical mixture powder of AASLN	71.33	-9.17289
	55.33	-5.94949
	46.33	-5.93368
Physical Mixture Powder of AANLC	46.00	-5.66175
	54.33	-5.20293
	71.67	-7.57573
Spray dried powder of AASLN chitosan-based	45.00	-0.87786
	56.67	-0.92568
	73.00	-1.41103
	36.67-164.00	-1.30727 – (-0.53692)

Continue

Sample	Temperature(⁰ C)	ΔH (W/g)
Spray dried powder of AANLC chitosan-based	44.00	-0.91639
	55.00	-0.86532
	73.00	-1.28651
	36.67-165.00	-1.33625 – (-0.60079)



APPENDIX E

WIDE XRD CHARACTERIZATION

จุฬาลงกรณ์มหาวิทยาลัย
CHULALONGKORN UNIVERSITY

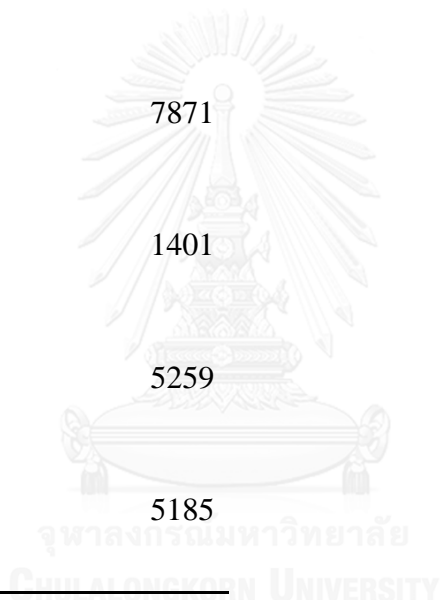
Bromocriptine

Angle 2 Theta ($^{\circ}$)	Intensity Count
5.0914928	3936
12.43379	4506
13.234352	1051
14.2865192	3936
15.7275308	1346
16.7568248	1025
17.1456692	2008
20.9197472	1339
22.3378856	1694



Tristearin

Angle 2 Theta ($^{\circ}$)	Intensity count
5.914928	2501
16.5967124	1035
16.9626836	1355
19.3414964	7871
22.2463928	1401
23.1613208	5259
24.2363612	5185



Pluronic f127

Angle 2 Theta ($^{\circ}$)	Intensity Count
14.636038	909
15.0870812	950
19.2042572	6865
23.3900528	5885
26.3635688	945



Trimyristin

Angle 2 Theta ($^{\circ}$)	Intensity count
7.4245592	3059
16.9398104	2040
17.5573868	1477
19.3872428	8440
22.0634072	1804
23.2299404	7231
24.0762488	7729



Nanospray dried powder of BMSLN chitosan-based


Angle 2 Theta (°)	Intensity Count
19.08989	1503
23.32143	1172
24.0305	1039

Nanospray dried powder of BMNLC chitosan-based

Angle 2 Theta (°)	Intensity Count
19.27288	1436
19.3415	1447
19.38724	1458
20.91975	1058
22.93259	1029
23.18419	1202

Asiatic acid

Angle 2 Theta (°)	Intensity Count
7.65971	793
12.60032	2035
12.94342	2205
13.69824	2757
15.07063	3005
16.09992	1059
16.67175	1152



จุฬาลงกรณ์มหาวิทยาลัย
CHULALONGKORN UNIVERSITY

Physical mixture powder of AASLN

Angle 2 Theta (°)	Intensity Count
5.875602	1468
19.39366	2733
23.07625	2294
24.197	1915

Physical mixture powder of AANLC

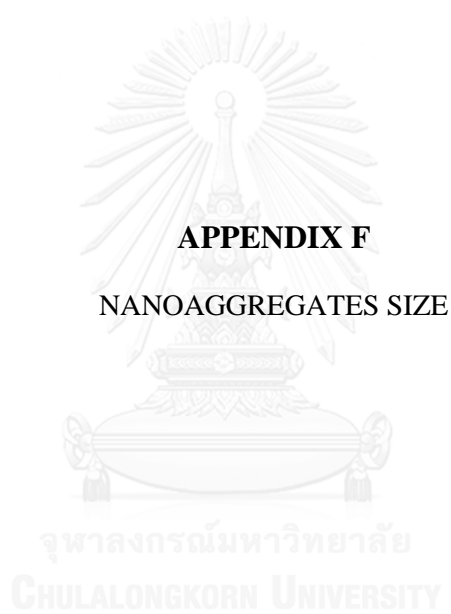
Angle 2 Theta (°)	Intensity Count
19.1649	3428
19.3708	3509
23.1449	3177
24.1055	2865

Spray dried powder of AASLN

Angle 2 Theta (°)	Intensity Count
19.3708	4357
23.1677	3959
24.0598	3785

Spray dried powder of AANLC

Angle 2 Theta (°)	Intensity Count
19.4165	5421
23.0991	5048
24.0141	4854



Redispersed Nanoaggregates size (nm)

SPSLN-Chi	SPSLN+Chi	SPNLC-Chi	SPNLC+Chi	NanoSPSLN-Chi	NanoSPSLN+Chi	NanoSPNLC-Chi	NanoSPNLC+Chi
494.4	638.1	305.6	471.5	397.6	556.1	341.9	523.5
536.1	580.5	328.3	455.4	411.4	821.5	331.7	655
523	663.8	323.3	543.9	318.5	752.7	321	656
537.2	665.6	300.6	531.5	367.1	643.5	303.8	659.9
537.5	614.8	282.6	456.1	355.8	504.5	311.5	568.4

Tests of Normality

group	Kolmogorov-Smirnov ^a		Shapiro-Wilk	
	Statistic	df	Statistic	Sig.
Nanosize				
AA-SPSLN-Chitosan	.209	5	.913	.484
AA-SPSLN+Chitosan	.209	5	.913	.484
AA-SPNLC-Chitosan	.196	5	.951	.743
AA-SPNLC+Chitosan	.282	5	.812	.102
AA-NanoSPSLN-Chitosan	.174	5	.967	.854
AA-NanoSPSLN+Chitosan	.174	5	.954	.768
AA-NanoSPNLC-Chitosan	.154	5	.978	.923
AA-NanoSPNLC+Chitosan	.350	5	.791	.068

a. Lilliefors Significance Correction

*. This is a lower bound of the true significance.

Multiple Comparisons
Nanoaggregates size
Bonferroni

(I) group_code	(J) group_code	Mean Difference (I-J)	Std. Error	Sig.	95% Confidence Interval	
					Lower Bound	Upper Bound
1.00	2.00	-130.02000*	36.58125	.034	-254.6773	-5.3627
	3.00	203.66000*	36.58125	.000	79.0027	328.3173
	4.00	-86.92000	36.58125	.662	-211.5773	37.7373
	5.00	155.56000*	36.58125	.005	30.9027	280.2173
	6.00	-106.92000	36.58125	.177	-231.5773	17.7373
	7.00	217.56000*	36.58125	.000	92.9027	342.2173
	8.00	33.96000	36.58125	1.000	-90.6973	158.6173
	2.00	1.00	130.02000*	36.58125	.034	5.3627
3.00		333.68000*	36.58125	.000	209.0227	458.3373
4.00		43.10000	36.58125	1.000	-81.5573	167.7573
5.00		285.58000*	36.58125	.000	160.9227	410.2373
6.00		23.10000	36.58125	1.000	-101.5573	147.7573
7.00		347.58000*	36.58125	.000	222.9227	472.2373
8.00		163.98000*	36.58125	.002	39.3227	288.6373

(I) group_code	(J) group_code	Mean Difference (I-J)	Std. Error	Sig.	95% Confidence Interval	
					Lower Bound	Upper Bound
3.00	1.00	-203.66000*	36.58125	.000	-328.3173	-79.0027
	2.00	-333.68000*	36.58125	.000	-458.3373	-209.0227
	4.00	-290.58000*	36.58125	.000	-415.2373	-165.9227
	5.00	-48.10000	36.58125	1.000	-172.7573	76.5573
	6.00	-310.58000*	36.58125	.000	-435.2373	-185.9227
	7.00	13.90000	36.58125	1.000	-110.7573	138.5573
	8.00	-169.70000*	36.58125	.002	-294.3573	-45.0427
	4.00	1.00	86.92000	36.58125	.662	-37.7373
2.00		-43.10000	36.58125	1.000	-167.7573	81.5573
3.00		290.58000*	36.58125	.000	165.9227	415.2373
5.00		242.48000*	36.58125	.000	117.8227	367.1373
6.00		-20.00000	36.58125	1.000	-144.6573	104.6573
7.00		304.48000*	36.58125	.000	179.8227	429.1373
8.00		120.88000	36.58125	.066	-3.7773	245.5373

(I) group_code	(J) group_code	Mean Difference (I-J)	Std. Error	Sig.	95% Confidence Interval	
					Lower Bound	Upper Bound
5.00	1.00	-155.56000*	36.58125	.005	-280.2173	-30.9027
	2.00	-285.58000*	36.58125	.000	-410.2373	-160.9227
	3.00	48.10000	36.58125	1.000	-76.5573	172.7573
	4.00	-242.48000*	36.58125	.000	-367.1373	-117.8227
	6.00	-262.48000*	36.58125	.000	-387.1373	-137.8227
	7.00	62.00000	36.58125	1.000	-62.6573	186.6573
	8.00	-121.60000	36.58125	.062	-246.2573	3.0573
	6.00	1.00	106.92000	36.58125	.177	-17.7373
2.00		-23.10000	36.58125	1.000	-147.7573	101.5573
3.00		310.58000*	36.58125	.000	185.9227	435.2373
4.00		20.00000	36.58125	1.000	-104.6573	144.6573
5.00		262.48000*	36.58125	.000	137.8227	387.1373
7.00		324.48000*	36.58125	.000	199.8227	449.1373
8.00		140.88000*	36.58125	.015	16.2227	265.5373

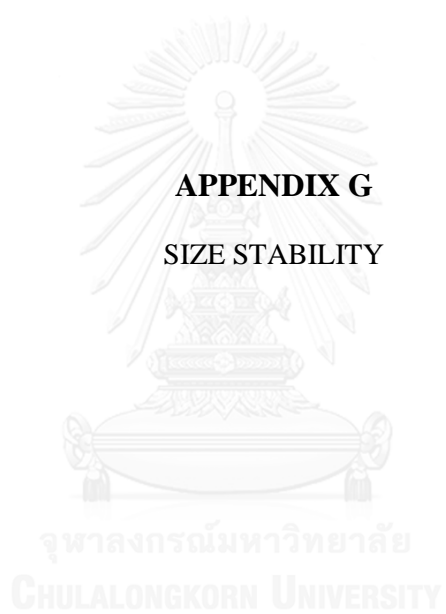
(I) group_code	(J) group_code	Mean Difference (I-J)	Std. Error	Sig.	95% Confidence Interval	
					Lower Bound	Upper Bound
7.00	1.00	-217.56000*	36.58125	.000	-342.2173	-92.9027
	2.00	-347.58000*	36.58125	.000	-472.2373	-222.9227
	3.00	-13.90000	36.58125	1.000	-138.5573	110.7573
	4.00	-304.48000*	36.58125	.000	-429.1373	-179.8227
	5.00	-62.00000	36.58125	1.000	-186.6573	62.6573
	6.00	-324.48000*	36.58125	.000	-449.1373	-199.8227
	8.00	-183.60000*	36.58125	.001	-308.2573	-58.9427
	8.00	1.00	-33.96000	36.58125	1.000	-158.6173
2.00		-163.98000*	36.58125	.002	-288.6373	-39.3227
3.00		169.70000*	36.58125	.002	45.0427	294.3573
4.00		-120.88000	36.58125	.066	-245.5373	3.7773
5.00		121.60000	36.58125	.062	-3.0573	246.2573
6.00		-140.88000*	36.58125	.015	-265.5373	-16.2227
7.00		183.60000*	36.58125	.001	58.9427	308.2573

*. The mean difference is significant at the 0.05 level.

Group codes

- 1.00 : Spray dried powder of BMSLN without chitosan
- 2.00 : Spray dried powder of BMSLN chitosan based
- 3.00 : Spray dried powder of BM NLC without chitosan
- 4.00 : B Spray dried powder of BM NLC chitosan based
- 5.00 : Nanospray dried powder of BMSLN without chitosan
- 6.00 : Nanospray dried powder of BMSLN chitosan based
- 7.00 : Nanospray dried powder of BMNLC without chitosan
- 8.00 : Nanospray dried powder of BMNLC chitosan based





Size Stability (mean (n=5) \pm SD (nm))

Formulation	Time (min)				
	0	15	30	60	90
SLN	122.96 \pm 5.63	120.65 \pm 12.01	132.48 \pm 9.65	157.89 \pm 12.34	160.74 \pm 9.34
SPAASLN	444.75 \pm 27.17	445.35 \pm 22.35	450.78 \pm 31.32	478.98 \pm 18.19	496.37 \pm 17.84
SPcAASLN	527.4 \pm 45.83	542.98 \pm 40.45	524.76 \pm 49.56	578.1 \pm 47.53	595.09 \pm 48.34
NLC	124.6 \pm 4.25	133.875 \pm 7.8	156.76 \pm 10.32	165.34 \pm 5.6	163 \pm 13.34
SPAANLC	398.89 \pm 30.00	402.32 \pm 31.76	420.65 \pm 26.56	418.23 \pm 34.67	426.64 \pm 28.97
SPcAANLC	584.6 \pm 58.63	594.73 \pm 42.9	590.43 \pm 49.57	619.75 \pm 48.43	630.34 \pm 47.89

Tests of Normality

Group	Formulation	Kolmogorov-Smirnov ^a			Shapiro-Wilk		
		Statistic	Df	Sig.	Statistic	df	Sig.
0 day	AANLC	.177	3	.	1.000	3	.961
	AASLN	.179	3	.	.999	3	.947
	RSPAANLC	.179	3	.	.999	3	.951
	RSPAASLN	.177	3	.	1.000	3	.971
90 day	AANLC	.180	3	.	.999	3	.945
	AASLN	.201	3	.	.995	3	.858
	RSPAANLC	.191	3	.	.997	3	.898
	RSPAASLN	.175	3	.	1.000	3	.997

Tests of Normality

	Group Formulation	Kolmogorov-Smirnov ^a			Shapiro-Wilk		
		Statistic	Df	Sig.	Statistic	df	Sig.
0 day	AANLC	.177	3	.	1.000	3	.961
	AASLN	.179	3	.	.999	3	.947
	RSPAANLC	.179	3	.	.999	3	.951
	RSPAASLN	.177	3	.	1.000	3	.971
90 day	AANLC	.180	3	.	.999	3	.945
	AASLN	.201	3	.	.995	3	.858
	RSPAANLC	.191	3	.	.997	3	.898
	RSPAASLN	.175	3	.	1.000	3	.997

a. Lilliefors Significance Correction

Paired Samples Statistics

Group Day	Mean	N	Std. Deviation	Std. Error Mean
0 day	272.2292	12	157.00221	45.32264
90 day	311.9392	12	159.14531	45.94129

Paired Samples Correlations

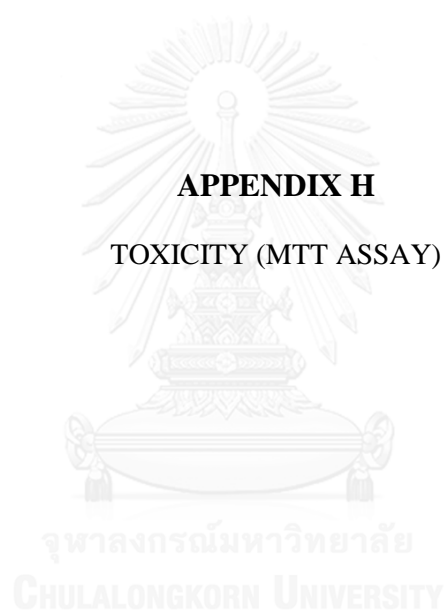
	N	Correlation	Sig.
0 day & 90 day	12	.997	.000

Paired Samples Test

	Paired Differences					t	df	Sig. (2-tailed)
	Mean	Std. Deviation	Std. Error Mean	95% Confidence Interval of the Difference				
				Lower	Upper			
0 day – 90 day	-39.71	12.78	3.69	-47.82990	-31.59	-10.76	11	.000

APPENDIX H

TOXICITY (MTT ASSAY)



Percentage of cell viability of toxicity study on Caco-2 cells between different groups (mean (n=3) \pm SD)

Group Treatment	Percentage cell viability (%)			
	100.0 μ M	50.0 μ M	25.0 μ M	12.5 μ M
Control	100.00 \pm 3.39	100.00 \pm 3.39	100.00 \pm 3.39	100.00 \pm 3.39
AA Free	77.66 \pm 1.68	81.56 \pm 1.36	85.18 \pm 3.08	86.62 \pm 4.59
SLN blank	79.80 \pm 3.11	81.84 \pm 5.17	83.98 \pm 3.64	88.25 \pm 4.04
RSPSLN blank	78.96 \pm 2.63	80.72 \pm 6.27	80.91 \pm 3.55	83.32 \pm 2.94
RSPcSLN blank	63.82 \pm 4.48	77.66 \pm 5.28	77.19 \pm 7.98	80.54 \pm 4.84
AASLN	78.56 \pm 3.49	78.40 \pm 4.18	80.82 \pm 2.94	82.58 \pm 6.18
RSPAASLN	76.92 \pm 2.94	77.66 \pm 4.91	82.02 \pm 5.30	83.14 \pm 7.94
RSPcAASLN	74.13 \pm 5.44	78.59 \pm 3.49	82.02 \pm 5.00	82.21 \pm 6.59
NLC blank	80.10 \pm 6.14	80.96 \pm 1.38	83.34 \pm 3.95	85.39 \pm 5.86
RSPNLC blank	80.21 \pm 2.96	80.77 \pm 5.83	82.41 \pm 2.90	85.06 \pm 1.61
RSPcNLC blank	73.71 \pm 9.62	77.06 \pm 6.16	78.70 \pm 4.11	79.49 \pm 5.94
AANLC	79.05 \pm 5.80	80.10 \pm 8.68	82.07 \pm 2.40	85.06 \pm 9.08
RSPAANLC	709.27 \pm 7.79	80.00 \pm 5.56	82.84 \pm 7.44	89.88 \pm 6.61
RSPcAANLC	78.34 \pm 4.90	80.00 \pm 7.26	81.17 \pm 6.10	84.31 \pm 4.93

Tests of Normality

Group Treatment		Kolmogorov-Smirnov ^a			Shapiro-Wilk		
		Statistic	df	Sig.	Statistic	df	Sig.
100.0 μ M	Control	.183	3	.	.999	3	.933
	AA free	.211	3	.	.991	3	.817
	SLN Blank	.318	3	.	.887	3	.344
	RSPSLN Blank	.304	3	.	.907	3	.407
	RSPcSLN Blank	.216	3	.	.988	3	.794
	AASLN	.198	3	.	.995	3	.868
	RSPAASLN	.204	3	.	.993	3	.843
	RSPcAASLN	.187	3	.	.998	3	.915
	NLC Blank	.175	3	.	1.000	3	.990
	RSPNLC Blank	.229	3	.	.981	3	.739
	RSPcNLC Blank	.186	3	.	.998	3	.920
	AANLC	.236	3	.	.977	3	.711
	RSPAANLC	.194	3	.	.996	3	.886
RSPcAANLC	.217	3	.	.988	3	.791	
50.0 μ M	Control	.183	3	.	.999	3	.933
	AA free	.349	3	.	.832	3	.194
	SLN Blank	.202	3	.	.994	3	.851
	RSPSLN Blank	.176	3	.	1.000	3	.975
	RSPcSLN Blank	.337	3	.	.855	3	.253
	AASLN	.184	3	.	.999	3	.927
	RSPAASLN	.219	3	.	.987	3	.780
	RSPcAASLN	.198	3	.	.995	3	.868
	NLC Blank	.198	3	.	.995	3	.870
	RSPNLC Blank	.189	3	.	.998	3	.909
	RSPcNLC Blank	.371	3	.	.785	3	.078
	AANLC	.192	3	.	.997	3	.896
	RSPAANLC	.205	3	.	.993	3	.841
RSPcAANLC	.183	3	.	.999	3	.933	

Continue

	Group Treatment	Kolmogorov-Smirnov ^a			Shapiro-Wilk		
		Statistic	df	Sig.	Statistic	df	Sig.
25.0 μ M	Control	.183	3	.	.999	3	.933
	AA free	.215	3	.	.989	3	.800
	SLN Blank	.207	3	.	.992	3	.831
	RSPSLN Blank	.357	3	.	.815	3	.150
	RSPcSLN Blank	.367	3	.	.794	3	.100
	AASLN	.204	3	.	.993	3	.843
	RSPAASLN	.181	3	.	.999	3	.942
	RSPcAASLN	.365	3	.	.797	3	.107
	NLC Blank	.278	3	.	.940	3	.528
	RSPNLC Blank	.198	3	.	.995	3	.870
	RSPcNLC Blank	.236	3	.	.977	3	.712
	AANLC	.178	3	.	.999	3	.956
	RSPAANLC	.237	3	.	.976	3	.705
	RSPcAANLC	.310	3	.	.899	3	.383
12.5 μ M	Control	.183	3	.	.999	3	.933
	AA free	.374	3	.	.776	3	.058
	SLN Blank	.177	3	.	1.000	3	.962
	RSPSLN Blank	.204	3	.	.993	3	.843
	RSPcSLN Blank	.365	3	.	.798	3	.110
	AASLN	.279	3	.	.939	3	.523
	RSPAASLN	.176	3	.	1.000	3	.981
	RSPcAASLN	.217	3	.	.988	3	.790
	NLC Blank	.181	3	.	.999	3	.941
	RSPNLC Blank	.339	3	.	.850	3	.240
	RSPcNLC Blank	.303	3	.	.909	3	.415
	AANLC	.233	3	.	.979	3	.723
	RSPAANLC	.271	3	.	.947	3	.558
	RSPcAANLC	.363	3	.	.802	3	.120

a. Lilliefors Significance Correction

Test of Homogeneity of Variances

Concentration	Levene Statistic	df1	df2	Sig.
100.0 μM	.957	13	28	.513
50.0 μM	.860	13	28	.600
25.0 μM	1.336	13	28	.251
12.5 μM	.888	13	28	.575

ANOVA

		Sum of Squares	df	Mean Square	F	Sig.
100.0 μM	Between Groups	741.409	13	57.031	2.251	.035
	Within Groups	709.332	28	25.333		
	Total	1450.740	41			
50.0 μM	Between Groups	104.979	13	8.075	.258	.994
	Within Groups	878.019	28	31.358		
	Total	982.999	41			
25.0 μM	Between Groups	160.318	13	12.332	.562	.863
	Within Groups	614.304	28	21.939		
	Total	774.622	41			
12.5 μM	Between Groups	399.764	13	30.751	.953	.516
	Within Groups	903.273	28	32.260		
	Total	1303.037	41			

Post Hoc Tests



Dependent Variable	Group Treatment	Group Treatment	Mean Difference	Std. Error	Sig.	95% Confidence Interval	
						Interval	
						Lower Bound	Upper Bound
100.0 μ M	Control	AA free	2.341	4.110	1.000	-13.685	18.368
		SLN Blank	0.205	4.110	1.000	-15.822	16.231
		RSPSLN Blank	1.041	4.110	1.000	-14.985	17.067
		RSPcSLN Blank	16.182*	4.110	0.045	0.1560	32.209
		AASLN	1.413	4.110	1.000	-14.614	17.439
		RSPAASLN	3.085	4.110	1.000	-12.942	19.111
		RSPcAASLN	5.871	4.110	1.000	-10.155	21.898
		NLC Blank	-0.103	4.110	1.000	-16.130	15.923
		RSPNLC Blank	-0.215	4.110	1.000	-16.241	15.812
		RSPcNLC Blank	6.288	4.110	1.000	-9.739	22.314
		AANLC	0.946	4.110	1.000	-15.081	16.972
		RSAANLC	0.727	4.110	1.000	-15.300	16.753
		RSPcAANLC	1.656	4.110	1.000	-14.371	17.682
		AA free	Control	-2.341	4.110	1.000	-18.368
	SLN Blank		-2.136	4.110	1.000	-18.163	13.890
	RSPSLN Blank		-1.300	4.110	1.000	-17.327	14.726
	RSPcSLN Blank		13.841	4.110	.202	-2.185	29.868
	AASLN		-.929	4.110	1.000	-16.955	15.098
	RSPAASLN		.743	4.110	1.000	-15.283	16.770
	RSPcAASLN		3.530	4.110	1.000	-12.496	19.556
	NLC Blank		-2.445	4.110	1.000	-18.471	13.582
	RSPNLC Blank		-2.556	4.110	1.000	-18.582	13.470
	RSPcNLC Blank		3.946	4.110	1.000	-12.080	19.973
	AANLC	-1.396	4.110	1.000	-17.422	14.630	
RSAANLC	-1.615	4.110	1.000	-17.641	14.412		
RSPcAANLC	-.686	4.110	1.000	-16.712	15.340		

Continue

Dependent Variable	Group Treatment	Group Treatment	Mean Difference	Std. Error	Sig.	95% Confidence Interval		
						Lower Bound	Upper Bound	
100.0 μ M	SLN Blank	Control	-.205	4.110	1.000	-16.231	15.823	
		AA free	2.136	4.110	1.000	-13.890	18.163	
		RSPSLN Blank	.836	4.110	1.000	-15.190	16.862	
		RSPcSLN Blank	15.978	4.110	.052	-.049	32.004	
		AASLN	1.208	4.110	1.000	-14.819	17.234	
		RSPAASLN	2.880	4.110	1.000	-13.147	18.906	
		RSPcAASLN	5.666	4.110	1.000	-10.360	21.693	
		NLC Blank	-.308	4.110	1.000	-16.335	15.718	
		RSPNLC Blank	-.4196	4.110	1.000	-16.446	15.607	
		RSPcNLC Blank	6.083	4.110	1.000	-9.944	22.109	
		AANLC	.740	4.110	1.000	-15.286	16.767	
		RSAANLC	.522	4.110	1.000	-15.505	16.548	
		RSPcAANLC	1.451	4.110	1.000	-14.576	17.477	
		RSPSLN Blank	Control	-1.0410	4.110	1.000	-17.067	14.985
			AA free	1.300	4.110	1.000	-14.726	17.327
	SLN Blank		-.8360	4.110	1.000	-16.862	15.190	
	RSPcSLN Blank		15.142	4.110	.089	-.885	31.168	
	AASLN		.372	4.110	1.000	-15.655	16.398	
	RSPAASLN		2.044	4.110	1.000	-13.983	18.070	
	RSPcAASLN		4.830	4.110	1.000	-11.196	20.857	
	NLC Blank		-1.144	4.110	1.000	-17.171	14.882	
	RSPNLC Blank		-1.256	4.110	1.000	-17.282	14.7708	
	RSPcNLC Blank		5.247	4.110	1.000	-10.780	21.273	
	AANLC		-.095	4.110	1.000	-16.122	15.931	
	RSAANLC		-.314	4.110	1.000	-16.341	15.712	
	RSPcAANLC		.615	4.110	1.000	-15.412	16.641	

Continue

Dependent Variable	Group Treatment	Group Treatment	Mean Difference	Std. Error	Sig.	95% Confidence Interval		
						Lower Bound	Upper Bound	
100.0 μ M	RSPcSLN Blank	Control	-16.182*	4.110	.045	-32.209	-.156	
		SLN Blank	-13.841	4.110	.202	-29.868	2.185	
		RSPSLN Blank	-15.978	4.110	.052	-32.004	.049	
		RSPcSLN Blank	-15.142	4.110	.089	-31.168	.885	
		AASLN	-14.770	4.110	.112	-30.796	1.256	
		RSPAASLN	-13.098	4.110	.320	-29.124	2.928	
		RSPcAASLN	-10.311	4.110	1.000	-26.338	5.715	
		NLC Blank	-16.286*	4.110	.042	-32.312	-.259	
		RSPNLC Blank	-16.397*	4.110	.039	-32.424	-.371	
		RSPcNLC Blank	-9.895	4.110	1.000	-25.921	6.132	
		AANLC	-15.237	4.110	.083	-31.263	.789	
		RSAANLC	-15.456	4.110	.072	-31.482	.570	
		RSPcAANLC	-14.527	4.110	.131	-30.553	1.500	
		AASLN	Control	-1.412	4.110	1.000	-17.439	14.614
			AA free	.929	4.110	1.000	-15.098	16.955
	SLN Blank		-1.208	4.110	1.000	-17.234	14.819	
	RSPSLN Blank		-.372	4.110	1.000	-16.398	15.655	
	RSPcSLN Blank		14.770	4.110	.112	-1.256	30.796	
	RSPAASLN		1.672	4.110	1.000	-14.354	17.698	
	RSPcAASLN		4.459	4.110	1.000	-11.568	20.485	
	NLC Blank		-1.516	4.110	1.000	-17.542	14.511	
	RSPNLC Blank		-1.627	4.110	1.000	-17.654	14.399	
	RSPcNLC Blank		4.875	4.110	1.000	-11.151	20.902	
	AANLC		-.467	4.110	1.000	-16.493	15.559	
	RSAANLC		-.686	4.110	1.000	-16.712	15.340	
	RSPcAANLC		.243	4.110	1.000	-15.783	16.270	

Continue

Dependent Variable	Group Treatment	Group Treatment	Mean Difference	Std. Error	Sig.	95% Confidence Interval	
						Lower Bound	Upper Bound
100 μ M	RSPAASLN	Control	-3.085	4.110	1.000	-19.111	12.942
		AA free	-.743	4.110	1.000	-16.770	15.283
		SLN Blank	-2.880	4.110	1.000	-18.906	13.147
		RSPSLN Blank	-2.044	4.110	1.000	-18.070	13.983
		RSPcSLN Blank	13.098	4.110	.320	-2.928	29.124
		AASLN	-1.672	4.110	1.000	-17.698	14.354
		RSPcAASLN	2.788	4.110	1.000	-13.240	18.813
		NLC Blank	-3.188	4.110	1.000	-19.214	12.838
		RSPNLC Blank	-3.300	4.110	1.000	-19.326	12.727
		RSPcNLC Blank	3.203	4.110	1.000	-12.823	19.230
		AANLC	-2.139	4.110	1.000	-18.166	13.887
		RSAANLC	-2.358	4.110	1.000	-18.384	13.668
		RSPcAANLC	-1.429	4.110	1.000	-17.455	14.597
		RSPcAASLN	Control	-5.871	4.110	1.000	-21.898
	AA free		-3.5300	4.110	1.000	-19.556	12.496
	SLN Blank		-5.666	4.110	1.000	-21.693	10.360
	RSPSLN Blank		-4.830	4.110	1.000	-20.857	11.196
	RSPcSLN Blank		10.311	4.110	1.000	-5.715	26.338
	AASLN		-4.459	4.110	1.000	-20.485	11.568
	RSPAASLN		-2.787	4.110	1.000	-18.813	13.240
	NLC Blank		-5.975	4.110	1.000	-22.001	10.052
	RSPNLC Blank		-6.086	4.110	1.000	-22.112	9.940
	RSPcNLC Blank		.4165	4.110	1.000	-15.610	16.443
	AANLC		-4.926	4.110	1.000	-20.952	11.100
	RSAANLC		-5.145	4.110	1.000	-21.171	10.882
	RSPcAANLC	-4.216	4.110	1.000	-20.242	11.811	

Continue

Dependent Variable	Group Treatment	Group Treatment	Mean Difference	Std. Error	Sig.	95% Confidence Interval		
						Lower Bound	Upper Bound	
100 μ M	NLC Blank	Control	.103	4.110	1.000	-15.923	16.130	
		AA free	2.445	4.110	1.000	-13.582	18.471	
		SLN Blank	.308	4.110	1.000	-15.718	16.335	
		RSPSLN Blank	1.144	4.110	1.000	-14.882	17.171	
		RSPcSLN Blank	16.286*	4.110	.042	.259	32.312	
		AASLN	1.516	4.110	1.000	-14.511	17.542	
		RSPAASLN	3.188	4.110	1.000	-12.838	19.214	
		RSPcAASLN	5.975	4.110	1.000	-10.052	22.001	
		RSPNLC Blank	-.111	4.110	1.000	-16.138	15.915	
		RSPcNLC Blank	6.391	4.110	1.000	-9.635	22.418	
		AANLC	1.049	4.110	1.000	-14.978	17.075	
		RSAANLC	.830	4.110	1.000	-15.196	16.856	
		RSPcAANLC	1.7589	4.110	1.000	-14.268	17.785	
		RSPNLC Blank	Control	.2146	4.110	1.000	-15.812	16.241
			AA free	2.556	4.110	1.000	-13.470	18.582
	SLN Blank		.420	4.110	1.000	-15.607	16.446	
	RSPSLN Blank		1.256	4.110	1.000	-14.771	17.282	
	RSPcSLN Blank		16.397*	4.110	.039	.371	32.424	
	AASLN		1.627	4.110	1.000	-14.399	17.654	
	RSPAASLN		3.299	4.110	1.000	-12.727	19.326	
	RSPcAASLN		6.086	4.110	1.000	-9.940	22.112	
	NLC Blank		.111	4.110	1.000	-15.915	16.138	
	RSPcNLC Blank		6.502	4.110	1.000	-9.524	22.529	
	AANLC		1.160	4.110	1.000	-14.866	17.187	
	RSAANLC		.941	4.110	1.000	-15.085	16.968	
	RSPcAANLC		1.870	4.110	1.000	-14.156	17.897	

Continue

Dependent Variable	Group Treatment	Group Treatment	Mean Difference	Std. Error	Sig.	95% Confidence Interval	
						Lower Bound	Upper Bound
100.0 μ M	RSPcNLC Blank	Control	-6.288	4.110	1.000	-22.314	9.738
		AA free	-3.946	4.110	1.000	-19.973	12.080
		SLN Blank	-6.083	4.110	1.000	-22.109	9.944
		RSPSLN Blank	-5.247	4.110	1.000	-21.273	10.7795
		RSPcSLN Blank	9.895	4.110	1.000	-6.132	25.921
		AASLN	-4.875	4.110	1.000	-20.902	11.151
		RSPAASLN	-3.203	4.110	1.000	-19.230	12.823
		RSPcAASLN	-.416	4.110	1.000	-16.443	15.610
		NLC Blank	-6.391	4.110	1.000	-22.418	9.635
		RSPNLC Blank	-6.502	4.110	1.000	-22.52	9.524
		AANLC	-5.342	4.110	1.000	-21.369	10.684
		RSAANLC	-5.561	4.110	1.000	-21.588	10.465
		RSPcAANLC	-4.632	4.110	1.000	-20.659	11.394
		AANLC	Control	-.946	4.110	1.000	-16.972
	AA free		1.396	4.110	1.000	-14.630	17.422
	SLN Blank		-.741	4.110	1.000	-16.767	15.286
	RSPSLN Blank		.0954	4.110	1.000	-15.931	16.122
	RSPcSLN Blank		15.237	4.110	.083	-.789	31.263
	AASLN		.467	4.110	1.000	-15.559	16.493
	RSPAASLN		2.139	4.110	1.000	-13.887	18.166
	RSPcAASLN		4.926	4.110	1.000	-11.100	20.952
	NLC Blank		-1.049	4.110	1.000	-17.075	14.978
	RSPNLC Blank		-1.160	4.110	1.000	-17.187	14.866
	RSPcNLC Blank		5.342	4.110	1.000	-10.684	21.369
	RSAANLC		-.219	4.110	1.000	-16.245	15.808
	RSPcAANLC	.711	4.110	1.000	-15.316	16.736	

Continue

Dependent Variable	Group Treatment	Group Treatment	Mean Difference	Std. Error	Sig.	95% Confidence Interval	
						Lower Bound	Upper Bound
100.0 μ M	RSPAANLC	Control	-.727	4.110	1.000	-16.753	15.300
		AA free	1.615	4.110	1.000	-14.412	17.641
		SLN Blank	-.522	4.110	1.000	-16.548	15.505
		RSPSLN Blank	.314	4.110	1.000	-15.712	16.341
		RSPcSLN Blank	15.456	4.110	.072	-.570	31.482
		AASLN	.6859	4.110	1.000	-15.340	16.712
		RSPAASLN	2.358	4.110	1.000	-13.668	18.384
		RSPcAASLN	5.145	4.110	1.000	-10.882	21.171
		NLC Blank	-.830	4.110	1.000	-16.856	15.196
		RSPNLC Blank	-.941	4.110	1.000	-16.968	15.085
		RSPcNLC Blank	5.561	4.110	1.000	-10.465	21.588
		AANLC	.219	4.110	1.000	-15.808	16.245
		RSPcAANLC	.929	4.110	1.000	-15.098	16.955
		RSPcAANLC	Control	-1.656	4.110	1.000	-17.682
	AA free		.6859	4.110	1.000	-15.340	16.712
	SLN Blank		-1.451	4.110	1.000	-17.477	14.576
	RSPSLN Blank		-.615	4.110	1.000	-16.641	15.412
	RSPcSLN Blank		14.527	4.110	.131	-1.500	30.553
	AASLN		-.243	4.110	1.000	-16.270	15.783
	RSPAASLN		1.429	4.110	1.000	-14.597	17.455
	RSPcAASLN		4.216	4.110	1.000	-11.811	20.242
	NLC Blank		-1.759	4.110	1.000	-17.785	14.268
	RSPNLC Blank		-1.870	4.110	1.000	-17.897	14.156
	RSPcNLC Blank		4.632	4.110	1.000	-11.394	20.659
	AANLC		-.710	4.110	1.000	-16.736	15.316
	RSAANLC	-.929	4.110	1.000	-16.955	15.098	

Percentage of cell viability of toxicity study on b.End3 cells between different groups
(mean (n=3) \pm SD)

Group Treatments	Percentage cell viability (%)
	100.0 μ M
Control	100.00 \pm 5.46
AA Free	90.24 \pm 4.79
SLN Blank	89.00 \pm 4.43
RSPSLN blank	87.09 \pm 2.44
RSPcSLN blank	84.69 \pm 3.08
AASLN	87.77 \pm 6.01
RSPAASLN	86.59 \pm 6.34
RSPcAASLN	84.36 \pm 3.26
NLC Blank	91.32 \pm 2.33
RSPNLC blank	96.88 \pm 6.81
RSPcNLC blank	96.22 \pm 4.34
AANLC	93.09 \pm 3.44
RSPAANLC	94.83 \pm 6.13
RSPcAANLC	9.32 \pm 6.44

		Tests of Normality					
Group Treatment		Kolmogorov-Smirnov ^a			Shapiro-Wilk		
		Statistic	df	Sig.	Statistic	df	Sig.
original	Control	.344	3	.	.842	3	.219
	AA free	.176	3	.	1.000	3	.982
	SLN Blank	.177	3	.	1.000	3	.973
	RSPSLN Blank	.248	3	.	.968	3	.658
	RSPcSLN Blank	.300	3	.	.912	3	.426
	AASLN	.176	3	.	1.000	3	.988
	RSPAASLN	.178	3	.	.999	3	.954
	RSPcAASLN	.362	3	.	.804	3	.124
	NLC Blank	.178	3	.	.999	3	.952
	RSPNLC Blank	.234	3	.	.978	3	.717
	RSPcNLC Blank	.332	3	.	.863	3	.276
	RSPAANLC	.312	3	.	.895	3	.371
	RSPAANLC	.197	3	.	.996	3	.875
	RSPcAANLC	.180	3	.	.999	3	.946

a. Lilliefors Significance Correction

Test of Homogeneity of Variances

Levene Statistic	df1	df2	Sig.
.512	13	28	.898

ANOVA

	Sum of Squares	df	Mean Square	F	Sig.
Between Groups	916.519	13	70.501	3.030	.007
Within Groups	651.477	28	23.267		
Total	1567.997	41			



Post Hoc Tests**Multiple Comparisons****Bonferroni**

Group Treatment	Group Treatment	Mean Difference	Std. Error	Sig.	95% Confidence Interval	
					Lower Bound	Upper Bound
Control	AA free	-10.239	3.938	1.000	-25.598	5.120
	SLN Blank	-8.994	3.938	1.000	-24.353	6.365
	RSPSLN Blank	-7.092	3.938	1.000	-22.451	8.267
	RSPcSLN Blank	-4.688	3.938	1.000	-20.047	10.671
	AASLN	-7.766	3.938	1.000	-23.125	7.593
	RSPAASLN	-6.585	3.938	1.000	-21.944	8.774
	RSPcAASLN	-4.365	3.938	1.000	-19.724	10.994
	NLC Blank	-11.318	3.938	.697	-26.677	4.041
	RSPNLC Blank	-16.883*	3.938	.018	-32.2412	-1.524
	RSPcNLC Blank	-16.225*	3.938	.028	-31.584	-.866
	AANLC	-13.085	3.938	.227	-28.444	2.274
	RSPAANLC	-14.833	3.938	.071	-30.192	.526
	RSPcAANLC	-11.318	3.938	.697	-26.677	4.041
AA free	Control	10.239	3.938	1.000	-5.120	25.598
	SLN Blank	1.244	3.938	1.000	-14.115	16.603
	RSPSLN Blank	3.147	3.938	1.000	-12.212	18.506
	RSPcSLN Blank	5.551	3.938	1.000	-9.808	20.910
	AASLN	2.473	3.938	1.000	-12.886	17.832
	RSPAASLN	3.654	3.938	1.000	-11.705	19.013
	RSPcAASLN	5.874	3.938	1.000	-9.485	21.233
	NLC Blank	-1.079	3.938	1.000	-16.438	14.280
	RSPNLC Blank	-6.644	3.938	1.000	-22.003	8.715
	RSPcNLC Blank	-5.986	3.938	1.000	-21.345	9.373
	AANLC	-2.847	3.938	1.000	-18.206	12.512
	RSPAANLC	-4.595	3.938	1.000	-19.954	10.764
	RSPcAANLC	-1.079	3.938	1.000	-16.4379	14.280

Continue

Group Treatment	Group Treatment	Mean Difference	Std. Error	Sig.	95% Confidence Interval	
					Lower Bound	Upper Bound
SLN Blank	Control	8.994	3.938	1.000	-6.365	24.353
	AA free	-1.244	3.938	1.000	-16.603	14.115
	RSPSLN Blank	1.903	3.938	1.000	-13.456	17.262
	RSPcSLN Blank	4.306	3.938	1.000	-11.053	19.665
	AASLN	1.229	3.938	1.000	-14.130	16.588
	RSPAASLN	2.410	3.938	1.000	-12.949	17.769
	RSPcAASLN	4.630	3.938	1.000	-10.729	19.989
	NLC Blank	-2.323	3.938	1.000	-17.682	13.036
	RSPNLC Blank	-7.888	3.938	1.000	-23.247	7.471
	RSPcNLC Blank	-7.230	3.938	1.000	-22.589	8.129
	AANLC	-4.091	3.938	1.000	-19.450	11.268
	RSPAANLC	-5.839	3.938	1.000	-21.198	9.520
	RSPcAANLC	-2.323	3.938	1.000	-17.682	13.036
	RSPSLN Blank	Control	7.092	3.938	1.000	-8.267
AA free		-3.147	3.938	1.000	-18.506	12.212
SLN Blank		-1.9023	3.938	1.000	-17.262	13.456
RSPcSLN Blank		2.404	3.938	1.000	-12.955	17.763
AASLN		-.674	3.938	1.000	-16.033	14.685
RSPAASLN		.507	3.938	1.000	-14.852	15.866
RSPcAASLN		2.727	3.938	1.000	-12.632	18.086
NLC Blank		-4.226	3.938	1.000	-19.585	11.133
RSPNLC Blank		-9.791	3.938	1.000	-25.150	5.568
RSPcNLC Blank		-9.133	3.938	1.000	-24.492	6.226
AANLC		-5.994	3.938	1.000	-21.353	9.365
RSPAANLC		-7.742	3.938	1.000	-23.101	7.617
RSPcAANLC		-4.226	3.938	1.000	-19.585	11.133

Continue

Group Treatment	Group Treatment	Mean Difference	Std. Error	Sig.	95% Confidence Interval		
					Lower Bound	Upper Bound	
RSPcSLN Blank	Control	4.688	3.938	1.000	-10.671	20.047	
	AA free	-5.551	3.938	1.000	-20.910	9.808	
	SLN Blank	-4.306	3.938	1.000	-19.665	11.053	
	RSPSLN Blank	-2.404	3.938	1.000	-17.763	12.955	
	AASLN	-3.078	3.938	1.000	-18.437	12.281	
	RSPAASLN	-1.897	3.938	1.000	-17.256	13.462	
	RSPcAASLN	.323	3.938	1.000	-15.036	15.682	
	NLC Blank	-6.630	3.938	1.000	-21.989	8.729	
	RSPNLC Blank	-12.195	3.938	.402	-27.554	3.164	
	RSPcNLC Blank	-11.537	3.938	.609	-26.896	3.822	
	AANLC	-8.397	3.938	1.000	-23.756	6.962	
	RSPAANLC	-10.145	3.938	1.000	-25.504	5.214	
	RSPcAANLC	-6.630	3.938	1.000	-21.989	8.729	
	AASLN	Control	7.766	3.938	1.000	-7.593	23.125
		AA free	-2.473	3.938	1.000	-17.832	12.886
SLN Blank		-1.229	3.938	1.000	-16.588	14.130	
RSPSLN Blank		.674	3.938	1.000	-14.685	16.033	
RSPcSLN Blank		3.078	3.938	1.000	-12.282	18.437	
RSPAASLN		1.181	3.938	1.000	-14.178	16.540	
RSPcAASLN		3.401	3.938	1.000	-11.958	18.760	
NLC Blank		-3.552	3.938	1.000	-18.911	11.807	
RSPNLC Blank		-9.117	3.938	1.000	-24.476	6.242	
RSPcNLC Blank		-8.459	3.938	1.000	-23.818	6.900	
AANLC		-5.320	3.938	1.000	-20.679	10.039	
RSPAANLC		-7.068	3.938	1.000	-22.427	8.291	
RSPcAANLC		-3.552	3.938	1.000	-18.911	11.807	

Continue

Group Treatment	Group Treatment	Mean Difference	Std. Error	Sig.	95% Confidence Interval	
					Lower Bound	Upper Bound
RSPAASLN	Control	6.585	3.938	1.000	-8.7743	21.944
	AA free	-3.654	3.938	1.000	-19.013	11.705
	SLN Blank	-2.410	3.938	1.000	-17.769	12.949
	RSPSLN Blnk	-.507	3.938	1.000	-15.866	14.852
	RSPcSLN Blank	1.897	3.938	1.000	-13.462	17.256
	AASLN	-1.181	3.938	1.000	-16.540	14.178
	RSPcAASLN	2.220	3.938	1.000	-13.139	17.579
	NLC Blank	-4.733	3.938	1.000	-20.092	10.626
	RSPNLC Blank	-10.298	3.938	1.000	-25.657	5.061
	RSPcNLC Blank	-9.640	3.938	1.000	-24.999	5.719
	AANLC	-6.501	3.938	1.000	-21.860	8.858
	RSPAANLC	-8.249	3.938	1.000	-23.608	7.110
	RSPcAANLC	-4.733	3.938	1.000	-20.092	10.626
	RSPcAASLN	Control	4.365	3.938	1.000	-10.994
AA free		-5.874	3.938	1.000	-21.233	9.485
SLN Blank		-4.630	3.938	1.000	-19.989	10.729
RSPSLN Blank		-2.727	3.938	1.000	-18.086	12.632
RSPcSLN Blank		-.323	3.938	1.000	-15.682	15.036
AASLN		-3.401	3.938	1.000	-18.760	11.958
RSPAASLN		-2.220	3.938	1.000	-17.579	13.139
NLC Blank		-6.953	3.938	1.000	-22.312	8.406
RSPNLC Blank		-12.518	3.938	.327	-27.877	2.841
RSPcNLC Blank		-11.860	3.938	.497	-27.219	3.499
AANLC		-8.721	3.938	1.000	-24.080	6.638
RSPAANLC		-10.469	3.938	1.000	-25.828	4.890
RSPcAANLC		-6.953	3.938	1.000	-22.312	8.406

Continue

Group Treatment	Group Treatment	Mean Difference	Std. Error	Sig.	95% Confidence Interval	
					Lower Bound	Upper Bound
NLC Blank	Control	11.318	3.938	.697	-4.041	26.677
	AA free	1.079	3.938	1.000	-14.280	16.438
	SLN Blank	2.323	3.938	1.000	-13.036	17.682
	RSPSLN Blnk	4.226	3.938	1.000	-11.133	19.585
	RSPcSLN Blank	6.630	3.938	1.000	-8.729	21.989
	AASLN	3.552	3.938	1.000	-11.807	18.911
	RSPcAASLN	4.733	3.938	1.000	-10.626	20.092
	NLC Blank	6.953	3.938	1.000	-8.406	22.312
	RSPNLC Blank	-5.565	3.938	1.000	-20.924	9.794
	RSPcNLC Blank	-4.907	3.938	1.000	-20.266	10.452
	AANLC	-1.768	3.938	1.000	-17.127	13.591
	RSPAANLC	-3.516	3.938	1.000	-18.875	11.843
	RSPcAANLC	.000	3.938	1.000	-15.359	15.359
	RSPNLC Blank	Control	16.883*	3.938	.018	1.524
AA free		6.644	3.938	1.000	-8.715	22.003
SLN Blank		7.888	3.938	1.000	-7.471	23.247
RSPSLN Blank		9.791	3.938	1.000	-5.568	25.150
RSPcSLN Blank		12.195	3.938	.402	-3.164	27.554
AASLN		9.117	3.938	1.000	-6.242	24.476
RSPAASLN		10.298	3.938	1.000	-5.061	25.657
NLC Blank		12.518	3.938	.327	-2.841	27.877
RSPNLC Blank		5.565	3.938	1.000	-9.794	20.924
RSPcNLC Blank		.658	3.938	1.000	-14.701	16.0169
AANLC		3.797	3.938	1.000	-11.562	19.156
RSPAANLC		2.049	3.938	1.000	-13.310	17.408
RSPcAANLC		5.565	3.938	1.000	-9.794	20.924

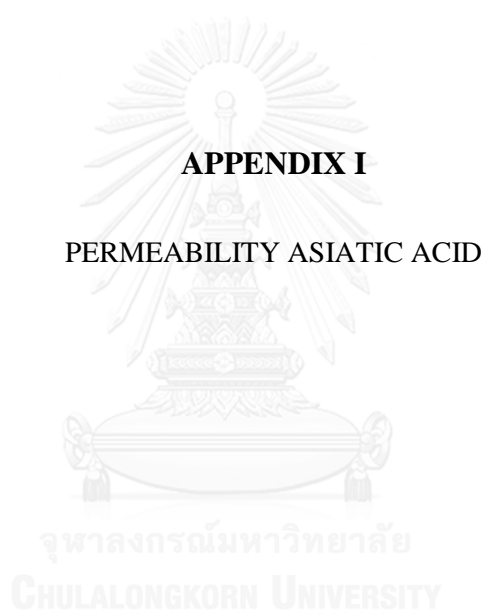
Continue

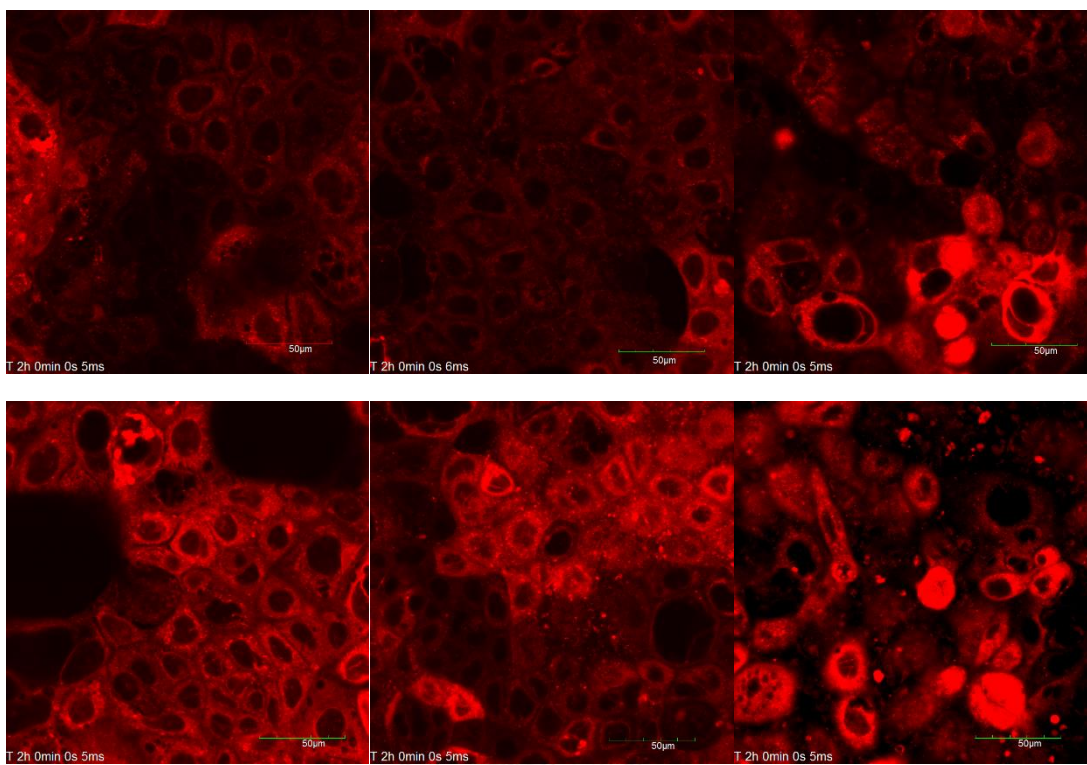
Group Treatment	Group Treatment	Mean Difference	Std. Error	Sig.	95% Confidence Interval	
					Lower Bound	Upper Bound
RSPcNLC Blank	Control	16.225*	3.938	.028	.866	31.584
	AA free	5.986	3.938	1.000	-9.373	21.345
	SLN Blank	7.230	3.938	1.000	-8.129	22.589
	RSPSLN Blnk	9.133	3.938	1.000	-6.226	24.492
	RSPcSLN Blank	11.537	3.938	.609	-3.822	26.896
	AASLN	8.459	3.938	1.000	-6.900	23.818
	RSPAASLN	9.640	3.938	1.000	-5.719	24.999
	RSPcAASLN	11.860	3.938	.497	-3.499	27.219
	NLC Blank	4.907	3.938	1.000	-10.452	20.266
	RSPNLC Blank	-.658	3.938	1.000	-16.017	14.701
	AANLC	3.139	3.938	1.000	-12.220	18.498
	RSPAANLC	1.391	3.938	1.000	-13.968	16.750
	RSPcAANLC	4.907	3.938	1.000	-10.452	20.266
	AANLC	Control	13.085	3.938	.227	-2.274
AA free		2.847	3.938	1.000	-12.512	18.206
SLN Blank		4.091	3.938	1.000	-11.268	19.450
RSPSLN Blank		5.9937	3.938	1.000	-9.365	21.353
RSPcSLN Blank		8.397	3.938	1.000	-6.962	23.756
AASLN		5.3197	3.938	1.000	-10.039	20.679
RSPAASLN		6.501	3.938	1.000	-8.858	21.860
RSPcAASLN		8.721	3.938	1.000	-6.638	24.080
NLC Blank		1.768	3.938	1.000	-13.591	17.127
RSPNLC Blank		-3.797	3.938	1.000	-19.156	11.562
RSPcNLC Blank		-3.139	3.938	1.000	-18.498	12.220
RSPAANLC		-1.748	3.938	1.000	-17.107	13.611
RSPcAANLC		1.768	3.938	1.000	-13.591	17.127

Continue

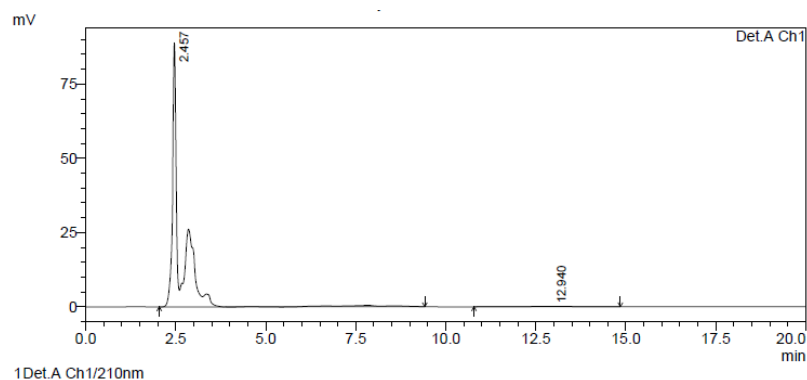
Group Treatment	Group Treatment	Mean Difference	Std. Error	Sig.	95% Confidence Interval	
					Lower Bound	Upper Bound
RSPAANLC	Control	14.833	3.938	.071	-.526	30.192
	AA free	4.595	3.938	1.000	-10.764	19.954
	SLN Blank	5.839	3.938	1.000	-9.520	21.198
	RSPSLN Blk	7.742	3.938	1.000	-7.617	23.101
	RSPcSLN Blank	10.145	3.938	1.000	-5.214	25.504
	AASLN	7.068	3.938	1.000	-8.291	22.427
	RSPAASLN	8.249	3.938	1.000	-7.110	23.608
	RSPcAASLN	10.469	3.938	1.000	-4.890	25.828
	NLC Blank	3.516	3.938	1.000	-11.843	18.875
	RSPNLC Blank	-2.049	3.938	1.000	-17.408	13.310
	RSPcNLC Blank	-1.391	3.938	1.000	-16.750	13.968
	AANLC	1.748	3.938	1.000	-13.611	17.107
	RSPcAANLC	3.516	3.938	1.000	-11.843	18.875
	RSPcAANLC	Control	11.318	3.938	.697	-4.041
AA free		1.079	3.938	1.000	-14.280	16.438
SLN Blank		2.323	3.938	1.000	-13.036	17.682
RSPSLN Blank		4.226	3.938	1.000	-11.133	19.585
RSPcSLN Blank		6.630	3.938	1.000	-8.729	21.989
AASLN		3.552	3.938	1.000	-11.807	18.911
RSPAASLN		4.733	3.938	1.000	-10.626	20.092
RSPcAASLN		6.953	3.938	1.000	-8.406	22.312
NLC Blank		.000	3.938	1.000	-15.359	15.359
RSPNLC Blank		-5.565	3.938	1.000	-20.924	9.794
RSPcNLC Blank		-4.907	3.938	1.000	-20.266	10.452
AANLC		-1.768	3.938	1.000	-17.127	13.591
RSPAANLC		-3.516	3.938	1.000	-18.875	11.843

*. The mean difference is significant at the 0.05 level.

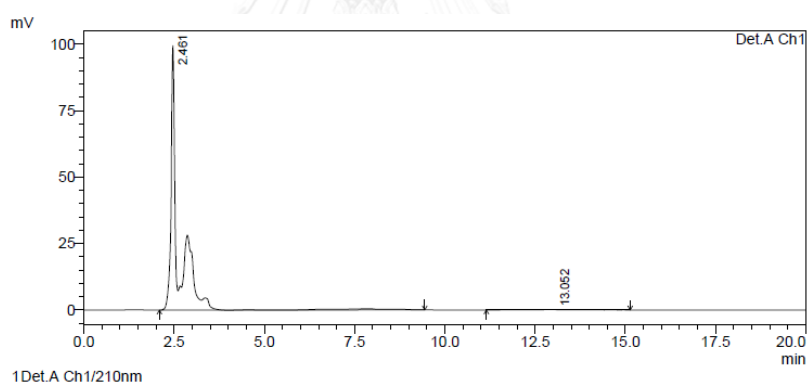




Confocal Laser Scanning Microscopy (CLSM) study of R6gSLN, RSPR6gSLN, RSPcR6gSLN (first row), R6gNLC, RSPR6gNLC and RSPcR6gNLC (second row) on Caco-2 cells at 2 h incubation. Paracellular localization of R6g fluorescence was noted (arrow).



Chromatogram of sample from basolateral site after 2 hour incubation on permeability study of RSPcAASLN, detected Asiatic acid (AA) with RT at 12.940 min and UC 9926 (HPLC condition of acetonitrile: 10 mM buffer phosphate = 28:72, v/v, pH 7.7, flow rate 1.0 mL/min, detected 210nm).



Chromatogram of sample from basolateral site after 2 hour incubation on permeability study of RSPcAANLC, detected Asiatic acid (AA) with RT at 13.052 min and AUC 10961 (HPLC condition of acetonitrile: 10 mM buffer phosphate = 28:72, v/v, pH 7.7, flow rate 1.0 mL/min, detected 210nm).

Drug Transport on Caco-2 cells (mean (n=3) \pm SD)

Treatment	Drug Transport at 2 h incubation (%)
AA free	10.29 \pm 0.15
AASLN	24.80 \pm 0.92
AANLC	26.20 \pm 0.58
RSPAASLN	35.11 \pm 0.38
RSPcAASLN	49.40 \pm 0.64
RSPAANLC	32.44 \pm 0.81
RSPcAANLC	42.90 \pm 0.41

Tests of Normality

Group Treatment	Kolmogorov-Smirnov ^a			Shapiro-Wilk		
	Statistic	Df	Sig.	Statistic	df	Sig.
AA free	.202	3	.	.994	3	.854
AASLN	.307	3	.	.903	3	.397
AANLC	.269	3	.	.949	3	.566
RSPAASLN	.343	3	.	.843	3	.222
RSPcAASLN	.262	3	.	.956	3	.599
RSPAANLC	.244	3	.	.971	3	.676
RSPcAANLC	.188	3	.	.998	3	.913

a. Lilliefors Significance Correction

Test of Homogeneity of Variances

Drug_transport			
Levene Statistic	df1	df2	Sig.
1.792	6	14	.173

ANOVA

Drug Transport					
	Sum of Squares	df	Mean Square	F	Sig.
Between Groups	2947.480	6	491.247	1326.718	.000
Within Groups	5.184	14	.370		
Total	2952.663	20			

Post Hoc Tests**Multiple Comparisons**

Drug Transport

Bonferroni

Group Treatment	Group Treatment	Mean Difference	Std. Error	Sig.	95% Confidence Interval	
					Lower Bound	Upper Bound
AA free	AASLN	-13.467*	.497	.000	-15.305	-11.629
	AANLC	-24.912*	.497	.000	-26.750	-23.074
	RSPAASLN	-38.376*	.497	.000	-40.214	-36.538
	RSPcAASLN	-16.543*	.497	.000	-18.381	-14.705
	RSPAANLC	-22.864*	.497	.000	-24.702	-21.026
	RSPcAANLC	-33.036*	.497	.000	-34.874	-31.198
AASLN	AA free	13.467*	.497	.000	11.629	15.305
	AANLC	-11.445*	.497	.000	-13.283	-9.607
	RSPAASLN	-24.909*	.497	.000	-26.747	-23.071
	RSPcAASLN	-3.076*	.497	.000	-4.914	-1.238
	RSPAANLC	-9.397*	.497	.000	-11.235	-7.560
	RSPcAANLC	-19.569*	.497	.000	-21.407	-17.731

Continue

Group Treatment	Group Treatment	Mean Difference	Std. Error	Sig.	95% Confidence Interval	
					Lower Bound	Upper Bound
AANLC	A free	24.912*	.497	.000	23.074	26.750
	AASLN	11.445*	.497	.000	9.607	13.283
	RSPAASLN	-13.464*	.497	.000	-15.302	-11.626
	RSPcAASLN	8.3694*	.497	.000	6.531	10.207
	RSPAANLC	2.048*	.497	.022	.210	3.886
	RSPcAANLC	-8.123*	.497	.000	-9.961	-6.286
RSPAASLN	A free	38.376*	.497	.000	36.538	40.214
	AASLN	24.909*	.497	.000	23.071	26.747
	AANLC	13.464*	.497	.000	11.626	15.302
	RSPcAASLN	21.833*	.497	.000	19.995	23.671
	RSPAANLC	15.512*	.497	.000	13.674	17.349
	RSPcAANLC	5.3402*	.497	.000	3.502	7.178
RSPcAASLN	AA free	16.543*	.497	.000	14.705	18.381
	AASLN	3.076*	.497	.000	1.238	4.9139
	AANLC	-8.369*	.497	.000	-10.207	-6.531
	RSPAASLN	-21.833*	.497	.000	-23.671	-19.995
	RSPAANLC	-6.321*	.497	.000	-8.159	-4.484
	RSPcAANLC	-16.493*	.497	.000	-18.331	-14.655
RSPAANLC	AA free	22.864*	.497	.000	21.026	24.702
	AASLN	9.397*	.497	.000	7.560	11.235
	AANLC	-2.0479*	.497	.022	-3.886	-.210
	RSPAASLN	-15.512*	.497	.000	-17.350	-13.674
	RSPcAASLN	6.3215*	.497	.000	4.484	8.159
	RSPcAANLC	-10.171*	.497	.000	-12.009	-8.333

Continue

Group Treatment	Group Treatment	Mean Difference	Std. Error	Sig.	95% Confidence Interval	
					Lower Bound	Upper Bound
RSPcAANLC	AA free	33.036*	.497	.000	31.198	34.874
	AASLN	19.569*	.497	.000	17.731	21.407
	AANLC	8.123*	.497	.000	6.286	9.961
	RSPAASLN	-5.340*	.497	.000	-7.178	-3.502
	RSPcAASLN	16.493*	.497	.000	14.655	18.3313
	RSPAANLC	10.171*	.497	.000	8.333	12.009

*. The mean difference is significant at the 0.05 level.



Permeability AA on Caco-2 cells (mean (n=3) \pm SD)

Treatment	Apparent Permeability (P_{app}) (cm/s)
AA free	5.19E-06 \pm 7.66E-08
AASLN	1.20E-05 \pm 4.76E-07
AANLC	1.36E-05 \pm 2.94E-07
RSPAASLN	1.78E-05 \pm 1.91E-07
RSPcAASLN	2.46E-05 \pm 3.22E-07
RSPAANLC	1.68E-05 \pm 4.11E-07
RSPcAANLC	2.19E-05 \pm 2.10E-07

Tests of Normality

Group Treatment	Kolmogorov-Smirnov ^a			Shapiro-Wilk		
	Statistic	df	Sig.	Statistic	df	Sig.
AA free	.176	3	.	1.000	3	.988
AASLN	.307	3	.	.903	3	.397
AANLC	.334	3	.	.859	3	.266
RSPAASLN	.302	3	.	.911	3	.421
RSPcAASLN	.262	3	.	.956	3	.598
RSPAANLC	.244	3	.	.971	3	.676
RSPcAANLC	.179	3	.	.999	3	.948

a. Lilliefors Significance Correction

Test of Homogeneity of Variances

Coefficient Permeability

Levene Statistic	df1	df2	Sig.
1.690	6	14	.196

ANOVA

Coefficient Permeability

	Sum of Squares	df	Mean Square	F	Sig.
Between Groups	.000	6	.000	2364.037	.000
Within Groups	.000	14	.000		
Total	.000	20			

Post Hoc Tests

Multiple Comparisons

Coefficient Permeability

Bonferroni

Group Treatment	Group Treatment	Mean Difference	Std. Error	Sig.	95% Confidence Interval	
					Lower Bound	Upper Bound
AA free	AASLN	-6.82708E-06*	2.567E-07	0.000	-7.78E-06	-5.88E-06
	AANLC	-.000011833510000*	2.567E-07	0.000	-1.28E-05	-1.09E-05
	RSPAASLN	-.000026900476667*	2.567E-07	0.000	-2.79E-05	-2.60E-05
	RSPcAASLN	-.000008382276667*	2.567E-07	0.000	-9.33E-06	-7.43E-06
	RSPAANLC	-.000011578343333*	2.567E-07	0.000	-1.25E-05	-1.06E-05
	RSPcAANLC	-.000019851010000*	2.567E-07	0.000	-2.08E-05	-1.89E-05
AASLN	AA free	.000006827076667*	2.567E-07	0.000	5.88E-06	7.78E-06
	AANLC	-.000005006433333*	2.567E-07	0.000	-5.96E-06	-4.06E-06
	RSPAASLN	-.000020073400000*	2.567E-07	0.000	-2.10E-05	-1.91E-05
	RSPcAASLN	-.000001555200000*	2.567E-07	0.001	-2.50E-06	-6.05E-07
	RSPAANLC	-.000004751266667*	2.567E-07	0.000	-5.70E-06	-3.80E-06
	RSPcAANLC	-.000013023933333*	2.567E-07	0.000	-1.40E-05	-1.21E-05
AANLC	AA free	.000011833510000*	2.567E-07	0.000	1.09E-05	1.28E-05
	AASLN	.000005006433333*	2.567E-07	0.000	4.06E-06	5.96E-06
	RSPAASLN	-.000015066966667*	2.567E-07	0.000	-1.60E-05	-1.41E-05
	RSPcAASLN	.000003451233333*	2.567E-07	0.000	2.50E-06	4.40E-06
	RSPAANLC	2.55167E-07*	2.567E-07	1.000	-6.95E-07	1.20E-06
	RSPcAANLC	-.000008017500000*	2.567E-07	0.000	-8.97E-06	-7.07E-06

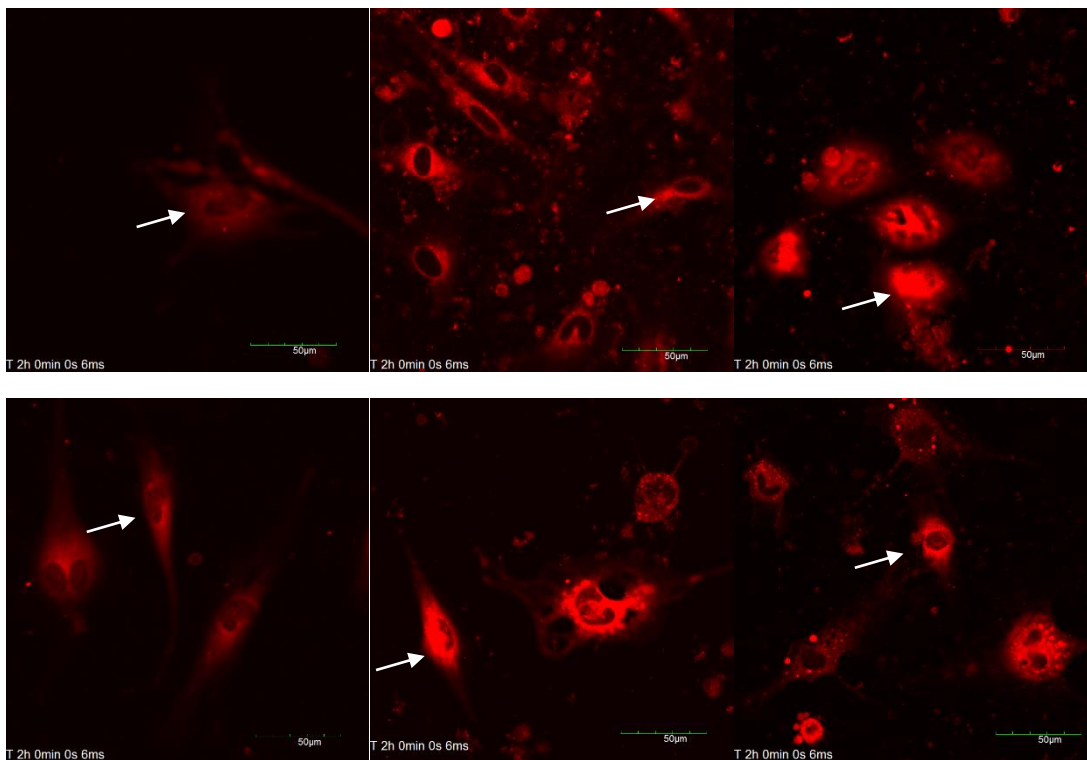
Continue

Group Treatment	Group Treatment	Mean Difference	Std. Error	Sig.	95% Confidence Interval	
					Lower Bound	Upper Bound
RSPAASLN	AA free	.000026900476667*	2.567E-07	0.000	2.60E-05	2.79E-05
	AASLN	.00002007340000*	2.567E-07	0.000	1.91E-05	2.10E-05
	AANLC	.000015066966667*	2.567E-07	0.000	1.41E-05	1.60E-05
	RSPcAASLN	.00001851820000*	2.567E-07	0.000	1.76E-05	1.95E-05
	RSPAANLC	.000015322133333*	2.567E-07	0.000	1.44E-05	1.63E-05
	RSPcAANLC	.000007049466667*	2.567E-07	0.000	6.10E-06	8.00E-06
RSPcAASLN	AA free	.000008382276667*	2.567E-07	0.000	7.43E-06	9.33E-06
	AASLN	.00000155520000*	2.567E-07	0.001	6.05E-07	2.50E-06
	AANLC	-.000003451233333*	2.567E-07	0.000	-4.40E-06	-2.50E-06
	RSPAASLN	-.00001851820000*	2.567E-07	0.000	-1.95E-05	-1.76E-05
	RSPAANLC	-.000003196066667*	2.567E-07	0.000	-4.15E-06	-2.25E-06
	RSPcAANLC	-.000011468733333*	2.567E-07	0.000	-1.24E-05	-1.05E-05
RSPAANLC	AA free	.000011578343333*	2.567E-07	0.000	1.06E-05	1.25E-05
	AASLN	.000004751266667*	2.567E-07	0.000	3.80E-06	5.70E-06
	AANLC	-2.55167E-07	2.567E-07	1.000	-1.20E-06	6.95E-07
	RSPAASLN	-.000015322133333*	2.567E-07	0.000	-1.63E-05	-1.44E-05
	RSPcAASLN	.000003196066667*	2.567E-07	0.000	2.25E-06	4.15E-06
	RSPcAANLC	-.000008272666667*	2.567E-07	0.000	-9.22E-06	-7.32E-06
RSPcAANLC	AA free	.000019851010000*	2.567E-07	0.000	1.89E-05	2.08E-05
	AASLN	.000013023933333*	2.567E-07	0.000	1.21E-05	1.40E-05
	AANLC	.00000801750000*	2.567E-07	0.000	7.07E-06	8.97E-06
	RSPAASLN	-.000007049466667*	2.567E-07	0.000	-8.00E-06	-6.10E-06
	RSPcAASLN	.000011468733333*	2.567E-07	0.000	1.05E-05	1.24E-05
	RSPAANLC	.000008272666667*	2.567E-07	0.000	7.32E-06	9.22E-06

*. The mean difference is significant at the 0.05 level

Uptake Drug Study on Caco-2 cells (mean n=3±SD)

Formulation	Drug uptake ($\mu\text{g}/\text{cm}^2$)
AA Free	$5.30\text{E-}07\pm 1.85\text{E-}07$
AASLN	$6.56\text{E-}07\pm 1.39\text{E-}07$
RSPAASLN	$8.51\text{E-}07\pm 2.27\text{E-}08$
RSPcAASLN	$7.90\text{E-}07\pm 3.69\text{E-}08$
AANLC	$7.25\text{E-}07\pm 4.33\text{E-}08$
RSPAANLC	$8.89\text{E-}07\pm 4.547\text{E-}08$
RSPcAANLC	$8.24\text{E-}07\pm 1.947\text{E-}08$



Confocal Laser Scanning Microscopy (CLSM) study of R6gSLN, RSPR6gSLN, RSPcR6gSLN (first row), R6gNLC, RSPR6gNLC and RSPcR6gNLC (second row) on bEnd3 cells at 2h incubation. Intracellular localization of R6g fluorescence was noted (arrow)

Drug Transport on bEnd3 cells cocultured with CTX-TNA2 cells (mean (n=3)±SD)

Formulation	Drug Transport (%)
AA Free	24.60 ± 2.48
AASLN	38.46 ± 2.37
RSPAASLN	32.64 ± 3.59
RSPcAASLN	47.26 ± 1.78
AANLC	54.31 ± 7.08
RSPAANLC	48.45 ± 3.88
RSPcAANLC	56.64 ± 1.46

Tests of Normality

Group Treatment	Kolmogorov-Smirnov ^a			Shapiro-Wilk		
	Statistic	Df	Sig.	Statistic	df	Sig.
AA Free	.323	3	.	.878	3	.318
AASLN	.314	3	.	.893	3	.362
RSPAASLN	.341	3	.	.847	3	.233
RSPcAASLN	.178	3	.	1.000	3	.959
AANLC	.270	3	.	.949	3	.564
RSPAANLC	.306	3	.	.904	3	.399
RSPcAANLC	.181	3	.	.999	3	.939

a. Lilliefors Significance Correction

Test of Homogeneity of Variances

Drug Transport			
Levene Statistic	df1	df2	Sig.
2.245	6	14	.100

ANOVA

Drug Transport					
	Sum of Squares	df	Mean Square	F	Sig.
Between Groups	2399.163	6	399.860	429.963	.000
Within Groups	13.020	14	.930		
Total	2412.183	20			

Post Hoc Tests

Multiple Comparisons

Drug Transport

Bonferroni

Group Treatment	Group Treatment	Mean Difference	Std. Error	Sig.	95% Confidence Interval	
					Lower Bound	Upper Bound
AA free	AASLN	-13.587*	.787	.000	-16.500	-10.674
	AANLC	-22.394*	.787	.000	-25.307	-19.481
	RSPAASLN	-29.214*	.787	.000	-32.127	-26.301
	RSPcAASLN	-7.291*	.787	.000	-10.203	-4.378
	RSPAANLC	-21.541*	.787	.000	-24.454	-18.628
	RSPcAANLC	-31.564*	.787	.000	-34.477	-28.651
AASLN	AA free	13.587*	.787	.000	10.674	16.500
	AANLC	-8.807*	.787	.000	-11.720	-5.894
	RSPAASLN	-15.627*	.787	.000	-18.540	-12.715
	RSPcAASLN	6.296*	.787	.000	3.384	9.209
	RSPAANLC	-7.954*	.787	.000	-10.867	-5.041
	RSPcAANLC	-17.977*	.787	.000	-20.890	-15.064

Continue

Group Treatment	Group Treatment	Mean Difference	Std. Error	Sig.	95% Confidence Interval	
					Lower Bound	Upper Bound
AANLC	AA free	22.394*	.787	.000	19.481	25.307
	AASLN	8.807*	.787	.000	5.894	11.720
	RSPAASLN	-6.820*	.787	.000	-9.733	-3.907
	RSPcAASLN	15.104*	.787	.000	12.191	18.016
	RSPAANLC	.853	.787	1.000	-2.060	3.766
	RSPcAANLC	-9.170*	.787	.000	-12.082	-6.257
RSPAASLN	AA free	29.214*	.787	.000	26.301	32.127
	AASLN	15.627*	.787	.000	12.715	18.540
	AANLC	6.820*	.787	.000	3.907	9.733
	RSPcAASLN	21.924*	.787	.000	19.011	24.836
	RSPAANLC	7.673*	.787	.000	4.761	10.586
	RSPcAANLC	-2.349	.787	.207	-5.262	.563
RSPcAASLN	AA free	7.291*	.787	.000	4.378	10.203
	AASLN	-6.296*	.787	.000	-9.209	-3.384
	AANLC	-15.104*	.787	.000	-18.016	-12.191
	RSPAASLN	-21.924*	.787	.000	-24.836	-19.011
	RSPAANLC	-14.250*	.787	.000	-17.163	-11.338
	RSPcAANLC	-24.273*	.787	.000	-27.186	-21.360

Continue

Group Treatment	Group Treatment	Mean Difference	Std. Error	Sig.	95% Confidence Interval	
					Lower Bound	Upper Bound
RSPAANLC	AA free	21.541*	.787	.000	18.628	24.454
	AASLN	7.954*	.787	.000	5.041	10.867
	AANLC	-.853	.787	1.000	-3.766	2.056
	RSPAASLN	-7.673*	.787	.000	-10.586	-4.761
	RSPcAASLN	14.250*	.787	.000	11.338	17.163
	RSPcAANLC	-10.023*	.787	.000	-12.936	-7.110
RSPcAANLC	AA free	31.564*	.787	.000	28.651	34.476
	AASLN	17.977*	.787	.000	15.064	20.890
	AANLC	9.1696*	.787	.000	6.257	12.082
	RSPAASLN	2.349	.787	.207	-.563	5.262
	RSPcAASLN	24.273*	.787	.000	21.360	27.186
	RSPAANLC	10.023*	.787	.000	7.110	12.936

*. The mean difference is significant at the 0.05 level.

Permeability AA on bEnd3 cells cocultured with CTX-TNA2 cells (mean (n=3)±SD)

Formulation	Apparent Permeability (P_{app}) (cm/s)
AA Free	1.27E-05±4.41E-07
AASLN	1.94E-05±2.80E-07
AANLC	1.64E-05±1.26E-07
RSPAASLN	2.40E-05±1.56E-07
RSPcAASLN	2.74E-05±3.66E-07
RSPAANLC	2.36E-05±8.18E-07
RSPcAANLC	2.86E-05±7.39E-07

Test of Normality

Group Treatment	Kolmogorov-Smirnov ^a			Shapiro-Wilk		
	Statistic	Df	Sig.	Statistic	Df	Sig.
AA free	.323	3	.	.878	3	.318
AASLN	.305	3	.	.905	3	.403
AANLC	.341	3	.	.847	3	.234
RSPAASLN	.178	3	.	1.000	3	.960
RSPcAASLN	.270	3	.	.949	3	.564
RSPAANLC	.306	3	.	.904	3	.399
RSPcAANLC	.181	3	.	.999	3	.939

a. Lilliefors Significance Correction

Test of Homogeneity of Variances

Coefficient Permeability

Levene Statistic	df1	df2	Sig.
2.220	6	14	.103

ANOVA

Coefficient Permeability

	Sum of Squares	Df	Mean Square	F	Sig.
Between Groups	.000	6	.000	417.767	.000
Within Groups	.000	14	.000		
Total	.000	20			



Post Hoc Tests

Multiple Comparisons

Coefficient Permeability

Bonferroni

Group Treatment	Group Treatment	Mean Difference	Std. Error	Sig.	95% Confidence Interval	
					Lower Bound	Upper Bound
AA free	AASLN	-.0000084*	3.99E-07	.000	-9.89E-06	-6.94E-06
	AANLC	-.0000113*	3.99E-07	.000	-1.28E-05	-9.85E-06
	RSPAASLN	-.0000148*	3.99E-07	.000	-1.62E-05	-1.33E-05
	RSPcAASLN	-.0000037*	3.99E-07	.000	-5.16E-06	-2.21E-06
	RSPAANLC	-.0000109*	3.99E-07	.000	-1.24E-05	-9.41E-06
	RSPcAANLC	-.0000156*	3.99E-07	.000	-1.74E-05	-1.45E-05
AASLN	AA free	.00000842*	3.99E-07	.000	6.94E-06	9.89E-06
	AANLC	-.00000290*	3.99E-07	.000	-4.38E-06	-1.43E-06
	RSPAASLN	-.00000635*	3.99E-07	.000	-7.83E-06	-4.88E-06
	RSPcAASLN	.00000473*	3.99E-07	.000	3.26E-06	6.21E-06
	RSPAANLC	-.00000247*	3.99E-07	.000	-3.95E-06	-9.97E-07
	RSPcAANLC	-.00000754*	3.99E-07	.000	-9.02E-06	-6.06E-06
AANLC	AA free	.0000113*	3.99E-07	.000	9.85E-06	1.28E-05
	AASLN	.0000029*	3.99E-07	.000	1.43E-06	4.38E-06
	RSPAASLN	-.0000034*	3.99E-07	.000	-4.92E-06	-1.97E-06
	RSPcAASLN	.0000076*	3.99E-07	.000	6.16E-06	9.11E-06
	RSPAANLC	.0000004	3.99E-07	1.000	-1.05E-06	1.91E-06
	RSPcAANLC	-.0000046*	3.99E-07	.000	-6.11E-06	-3.16E-06

Continue

Group Treatment	Group Treatment	Mean Difference	Std. Error	Sig.	95% Confidence Interval	
					Lower Bound	Upper Bound
RSPAASLN	AA free	.0000148*	3.99E-07	.000	1.33E-05	1.62E-05
	AASLN	.0000064*	3.99E-07	.000	4.88E-06	7.83E-06
	AANLC	.0000034*	3.99E-07	.000	1.97E-06	4.92E-06
	RSPcAASLN	.0000111*	3.99E-07	.000	9.61E-06	1.26E-05
	RSPAANLC	.0000039*	3.99E-07	.000	2.40E-06	5.36E-06
	RSPcAANLC	-.0000012	3.99E-07	.210	-2.66E-06	2.89E-07
RSPcAASLN	AA free	.0000037*	3.99E-07	.000	2.21E-06	5.16E-06
	AASLN	-.0000047*	3.99E-07	.000	-6.21E-06	-3.26E-06
	AANLC	-.0000076*	3.99E-07	.000	-9.11E-06	-6.16E-06
	RSPAASLN	-.0000111*	3.99E-07	.000	-1.26E-05	-9.61E-06
	RSPAANLC	-.0000072*	3.99E-07	.000	-8.68E-06	-5.73E-06
	RSPcAANLC	-.0000123*	3.99E-07	.000	-1.37E-05	-1.08E-05
RSPAANLC	AA free	.0000109*	3.99E-07	.000	9.41E-06	1.24E-05
	AASLN	.0000025*	3.99E-07	.000	9.97E-07	3.95E-06
	AANLC	-.0000004	3.99E-07	1.000	-1.91E-06	1.05E-06
	RSPAASLN	-.0000039*	3.99E-07	.000	-5.36E-06	-2.40E-06
	RSPcAASLN	.0000072*	3.99E-07	.000	5.73E-06	8.68E-06
	RSPcAANLC	-.0000051*	3.99E-07	.000	-6.54E-06	-3.59E-06
RSPcAANLC	AA free	.0000160*	3.99E-07	.000	1.45E-05	1.74E-05
	AASLN	.0000075*	3.99E-07	.000	6.06E-06	9.02E-06
	AANLC	.0000046*	3.99E-07	.000	3.16E-06	6.11E-06
	RSPAASLN	.0000012	3.99E-07	.210	-2.89E-07	2.66E-06
	RSPcAASLN	.0000123*	3.99E-07	.000	1.08E-05	1.37E-05
	RSPAANLC	.0000051*	3.99E-07	.000	3.59E-06	6.54E-06

*. The mean difference is significant at the 0.05 level.

Drug Uptake of AA on bEnd3 cells cocultured with CTX-TNA2 cells (mean (n=3)±SD)

Formulation	Drug uptake (mg/cm ²)
AA Free	2.63E-05±1.08E-05
AASLN	4.18E-05±5.60E-06
RSPAASLN	4.78E-05±3.81E-06
RSPcAASLN	6.13E-05±8.10E-06
AANLC	6.68E-06±7.05E-06
RSPAANLC	6.20E-05±5.70E-06
RSPcAANLC	6.34E-05±1.16E-05

Tests of Normality

Group Treatment	Kolmogorov-Smirnov ^a			Shapiro-Wilk		
	Statistic	df	Sig.	Statistic	df	Sig.
AA free	.323	3	.	.878	3	.318
AASLN	.314	3	.	.893	3	.362
AANLC	.341	3	.	.847	3	.233
RSPAASLN	.178	3	.	1.000	3	.959
RSPcAASLN	.270	3	.	.949	3	.564
RSPAANLC	.306	3	.	.904	3	.399
RSPCANLC	.181	3	.	.999	3	.939

Tests of Normality

Group Treatment	Kolmogorov-Smirnov ^a			Shapiro-Wilk		
	Statistic	df	Sig.	Statistic	df	Sig.
AA free	.323	3	.	.878	3	.318
AASLN	.314	3	.	.893	3	.362
AANLC	.341	3	.	.847	3	.233
RSPAASLN	.178	3	.	1.000	3	.959
RSPcAASLN	.270	3	.	.949	3	.564
RSPAANLC	.306	3	.	.904	3	.399
RSPCANLC	.181	3	.	.999	3	.939

a. Lilliefors Significance Correction

Test of Homogeneity of Variances

Drug Transport

Levene Statistic	df1	df2	Sig.
2.245	6	14	.100

ANOVA

Drug Transport

	Sum of Squares	df	Mean Square	F	Sig.
Between Groups	2399.163	6	399.860	429.963	.000
Within Groups	13.020	14	.930		
Total	2412.183	20			

Post Hoc Tests

Multiple Comparisons

Drug Transport

Bonferroni

Group Treatment	Group Treatment	Mean Difference	Std. Error	Sig.	95% Confidence Interval	
					Lower Bound	Upper Bound

AA free	AASLN	-13.587*	.787	.000	-16.500	-10.674
	AANLC	-22.394*	.787	.000	-25.307	-19.481
	RSPAASLN	-29.214*	.787	.000	-32.127	-26.301
	RSPcAASLN	-7.291*	.787	.000	-10.203	-4.378
	RSPAANLC	-21.541*	.787	.000	-24.454	-18.628
	RSPcAANLC	-31.564*	.787	.000	-34.476	-28.651
AASLN	AA free	13.587*	.787	.000	10.674	16.4996
	AANLC	-8.807*	.787	.000	-11.720	-5.8945
	RSPAASLN	-15.627*	.787	.000	-18.540	-12.7147
	RSPcAASLN	6.296*	.787	.000	3.384	9.2090
	RSPAANLC	-7.954*	.787	.000	-10.867	-5.0413
	RSPcAANLC	-17.977*	.787	.000	-20.890	-15.0641

Continue

Group Treatment	Group Treatment	Mean Difference	Std. Error	Sig.	95% Confidence Interval	
					Lower Bound	Upper Bound
AANLC	AA free	22.394*	.787	.000	19.481	25.307
	AASLN	8.807*	.787	.000	5.894	11.720
	RSPAASLN	-6.820*	.787	.000	-9.733	-3.907
	RSPcAASLN	15.104*	.787	.000	12.191	18.016
	RSPAANLC	.853	.787	1.000	-2.060	3.766
	RSPcAANLC	-9.170*	.787	.000	-12.082	-6.257
RSPAASLN	AA free	29.214*	.787	.000	26.301	32.127
	AASLN	15.627*	.787	.000	12.715	18.540
	AANLC	6.820*	.787	.000	3.907	9.733
	RSPcAASLN	21.924*	.787	.000	19.011	24.836

	RSPAANLC	7.67334*	.787	.000	4.761	10.586
	RSPcAANLC	-2.349	.787	.207	-5.262	.563
RSPcAASLN	AA free	7.291*	.787	.000	4.378	10.203
	AASLN	-6.296*	.787	.000	-9.209	-3.384
	AANLC	-15.104*	.787	.000	-18.016	-12.191
	RSPAASLN	-21.924*	.787	.000	-24.836	-19.011
	RSPAANLC	-14.250*	.787	.000	-17.163	-11.338
	RSPcAANLC	-24.273*	.787	.000	-27.186	-21.360

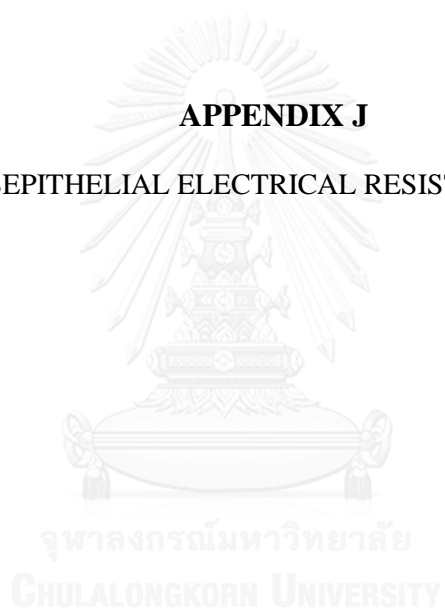


Group Treatment	Group Treatment	Mean Difference	Std. Error	Sig.	95% Confidence Interval	
					Lower Bound	Upper Bound
RSPAANLC	AA free	21.541*	.787	.000	18.628	24.454
	AASLN	7.954*	.787	.000	5.041	10.867
	AANLC	-.853	.787	1.000	-3.766	2.060
	RSPAASLN	-7.673*	.787	.000	-10.586	-4.761
	RSPcAASLN	14.250*	.787	.000	11.338	17.163
	RSPcAANLC	-10.023*	.787	.000	-12.936	-7.110
RSPcAANLC	AA free	31.564*	.787	.000	28.651	34.476
	AASLN	17.977*	.787	.000	15.064	20.890
	AANLC	9.170*	.787	.000	6.257	12.082
	RSPAASLN	2.349	.787	.207	-.563	5.262
	RSPcAASLN	24.273*	.787	.000	21.360	27.186
	RSPAANLC	10.023*	.787	.000	7.110	12.936

*. The mean difference is significant at the 0.05 level.

APPENDIX J

TRANSEPITHELIAL ELECTRICAL RESISTANCE (TEER)



Decrease of TEER value on Caco-2 cells (mean (n=3) \pm SD)

Treatment	Percentage TEER decrease at 2 h (%)
Control	96.97 \pm 0.51
AA free	83.75 \pm 3.98
AASLN	92.21 \pm 2.41
AANLC	93.74 \pm 2.53
RSPAASLN	59.79 \pm 6.36
RSPcAASLN	39.25 \pm 4.32
RSPAANLC	56.48 \pm 3.00
RSPcAANLC	47.19 \pm 5.37

Tests of Normality

Group Treatment	Kolmogorov-Smirnov ^a			Shapiro-Wilk		
	Statistic	df	Sig.	Statistic	df	Sig.
Control	.313	3	.	.895	3	.368
AA free	.310	3	.	.899	3	.382
AASLN	.199	3	.	.995	3	.866
AANLC	.249	3	.	.968	3	.654
RSPAASLN	.311	3	.	.897	3	.377
RSPcAASLN	.196	3	.	.996	3	.877
RSPAANLC	.177	3	.	1.000	3	.963
RSPcAANLC	.247	3	.	.969	3	.662

a. Lilliefors Significance Correction

Test of Homogeneity of Variances

TEER				
Levene Statistic	df1	df2	Sig.	
1.525	7	16	.229	

ANOVA

TEER					
	Sum of Squares	df	Mean Square	F	Sig.
Between Groups	9926.137	7	1418.020	124.082	.000
Within Groups	182.849	16	11.428		
Total	10108.986	23			

Post Hoc Tests

Multiple Comparisons

TEER

Bonferroni

Group Treatment	Group Treatment	Mean Difference	Std. Error	Sig.	95% Confidence Interval	
					Lower Bound	Upper Bound
Control	AA free	6.566	2.760	.845	-3.757	16.888
	AASLN	-4.541	2.760	1.000	-14.864	5.781
	AANLC	-3.226	2.760	1.000	-13.549	7.097
	RSPAASLN	8.991	2.760	.138	-1.331	19.314
	RSPcAASLN	53.232*	2.760	.000	42.909	63.555
	RSPAANLC	18.031*	2.760	.000	7.708	28.353
	RSPcAANLC	43.145*	2.760	.000	32.823	53.468
AA free	AA free	-6.566	2.760	.845	-16.888	3.757
	AASLN	-11.107*	2.760	.027	-21.430	-.784
	AANLC	-9.792	2.760	.075	-20.114	.531
	RSPAASLN	2.425	2.760	1.000	-7.897	12.748
	RSPcAASLN	46.666*	2.760	.000	36.344	56.989
	RSPAANLC	11.465*	2.760	.021	1.142	21.787
	RSPcAANLC	36.579*	2.760	.000	26.257	46.902

Continue

Group Treatment	Group Treatment	Mean Difference	Std. Error	Sig.	95% Confidence Interval	
					Lower Bound	Upper Bound
AASLN	AA free	4.541	2.760	1.000	-5.7814	14.864
	AASLN	11.107*	2.760	.027	.7845	21.430
	AANLC	1.315	2.760	1.000	-9.0074	11.638
	RSPAASLN	13.533*	2.760	.004	3.2099	23.855
	RSPcAASLN	57.773*	2.760	.000	47.4507	68.096
	RSPAANLC	22.572*	2.760	.000	12.2491	32.894
	RSPcAANLC	47.686*	2.760	.000	37.3639	58.009
AANLC	AA free	3.226	2.760	1.000	-7.0966	13.549
	AASLN	9.792	2.760	.075	-.5308	20.114
	AANLC	-1.315	2.760	1.000	-11.6380	9.007
	RSPAASLN	12.217*	2.760	.012	1.8947	22.540
	RSPcAASLN	56.458*	2.760	.000	46.1354	66.781
	RSPAANLC	21.256*	2.760	.000	10.9339	31.579
	RSPcAANLC	46.371*	2.760	.000	36.0486	56.694
RSPAASLN	AA free	-8.991	2.760	.138	-19.3140	1.331
	AASLN	-2.425	2.760	1.000	-12.7481	7.897
	AANLC	-13.533*	2.760	.004	-23.8553	-3.210
	RSPAASLN	-12.217*	2.760	.012	-22.5400	-1.85
	RSPcAASLN	44.241*	2.760	.000	33.9181	54.563
	RSPAANLC	9.039	2.760	.133	-1.2835	19.362
	RSPcAANLC	34.154*	2.760	.000	23.8313	44.477

Continue

Group Treatment	Group Treatment	Mean Difference	Std. Error	Sig.	95% Confidence Interval	
					Lower Bound	Upper Bound
RSPcAASLN	AA free	-53.232*	2.760	.000	-63.555	-42.909
	AASLN	-46.666*	2.760	.000	-56.989	-36.344
	AANLC	-57.773*	2.760	.000	-68.096	-47.451
	RSPAASLN	-56.458*	2.760	.000	-66.781	-46.135
	RSPcAASLN	-44.241*	2.760	.000	-54.563	-33.918
	RSPAANLC	-35.202*	2.760	.000	-45.524	-24.879
	RSPcAANLC	-10.087	2.760	.060	-20.410	.236
RSPAANLC	AA free	-18.031*	2.760	.000	-28.353	-7.708
	AASLN	-11.465*	2.760	.021	-21.787	-1.142
	AANLC	-22.572*	2.760	.000	-32.894	-12.249
	RSPAASLN	-21.256*	2.760	.000	-31.579	-10.934
	RSPcAASLN	-9.039	2.760	.133	-19.362	1.284
	RSPAANLC	35.202*	2.760	.000	24.879	45.524
	RSPcAANLC	25.115*	2.760	.000	14.792	35.437
RSPcAANLC	AA free	-43.145*	2.760	.000	-53.468	-32.823
	AASLN	-36.579*	2.760	.000	-46.902	-26.257
	AANLC	-47.686*	2.760	.000	-58.009	-37.364
	RSPAASLN	-46.371*	2.760	.000	-56.694	-36.049
	RSPcAASLN	-34.154*	2.760	.000	-44.477	-23.831
	RSPAANLC	10.087	2.760	.060	-.236	20.410
	RSPcAANLC	-25.115*	2.760	.000	-35.437	-14.792

*. The mean difference is significant at the 0.05 level.

TEER value on bEnd3 cells cocultured with CTX-TNA2 cells (mean (n=3)±SD)

Treatment	TEER ($\Omega \cdot \text{cm}^2$)	
	0 h	6 h
Control	418.00±31.19	420.67±24.13
AA Free	441.33±20.03	373.67±6.51
AASLN	466.67±36.02	400.33±17.89
AANLC	449.67±31.09	384.00±42.15
RSPAASLN	451.33±29.14	407.33±11.01
RSPcAASLN	628.67±44.66	542.67±15.28
RSP-AANLC	487.33±14.05	388.67±9.02
RSPcAANLC	449.00±23.52	288.67±11.59

Paired Samples Statistics

		Mean	N	Std. Deviation	Std. Error Mean
Pair 1	TEER at T ₀	474.0000	24	67.47818	13.77393
	TEER at T ₆	383.1667	24	68.28945	13.93953

Paired Samples Correlations

		N	Correlation	Sig.
Pair 1	TEER at T ₀ & TEER at T ₆	24	.716	.000

Paired Samples Test

	Paired Differences					t	df	Sig. (2-tailed)
	Mean	Std. Deviation	Std. Error Mean	95% Confidence Interval of the Difference				
				Lower	Upper			
				Difference				
TEER T ₀ – TEER T ₃₆₀	90.833	51.196	10.450	69.215	112.451	8.692	23	.000



TEER value change on bEnd3 cells cocultured with CTX-TNA2 cells (mean $n=3\pm SD$)

Treatment	Percentage TEER change at 2 h (%)
Control	100.80 \pm 5.41
AA Free	84.80 \pm 4.79
AASLN	85.93 \pm 3.15
AANLC	85.44 \pm 8.16
RSPAASLN	90.40 \pm 3.88
RSPcAASLN	86.67 \pm 7.72
RSPAANLC	79.76 \pm 0.44
RSPcAANLC	64.49 \pm 5.95

Tests of Normality

Group Treatment	Kolmogorov-Smirnov ^a			Shapiro-Wilk		
	Statistic	Df	Sig.	Statistic	df	Sig.
1.00	.175	3	.	1.000	3	.998
2.00	.282	3	.	.936	3	.510
3.00	.274	3	.	.945	3	.547
4.00	.337	3	.	.854	3	.250
5.00	.362	3	.	.804	3	.124
6.00	.344	3	.	.841	3	.218
7.00	.326	3	.	.873	3	.304
8.00	.209	3	.	.992	3	.825

a. Lilliefors Significance Correction

Test of Homogeneity of Variances

TEER				
Levene Statistic	df1	df2	Sig.	
1.796	7	16	.157	

ANOVA

TEER						
	Sum of Squares	df	Mean Square	F	Sig.	
Between Groups	2339.981	7	334.283	17.889	.000	
Within Groups	298.986	16	18.687			
Total	2638.967	23				

Post Hoc Tests**Multiple Comparisons**

TEER						
Bonferroni						
Group Treatment	Group Treatment	Mean Difference	Std. Error	Sig.	95% Confidence Interval	
					Lower Bound	Upper Bound
Control	AA free	15.804*	3.530	.011	2.604	29.004
	AASLN	14.177*	3.530	.028	.977	27.377
	AANLC	14.278*	3.530	.026	1.078	27.478
	RSPAASLN	15.960*	3.530	.010	2.760	29.160
	RSPcAASLN	14.080*	3.530	.030	.880	27.280
	RSPAANLC	27.357*	3.530	.000	14.157	40.557
	RSPcAANLC	35.911*	3.530	.000	22.711	49.111
AA free	AA free	-15.804*	3.530	.011	-29.004	-2.604
	AASLN	-1.627	3.530	1.000	-14.827	11.573
	AANLC	-1.526	3.530	1.000	-14.726	11.674
	RSPAASLN	.1555	3.530	1.000	-13.044	13.355
	RSPcAASLN	-1.724	3.530	1.000	-14.924	11.476
	RSPAANLC	11.553	3.530	.134	-1.647	24.753
	RSPcAANLC	20.106*	3.530	.001	6.907	33.306

Continue

Group Treatment	Group Treatment	Mean Difference	Std. Error	Sig.	95% Confidence Interval	
					Lower Bound	Upper Bound
AASLN	Control	-14.177*	3.530	.028	-27.377	-.977
	AA free	1.6270	3.530	1.000	-11.573	14.827
	AANLC	.1013	3.530	1.000	-13.099	13.301
	RSPAASLN	1.782	3.530	1.000	-11.418	14.982
	RSPcAASLN	-.097	3.530	1.000	-13.297	13.103
	RSPAANLC	13.180	3.530	.051	-.020	26.380
	RSPcAANLC	21.734*	3.530	.000	8.534	34.933
AANLC	Control	-14.278*	3.530	.026	-27.478	-1.078
	AA free	1.526	3.530	1.000	-11.674	14.726
	AASLN	-.101	3.530	1.000	-13.301	13.099
	RSPAASLN	1.681	3.530	1.000	-11.519	14.881
	RSPcAASLN	-.198	3.530	1.000	-13.398	13.001
	RSPAANLC	13.079	3.530	.054	-.121	26.279
	RSPcAANLC	21.632*	3.530	.000	8.432	34.832
RSPAASLN	Control	-15.960*	3.530	.010	-29.160	-2.760
	AA free	-.155	3.530	1.000	-13.355	13.044
	AASLN	-1.782	3.530	1.000	-14.982	11.418
	AANLC	-1.681	3.530	1.000	-14.881	11.519
	RSPcAASLN	-1.880	3.530	1.000	-15.080	11.320
	RSPAANLC	11.398	3.530	.147	-1.802	24.598
	RSPcAANLC	19.951*	3.530	.001	6.751	33.151

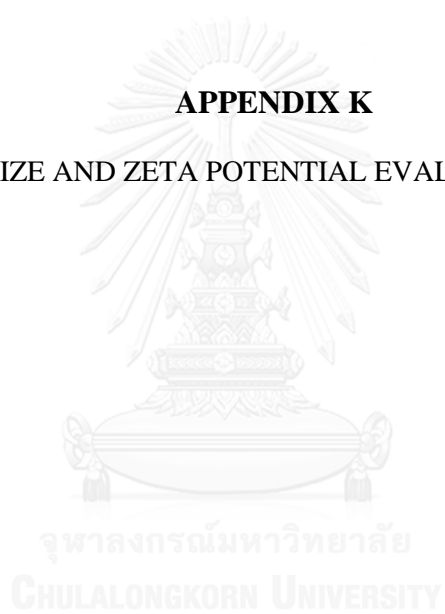
Continue

Group Treatment	Group Treatment	Mean Difference	Std. Error	Sig.	95% Confidence Interval	
					Lower Bound	Upper Bound
RSPcAASLN	Control	-14.080*	3.530	.030	-27.280	-.880
	AA free	1.724	3.530	1.000	-11.476	14.924
	AASLN	.097	3.530	1.000	-13.103	13.297
	AANLC	.198	3.530	1.000	-13.001	13.398
	RSPAASLN	1.880	3.530	1.000	-11.320	15.080
	RSPAANLC	13.277*	3.530	.048	.077	26.477
	RSPcAANLC	21.831*	3.530	.000	8.631	35.031
RSPAANLC	Control	-27.357*	3.530	.000	-40.557	-14.157
	AA free	-11.553	3.530	.134	-24.753	1.647
	AASLN	-13.180	3.530	.051	-26.380	.020
	AANLC	-13.079	3.530	.054	-26.279	.121
	RSPAASLN	-11.398	3.530	.147	-24.598	1.802
	RSPcAASLN	-13.277*	3.530	.048	-26.477	-.077
	RSPcAANLC	8.553	3.530	.773	-4.646	21.753
RSPcAANLC	Control	-35.911*	3.530	.000	-49.111	-22.711
	AA free	-20.107*	3.530	.001	-33.306	-6.907
	AASLN	-21.734*	3.530	.000	-34.933	-8.534
	AANLC	-21.632*	3.530	.000	-34.832	-8.432
	RSPAASLN	-19.951*	3.530	.001	-33.151	-6.751
	RSPcAASLN	-21.831*	3.530	.000	-35.031	-8.631
	RSPAANLC	-8.554	3.530	.773	-21.753	4.647

*. The mean difference is significant at the 0.05 level.

APPENDIX K

SIZE AND ZETA POTENTIAL EVALUATION



Sample	Size (d.nm)	PdI	Zeta Potential
AASLNapicalsite1	123.1	0.369	-5.96
AASLNapicalsite2	129.9	0.438	-7.07
AASLNapicalsite3	126.9	0.432	-6.85
AASLNapicalsite4	122.1	0.396	-5.93
AASLNapicalsite5	115.1	0.426	-6.05
Mean	123.42	0.4122	-6.372
SD	5.59392528	0.029055	0.544169091
AANLCapicalsite1	151.3	0.489	-5.8
AANLCapicalsite2	148.4	0.484	-6.25
AANLCapicalsite3	148.3	0.476	-7.11
AANLCapicalsite4	145.8	0.485	-6.11
AANLCapicalsite5	150	0.483	-5.53
Mean	148.76	0.4834	-6.16
SD	2.06712361	0.004722	0.599916661
RSPAASLN-apicalsite1	414.2	0.362	-16.9
RSPAASLN-apicalsite2	427.5	0.261	-14.9
RSPAASLN-apicalsite3	467.6	0.42	-17.8
RSPAASLN-apicalsite4	477.8	0.526	-17.6
RSPAASLN-apicalsite5	434.3	0.589	-17.4
Mean	444.28	0.4316	-16.92
SD	27.1725413	0.130163	1.177709642
RSPcAASLN-apicalsite1	583.9	0.388	42.6
RSPcAASLN-apicalsite2	545.3	0.336	39.3
RSPcAASLN-apicalsite3	467.7	0.355	42.7
RSPcAASLN-apicalsite4	495.4	0.407	42.3
RSPcAASLN-apicalsite5	544.7	0.343	41.3
Mean	527.4	0.3658	41.64
SD	45.8258661	0.030475	1.420563269
RSPAANLC-picalsite1	380.3	0.416	-19.3
RSPAANLC-apicalsite2	370.8	0.414	-16.9
RSPAANLC-apicalsite3	424.8	0.387	-15.3
RSPAANLC-apicalsite4	387.9	0.367	-14.8
RSPAANLC-apicalsite5	435.1	0.398	-17.2
Mean	399.78	0.3964	-16.7
SD	28.4339058	0.020305	1.776231967
RSPcAANLC-picalsite1	596.2	0.383	31.8
RSPcAANLC-apicalsite2	545.1	0.391	33.9
RSPcAANLC-apicalsite3	505.3	0.458	32.1
RSPcAANLC-apicalsite4	635.1	0.576	37
RSPcAANLC-apicalsite5	641.3	0.49	31.3
Mean	584.6	0.4596	33.22
SD	58.626871	0.079135	2.329592239

Continue

Sample	Size (d.nm)	PdI	Zeta Potential
AASLNbasolateralsite(after120min)1	209.7	0.442	-12.5
AASLNbasolateralsite(after120min)2	221.6	0.356	-11.2
AASLNbasolateralsite(after120min)3	217	0.465	-11
AASLNbasolateralsite(after120min)4	213.3	0.37	-9.71
AASLNbasolateralsite(after120min)5	254.9	0.472	-11.9
Mean	223.3	0.421	-11.262
SD	18.207828	0.054323	1.05129444
AANLCbasolateralsite(after120min)1	247.8	0.374	-16.6
AANLCbasolateralsite(after120min)2	271.4	0.422	-11.2
AANLCbasolateralsite(after120min)3	267.1	0.344	-14.1
AANLCbasolateralsite(after120min)4	240.9	0.378	-12.4
AANLCbasolateralsite(after120min)5	233.5	0.313	-9.43
Mean	252.14	0.3662	-12.746
SD	16.4876621	0.040733	2.747376931
RSPAASLN-basolateralsite(after120min)1	335.7	0.789	-9.86
RSPAASLN-basolateralsite(after120min)2	272.3	0.65	-7.51
RSPAASLN-basolateralsite(after120min)3	269.3	0.693	-11.6
RSPAASLN-basolateralsite(after120min)4	371.9	0.636	-7.98
RSPAASLN-basolateralsite(after120min)5	381.4	0.679	-8.92
RSPAASLN-basolateralsite(after120min)	326.12	0.6894	-9.174
SD	53.3117435	0.060094	1.629042664
RSPcAASLN-basolateralsite(after120min)1	396	0.693	-3.83
RSPcAASLN-basolateralsite(after120min)2	438.8	0.697	5.32
RSPcAASLN-basolateralsite(after120min)3	401.1	0.671	-2.63
RSPcAASLN-basolateralsite(after120min)4	524.5	0.562	5.32
RSPcAASLN-basolateralsite(after120min)5	483.1	0.559	4.53
Mean	448.7	0.6364	1.742
SD	54.9319124	0.069999	4.569974836

Continue

Sample	Size (d.nm)	PdI	Zeta Potential
RSPAANLC-basolateralsite(after120min)1	372.9	0.595	-18.4
RSPAANLC-basolateralsite(after120min)2	309.5	0.539	-7.57
RSPAANLC-basolateralsite(after120min)3	350	0.451	-8.49
RSPAANLC-basolateralsite(after120min)4	367.3	0.428	-14.8
RSPAANLC-basolateralsite(after120min)5	321.7	0.404	-13.8
Mean	344.28	0.4834	-12.612
SD	27.8444249	0.080575	4.530791322
RSPcAANLC-basolateralsite(after120min)1	547.7	0.358	-19.9
RSPcAANLC-basolateralsite(after120min)2	463	0.451	-3.13
RSPcAANLC-basolateralsite(after120min)3	443.1	0.39	-11.5
RSPcAANLC-basolateralsite(after120min)4	423.6	0.489	-1.75
RSPcAANLC-basolateralsite(after120min)5	526.5	0.369	-9.91
Mean	480.78	0.4114	-9.238
SD	53.7914212	0.056341	7.290820941

VITA

Siti Zahliyatul Munawiroh was born on November 2, 1978, in Kudus, Central Jawa, Indonesia. She graduated with Bachelor of Pharmacy from Gadjah Mada University, Yogyakarta, Indonesia on 2002. She also received Apothecary Degree from Gadjah Mada University, Yogyakarta, Indonesia on 2003. Now she is working as one of junior lecturers at Faculty of Mathematics and Sciences, Universitas Islam Indonesia, Yogyakarta, Indonesia.



